Università degli Studi
di Modena e Reggio Emilia

PhD course in

“Models and Methods for Material and Environmental Sciences”

XXXIII Cycle – Director: Prof. Alfonso Pedone

Atom Transfer Radical Reactions: Polymerization of Styrene and Synthesis of γ-Lactones

Candidate: **Mirko Buffagni**

Supervisor: Prof. **Franco Ghelfi** Co-supervisor: Dr. **Francesca Parenti**

"I am utterly convinced that Science and Peace will triumph over Ignorance and War, that nations will eventually unite not to destroy but to edify, and that the future will belong to those who have done the most for the sake of suffering humanity."

—Louis Pasteur (1822–1895)

Title

Atom Transfer Radical Reactions: Polymerization of Styrene and Synthesis of γ-Lactones

Submission date

December 30, 2020

Final revisions

March 22, 2021

Defense date

April 12, 2021

Supervisors

Prof. Franco Ghelfi, Department of Chemical and Geological Sciences, University of Modena and Reggio Emilia

Dr. Francesca Parenti, Department of Chemical and Geological Sciences, University of Modena and Reggio Emilia

Opponents

Prof. Marco Borsari, Department of Chemical and Geological Sciences, University of Modena and Reggio Emilia

Prof. Marco Giardino, Department of Earth Sciences, University of Turin

Prof. Alberto Castelli, Department of Biology, University of Pisa

Mirko Buffagni PhD Thesis

Preface

During my PhD period, I mainly worked on two different research projects. Both of these projects involve atom transfer radical reactions. The thesis is therefore divided into two parts.

In Part I, the mechanistic aspects of an anomalous gelation during the synthesis of PS via ATRP were investigated. I dedicated the majority of my time to this project, under the guidance of Prof. Franco Ghelfi and Dr. Francesca Parenti.

In Part II, it is described the ATRA-L, a new type of organic reaction. The ATRA-L project was conceived and developed during my six-month period within the Matyjaszewski Polymer Group (Carnegie Mellon University, Pittsburgh PA, USA), under the supervision of Prof. Krzysztof Matyjaszewski.

The abstracts of this thesis and the publications that have been made during my PhD period are reported hereafter.

Abstracts

English

Atom transfer radical polymerization (ATRP) is a powerful technique for the synthesis of controlled macromolecular structures. In this work, an activator regenerated by electron transfer (ARGET) ATRP system is used as a new green system for the synthesis of polystyrene (PS). This ARGET ATRP system is Cu-catalyzed and the reducing system is composed of ascorbic acid and Na_2CO_3. The solvent mixture is made up of EtOAc and EtOH. Surprisingly, in specific ARGET ATRP conditions, the PS gelled. The gelation is surprising since no branching nor crosslinking agents were added to the reaction mixture and their formation in situ was excluded. The experimental results led to the hypothesis that a polycatenane network with interpen-

etrating macrocycles is formed. Furthermore, a patent was filed with the surprising discovery. In this thesis, it is studied the mechanism of the anomalous gelation with the supporting evidence to the polycatenane hypothesis.

Besides, atom transfer radical addition (ATRA) was also studied to synthesize γ-halocarboxylic acids, starting from α-halocarboxylic acids and alkenes. The γ-halocarboxylic acids can rapidly cyclize to form γ-lactones, following a substitution reaction of the halogenated moiety by the carboxylic acid. A new acronym is then proposed for the combination of ATRA with the subsequent lactonization (ATRA-L). Since the halogenated moiety is rapidly lost, the ATRA-L allows the use of alkenes that are generally prohibited in ATRA. In fact, following an ATRA reaction, the halogen of the product is required to be inactive toward a second ATRA, otherwise an oligomer is obtained. In ATRA-L, the halogen is lost and there are no restrictions on the choice of the alkene. An in-depth study of the literature was done to find the reactions related to ATRA-L and to connect them from a common point of view. A Cu-catalyzed ATRA-L system in H_2O is then studied, focusing on the effect of the pH on the reaction, on how the variables affect the system, and on the reaction mechanism.

Italian

La polimerizzazione radicalica a trasferimento di atomo (ATRP) è una tecnica versatile per la sintesi controllata di strutture macromolecolari. In questo lavoro, un sistema ATRP ad attivatore rigenerato mediante trasferimento elettronico (ARGET) viene utilizzato come un nuovo sistema *green* per la sintesi del polistirene (PS). Tale processo ARGET ATRP è catalizzato da Cu e il sistema riducente è composto da acido ascorbico e Na_2CO_3. La miscela di solventi è composta da EtOAc e EtOH. Sorprendentemente, in specifiche condizioni ARGET ATRP, il PS è gelificato. La gelificazione è sorprendente poiché non sono stati aggiunti agenti ramificanti o reticolanti alla miscela di reazione e la loro formazione in situ è stata esclusa. I risultati sperimentali portano all'ipotesi che si formi una rete di policatenani con macrocicli compenetranti. Questa innovativa scoperta è stata inoltre oggetto di un brevetto depositato. In questa tesi viene studiato il meccanismo della gelificazione anomala con le prove a supporto dell'ipotesi della rete di policatenani.

Inoltre, è stata studiata anche l'addizione radicalica a trasferimento di atomo (ATRA) per sintetizzare acidi γ-alocarbossilici, partedo da da acidi α-alocarbossilici e alcheni. Gli acidi γ-alocarbossilici possono ciclizzare rapidamente per formare γ-lattoni, a seguito di una reazione di sostituzione della funzione alogenata da parte dell'acido carbossilico. Viene quindi proposto un nuovo acronimo per l'accoppiamento dell'ATRA con la successiva lattonizzazione (ATRA-L). Poiché la frazione alogenata viene persa rapidamente, l'ATRA-L consente l'uso di alcheni generalmente proibiti in ATRA. Infatti, a seguito di una reazione ATRA, l'alogeno del prodotto deve essere inattivo nei confronti di una seconda ATRA, altrimenti si otterrebbe un oligomero. In ATRA-L, l'alogeno viene perso e non ci sono restrizioni sulla scelta dell'alchene. È stato condotto uno studio approfondito della letteratura per trovare le reazioni correlate all'ATRA-L e per collegarle da un punto di vista comune. Viene quindi studiato un sistema ATRA-L catalizzato da Cu in H_2O, concentrandosi sull'effetto del pH sulla reazione, su come le variabili influenzano il sistema e sul meccanismo di reazione.

Publications

1. M. Caselli, D. Vanossi, M. Buffagni, M. Imperato, L. Pigani, A. Mucci, and F. Parenti, Optoelectronic properties of A-π-D-π-A thiophene-based materials with a dithienosilole core: An experimental and theoretical study, *ChemPlusChem* **84**(9), 1314–1323 (2019), DOI: 10.1002/cplu.201900092.

2. F. Ghelfi, A. Ferrando, A. Longo, and M. Buffagni, Polymerization process for the synthesis of vinyl aromatic polymers with a controlled structure, 2019, Patent number WO2019215626.

3. N. Braidi, M. Buffagni, F. Ghelfi, M. Imperato, A. Menabue, F. Parenti, A. Gennaro, A. A. Isse, E. Bedogni, L. Bonifaci, G. Cavalca, A. Ferrando, A. Longo, and I. Morandini, Copper-catalysed "activators regenerated by electron transfer" "atom transfer radical polymerisation" of styrene from a bifunctional initiator in ethyl acetate/ethanol, using ascorbic acid/sodium carbonate as reducing system, *Macromolecular Research* **28**(8), 751–761 (2020), DOI: 10.1007/s13233-020-8091-3.

4. N. Braidi, M. Buffagni, F. Ghelfi, F. Parenti, A. Gennaro, A. A. Isse, E. Bedogni, L. Bonifaci, G. Cavalca, A. Ferrando, A. Longo, and I. Morandini, ARGET ATRP of styrene in EtOAc/EtOH using only Na_2CO_3 to promote the copper catalyst regeneration, *Journal of Macromolecular Science, Part A* (2021), DOI: 10.1080/10601325.2020.1866434.

5. N. Braidi, M. Buffagni, V. Buzzoni, F. Ghelfi, F. Parenti, M. L. Focarete, C. Gualandi, E. Bedogni, L. Bonifaci, G. Cavalca, A. Ferrando, A. Longo, I. Morandini, and N. Pettenuzzo, Unusual cross-linked polystyrene by copper-catalyzed ARGET ATRP using a bifunctional initiator and no cross-linking agent, *submitted for publication.*

The first published article is about a research that has been done during my master thesis and it does not concern atom transfer radical reactions. The third and fourth publications relate to initial studies on the ARGET ATRP system developed by my research group. The fourth entry was accepted for publication and the DOI was generated, but to date it lacks other journal information (volume, issue, and pages). The second and the fifth publications are related to the anomalous gelation. Among these, the fifth has been submitted, but it is still under the review process. Furthermore, a sixth article is in preparation still concerning the anomalous gelation.

Contents

Part I

Anomalous Gelation During the Atom Transfer Radical Polymerization of Styrene

Chapter 1

Introduction to atom transfer radical polymerization

1.1 Reversible-deactivation radical polymerization

Reversible-deactivation radical polymerization (RDRP) is a class of RP processes that allow the synthesis of polymers with controlled molecular architecture and low dispersity ($Đ$).[1] For a long time, the control of molecular architecture was thought to be impossible in radical polymerization (RP) since the reaction between two radicals is very fast. In fact, radical–radical coupling is a diffusion-controlled termination reaction. RDRP techniques exploit an equilibrium between dormant and active species and only the active species can react with monomers and propagate. The RDRP equilibrium is shifted toward the dormant species to prevent radical–radical coupling. In the ideal case, polymer chains grow with uniform molecular weights and in a predictable way. Furthermore, a chain-end functionality is preserved in the dormant species, which can be used for post-functionalization reactions.

Various RDRP have been developed, such as atom transfer radical polymerization (ATRP),[2] reversible addition-fragmentation chain transfer (RAFT) polymerization,[3] nitroxide-mediated radical polymerization (NMP),[4] and organometallic-mediated radical polymerization (OMRP).[5] Among them, ATRP is the most popular and widespread.[6,7] ARTP was first independently developed in 1995 by Sawamoto[8] and Matyjaszewski,[9] and can be described as a particular case of atom transfer radical addition (ATRA). Differently from ATRA, ATRP performs multiple additions of unsaturated compounds (i.e. monomers), instead of a single one.

1.2 Mechanism of ATRP

ATRP is controlled by the equilibrium between dormant halogenated species ($P_n{-}X$) and propagating radicals ($P_n\cdot$) (Scheme 1.1).[2] The equilibrium is catalyzed by the complex Mt^mL, where Mt^m is the transition metal with the oxidation state m and L is a ligand. The complex in its lower oxidation state (Mt^mL) is called activator, while the higher oxidation state ($X{-}Mt^{m+1}L$) is named deactivator. The activator periodically reacts with the dormant species by abstracting a halogen with rate constant k_a, to give the propagating radicals and the deactivator. In their turn, the propagating radicals and the deactivator react with the deactivation rate constant k_d to give back the dormant species and the activator. The rate constant of ATRP (K_{ATRP}) is the defined as the ratio between k_a and k_d.

In their lifetime, the radical species can propagate adding a monomer (M) with rate constant k_p, or they can terminate by radical–radical coupling with constant rate k_t. The termination reaction gives the completely inactive species $P_n{-}P_n$. Its inactivity is due to the loss of the halogenated functions. The control of ATRP is ensured by keeping low the concentration of propagating radicals, minimizing termination reactions. Therefore, the deactivation rate constant (k_d) should be higher than the activation one (k_a), shifting the equilibrium toward the dormant species.

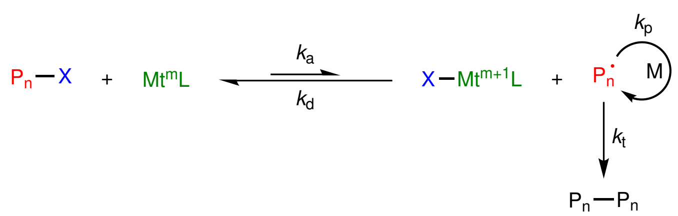

Scheme 1.1: ATRP equilibrium.

ATRP initiators ($P_n{-}X$ with $n = 0$) are chosen in a way that their activation rate is higher than the one of the other halogenated species which have added at least one monomer ($n > 0$). In this way, a slow initiation is avoided and the $Đ$ is kept as small as possible. In other words, in the ideal case, the monoaddition products ($n = 1$) start reacting only after the initiator is completely consumed.

Typically, the monomers employed in ATRP have a vinyl moiety. Nevertheless, there is a limitation in the monomers that can be used. This limitation is related to the activation of the dormant species, for which an active halogen is required. It is therefore necessary an α-stabilizing substituent adjacent to the transferable halogen. Otherwise, the activator would not be able to reactivate the dormant species. This does not exclude that in the future there will be more active catalysts able to activate some of the less activated halogens.[10] However, simple alkenes (which are not suitable for the ATRP equilibrium) can be copolymerized, principally with acrylates.[11]

In ATRP, the polymerization rate R_p is directly proportional to the growing radicals $\mathrm{P_n\cdot}$ and to the concentration of the monomer [M], through the rate constant k_p (Equation 1.1).[7,12–14] When the equilibrium is reached, $\mathrm{P_n\cdot}$ is constant and the K_ATRP is expressed by Equation 1.2. Equation 1.3 is obtained by solving the differential Equation 1.1. In the solution, the differential ∂[M] is integrated within the initial and the current concentration of monomer ($[\mathrm{M}]_0$ and [M] respectively). On the other side, the integration limits of ∂t are 0 and t. The value $[\mathrm{R}\cdot]$ represents the concentration of radicals, which is equivalent to $[\mathrm{P_n\cdot}]$. Equation 1.3 is used in kinetic analysis to determine whether or not a process is controlled. If it is controlled, $[\mathrm{R}\cdot]$ is constant and, therefore, there is a linear dependence between $ln\frac{[\mathrm{M}]_0}{[\mathrm{M}]}$ and t. The k_p is constant for a specific monomer at a constant temperature.

$$R_\mathrm{p} = -\frac{\partial[\mathrm{M}]}{\partial t} = k_\mathrm{p} \cdot [\mathrm{M}] \cdot [\mathrm{P_n}\cdot] \tag{1.1}$$

$$K_\mathrm{ATRP} = \frac{k_\mathrm{a}}{k_\mathrm{d}} = \frac{[\mathrm{P_n}\cdot] \cdot [\mathrm{X{-}Mt^{m+1}L}]}{[\mathrm{P_n{-}X}] \cdot [\mathrm{Mt^mL}]} \tag{1.2}$$

$$ln\frac{[\mathrm{M}]_0}{[\mathrm{M}]} = k_\mathrm{p} \cdot [\mathrm{R}\cdot] \cdot t \tag{1.3}$$

1.3 Catalyst regeneration

The most employed transition metal for ATRP catalysis is Cu.[2] Other transition metals used in ATRP include Fe,[15–17] Ti,[18] Ni,[19–21] Co,[22] Pd,[23] Ru,[8,24,25] Mo,[26–28] Rh,[29,30] Os,[31] and Re.[32,33] The metals are usually complexed with polydentate N-based ligands.

As already stated, termination reactions are strongly suppressed in an ATRP system. However, the process is not ideal and a few termination reactions are occurring. This causes an increase in the concentration of the deactivator, slowing down the polymerization until it stops. To avoid the stoppage, a high amount of activator can be used. Nevertheless, increasing the concentration of the catalyst prejudices the atom efficiency of the process and raises the problem of metal removal from the final polymeric material.[34–36] To avoid these problems, catalyst regeneration techniques were developed, coupling a reducing agent with the catalytic system.

The catalyst regeneration has three main advantages. *(i)* As already mentioned, it quenches the accumulation of the deactivator, which is a consequence of termination reactions. *(ii)* It allows the usage of small amounts of metal catalyst, down to ppm levels. *(iii)* The metal can be added to the reaction mixture in its higher oxidation state (the deactivator), which is generally stable in air. Following this last advantage, the activator is not only regenerated but also generated in situ.[37–39] The addition of the metal in its higher oxidation state defines what is known as "reverse" ATRP.

Various methods have been developed with different reducing agents as catalyst regeneration techniques:

- **Initiators for continuous activator regeneration (ICAR) ATRP**. Free radicals are slowly and constantly added to the polymerizing mixture to reduce the deactivator. Free radicals are obtained by decomposition of conventional radical initiators like azobisisobutyronitrile (AIBN).[40–42]

- **Activators regenerated by electron transfer (ARGET) ATRP**. Non-radical reducing agents are employed, such as tin(II) 2-ethylhexanoate ($Sn(EH)_2$),[43–46] ascorbic acid (AsAc),[47–50] or aliphatic tertiary amines.[51–53]

- **Supplemental activator and reducing agent (SARA) ATRP**. A zerovalent metal is used to regenerate the activator and as additional activator, following a comproportionation reaction with the deactivator.[54–57] This type of regeneration method was rationalized also as single-electron transfer living radical polymerization (SET-LRP).[58,59]

- **Electrochemically mediated ATRP (*e*ATRP)**. The reduction is performed and controlled using electrochemical methods.[60–63]

- **Photoinduced ATRP (photo-ATRP)**. The activator regeneration by the reducing agent is made possible by irradiation with visible or UV light.[64–66]

- **Mechanically induced ATRP (mechano-ATRP)**. Piezoelectric nanoparticles under ultrasonication are exploited for the electron transfer.[67,68]

Furthermore, metal-free ATRP systems have been studied. These systems exploit uncatalyzed iodine atom transfer or organic redox carriers.[69–74]

1.4 Polymer architecture

ATRP allows the synthesis of (co)polymers with controlled architectures. Other than homopolymers, it is possible to prepare statistical, block, alternating, periodic, and gradient copolymers (Figure 1.1a). As already mentioned in section 1.2, the synthesis of copolymers allows the usage of monomers that are generally forbidden in ATRP.

Furthermore, it is possible to build more complex architectures than simple linear polymer chains. Several methods allow the construction of graft and comb-shaped copolymers, (hyper)branched, stars, rings, and even network structures (Figure 1.1b).[75]

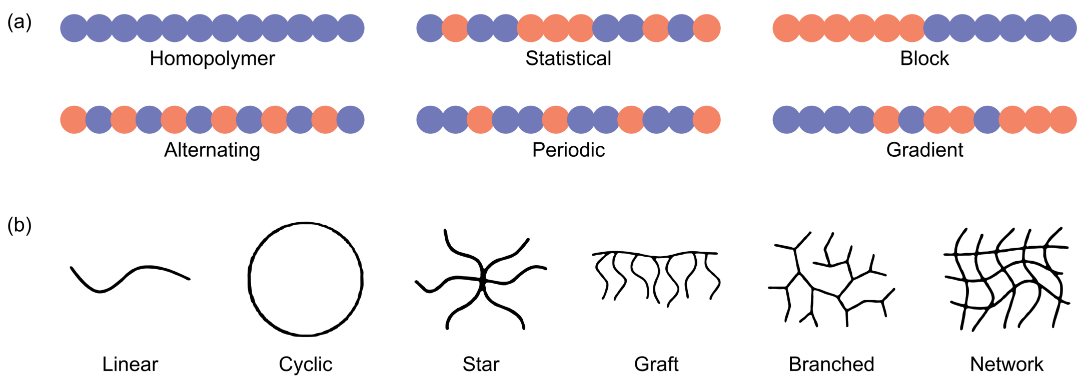

Figure 1.1: Composition (a) and topology (b) of polymers prepared by ATRP.

1.4.1 Synthesis of branched (co)polymers by ATRP

Hyperbranched polymer architectures can lead to the formation of macroscopic gels. To obtain a branched structure, a crosslinker is generally required. The molecular weight of branched polymers is exponentially increased by the level of crosslinking.[76] In general, four strategies are exploited to obtain a branched architecture. *(i)* Grafting onto, grafting from, and grafting through are two-step processes used to insert branching points. *(ii)* Divinyl comonomers are also employed as crosslinkers. If the molar amount of the divinyl compound is lower than the one of the initiator, a branched copolymer is generally obtained. Otherwise, if the amount of divinyl compound is greater than the initiator, a gel is achieved.[77] *(iii)* Multifunctional initiators (at least trifunctional) can add a branching point, generating a star.[78] *(iv)* The last strategy involves the usage of inimers, which are particular compounds that have both an alkyl halide to initiate and a double bond to polymerize. If an inimer is used in a copolymerization, then a relatively loosely branched polymer is obtained. The homopolymerization of an inimer gives a hyperbranched structure instead.[79]

RDRP techniques (ATRP included) offer important differences in the ability to manipulate the structures of branched polymers and gels.[77] Such techniques provide more homogeneous incorporation of branching points in branched copolymers and more regular network structures in gels, compared to polymers produced by conventional FRP.[80]

1.5 The ARGET ATRP process developed by our research group

Recently, our research group reported the synthesis of γ-lactams from *N*-substituted *N*-allyl-2,2-dichloroamides via ARGET atom transfer radical cyclization (ATRC).[81–83] The process was Cu-catalyzed and tris(2-pyridylmethyl)amine (TPMA) was used as ligand. The reducing agent was AsAc, coupled with Na_2CO_3 as neutralizing agent. The solvent was a mixture of EtOAc and EtOH. Following a collaboration with the “Claudio Buonerba” research center of Versalis (Eni) S.p.A. in Mantua (Italy), the ARGET ATRC was adapted to the ARGET ATRP of styrene (St). The high versatility of the ATRP process is indeed well suited for the preparation of precisely tailored and valuable St-based materials, such as surface-active polymers, electrolyte gels, functional membranes, and various hybrid materials.[84–88]

The ARGET ATRP system derived from the ATRC process is highlighted in Scheme 1.2. Ethyl 2,2-dichloropropionate (EDCP) was chosen as bifunctional initiator since it retains a functionality ($CCl_2C{=}O$) similar to the N-substituted N-allyl-2,2-dichloroamides. This type of initiators can be synthesized by simple esterification of 2,2-dichlorocarboxylic acids or of the corresponding acyl chlorides, substrates that are easily obtainable on a large scale with simple procedures.[89–91] In particular, EDCP was chosen because it is a derivative of 2,2-dichloropropionic acid, which is a cheap industrial product, mostly used as herbicide. In addition, the activation of both chlorinated functions of EDCP is faster than the activation of the benzylic halide from the polystyrene (PS) chain end.[92] Ideally, the addition of St monomers on the PS chain end occurs only after both the chlorinated functions of EDCP reacted. Lastly, an ethyl ester was chosen as initiator to cancel the effect of the transesterification reaction with the EtOH from the solvent mixture. The basic conditions of the reaction mixture (due to the presence of Na_2CO_3) can indeed promote transesterification reactions.[93]

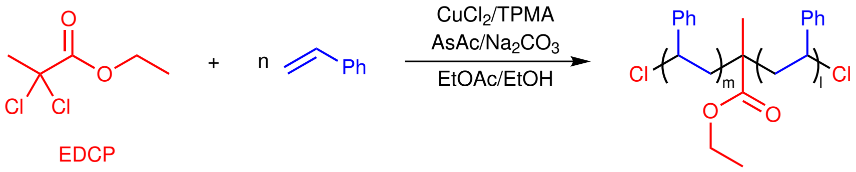

Scheme 1.2: ARGET ATRP from EDCP to synthesize α,ω-telechelic PS.

Cu-catalyzed ARGET ATRP with AsAc is a well-known practice.[49,50,94–97] However, we were unable to find examples where AsAc and Na_2CO_3 are coupled. The addition of catalytic amounts of a base (NaOH) to AsAc was studied only in one example of Fe-catalyzed bulk polymerization of St.[98] The combination of inorganic bases (including Na_2CO_3) with AsAc was also reported for a few polymerizations of methyl methacrylate by ARGET ATRP.[99–102] These examples, however, are always catalyzed by Fe and never in the presence of protic solvents.

Scheme 1.3 shows the ARGET ATRP mechanism with AsAc and Na_2CO_3. AsAc reacts with the deactivator, giving dehydroascorbic acid (DHAs), the activator, and a halogenic acid (HX). The acidity of the halogenic acid is then quenched by Na_2CO_3 in an acid–base reaction, releasing NaX, CO_2, and H_2O. For simplicity of the scheme, the reaction is not balanced. One mole of AsAc is able to reduce two moles of activator and to produce two moles of halogenic acid. The two moles of halogenic

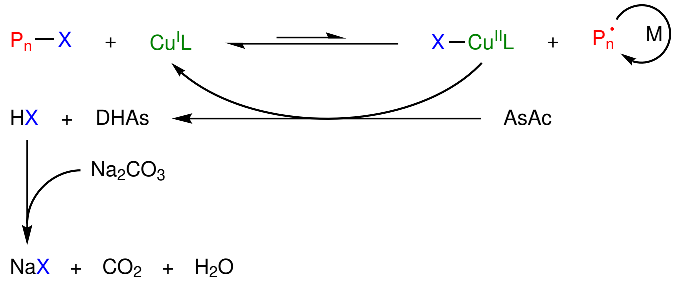

Scheme 1.3: ARGET ATRP process with AsAc and Na_2CO_3.

acid can be neutralized by only one mole of Na_2CO_3.

The use of the EtOAc/EtOH solvent mixture appears to have never been used in ATRP as well. This solvent mixture is interesting because it is a green choice and the two components derive from renewable resources.[103] Furthermore, the change in the ratio between EtOAc and EtOH can be exploited to modulate the electric and the solvent properties of the medium. In fact, EtOAc is a moderately polar aprotic solvent able to dissolve PS. On the other side, EtOH is a polar protic component, in which PS is not soluble. This solvent mixture is more versatile and cheaper than ethyl lactate, which was recently proposed as a green solvent for ARGET ATRP and SET-LRP processes.[103,104]

TPMA is a suitable ligand for various reasons. *(i)* Its complex with Cu is proved to be quite robust and efficient in our reaction system.[81–83] *(ii)* TPMA is one of the most used ligands for the Cu-catalyzed ATRA.[105,106] *(iii)* Its good chelating properties allow to work with low concentrations of Cu.[107] *(iv)* TPMA is known to prevent the disproportionation between Cu^{I} species, even in H_2O, with the consequent release of Cu^{0} in the reaction system.[108] *(v)* Being solid, TPMA is foreseeably fit for process scale-up.[109]

Usually, atom transfer radical reactions are performed with an excess of the ligand (compared to the amount of transition metal). However, the ARGET ATRP that we developed uses only a stoichiometric amount of TPMA. The molar amount of TPMA is 1:1 relative to Cu. The aim is to make the process more practical and economic.

Chapter 2

Materials and methods

Unless differently stated, the molar ratio (MR) of St is always set to 100. Therefore, the MR of other reagents is equivalent to their mol %.

2.1 Experimental section

2.1.1 Chemicals

St (stabilized with 10–15 ppm of 4-*tert*-butylcatechol, TBC) is supplied by Versalis (Eni) S.p.A. and used without purification. Ethyl methacrylate (EMA) (Sigma-Aldrich, 99%), ethyl acrylate (EA) (Sigma-Aldrich, 99%), St-d_8 (Sigma-Aldrich, 98%), methyl 2-chloroactylate (MCA) (Sigma-Aldrich, 98%), benzal chloride (BC) (Sigma-Aldrich, 95%), benzal bromide (BB) (Sigma-Aldrich, 95%), $CuCl_2$ (Riedel-de Haën, 97%), CuCl (Fluka, 97.0%), $CuBr_2$ (Acros Organics, 99%), TPMA (TCI Europe, 98%), N,N,N',N'',N''-pentamethyldiethylenetriamine (PMDETA) (TCI Europe, 99.0%), 4,4′-dinonyl-2,2′-bipyridine (dNbpy) (TCI Europe, 98%), AsAc (Sigma-Aldrich, 99.5%), Na_2CO_3 (Carlo Erba, 99.5%), $Sn(EH)_2$ (TCI Europe, 85.0%), TBC (Sigma-Aldrich, 99%), 5,6-O,O-isopropylidene-ascorbic acid (IPIAA) (Sigma-Aldrich, 98%), EtOH (98%), EtOAc (98%), and toluene (Tol) (Carlo Erba, 99.5%) are used without purification. EDCP (99%, determined via gas chromatography, GC) is prepared by esterification of 2,2-dichloropropanoyl chloride acid with EtOH; 2,2-dichloropropanoyl chloride is synthesized following a literature method.[89] Methyl 2,2-dichlorobutanoate (MDCB) (GC purity 99%) is obtained in an analogous way as EDCP. Ethyl 2-chloroisobutyrate (ECiB) is synthesized from ethyl

2-hydroxyisobutyrate by adaptation of literature procedures.[110,111] CH_2Cl_2 and MeOH, used for the reaction work-up, are recycled products purified by fractional distillation.

2.1.2 General procedure

Entry P018 of Table 3.3 is described as a typical experiment. 23.0 mg of AsAc (0.130 mmol) and 41.5 mg of Na_2CO_3 (0.391 mmol) are transferred to a 25 mL Schlenk tube. After 3 cycles of vacuum/Ar, the reagents are added in the following order: 3 mL of St (26.1 mmol), 2 mL of EtOAc, 1 mL of 0.276 mol L^{-1} EDCP stock solution in EtOAc (0.276 mmol), 0.75 mL of EtOH, and 0.25 mL of 0.0520 mol L^{-1} $CuCl_2$/TPMA stock solution in EtOH (0.0130 mmol of $CuCl_2$ and 0.0130 mmol of TPMA). The Schlenk tube is sealed and submerged in an oil bath thermostated at 70 °C and the reaction mixture is stirred for 18 h at 400 rpm (oval stirring bar: l = 20 mm, d = 10 mm). Afterward, the Schlenk is allowed to cool to room temperature. The recovery of the gel is made easier by the addition of MeOH. The gel is extracted in Soxhlet with MeOH for 7 days and then dried in a vacuum oven till constant weight (T = 60 °C, P = 1–2 mbar). 2.25 g of crosslinked PS are obtained (83% yield).

When the final reaction mixture does not gel, it is diluted with CH_2Cl_2. The PS is then precipitated in 300 mL of MeOH, dropping the diluted reaction mixture under adequate stirring. To improve the coagulation, HCl_{aq} 10% (2 mL) is added. The PS is then filtered with a filter funnel (porosity P4) and washed two times with MeOH. The funnel with the PS is first dried under vacuum (P = 1–2 mbar) for 1–2 h, then under aspiration for 15–20 h till constant weight. The conversion (conv) is calculated by subtracting the contribution of the initiator from the measured mass of the isolated material. Gravimetry is an easy and common method for conversion measurement. The only error is due to the fractionation of PS chains with a very low molecular weight (MW) during the reaction work-up. However, this error is negligible for conversions which yield PS with $M_n > 3000$ Da.[112] Since MeOH is a good solvent for the $CuCl_2$/TPMA complex, the typical filtration over basic Al_2O_3 is avoided. The recovered PS is indeed white.

2.2 Characterizations

2.2.1 Gel permeation chromatography

The MW distributions, molar mass averages (M_n and M_w) and $Đ$ are obtained using a conventional gel permeation chromatography (GPC). The GPC is equipped with only a concentration detector and is calibrated with standards of monodisperse polymers matching those subsequently analyzed. In order to study the branching of some samples, a GPC-VISCO-MALLS is used instead, which is equipped with a multiangle laser light scattering (MALLS) detector and a viscometer (VISCO) detector. For details about the MALLS analysis, see subsection 2.2.2.

In the conventional GPC, the MW distributions are determined using a Waters GPC system composed of a Waters Alliance 2695 separation module and a Waters 2414 differential refractometer detector. Empower 2 (Waters) is used as chromatographic analysis software. The system is calibrated with 20 narrow distribution standards of PS with MW ranging from 1.3 kDa to 7000 kDa. Four GPC Phenogel (Phenomenex) columns (size 300×7.6 mm, particle size 5 µm, porosity 10^6, 10^5, 10^4, and 10^3 Å) are connected and housed in an oven at 30 °C. Tetrahydrofuran (THF) is used as the mobile phase for the high-performance liquid chromatography (HPLC). The elution conditions are: flow rate 1 mL min^{-1}, injection volume 200 µL, sample concentration 2.5 mg mL^{-1}, and Tol is used as internal standard.

2.2.2 Multiangle laser light scattering

GPC-VISCO-MALLS analyses are performed using the same GPC system additionally equipped with a DAWN EOS MALLS (Wyatt Technology) and a Viscotek T50 as light scattering and VISCO detectors. The analytical conditions are the same used in conventional GPC but the sample concentration is 1.0 mg mL^{-1}. Two different samples of PS with broad distribution are used for comparison: a linear one (commercial product) and a branched one. The branched PS is synthesized by free-radical polymerization (FRP) between St and divinylbenzene.

The $\Delta M_\mathrm{w}\%$ (Equation 2.6 of section 2.3) is used to roughly evaluate the degree of branching. The $\Delta M_\mathrm{w}\%$ shows the difference between the real $M_\mathrm{w}^\mathrm{MALLS}$ and the estimated $M_\mathrm{w}^\mathrm{GPC}$. The comparison of the $\Delta M_\mathrm{w}\%$ values between a specific sample and the branched PS allowed us to understand which samples are branched. The arbitrary limit between a linear and a branched sample is set as 60% of the $\Delta M_w\%$ value of the branched PS (second entry of Table 2.1). Thus, this limit is equal to 10.9% ($= 18.2 \cdot 60$). Briefly, every PS sample with a $\Delta M_w\%$ value above 10.9% is considered branched.

Table 2.1 reports the $\Delta M_w\%$ values of the reactions of chapter 3.

Entry	**Table**	$M_w^{\mathbf{MALLS}}$ [kDa]	$M_w^{\mathbf{GPC}}$ [kDa]	$M_w^{\mathbf{MALLS}}/M_w^{\mathbf{GPC}}$	$\Delta M_w\%$
Linear PS	—	288.9	288.0	1.00	0.3
Branched PS	—	387.2	316.8	1.22	18.2
P010	3.2	244.9	174.2	1.41	28.9
P027	3.5	60.3	47.5	1.27	21.2
P035	3.7	31.5	29.1	1.08	7.6
P044	3.8	28.2	27.4	1.03	2.8
P048	3.10	19.5	18.9	1.03	3.1
P050	3.10	384.7	198.9	1.93	48.3
P051	3.10	377.2	228.5	1.65	39.4
P065	3.13	126.8	73.6	1.72	42.0
P067	3.13	415.5	204.6	2.03	50.8
P068	3.13	131.8	92.1	1.43	30.1
P069	3.13	10.3	10.3	1.00	0.0
P070	3.14	481.0	173.2	2.78	64.0
P071	3.14	169.5	116.7	1.45	31.2
P072	3.14	61.3	51.8	0.30	15.5
P073	3.15	193.2	124.0	1.56	35.8
P074	3.15	76.0	61.7	1.23	18.8
P075	3.15	47.1	41.9	1.12	11.0
P109	3.24	249.3	159.0	1.57	36.2
P108	3.24	293.5	196.7	1.49	33.0

Table 2.1: Results of the MALLS analyses. Samples are considered branched if $\Delta M_w\% > 10.9\%$.

2.2.3 Nuclear magnetic resonance

Nuclear magnetic resonance (NMR) spectra are recorded with a Bruker AV-400 spectrometer (resonance frequency 400.13 MHz), equipped with a 5 mm PABBO BB/19F-1H/D x,y,z-field gradient probe-head. The spectra are analyzed with Topspin 3.6 software package, operating in Fourier transform. Typical acquisition parameters: 512 transients, spectral width 7.5 kHz, and delay time of 7.0 s. Chemical shifts are referred to solvent peak. All the spectra are acquired using $CDCl_3$ as solvent at 25 °C.

2.2.4 Scanning electron microscope

Images of the crosslinked PS are obtained with a scanning electron microscope (SEM) field emission gun (FEG) TESCAN MIRA II (TESCAN). The sample is prepared by cutting a small amount of material that was then sputtered with Au (thickness ≈ 20 nm).

2.3 Equations

The number average molar mass (M_n) and the mass average molar mass M_w are defined by Equations 2.1 and 2.2, respectively. They represent the weighted mean taken with the mole fraction (M_n) and with the weight fraction (M_w). These two values are determined via GPC. The $Đ$ is calculated as the ratio between M_w and M_n, as shown in Equation 2.3.

$$M_\mathrm{n} = \frac{\sum M_i N_i}{\sum N_i} \tag{2.1}$$

$$M_\mathrm{w} = \frac{\sum M_i^2 N_i}{\sum M_i N_i} \tag{2.2}$$

$$Đ = \frac{M_\mathrm{w}}{M_\mathrm{n}} \tag{2.3}$$

The theoretical number average molar mass (M_n^th) is calculated with Equation 2.4. The moles of St and initiator are n_{St} and n_{Ini} respectively. The molar mass of St and initiator are M_{St} and M_{Ini}. The conversion ($conv$) is the mass of the final recovered PS without the contribution of the initiator (assuming a 100% yield of the initiator). Equation 2.5 is used to calculate the $\Delta M_\mathrm{n}\%$, i.e. the percentage difference between the experimental M_n and the theoretical M_n^th.

$$M_\mathrm{n}^\mathrm{th} = \frac{n_{St}}{n_{Ini}} \cdot M_{St} \cdot conv + M_{Ini} \tag{2.4}$$

$$\Delta M_{\mathrm{n}}\% = \frac{M_{\mathrm{n}} - M_{\mathrm{n}}^{\mathrm{th}}}{M_{\mathrm{n}}} \cdot 100\% \tag{2.5}$$

The percentage difference between the two M_{w} values, one determined via MALLS ($M_{\mathrm{w}}^{\mathrm{MALLS}}$) and one via GPC ($M_{\mathrm{w}}^{\mathrm{GPC}}$), is calculated with Equation 2.6. This value is used to discriminate linear from branched PS chains, as described in subsection 2.2.2.

$$\Delta M_{\mathrm{w}}\% = \frac{M_{\mathrm{w}}^{\mathrm{MALLS}} - M_{\mathrm{w}}^{\mathrm{GPC}}}{M_{\mathrm{w}}^{\mathrm{MALLS}}} \cdot 100\% \tag{2.6}$$

Chapter 3

Results and discussion

3.1 Anomalous gelation

The ARGET ATRP of St was studied in the temperature range 25–100 °C, as reported in Table 3.1.[92] The targeted degree of polymerization (TDP) is ~100 and the reaction time was kept constant at 18 h. As expected, conversions decreased while lowering the reaction temperature. The reactions went from full conversion at 100 °C to 23% at 25 °C (entries P006 and P001, respectively). Surprisingly, the control of the polymerization deteriorated below 90 °C, as can be seen from the values of $\Delta M_\mathrm{n}\%$ and $Đ$.

Entry	$\boldsymbol{T}$ [°C]	**Conv** [%]	$\boldsymbol{M_\mathrm{n}}$ [kDa]	$\boldsymbol{M_\mathrm{n}^\mathrm{th}}$ [kDa]	$\boldsymbol{\Delta M_\mathrm{n}\%}$	$\boldsymbol{Đ}$
P001	25	23	7.2	2.4	67	1.76
P002	43	44	21.8	4.4	80	3.48
P003	60	gel	—	—	—	—
P004	80	87	32.2	8.7	73	3.14
P005	90	88	15.0	8.8	41	1.54
P006	100	101	22.4	10.0	55	1.87

Table 3.1: Effect of the temperature on the ARGET ATRP of St. Conditions: St:EDCP:$CuCl_2$/TPMA:AsAc:Na_2CO_3 = 100:1.06:0.2:0.5:1.5, V_St = 3 mL, V_EtOAc = 3 mL, V_EtOH = 1 mL, t = 18 h.

The loss of control was probably due to an unexpected branching. However, no crosslinking agent was added to the reaction mixture. At 60 °C, the phenomenon was so accentuated that the reaction mixture even gelled. The gel is insoluble in CH_2Cl_2 and Tol, two good solvents for PS.[113] Figure 3.1 shows how the GPC traces

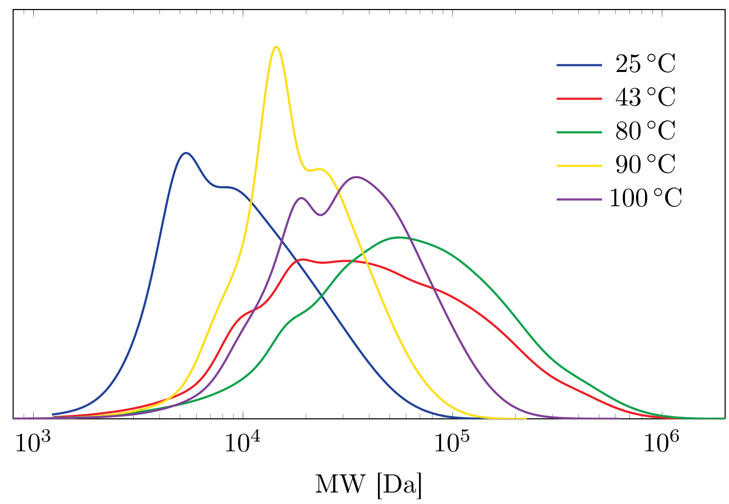

Figure 3.1: GPC analyses of the PSs obtained at different temperatures (entries of Table 3.1).

of the polymers are polymodal. Obviously, the PS gel obtained at 60 °C could not be analyzed via GPC.

As far as we are aware, no one ever reported this type of anomalous gelation during the polymerization of St. The discovery was therefore patented.[114] The preparation of branched or crosslinked polymers by ATRP is known and widely employed.[77,115] Nevertheless, the branching and crosslinking occur through the addition of specific reagents to the reaction mixture, like inimers. The inimer is a particular compound containing both a polymerizable vinyl moiety and an initiator function. Most commonly, branching is obtained by copolymerization of a vinyl monomer with an adequate low amount of divinyl compound (known as crosslinker)[116,117] or polymerization of the same crosslinker via deactivation enhanced ATRP.[118–120] When no particular precaution is adopted, the use of crosslinkers leads to the formation of insoluble networks instead.[121,122] Another path to obtain polymeric gels exploits coupling between radical centers through atom transfer radical coupling of multifunctional initiators (at least trifunctional).[123–125]

3.2 Effect of the reagent ratios on gelation

Initial efforts to understand the causes of the atypical gelation examined the influence of reagent ratios (Table 3.2). The first experiments aimed to decrease the load of catalyst from 0.2 mol % to 0.1 mol % and 0.05 mol % (entries P003, P007, and P008). The reaction mixture gelled even using these lower amounts of catalyst. The lowest

Entry	EDCP [MR]	Cat[a] [MR]	AsAc [MR]	Na_2CO_3 [MR]	Conv [%]	M_n [kDa]	M_n^{th} [kDa]	$\Delta M_n\%$	$Đ$
P003	1.06	0.2	0.5	1.5	gel	—	—	—	—
P007	1.06	0.1	0.5	1.5	gel	—	—	—	—
P008	1.06	0.05	0.5	1.5	gel	—	—	—	—
P009	0.53	0.05	0.5	1.5	31	44.6	6.3	86	9.11
P010[b]	0.53	0.025	0.25	0.75	68	52.1	13.6	74	3.22
P011	1.06	0.05	0.25	1.5	51	11.1	5.2	53	1.61
P012	1.06	0.05	0.25	0.75	50	9.1	5.1	44	1.47
P013	1.06	0.05	0.5	1.0	56	26.1	5.7	78	3.39
P014	1.06	0.05	0.75	1.5	gel	—	—	—	—

Table 3.2: Effect of the reagent ratios on gelation. Conditions: $V_{St} = 3\,mL$, $V_{EtOAc} = 3\,mL$, $V_{EtOH} = 1\,mL$, $T = 60\,°C$, $t = 18\,h$. [a]Catalyst (i.e $CuCl_2$/TPMA). [b]$V_{St} = 6\,mL$.

amount (0.05 mol %) was considered adequate and was adopted as the standard for all the following experiments. A further decrease in the catalyst load will be discussed in subsection 3.14.3.

The amount of EDCP was then halved from 1.06 mol % to 0.53 mol % (entries P008 and P009, Table 3.2), bringing the TDP to ∼200. No gelation occurred by halving the quantity of EDCP. However, the very high values of $\Delta M_n\%$ and $Đ$ suggested that branching is occurring. The probable branching is also confirmed by the polimodality of the GPC trace (Figure 3.2).

In entry P009, the St:EDCP = 100:0.53 ratio was obtained by having the amount

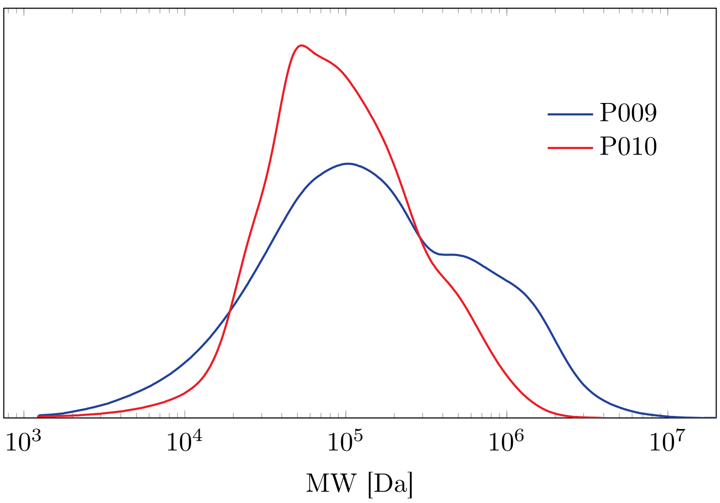

Figure 3.2: GPC analyses of ARGET ATRPs with TDP of ∼200 (entries P009 and P010 of Table 3.2).

of EDCP. Similarly in entry P010, the same ratio was obtained by doubling the amount of St. Even if the GPC trace of entry P010 is still polymodal (Figure 3.2), the control over polymerization appeared to be better. However, $\Delta M_\mathrm{n}\%$ and $Đ$ of entry P010 are still quite high. The MALLS analysis (subsection 2.2.2) confirmed that the PS from entry P010 is branched.

Entry P010 is more controlled than P009 for reasons related to the polarity of the medium. The higher amount of St of entry P010 decreases the polarity of the reaction mixture. As previously observed by our research group, [92] the lower polarity makes the reduction by AsAc and Na_2CO_3 on the Cu catalyst milder. This allows a higher concentration of Cu^{II} in solution. Following Equation 1.2, a higher concentration of Cu^{II} corresponds to a lower concentration of radicals, which improves the control by slowing down the process.

Gelation is also greatly influenced by the amount of AsAc used. In fact, gelation did not occur either in its absence, [126] or lowering its amount from 0.5 mol % to 0.25 mol % (entries P003 and P011, Table 3.2). Even halving both AsAc and Na_2CO_3 (entry P012, Table 3.2) yielded a quite controlled PS, as evidenced by the values of $\Delta M_\mathrm{n}\%$ and $Đ$, and by the GPC (Figure 3.3). As already stated, the improvement in control is likely due to a higher amount of Cu^{II} in the reaction mixture.

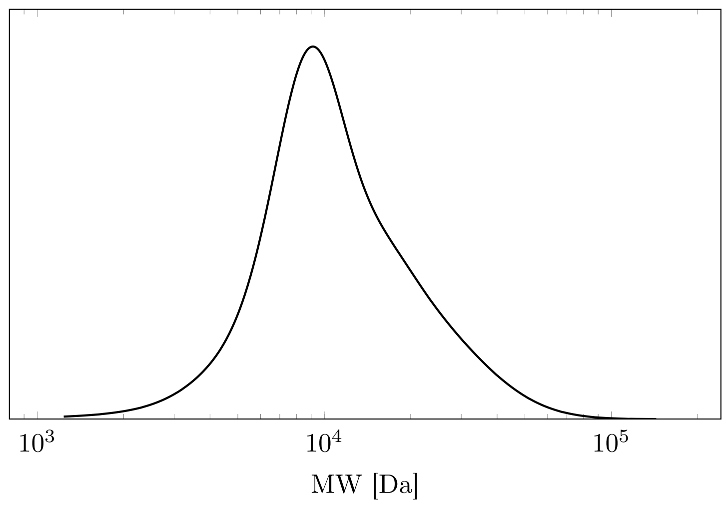

Figure 3.3: GPC analysis halving the loads of AsAc and Na_2CO_3, compared to a typical gelation reaction (entry P012 of Table 3.2).

In entry P013 (Table 3.2), the AsAc:Na_2CO_3 ratio was increased from 1:3 to 1:2 by decreasing the amount of Na_2CO_3. Even if the gelation did not occur in this case, the PS was likely branched, considering the large values of $\Delta M_\mathrm{n}\%$ and $Đ$. Contrarily, raising the amount of AsAc to 0.75 mol % gave gelation, even if the AsAc:Na_2CO_3 was 1:2 (entry P014, Table 3.2). However, the less consistency in the morphology of the obtained gel suggested that the PS was less crosslinked than the one obtained from entry P008.

3.3 Effect of the reaction medium and temperature on gelation

Entry	**EtOAc** [mL]	**EtOH** [mL]	T [°C]	t [h]	**Conv** [%]	M_n [kDa]	M_n^{th} [kDa]	$\Delta M_n\%$	$Đ$
P008	3	1	60	18	gel	—	—	—	—
P015	3.5	0.5	60	18	64	17.4	6.5	63	2.11
P016	6	2	60	18	46	34.7	4.7	86	5.80
P017	3	1	50	18	49	28.2	5.0	82	4.67
P018	3	1	70	18	gel	—	—	—	—
P019	3	1	60	4.5	41	17.5	4.2	76	2.79
P020	3	1	70	4.5	52	25.8	5.2	80	3.69

Table 3.3: Effect of the reaction medium and temperature on the gelation process. Conditions: St:EDCP:$CuCl_2$/TPMA:AsAc:Na_2CO_3 = 100:1.06:0.05:0.5:1.5, V_{St} = 3 mL.

The polymerization in a less polar environment (entry P015 compared to entry P008, Table 3.3) was more controlled, with a relatively low $Đ$. This result resembles the one already discussed after doubling the amount of St (entry P010, Table 3.2 of section 3.2). Likely, the reason for the recovered control is the same: a less polar environment corresponds to a more controlled polymerization system. The GPC traces of entries P015 (with increased EtOAc/EtOH ratio) and P010 (increased amount of St) are depicted in Figure 3.4. Surprisingly, their outlines are similar. Furthermore in section 3.15, the study of the polarity of the solvent mixture is deepened, confirming that the increase in polarity stimulates the branching phenomenon.

In addition, the dilution of the reaction mixture prevented the gelation (entry P016, Table 3.3). Reasonably, all the processes became slower. The polymodality of the GPC trace (Figure 3.5) and the high values of $\Delta M_n\%$ and $Đ$ clearly indicate that the recovered PS was probably branched.

All the observations that have been made so far in this section and in section 3.2

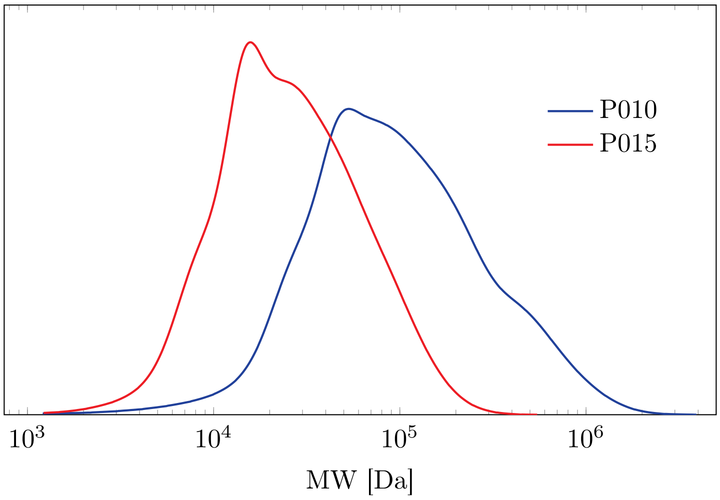

Figure 3.4: GPC analyses of ARGET ATRPs with lower polarity of the medium (entries P010 and P015 of Tables 3.2 and 3.3, respectively).

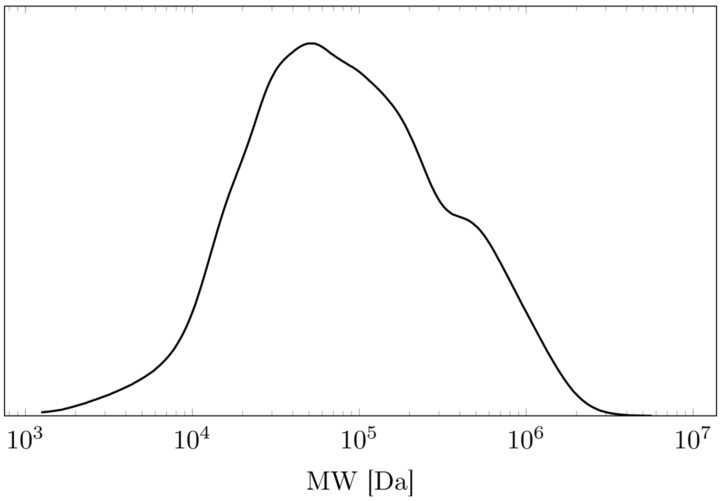

Figure 3.5: GPC analysis of a PS obtained in a more diluted ARGET ATRP system (entry P016 Table 3.3).

agree with the mechanistic frame that our research group defined for the controlled ARGET ATRP process with AsAc and Na_2CO_3 at 100 °C.[92] Generally, the reaction conditions which yield a better control over the polymerization are the ones that promote higher concentrations of Cu^{II}. The better control suppresses the branching phenomenon and, thus, the gelation of the reaction mixture.

Temperatures around 60 °C were then explored. No gelation occurred at 50 °C (entry P017, Table 3.3). However, the relatively high $\Delta M_n\%$ and $Đ$ indicate that the PS is branched and that the lower temperature maybe slowed down the process. The higher temperature of 70 °C was also explored (entry P018, Table 3.3) and the reaction mixture gelled. The obtained gel was more consistent and less sticky than the one obtained at 60 °C. Apparently, at 70 °C, the crosslinking process meets more favorable conditions. As already discussed in section 3.1 however, a further increase of the reaction temperature discourages the gelation phenomenon, rerouting the polymerization toward a more typical ATRP behavior.

An SEM image of the gel obtained from entry P018 is reported in Figure 3.6. The image shows that the material is composed of cavities with different dimensions. Curiously, in some of these cavities, single cubic crystals can be found. From the X-ray analysis (Figure 3.7), the elemental composition of the cubic crystals revealed that they are composed of NaCl. In fact, NaCl is a by-product of the catalyst reactivation by AsAc and Na_2CO_3, as showed in Scheme 1.3.

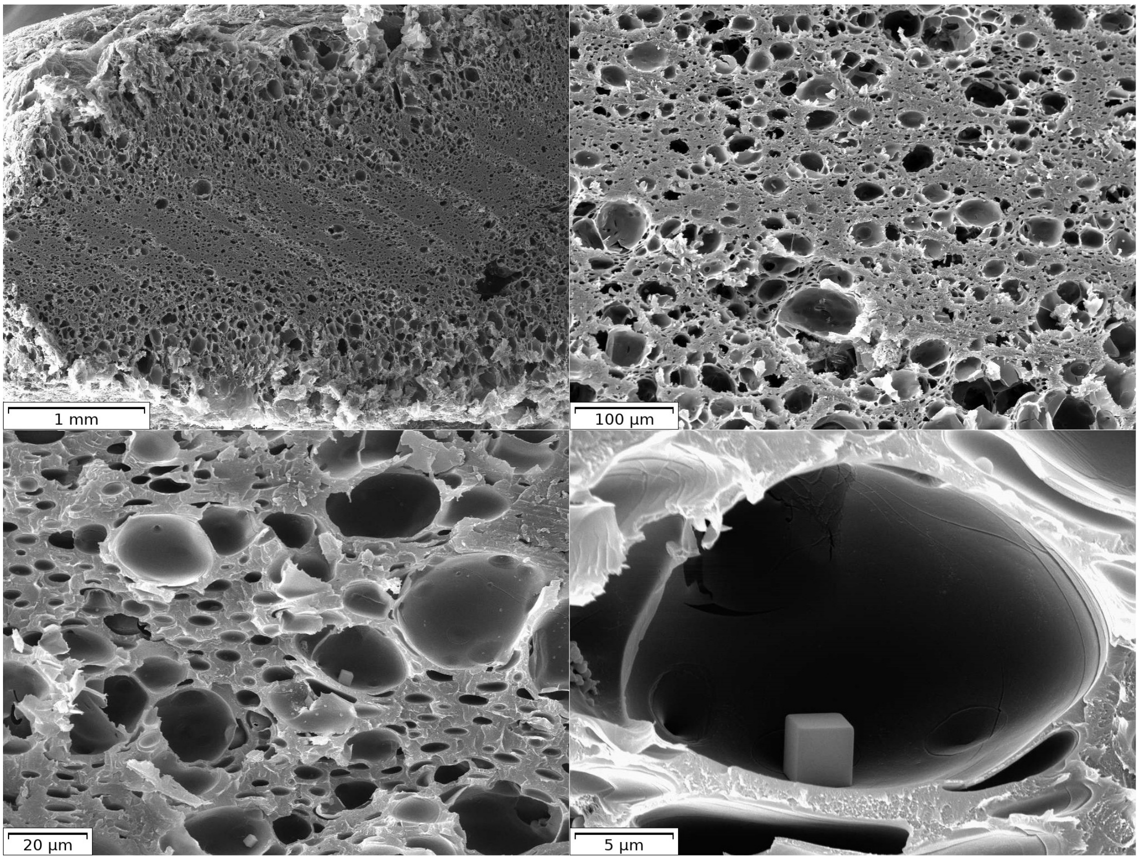

Figure 3.6: SEM image of a slice of the gel obtained in entry P018 (Table 3.3). Magnifications from top left to bottom right: 70×, 500×, 2000×, and 10 000×.

To better characterize via GPC the gels obtained at 60 °C and 70 °C (entries P008 and P018, Table 3.3), the reaction time was shortened to 4.5 h (entries P019 and P020, Table 3.3). The quite large values of $\Delta M_{\mathrm{n}}\%$ and $Đ$ suggest that the branching phenomenon even starts at the early stages of the polymerization. Moreover, the GPC analyses show polymodal traces (Figure 3.8).

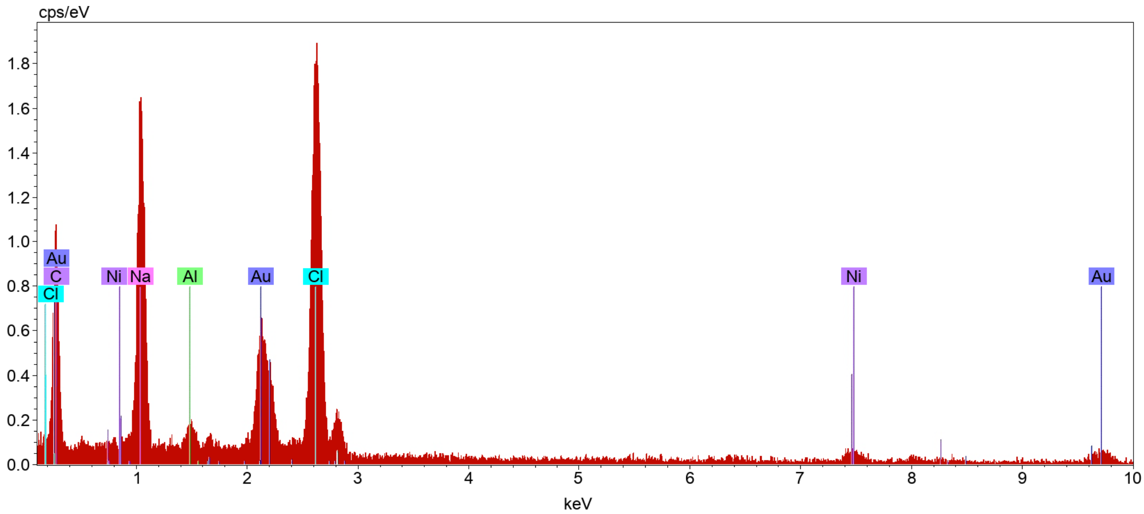

Figure 3.7: X-ray spectrum of the cubic crystals inside the cavities of the gel.

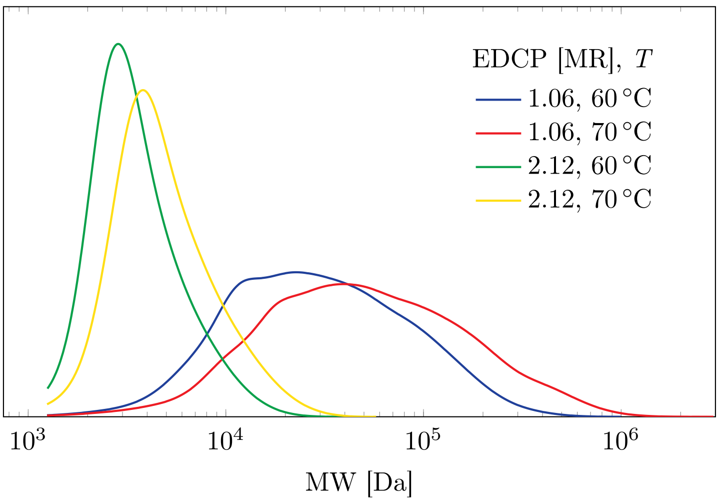

Figure 3.8: GPC analyses of reactions that go toward gelation in comparison with reactions where EDCP was doubled (entries P019 and P020 of Table 3.3, and entries P021 and P022 of Table 3.4).

3.4 Effect of the initiator concentration on gelation

Aiming for a more crosslinked material, the amount of EDCP was increased from 1.06 mol % to 2.12 mol % in the two reaction systems that previously gave gelation at 60 °C and at 70 °C (entries P008 and P018 of Table 3.3). Unexpectedly, after 4.5 h (entries P021 and P022, Table 3.4), the recovered PSs presented low $Đ$ (< 1.4) and monomodal GPC traces (Figure 3.8). Even extending the reaction time to 18 h (entry P023, Table 3.4), the polymerization at 70 °C appeared to be controlled with relatively low values of $Đ$. However, the not so low values of $\Delta M_\mathrm{n}\%$ may mean that part of the initiator was consumed by radical coupling processes.

The gelation phenomenon is discouraged by the increase of the EDCP concen-

Entry	AsAc [MR]	Na_2CO_3 [MR]	T [°C]	t [h]	Conv [%]	M_n [kDa]	M_n^{th} [kDa]	$\Delta M_n\%$	$Đ$
P021	0.5	1.5	60	4.5	31	3.1	1.7	46	1.30
P022	0.5	1.5	70	4.5	48	4.1	2.5	39	1.39
P023	0.5	1.5	70	18	75	6.8	3.8	44	1.54
P024	1.0	3.0	70	18	gel	—	—	—	—

Table 3.4: Gelation with 2.12 mol % of EDCP. Conditions: St:EDCP:$CuCl_2$/TPMA = 100:2.12:0.05, V_{St} = 3 mL, V_{EtOAc} = 3 mL, V_{EtOH} = 1 mL.

tration. This result can be explained by the consequent increase of Cu^{II}. In fact, following the ATRP equilibrium (Scheme 1.1), increasing the concentration of the initiator increases also the concentration of Cu^{II}. However, gelation was recovered when the amounts of AsAc and Na_2CO_3 were also doubled (entry P024, Table 3.4). The more reductive environment decreases the concentration of Cu^{II}, re-establishing the gelation phenomenon.

3.5 Kinetic analysis

To have a better understanding of the mechanism of the gelation process, a kinetic analysis of entry P018 (Table 3.3) was carried out. As shown in Table 3.5, the time of the reaction was kept below 6.5 h to prevent the gelation of the reaction mixture.

Entry	t [h]	Conv [%]	M_n [kDa]	M_n^{th} [kDa]	$\Delta M_n\%$	$Đ$
P025	1.0	16	3.5	1.7	50	1.35
P026	2.0	32	10.0	3.3	67	2.00
P027	3.3	41	18.3	4.2	77	2.90
P028	4.5	46	24.1	4.7	80	3.62
P029	6.5	53	32.2	5.4	83	7.47

Table 3.5: Kinetics of the gelation phenomenon. Conditions: St:EDCP:$CuCl_2$/TPMA:AsAc:Na_2CO_3 = 100:1.06:0.05:0.5:1.5, V_{St} = 3 mL, V_{EtOAc} = 3 mL, V_{EtOH} = 1 mL, T = 70 °C.

The results of the kinetics are reported in Figure 3.9. The plot of $ln\frac{[M]_0}{[M]}$ is linear until about 2 h, meaning that the $[R\cdot]$ is approximately constant within this interval. Above 2 h, the $[R\cdot]$ is decreasing, suggesting that there is an annihilation of the C−Cl functions by termination reactions. On the right of Figure 3.9, $Đ$ and M_n are instead increasing with the increasing of the conversion. It is clear that the polymerization proceeds progressively losing control. The GPCs of the isolated PSs are reported in Figure 3.10 and they show how the polymodality is increasing with reaction time. Furthermore, the MALLS analysis of the PS from entry P027 (subsection 2.2.2) revealed that the branching phenomenon was already present at 3.3 h.

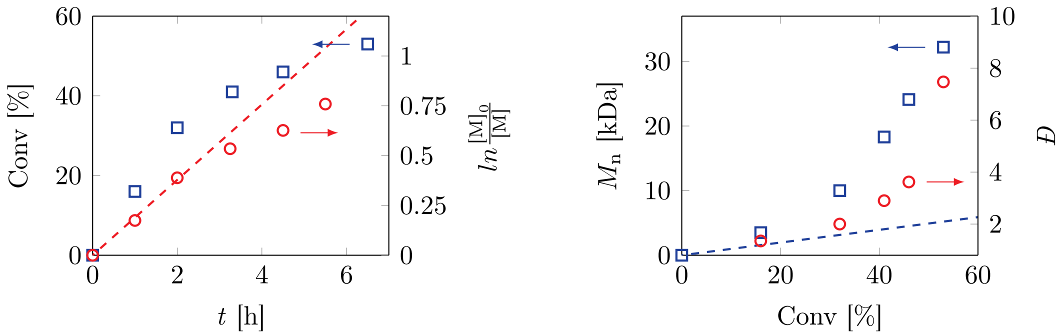

Figure 3.9: Kinetics of the gelation (entries of Table 3.5). *Left:* The red line shows the linear regression of the data in the interval 0–2 h, forcing the intercept at 0 ($R^2 = 0.998$). *Right:* The blue line shows the trend of the M_n^{th}.

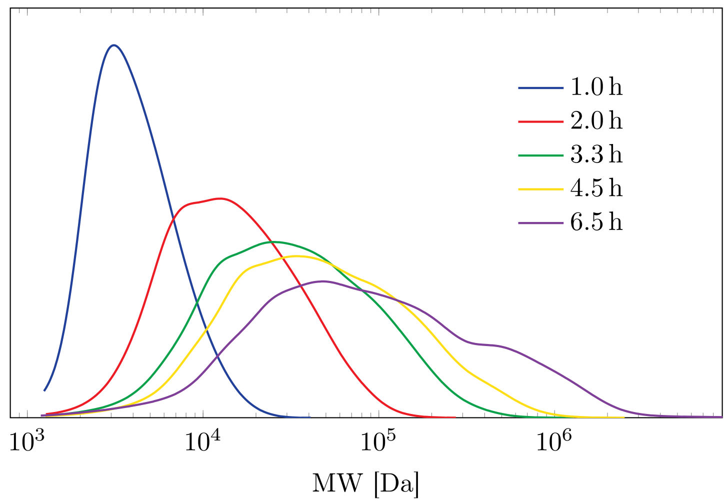

Figure 3.10: GPC analyses of the kinetics (entries of Table 3.5).

To note that the remarkable increase of M_n is not related to monomer conversion, but it is related to coupling between different PS chains. This increase is therefore associated with a drop of the polymerization rate, which is a consequence of the consumption of the C−Cl chain-end functions. This suggests that the gelation may be a consequence of the coupling phenomenon between the PS chains. The loss of the C−Cl functions was also supported by the ^{1}H NMR spectra of the isolated PS after 1 h and 6.5 h (Figure 3.11). The NMR shows a significant drop of the integral related to the C−Cl chain end (signal at 4.2–4.5 ppm).

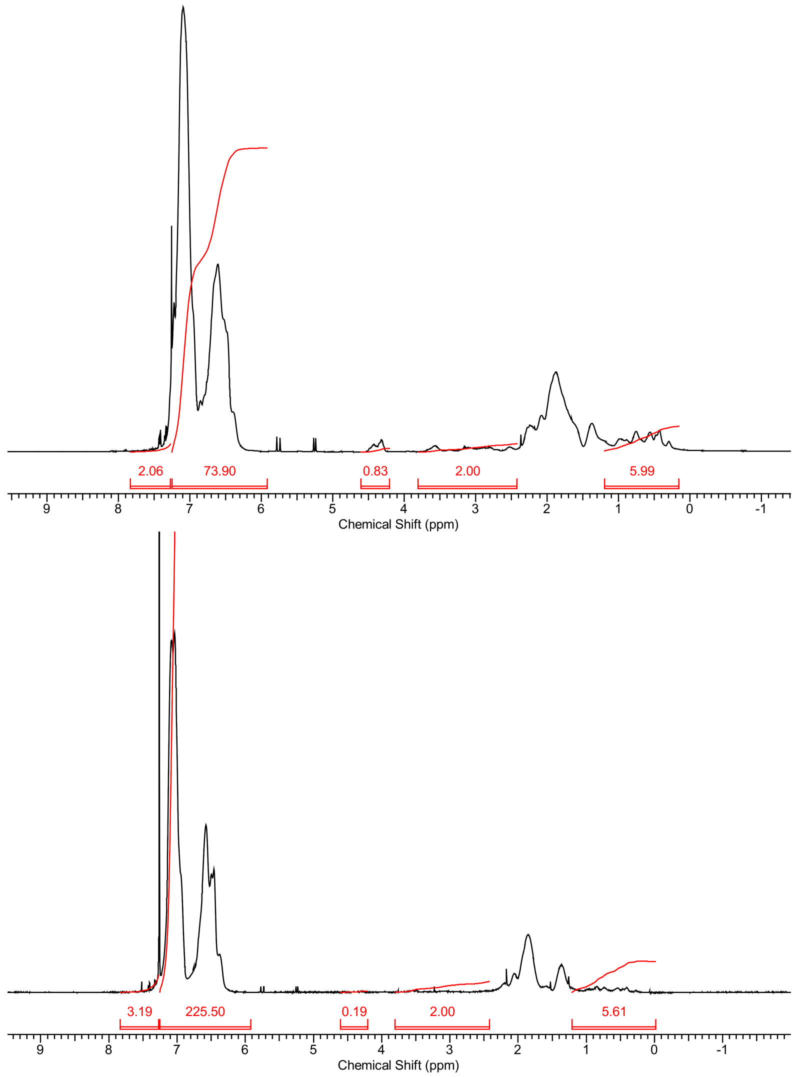

Figure 3.11: ^{1}H NMR of the kinetic analysis after 1 h (*top*) and 6.5 h (*bottom*) (entries P025 and P029 of Table 3.5, respectively).

3.6 Change of monomer

The anomalous gelation was also tested with two different monomers from St: a methacrylate (EMA) and an acrylate (EA) (Figure 3.12). Ethyl esters were chosen in order to cancel any transesterification reaction with the solvent (EtOH). The reaction conditions are the ones that led to gelation with only St (entry P008, Table 3.6).

In entry P030 (Table 3.6), St was completely substituted with EMA and no

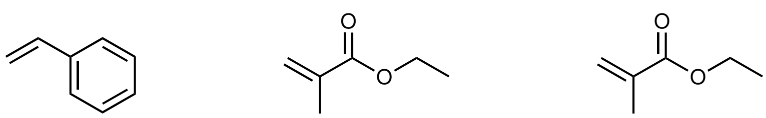

St EMA EA

Figure 3.12: Tested monomers.

Entry	**St**	**EA**	**EMA**	**Conv**	$\boldsymbol{M_n}$	$\boldsymbol{M_n^{th}}$	$\boldsymbol{\Delta M_n\%}$	$\boldsymbol{Đ}$
	[MR]	[MR]	[MR]	[%]	[kDa]	[kDa]		
P008	100	—	—	gel	—	—	—	—
P030	—	—	100	95	20.4	10.4	49	1.52
P031	90	10	—	gel	—	—	—	—
P032	50	50	—	no gel	—	—	—	—

Table 3.6: Effect of the monomer on the gelation process. Conditions: EDCP:$CuCl_2$/TPMA:AsAc:Na_2CO_3 = 1.06:0.05:0.5:1.5, V_{EtOAc} = 3 mL, V_{EtOH} = 1 mL, T = 60 °C, t = 18 h. An MR of 100 corresponds to 26.1 mmol of monomer.

gelation was observed. The recovered poly(ethyl methacrylate) (PEMA) was not branched due to the relatively low $Đ$ and the bimodal GPC trace (Figure 3.13). The $\Delta M_n\%$ value is not particularly low, but this is probably due to the high conversion and the bimodality of the GPC.

Compared to St, EMA has a higher k_p/k_t ratio and preferentially terminates by disproportionation.[127] In fact, the bimodality of the GPC is probably a consequence of the disproportionation (two populations of PEMA are present, one with two living chain ends and the other with only one). The failed gelation is consistent with the fact that radical coupling is at the base of the anomalous branching phenomenon.

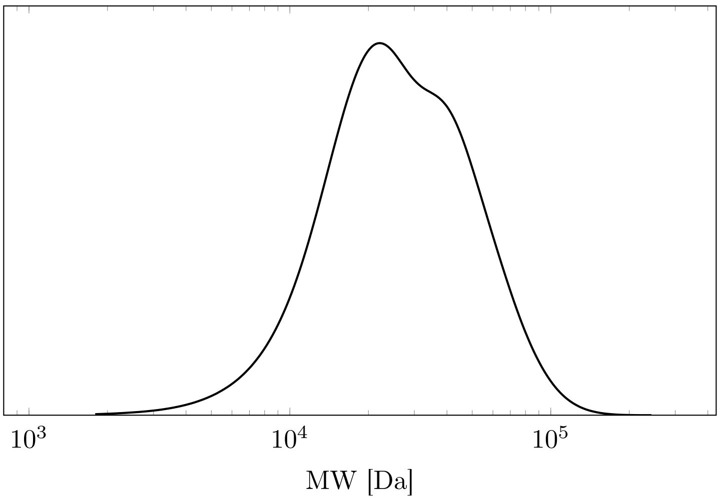

Figure 3.13: GPC analysis of PEMA (entry P030 of Table 3.6).

The ARGET ATRP with EA was instead investigated in copolymerization with St (entries P031 and P032, Table 3.6). In entry P031, the load of EA and St were 10% and 90%, respectively. In entry P032 instead, the two loads were 50%. As a result, gelation was achieved only with the higher load of St (90% of entry P031).

With a 50% load, a very viscous solution was obtained, but the copolymer was not recovered and analyzed. These results confirm the importance of St in the anomalous branching and consequent gelation.

3.7 The role of the reducing agent

To better understand the role of the reducing agent regarding the gelation, AsAc was substituted with other reducing agents, like $Sn(EH)_2$, TBC, and IPIAA (Figure 3.14).

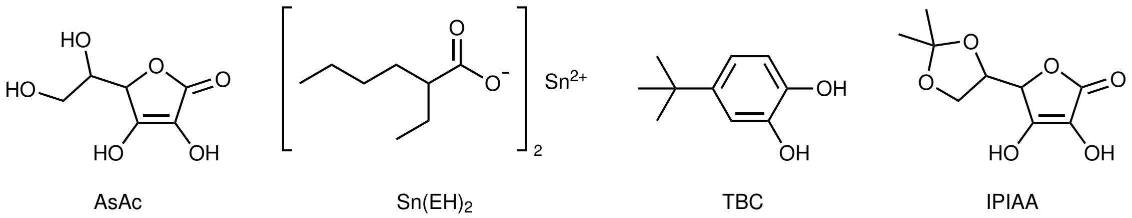

Figure 3.14: Tested reducing agents.

Entry	**RA**[a]	$\mathbf{Na_2CO_3}$ [MR]	$\boldsymbol{t}$ [h]	**Conv** [%]	$\boldsymbol{M_n}$ [kDa]	$\boldsymbol{M_n^{th}}$ [kDa]	$\boldsymbol{\Delta M_n\%}$	$\boldsymbol{Đ}$
P020	AsAc	1.5	4.5	52	25.8	5.2	80	3.69
P018	AsAc	1.5	18	gel	—	—	—	—
P033	AsAc	—	4.5	0	—	—	—	—
P034	$Sn(EH)_2$	1.5	4.5	30	5.2	3.1	40	1.65
P035	$Sn(EH)_2$	1.5	18	64	12.6	6.4	49	2.32
P036	$Sn(EH)_2$	—	4.5	0	—	—	—	—
P037	TBC	1.5	4.5	2	2.3	0.4	82	1.11
P038	TBC	1.5	18	43	6.0	4.4	27	1.43
P039	TBC	—	4.5	0	—	—	—	—
P040[b]	AsAc	1.5	18	gel	—	—	—	—

Table 3.7: Change of the reducing agent. Conditions: St:EDCP:$CuCl_2$/TPMA:RA = 100:1.06:0.05:0.5, $V_{St} = 3\,mL$, $V_{EtOAc} = 3\,mL$, $V_{EtOH} = 1\,mL$, $T = 70\,°C$. [a]Reducing agent. [b]Non-stabilized St is used.

In Table 3.7, entries P034, P035, and P036 with $Sn(EH)_2$ should be compared with entries P020, P018, and P033 with AsAc. Surprisingly, crosslinking with $Sn(EH)_2$ failed. Entry P018 with AsAc gave a gel, while the same reaction conditions with $Sn(EH)_2$ (entry P035) did not. A MALLS analysis (subsection 2.2.2) confirmed the not branched nature of the PS obtained with $Sn(EH)_2$. In addition, the GPC analysis of the two reactions with $Sn(EH)_2$ and Na_2CO_3 (entries P034 and P035) showed two monomodal curves (Figure 3.15). It seems that the role of AsAc is more complex than just a simple reducing agent.

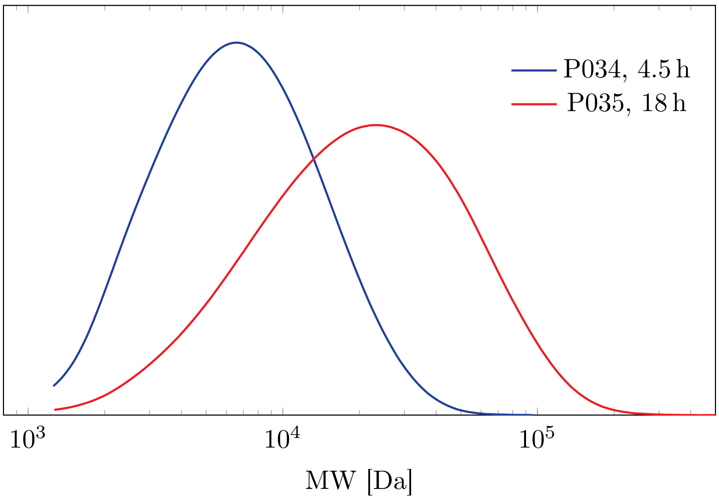

Figure 3.15: GPC analyses of ARGET ATRPs with $Sn(EH)_2$ as reducing agent (entries P034 and P035 of Table 3.7).

As observed by my research group, the ARGET ATRP system here described is not working in the absence of Na_2CO_3.[92] No polymerization was therefore observed without Na_2CO_3, both using AsAc or $Sn(EH)_2$ as reducing agent (entries P033 and P036 of Table 3.7, respectively).

Since St is not purified from TBC before every experiment (as described in subsection 2.1.1), it was thought that TBC could be involved in the branching process. In entry P040 (Table 3.7), St was passed through basic alumina to remove TBC. However, the reaction mixture gelled even in the absence of TBC. Thus, TBC is not involved in the branching process.

Furthermore, the structure of TBC has a vicinal diol like AsAc. This means that TBC could work like AsAc and could potentially regenerate the catalyst following a redox reaction. Therefore, in entries P037–P039 of Table 3.7, AsAc was substituted with TBC (compared to entries P020, P018, and P033). The gelation was not observed while using TBC as catalyst regenerator. In addition, the relative low $Đ$ values of entries P037 and P038 (4.5 h and 18 h, respectively) suggest that the branching phenomenon is not occurring. However, the yields obtained with TBC are lower than the one obtained with AsAc and $Sn(EH)_2$. In 4.5 h, AsAc reached 52% conversion, $Sn(EH)_2$ reached 30%, and TBC only reached 4% (entries P020, P034, and P037 respectively). The lower yield with TBC is probably due to its property of radical inhibitor. Finally, without Na_2CO_3, no polymerization was again observed even using TBC as reducing agent (entry P039, Table 3.7).

Afterward, IPIAA was tested as reducing agent. IPIAA has the same structure as AsAc, but the vicinal diol on the side chain has been protected as acetonide. On the contrary, the vicinal diol of AsAc bound to the ring and involved in the redox processes is kept the same. Therefore, the reactivity of IPIAA toward the regeneration of the complex is expected to be similar to AsAc. However, there is an important difference between AsAc and IPIAA. AsAc, like Na_2CO_3, is poorly soluble in the reaction mixture composed of EtOAc, EtOH, and St. On the contrary, IPIAA was found to be very soluble in systems with a modest amount of EtOH. As previously reported by our research group, a more polar reaction mixture increases the solubility of AsAc and, consequently, the regeneration of the catalyst.[92] IPIAA, being more soluble, should increase the amount of Cu^I, increasing also the polymerization rate.

Table 3.8 reports the results of two different ARGET ATRP systems, studied both with AsAc and IPIAA. The initiator is not EDCP but BC, which is another bifunctional initiator. As it will be discussed in subsection 3.11.1, the two initiators are equivalent in our ARGET ATRP system.

Entry	**RA**	**Conv** [%]	$\boldsymbol{M_\mathrm{n}}$ [kDa]	$\boldsymbol{M_\mathrm{n}^\mathrm{th}}$ [kDa]	$\boldsymbol{\Delta M_\mathrm{n}\%}$	$\boldsymbol{Đ}$
P041[a]	AsAc	46	9.5	9.5	0.1	1.23
P042[a]	IPIAA	67	23.0	13.6	41	1.66
P043[b]	AsAc	—	—	—	—	—
P044[b]	IPIAA	65	15.6	6.7	57	1.75

Table 3.8: Comparison between AsAc and IPIAA as reducing agents. [a]Conditions: St:BC:$CuCl_2$/TPMA:RA:Na_2CO_3 = 100:0.52:0.025:0.25:0.75, V_St = 6 mL, V_EtOAc = 3.5 mL, V_EtOH = 0.5 mL, T = 100 °C, t = 4 h. [b]Conditions: St:BC:$CuCl_2$/TPMA:RA:Na_2CO_3 = 100:1.04:0.05:0.5:1.5, V_St = 3 mL, V_EtOAc = 3 mL, V_EtOH = 1 mL, T = 70 °C, t = 18 h.

Entries P041 and P042 belong to a controlled ARGET ATRP which never showed the branching phenomenon.[92] Entry P041 with AsAc yielded a very controlled PS with low $Đ$ and a perfectly predicted M_n ($\Delta M_\mathrm{n}\%$ is close to zero). Entry P042 with IPIAA has not a particularly high $Đ$, but the $\Delta M_\mathrm{n}\%$ value is quite high. As can be seen from the GPC traces (Figure 3.16), a bimodality is obtained if IPIAA is used. For this reason the value of $\Delta M_\mathrm{n}\%$ is quite high. As already stated, IPIAA

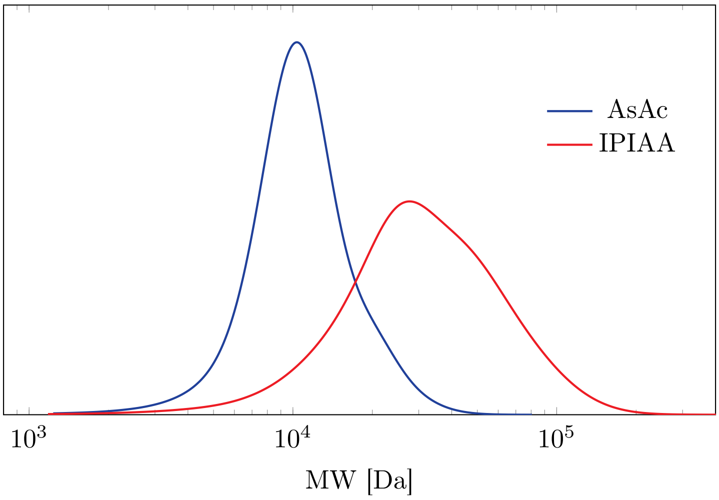

Figure 3.16: GPC analyses of ARGET ATRP with AsAc and with IPIAA (entries P041 and P042 of Table 3.8).

is more soluble and therefore more active as a reducing agent. This higher activity increases the concentration of Cu^{I} and, consequently, the concentration of radicals. More radicals increase termination reactions and, as a result, the bimodality appears. Moreover, entry P042 with IPIAA returned a 67% conversion, while entry P041 with AsAc only reached 46% conversion. As previously observed by our research group, the bimodality of these systems with AsAc usually appears above 50% conversion.[92] Anyway, the higher conversion with IPIAA is proof of its higher activity related to its higher solubility.

The reaction conditions of entries P043 and P044 of Table 3.8 are the ones that lead to gelation. Entry P043 with AsAc returned a gel, but entry P044 with IPIAA did not gel. However, even with IPIAA, the polymerization system did not show a good control: the $\Delta M_{\mathrm{n}}\%$ is quite high and the $Đ$ is not particularly low. Nevertheless, the system with IPIAA seems to be far from gelation. The poor control is a direct consequence of the long reaction time (18 h) and the higher activity of IPIAA. Also, a MALLS analysis (subsection 2.2.2) confirmed the non-branched nature of the PS with IPIAA from entry P044.

In conclusion, gelation was never observed with reducing agents different from AsAc. This probably depends on the different reducing activity on the Cu catalyst. Termination reactions were indeed proved to be important for the gelation to take place (section 3.5) and they can be highly influenced by the relative quantities of Cu^{I} and Cu^{II}. Anyhow, AsAc may have a different role from a simple reducing agent, since gelation was never observed without it. Could AsAc be included in the polymer backbone and act as a crosslinker? To answer this question, a reaction that goes toward gelation was stopped after 2 h and the recovered PS was analyzed via ^{1}H NMR (Figure 3.17). As can be seen, the typical signals of AsAc are missing, like the H bonded to the ring, whose chemical shift should be found at 4.5–5.0 ppm.[128–131] Furthermore, as it will be discussed in section 3.11, no branching was observed with a monofunctional initiator like ECiB, even if AsAc was present in the reaction mixture. This definitely excludes any involvement of AsAc in the branching phenomenon.

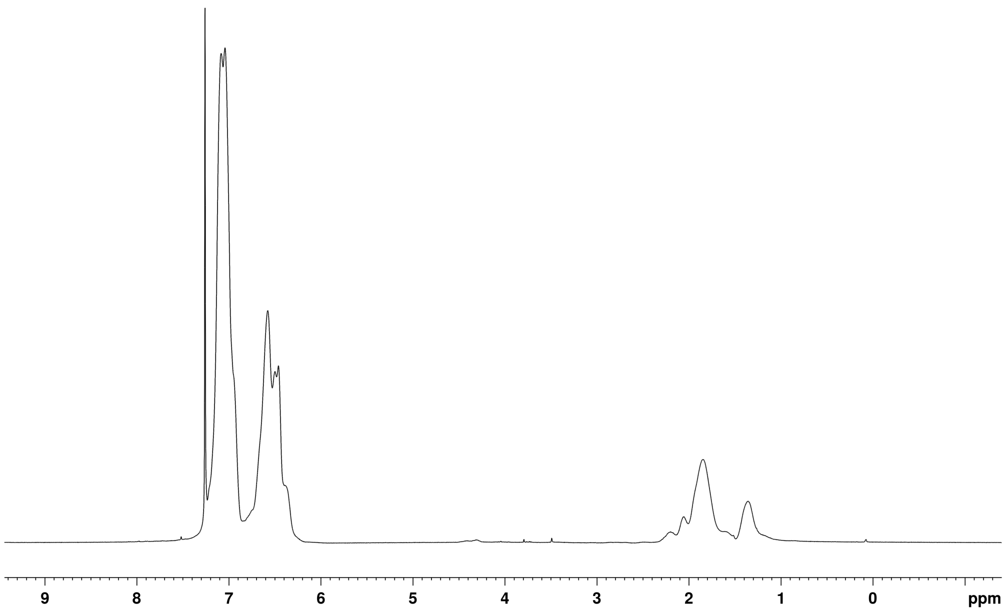

Figure 3.17: ^{1}H NMR of an ARGET ATRP system that goes toward gelation but stopped after 2 h (entry P052 of Table 3.11.

3.8 Inimer hypothesis

Gelation could be caused by the formation of an inimer. The inimer is a species that can react both as initiator and as monomer, generating a branching point with three arms. Following termination reactions, a polymer network can be formed and the result is a gel. In our system, an inimer can be formed by dehydrohalogenation of EDCP to ethyl 2-chloroactylate (ECA) (Scheme 3.1). Dehydrohalogenation is indeed stimulated by a base, and Na_2CO_3 is present in our reaction mixture.

However, two experimental pieces of evidence disproved the formation of ECA or its involvement in the branching process. The first is the ^{1}H NMR integral analysis

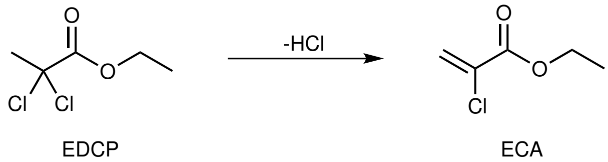

Scheme 3.1: Dehydrohalogenation of EDCP to ECA.

of the signals from EDCP. In fact, EDCP has a CH_3:CH_2 ratio of 6:2, while ECA has a ratio of 3:2. Both EDCP and ECA have the $-CH_2CH_3$ group bound to the ester O atom, but EDCP has an additional $-CH_3$. ECA has a $=CH_2$ instead, which should react and end in the polymer backbone.

To analyze the ^{1}H NMR integrals of EDCP (or ECA), St-d_8 is used to synthesize a deuterated PS. The usage of St-d_8 leads to easier discrimination between the signals from EDCP (or ECA) and the signals from the polymer backbone. Apart from the use of St-d_8, the reaction conditions are the same as entry P025 (Table 3.5). In other words, it is a reaction which is going toward gelation, but stopped after 1 h. Anyhow, all the initiator should be depleted within 1 h. The resulting ^{1}H NMR analysis is reported in Figure 3.18 and shows a CH_3:CH_2 ratio of 6:2. This result confirms the presence of EDCP in the PS and disproves the formation of the inimer ECA.

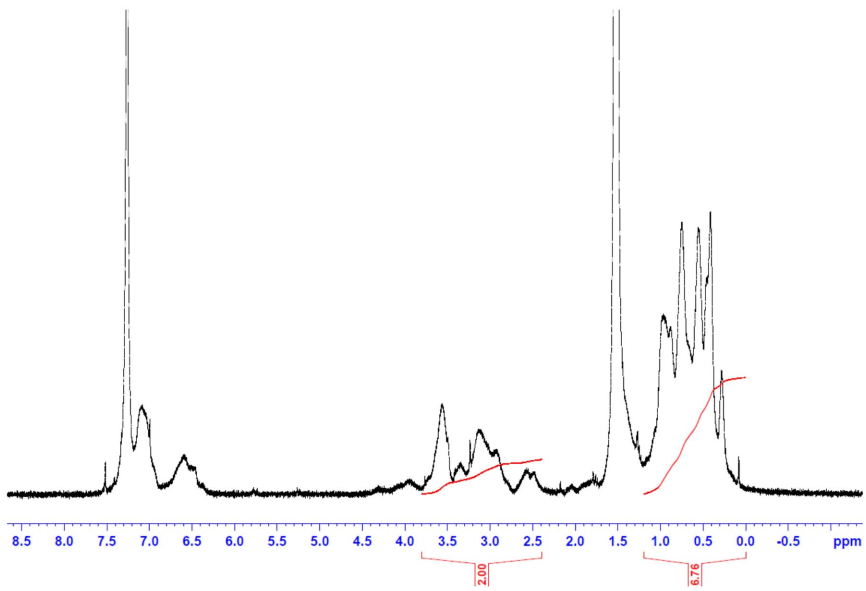

Figure 3.18: ^{1}H NMR of a gelation reaction with St-d_8 stopped after 1 h.

The second experimental evidence to confirm the non-formation of ECA is the intentional addition of an inimer. MCA (a commercial inimer, analogous to ECA) was deliberately added in variable amounts to an ARGET ATRP system with only Na_2CO_3 as catalyst regenerator. With only Na_2CO_3, any form of branching has never been observed.[126] The experiments are summarized in Table 3.9. MCA was added in 25 mol % and 50 mol % compared to EDCP (entries P046 and P047, respectively). As can be seen from the results, the control was not affected by the addition of MCA.

Furthermore, as it will be discussed in section 3.11, gelation was also observed with initiators unable to dehydrohalogenate to inimers, like BC. This is a third proof against the inimer hypothesis. At this point, the inimer hypothesis should be considered completely disproved.

Entry	**MCA** [MR]	**Conv** [%]	$\boldsymbol{M}_\mathbf{n}$ [kDa]	$\boldsymbol{M}_\mathbf{n}^\mathbf{th}$ [kDa]	$\boldsymbol{Đ}$
P045	—	48	6.5	4.9	1.33
P046	0.265	43	6.0	—	1.34
P047	0.53	44	5.5	—	1.36

Table 3.9: ARGET ATRP in the presence of MCA. Conditions: St:EDCP:$CuCl_2$/TPMA:Na_2CO_3 = 100:1.06:0.05:1.5, $V_{\mathrm{St}} = 3\,\mathrm{mL}$, $V_{\mathrm{EtOAc}} = 3\,\mathrm{mL}$, $V_{\mathrm{EtOH}} = 1\,\mathrm{mL}$, $T = 60\,°\mathrm{C}$, $t = 18\,\mathrm{h}$.

3.9 Unsaturation of PS chain ends hypothesis

In section 3.8, the dehydrohalogenation of the EDCP has been proved to be a false hypothesis. However, dehydrohalogenation could take place in the PS chain ends, forming a double bond which could generate branching points.

Sarbu et al. studied the ATRP reaction of α,ω-dibromopolystyrene (DBPS) in a monomer-free system.[132] Without monomer, they observed a step-growth polymerization due to radical coupling. Interestingly, they also obtained hyperbranched materials, like in our case. They suggested that the branching phenomenon was probably due to the formation of unsaturated chain ends through dehydrohalogenation reactions (Scheme 3.2). The resulting PSs with unsaturated chain ends are macroinimers and, therefore, they are possible branching points. Since the Cu^{II}-catalyzed elimination can be virtually excluded in ARGET ATRP systems,[133,134] they suggested the intervention of the N-based ligand.[132]

In our ARGET ATRP system, the explanation of Sarbu et al. is unsatisfactory for several reasons.

(i) Dehydrohalogenation should be boosted by increasing the reaction temperature.[135] However, as discussed in section 3.1, the opposite was observed. As a

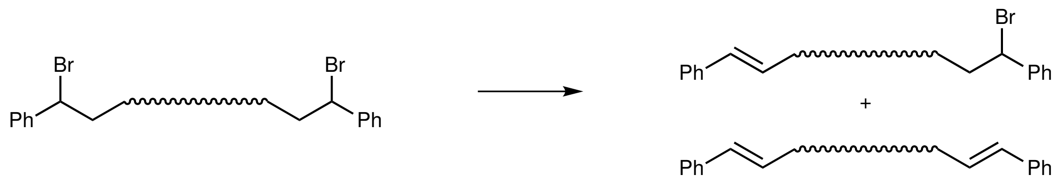

Scheme 3.2: Single and double dehydrohalogenation of DBPS from reference [132].

matter of fact, we observed the disappearance of the gelation phenomenon at higher temperatures.

(ii) Dehydrohalogenation is also influenced by the bond-dissociation energy (BDE) and, therefore, by the involved halogen atom.[135] Sarbu et al. were working with Br, while we are working with Cl. The phenomenon observed by Sarbu et al. should be less effective in our case due to the higher BDE of Cl (compared to Br). Furthermore, the dehydrohalogenation should be further discouraged in the case of deuterated PS. In fact, due to the kinetic isotope effect, the rate of a reaction involving a C−D bond is 6–10 times slower than the corresponding C−H bond.[136] As already discussed in section 3.8, normal St and St-d_8 yielded the same gel in specific reaction conditions.

(iii) As shown in Scheme 3.2, the dehydrohalogenation would yield a β-substituted double bond. This newly generated double bond is sterically hindered and thus less reactive than the vinyl moiety of the St monomer.[137] As reported in section 3.5, the unreacted St was still ~50% when the reaction mixture was close to gel and branching was already present. It is therefore unlikely that any double bond generated from dehydrohalogenation could give radical addition with consequent branching.

(iv) The ^{1}H NMR spectra of the kinetic analysis after 1 h and 6.5 h (Figure 3.11) did not show the typical signals at 6.05 ppm and 6.05 ppm of unsaturated chain ends.[138]

(v) A dehydrohalogenation experiment of linear α,ω-dichloropolystyrene (DCPS) was also carried out. DCPS was synthesized via an ARGET ATRP system with only Na_2CO_3 as reducing agent.[126] Reaction reagents and conditions were St:EDCP:$CuCl_2$/TPMA:Na_2CO_3 = 100:1.06:0.1:0.5, with $V_{\mathrm{St}} = 9\,\mathrm{mL}$, $V_{\mathrm{EtOAc}} = 9\,\mathrm{mL}$, $V_{\mathrm{EtOH}} = 3\,\mathrm{mL}$, $T = 100\,°\mathrm{C}$, and $t = 4.5\,\mathrm{h}$. The resulting conversion was 47%, with $M_{\mathrm{n}} = 5.0\,\mathrm{kDa}$, $M_{\mathrm{n}}^{\mathrm{th}} = 4.8\,\mathrm{kDa}$, $\Delta M_{\mathrm{n}}\% = 6$, and $Đ = 1.19$. The ^{1}H NMR is depicted in Figure 3.19.

The synthesized DCPS was used in a gelation reaction with the same conditions

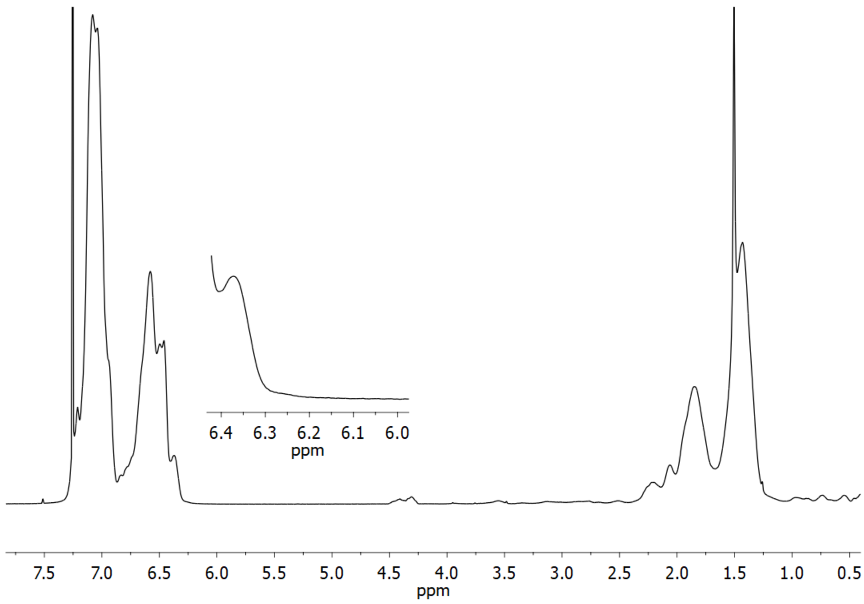

Figure 3.19: ^{1}H NMR of the DCPS used in the dehydrohalogenation experiment.

of entry P028 of Table 3.5. The only differences were that St was replaced with Tol and $CuCl_2$/TPMA was not added. The ^{1}H NMR of Figure 3.20 shows that dehydrohalogenation did not occur in the resulting PS. The experiment was repeated even with the addition of TPMA in the same quantity as entry P028. Even in this case, the dehydrohalogenation was not observed (Figure 3.21).

With all this evidence, it can be stated that the dehydrohalogenation of the PS chain ends is not occurring and that is not involved in the branching phenomenon.

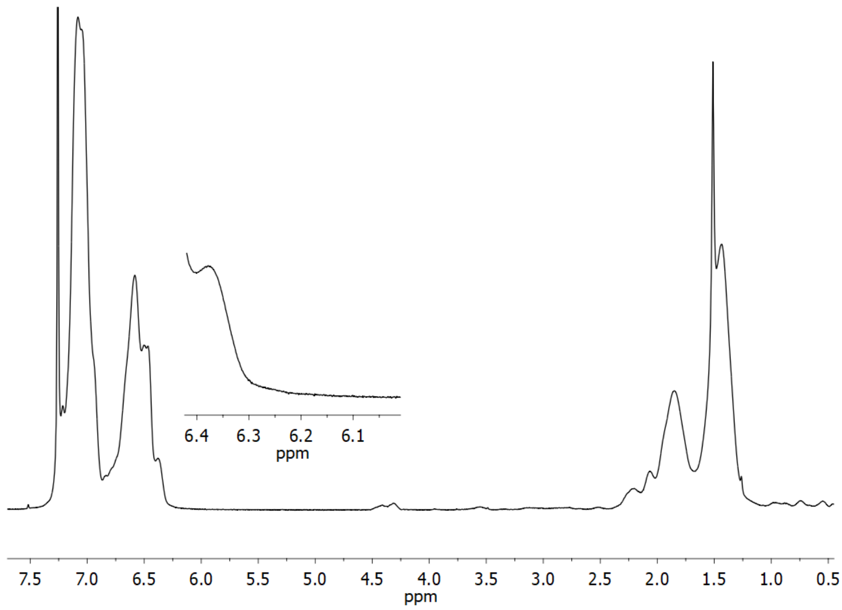

Figure 3.20: ^{1}H NMR of the DCPS after the dehydrohalogenation experiment.

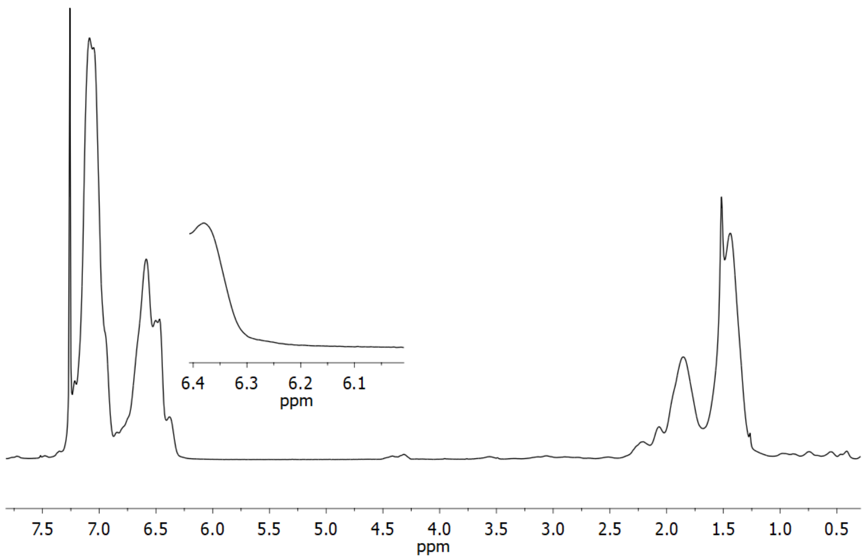

Figure 3.21: ^{1}H NMR of the DCPS after the dehydrohalogenation experiment in the presence of TPMA.

3.10 Chain transfer hypothesis

A radical chain transfer process may be the cause of branching. A radical can be formed along the polymer backbone chain and it can react with a radical chain end, generating a branching point (Scheme 3.3). Following termination reactions, a gel may be formed.

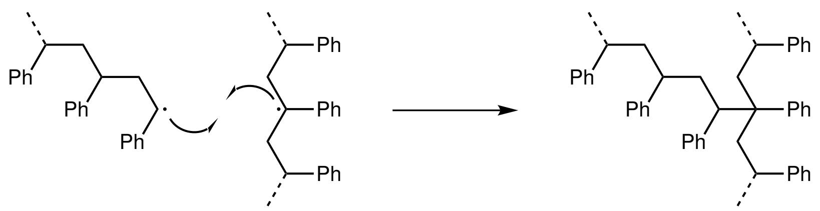

Scheme 3.3: Chain transfer to PS.

The radical along the polymer backbone can be formed as a result of the homolytic cleavage of a C−H bond. To prove or disprove the chain transfer hypothesis, a reaction leading to gelation (entry P008 of Table 3.2, section 3.2) was repeated with St-d_8. As already stated in section 3.9, the reaction rate of a C−D bond is 6–10 times slower (compared to the corresponding C−H bond).[136] Therefore, using St-d_8 should slow down the branching process if it comes from chain transfer processes. However, gelation was observed even with St-d_8. Clearly, gelation cannot be attributed to radical chain transfer processes.

This result also rules out the intervention of intrachain migrations of the apical radical center and relative β-scission[139,140] as the cause of gelation, confirming that St has difficulty to branch in the absence of a crosslinking agent.[141]

3.11 The importance of a bifunctional initiator

The role of the initiator on the branching phenomenon was then investigated. The aim is to better understand the role of EDCP and if the bifunctionality is a fundamental prerequisite for gelation. In addition to EDCP, the initiators of Figure 3.22 were also tested in reaction conditions which usually lead to gelation.

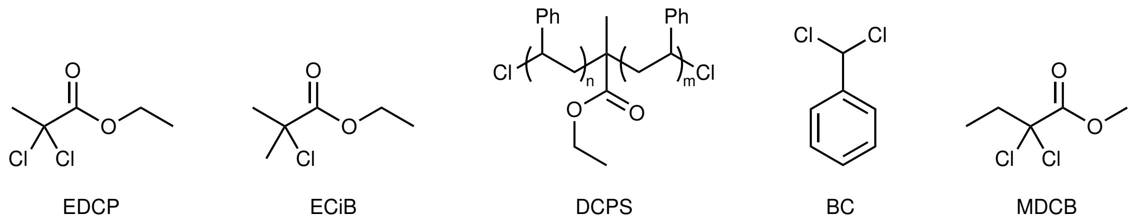

Figure 3.22: Tested initiators.

Entry	Ini[a] (MR)	Cat[b]	T [°C]	Conv [%]	M_n [kDa]	M_n^{th} [kDa]	$\Delta M_n\%$	$Đ$
P018	EDCP (1.06)	0.05	70	gel	—	—	—	—
P048	ECiB (1.04)	0.05	70	33	7.9	3.5	55	2.25
P049	ECiB (2.08)	0.05	70	63	7.9	3.3	58	2.38
P043	BC (1.04)	0.05	70	gel	—	—	—	—
P003	EDCP (1.06)	0.2	60	gel	—	—	—	—
P050	MDCB (1.09)	0.2	60	58	36.9	5.7	85	5.64
P051	DCPS[c] (1.11)	0.05	70	87	46.4	13.9	70	4.56

Table 3.10: Effect of the initiator on the gelation process. Conditions: St:AsAc:Na_2CO_3 = 100:0.5:1.5, $V_{St} = 3\,mL$, $V_{EtOAc} = 3\,mL$, $V_{EtOH} = 1\,mL$, $T = 70\,°C$, $t = 18\,h$. [a]Initiator. [b]$CuCl_2$/TPMA. [c]DCPS with $M_n = 5.3\,kDa$ and $Đ = 1.34$ prepared with a controlled ARGET ATRP, conditions: St:EDCP:$CuCl_2$/TPMA:AsAc:Na_2CO_3 = 100:0.53:0.025:0.25:0.75, $V_{St} = 6\,mL$, $V_{EtOAc} = 3.5\,mL$, $V_{EtOH} = 0.5\,mL$, $T = 100\,°C$, $t = 2\,h$.

As reported in Table 3.10, ECiB was used in two experiments (entries P049 and P048), which should be compared to the one with EDCP that gelled (entry P018). ECiB is the isosteric analogous of EDCP, but monofunctional. ECiB was added to the reaction mixture in two amounts, one isomolar to EDCP (entry P048) and one isoequivalent to EDCP (entry P049). In both cases, no gelation was observed. Even if the $\Delta M_n\%$ and the $Đ$ are not particularly low, the GPC traces are monomodal (Figure 3.23). The MALLS analysis (subsection 2.2.2) confirmed that the PS obtained from entry P048 was not branched.

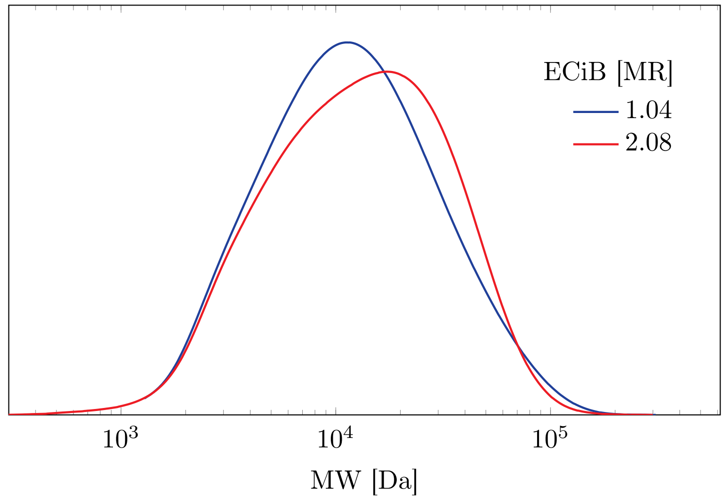

Figure 3.23: GPC analyses of ARGET ATRPs with ECiB as initiator (entries P048 and P049 of Table 3.10).

The results with ECiB tells us an important thing. The branching phenomenon is not originating from any crosslinking agent generated by any side reaction between St, Cu complexes, AsAc, or Na_2CO_3. If not, gelling should have been observed also in this case where only the initiator was changed. It seems that EDCP is the protagonist of the branching phenomenon. However, branching was also observed with other initiators. EDCP was substituted with BC (entry P043, Table 3.10) and the system gelled. Even MDCB of entry P050 (Table 3.10) yielded a branched PS with a high $Đ$. Entry P050 with MDCB should be compared to entry P003 (Table 3.10) with EDCP, which gelled.

From the results of Table 3.10, it is clear that bifunctionality is a prerequisite for gelation. The PSs obtained from the monofunctional ECiB resulted to be linear. On the contrary, the PSs obtained from bifunctional initiators (EDCP, BC, and MDCB) were branched and some of them even gelled. However, all the bifunctional initiators were geminal (i.e. with the two Cl atoms bonded to the same C atom). To verify if the bifunctional initiator has to be geminal in order to have gelation, a linear DCPS was synthesized and used as macroinitiator in entry P051 of Table 3.10. The final high $Đ$ of entry P051 tells us that branching is occurring even without a geminal initiator. In addition, the GPC of the DCPS used as macroinitiator and the resulting PS after the reaction are reported in Figure 3.24. The GPC trace went from monomodal for the DCPS to polymodal after reaction P051. The MALLS analysis (subsection 2.2.2) confirmed the branched nature of the PS obtained from entry P051.

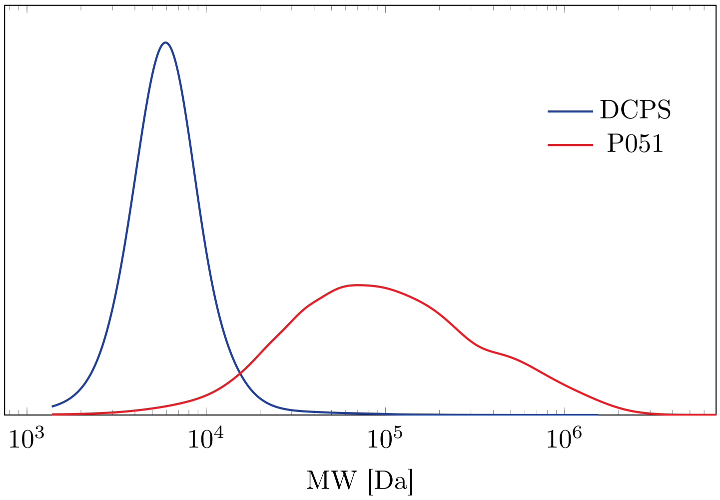

Figure 3.24: GPC analyses of the DCPS before and after its usage as macroinitiator (entry P051 of Table 3.10).

As discussed in section 3.8, the inimer hypothesis for the branching phenomenon was disproved and the dehydrohalogenation of EDCP with the formation of ECA is not occurring. ECA is an inimer and could form a branching point in the polymer backbone. The fact that branching and gelation took place even with BC and MDCB (entries P043 and P050 respectively) is another proof that dehydrohalogenation of the initiator is not at the origin of the branching phenomenon. In fact, BC cannot give dehydrohalogenation for the lack of β-H atoms. Differently, MDCB could give dehydrohalogenation, but the resulting alkene would be sterically hindered and, consequently, less reactive than the vinyl moiety of St.[137] Therefore, the dehydrohalogenation product of MDCB probably cannot be considered an inimer.

3.11.1 Change of initiator

As reported in Table 3.10, BC as initiator gave the same result ad EDCP in the same reaction conditions (entries P043 and P018 of Table 3.10). As a consequence, the idea of replacing EDCP with BC for future experiments was considered. BC has the advantages to be the homolog of St, less expensive, and more commercially available.

Eight experiments were thus performed to compare the obtained PSs with both EDCP and BC. The experiments and their results are reported in Table 3.11, where each pair of lines denotes the same reaction conditions. Obviously, the only difference in each pair is the used initiator (EDCP or BC). The small difference in the MRs between EDCP and BC depends on experimental laboratory necessities, but it should not be particularly significant.

Entry	**Ini (MR)**	t [h]	**Conv** [%]	M_n [kDa]	M_n^{th} [kDa]	$\Delta M_n\%$	$Đ$
P026[a]	EDCP (1.06)	2	32	10.0	3.3	67	2.00
P052[a]	BC (1.04)	2	33	14.5	3.5	76	2.52
P053[b]	EDCP (0.53)	4	53	11.8	10.5	11	1.31
P041[b]	BC (0.52)	4	46	9.5	9.5	0.1	1.23
P054[c]	EDCP (0.53)	1	20	4.3	4.2	2.1	1.27
P055[c]	BC (0.52)	1	23	4.9	4.9	0.2	1.27
P056[c]	EDCP (0.53)	4	47	9.7	9.5	2.2	1.27
P057[c]	BC (0.52)	4	43	9.5	8.9	7.2	1.25

Table 3.11: Comparison between EDCP and BC as initiators. [a]Conditions: St:$CuCl_2$/TPMA:AsAc:Na_2CO_3 = 100:0.05:0.5:1.5, V_{St} = 3 mL, V_{EtOAc} = 3 mL, V_{EtOH} = 1 mL, T = 70 °C. [b]Conditions: St:$CuCl_2$/TPMA:AsAc:Na_2CO_3 = 100:0.025:0.25:0.75, V_{St} = 6 mL, V_{EtOAc} = 3.5 mL, V_{EtOH} = 0.5 mL, T = 100 °C. [c]Conditions: St:$CuCl_2$/TPMA:Na_2CO_3 = 100:0.05:0.25, V_{St} = 6 mL, V_{EtOAc} = 3 mL, V_{EtOH} = 1 mL, T = 100 °C.

The first pair of reactions (P026 and P052 of Table 3.11) are performed under conditions that gave gelation, but shortened to 2 h. As expected, both these reactions resulted in an uncontrolled polymerization. However, a small gap is present between the values of $\Delta M_n\%$ and $Đ$, even if the yields are very close to each other. GPC traces also appear slightly different (Figure 3.25a), but they are both polymodal. However, the results of these two reactions are not very different if it is taken into account the uncontrolled nature of the reaction conditions. Indeed, the important result is that they both give rise to the branching phenomenon.

Entries P053 and P041 of Table 3.11 were performed in reaction conditions that never showed any signs of branching.[92] Unfortunately, the results show a greater $\Delta M_n\%$ and $Đ$ when EDCP is used. The reason for the higher values of $\Delta M_n\%$ and $Đ$ can be found in the GPC analyses (Figure 3.25b). In fact, when EDCP is used, a bimodality is reached, and the bimodality is much less present with BC.

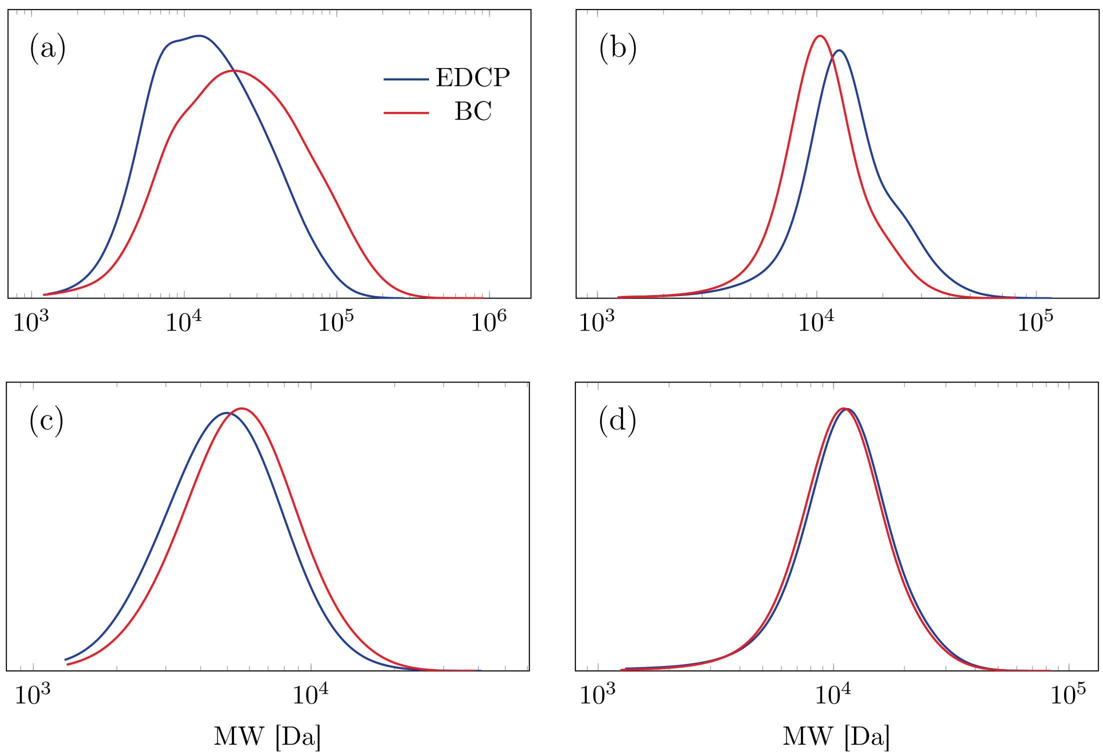

Figure 3.25: GPC analyses of the comparison between EDCP and BC as initiators (entries P026 and P052 (a), P053 and P041 (b), P054 and P055 (c), P056 and P057 (d) of Table 3.11).

However, the more pronounced bimodality with EDCP is a direct consequence of the higher yield. In fact, the system with EDCP had a 53% conversion, while BC only had 46%. As already observed by our research group, the bimodality arises just at ∼50% conversion.[92] Thus, all the differences between reactions P053 and P041 are consequences of the different yields. If the two reactions had returned the same conversion, their final results probably would have matched. Then why entry P053 with EDCP returned a higher conversion? There are two possible explanations. The first is that BC could give a slightly slower initiation than EDCP. The other one is that this result lies within the experimental error. In fact, experimentally, the two reactions were not performed consecutively, but a certain amount of time passed between the two. The second explanation is more likely since BC returned higher yields than EDCP only in half of the reactions of Table 3.11.

A third type of polymerization was then used to evaluate the differences between EDCP and BC as initiators. In entries P054–P057 of Table 3.11, a controlled ARGET ATRP with only Na_2CO_3 as catalyst regenerator was used.[126] Two reactions (entries P054 and P055) were stopped after 1 h and the other two (entries P056 and P057) after 4 h. As can be observed from the GPC analyses (Figures 3.25c and 3.25d), EDCP and BC yielded the same PS with the same characteristics. There are small differences in the conversion and in the ΔM_n%, but the values of the $Đ$ match.

Overall, no particular differences can be reported by using EDPC or BC. The only significant difference can be found in the system that undergoes gelation (entries P026 and P052), but the result is expected since this ATRP system is not controlled. Therefore, BC is used from now on for the following experiments instead of EDCP. It is also possible to compare together reactions with BC and with EDCP.

3.12 Polycatenane hypothesis

As reported so far by the experimental results, the gelation starts with a controlled ATRP, which is soon joined by step-growth polymerization. This leads to a decrease of the number of growing chains and free radicals in the reaction mixture, making more probable the intramolecular coupling between the C−Cl end functions.[142] This should produce macrocycles, which are interpenetrated and form a network (Figure 3.26). The generated network clearly lacks crosslinking points and it is supported only by mechanical bonds instead of chemical bonds. This type of polymer architecture is named polycatenane.[143] Reasonably, polycatenanes have a morphology very similar to a gel.

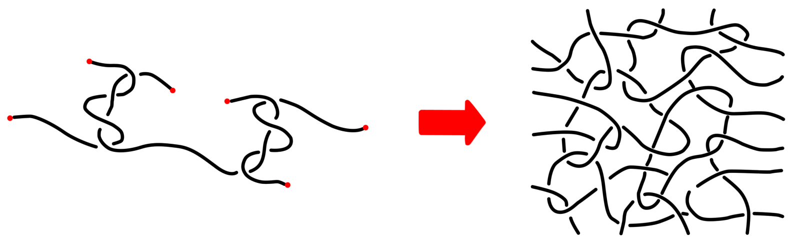

Figure 3.26: Formation of a polycatenane from bifunctional polymer chains.

The formation of a polycatenane network starting from bifunctional polymer chains is certainly an unusual phenomenon, but it was reported before. Rigby and Mark obtained an insoluble product while studying the chain extension of dihydroxy-terminated polydimethylsiloxane with dimethyldiethoxysilane. The insoluble product was rationalized as a polycatenane.[144] Recently, concatenated polysiloxane rings from heterotelechelic oligomers were prepared and actively studied.[145,146] A similar network of macrocycles was also prepared by thermal polymerization of 1,2-dithiane.[147] Interestingly, Vollmert and Huang hypothesized the formation of entangled rings during the polymerization of St, with the final generation of microgels.[148] Furthermore, various studies stressed that in the course of irreversible polycondensations, to which our system is strictly analogous, end-to-end cyclization competes with chain-growth at any stage and at any monomer concentration.[149]

So far, the polycatenane hypothesis was never disproved and it seems to be the most reasonable explanation of the anomalous gelation.

3.13 Gelation of linear telechelic PS in the absence of monomer

The kinetic analysis (section 3.5) revealed that termination reactions are involved in the anomalous branching and, as formulated in section 3.12, they are fundamental to the formation of a polycatenane network. To better understand the role of termination reactions, they were promoted between linear DCPS chains in reaction systems without St monomer and without any other initiator. In this way, the DCPS chains are forced to react inter- and intra-molecularly.

3.13.1 Linear telechelic PS synthesis

The synthesis of the DCPSs is described in Table 3.12 and it is performed via the ARGET ATRP with only Na_2CO_3 as reducing system, which never showed the branching phenomenon.[126] DCPSs with M_n in the range 2.3–10.5 kDa were prepared. For entries P055 and P059–P063, the targeted M_n was ~5 kDa and the reaction time was 60 min, except for reaction P063 which took 120 min to reach the same M_n. P063 was scaled up 4 times and thus required a different reaction time to reach the same result. In fact, all the GPC traces of entries P055 and P059–P063 are very similar to each other (Figure 3.27). Only entry P060 returned a DCPS with a smaller M_n, but the results obtained from it as macroinitiator were in agreement with the others (subsection 3.13.3). Therefore, the DCPS from entry P060 was used anyway, even if its M_n is slightly smaller than the others.

Entry	t [min]	**Conv** [%]	M_n [kDa]	M_n^{th} [kDa]	$\Delta M_n\%$	$Đ$
P058	20	6	2.3	1.4	38	1.14
P055	60	23	4.9	4.9	0.2	1.27
P059	60	25	5.2	5.2	−0.9	1.27
P060	60	19	3.8	3.9	−0.7	1.21
P061	60	25	4.8	5.1	−5	1.33
P062	60	24	4.6	4.9	−7	1.31
P063[a]	120	22	5.2	4.6	11	1.21
P064	240	48	10.5	9.7	8	1.25

Table 3.12: Synthesis of linear DCPSs. Conditions: St:BC:$CuCl_2$/TPMA:Na_2CO_3 = 100:0.52:0.05:0.25, $V_{St} = 6\,mL$, $V_{EtOAc} = 3\,mL$, $V_{EtOH} = 1\,mL$, $T = 100\,°C$. [a]Reaction scaled up 4 times.

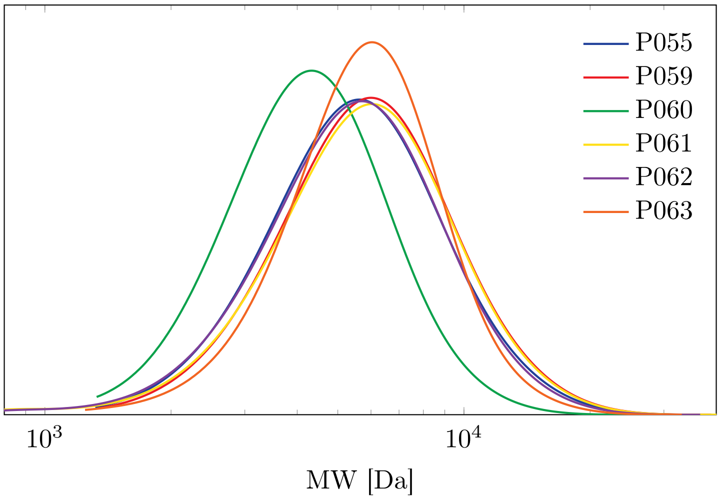

Figure 3.27: GPC analyses of the linear DCPSs (entries P055 and P059–P063 of Table 3.12).

3.13.2 Gelation of linear telechelic PS

The results of first set of the forced termination reactions are reported in Table 3.13. The M_n^i indicates the initial molar mass of the DCPS, while the M_n^f indicates the final molar mass. The same thing is applied to initial $Đ^i$ and final $Đ^f$. St is substituted with the same volume of Tol to ensure the same properties of the solvent mixture.

Entries P065–P067 of Table 3.13 were conducted under conditions that lead to gelation, but with DCPS as macroinitiators and without St monomer. The only difference between these 3 reactions were the M_n^i of the starting DCPS: ~2.5, ~5, and ~10 kDa. Interestingly, gelation of the reaction mixture was observed only with a DCPS with ~5 kDa (entry P066). However, the obtained gel was deformable and sticky. Also P065 and P067 yielded branched polymers due to their high $Đ$ values

Entry	**DCPS**[a]	**AsAc** [MR]	$\boldsymbol{T}$ [°C]	$\boldsymbol{M_n^i}$ [kDa]	$\boldsymbol{Đ^i}$	$\boldsymbol{M_n^f}$ [kDa]	$\boldsymbol{Đ^f}$
P065	P058	0.5	70	2.3	1.14	16.3	7.74
P066	P059	0.5	70	5.2	1.27	gel	—
P067	P064	0.5	70	10.5	1.25	40.3	5.69
P068	P063	0.5	100	5.2	1.21	25.9	4.38
P069	P063	—	70	5.2	1.21	6.7	1.48

Table 3.13: Gelation of DCPS in the absence of St. Conditions: DCPS:$CuCl_2$/TPMA:Na_2CO_3 = 1.04:0.05:1.5[b], $V_{\mathrm{Tol}} = 3\,\mathrm{mL}$, $V_{\mathrm{EtOAc}} = 3\,\mathrm{mL}$, $V_{\mathrm{EtOH}} = 1\,\mathrm{mL}$, $t = 18\,\mathrm{h}$. [a]The origin of the DCPSs, which are synthesized in Table 3.12. [b]For convenience, MRs are referred to 3 mL of St (which has MR = 100), even if St is not present.

and their MALLS results (subsection 2.2.2). Hence, branching was observed for all these three reaction systems.

For the other reactions (entries P068 and P069, Table 3.13), it was chosen a starting DCPS with a M_n^i of ∼5 kDa like entry P066 (the one that gelled). Entry P068 differs from entry P066 only for the reaction temperature, which was raised from 70 °C to 100 °C. At 100 °C, no gelation was observed, but a quite high value of $Đ$ was obtained. Even in this case, a MALLS analysis (subsection 2.2.2) confirmed that the final PS is branched. This can be a significant result because branching was not observed for temperatures higher than 90 °C (section 3.1). So far, it seemed that the branching phenomenon was only present in a specific temperature range.

Lastly in entry P069, AsAc was not added, making this system one of those with only Na_2CO_3 as reducing agent.[126] The only difference between P069 and P066 is indeed the presence of AsAc. Without AsAc, no gelation was observed and the reaction did not proceed a lot. The higher values of M_n^f and $Đ$ from the original DCPS are only due to the onset of bimodality (Figure 3.28).

3.13.3 Dilution of the reaction system

As formulated in section 3.12, the branching phenomenon seems to be based on the formation of macrocycles via an intramolecular reaction between the two chain ends. The competition between intra- and inter-molecular reaction is primarily influenced by the concentration of the substrate. It was therefore studied the effect of the dilution on the reaction with DCPS and without St which yielded a gel (P066, Table 3.13). Furthermore, if non-concatenated macrocycles are formed due to

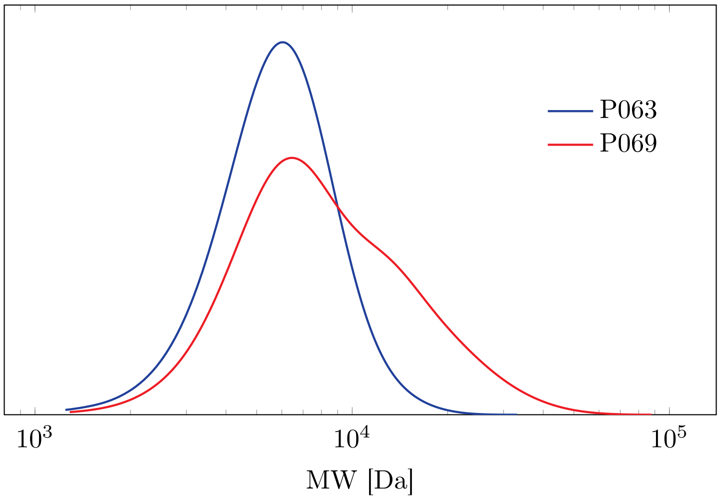

Figure 3.28: GPC analyses of DCPS before and after a reaction without St to promote termination reactions (entries P063 and P069 of Table 3.13).

dilution, they may be identified from GPC. In fact, linear and cyclic PSs with the same MW have different retention times in GPC analysis.[150,151]

In Table 3.14 are reported three different levels of dilution of entry P066. The result is a progressive decrease of M_n and $Đ$ by increasing the dilution factor (DF). Interestingly, as shown in Figure 3.29, the progressive decrease is linearly related to the logarithm of the DF. Figure 3.29 shows also the GPC analysis: as expected, the polymodality is more pronounced for lower DFs. A MALLS analysis (subsection 2.2.2) reported that all the PS obtained from Table 3.14 are branched. Unfortunately, it was not possible to identify single macrocycles from GPC, based on different retention times of linear and cyclic PSs. This because it is difficult to separate the peaks by deconvolution from the GPC eluogram.

Entry	**DCPS**[a]	**DF**	$\boldsymbol{M_\mathrm{n}^\mathrm{i}}$ [kDa]	$\boldsymbol{Đ^\mathrm{i}}$	$\boldsymbol{M_\mathrm{n}^\mathrm{f}}$ [kDa]	$\boldsymbol{Đ^\mathrm{f}}$
P066	P059	1	5.2	1.27	gel	—
P070	P055	2	4.9	1.27	28.4	7.76
P071	P060	4	3.8	1.21	23.3	5.37
P072	P061	8	4.8	1.33	18.5	2.80

Table 3.14: Effect of the dilution on the gelation of DCPS in the absence of St. Conditions: DCPS:$CuCl_2$/TPMA:AsAc:Na_2CO_3 = 1.04:0.05:0.5:1.5[b], V_Tol = (3 × DF) mL, V_EtOAc = (3 × DF) mL, V_EtOH = (1 × DF) mL, T = 70 °C, t = 18 h. [a]The origin of the DCPSs, which are synthesized in Table 3.12. [b]For convenience, MRs are referred to 3 mL of St (which has MR = 100), even if St is not present.

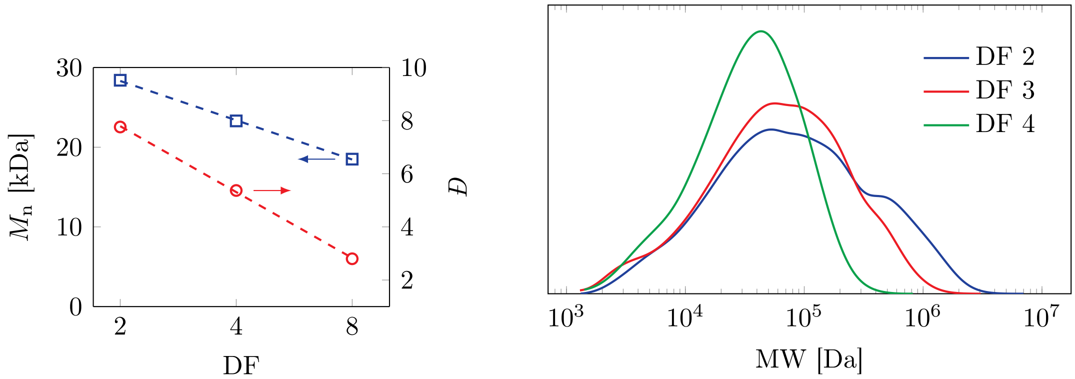

Figure 3.29: Effect of the dilution on the gelation of DCPS in the absence of St: M_n and $Đ$ versus DF (*left*), and GPC analysis (*right*) (entries P070–P072 of Table 3.14). The two straight lines on the left show the linear regressions ($R^2_{M_n} = 0.9996$, $R^2_{Đ} = 0.9996$).

3.13.4 Decreasing the linear telechelic PS concentration

A similar strategy to the dilution of subsection 3.13.3 is decreasing the concentration of DCPS, leaving unchanged the concentrations of other reagents. Differently from dilution, decreasing the concentration of DCPS changes the ATRP equilibrium, increasing the ratio between propagating radicals and dormant species. In Table 3.15, the concentration of DCPS is progressively halved until it reaches an eighth of the concentration of reaction P066, which yielded a gel.

Entry	**DCPS**[a] **(MR)**	M_n^i [kDa]	$Đ^i$	M_n^f [kDa]	$Đ^f$
P066	P059 (1.04)	5.2	1.27	gel	—
P073	P062 (0.52)	4.6	1.31	26.3	5.50
P074	P062 (0.26)	4.6	1.31	21.1	3.05
P075	P062 (0.13)	4.6	1.31	17.8	2.44

Table 3.15: Effect of the DCPS concentration on the gelation of DCPS in the absence of St. Conditions: $CuCl_2$/TPMA:AsAc:Na_2CO_3 = 0.05:0.5:1.5[b], V_{Tol} = 3 mL, V_{EtOAc} = 3 mL, V_{EtOH} = 1 mL, T = 70 °C, t = 18 h. [a]The origin of the DCPSs, which are synthesized in Table 3.12. [b]For convenience, MRs are referred to 3 mL of St (which has MR = 100), even if St is not present.

As expected, the decrease of DCPS concentration is followed by a decrease in M_n^f and $Đ^f$. Figure 3.30 shows the trend of M_n^f and $Đ^f$ and the GPC analysis with respect to the concentration of DCPS. All the GPC traces appear polymodal, except for entry P075 with the lowest MR of DCPS which appears bimodal. The MALLS analysis (subsection 2.2.2) revealed the branched nature of all the PS obtained from Table 3.15, even if the one obtained from entry P075 was just above the boundary between branched and linear.

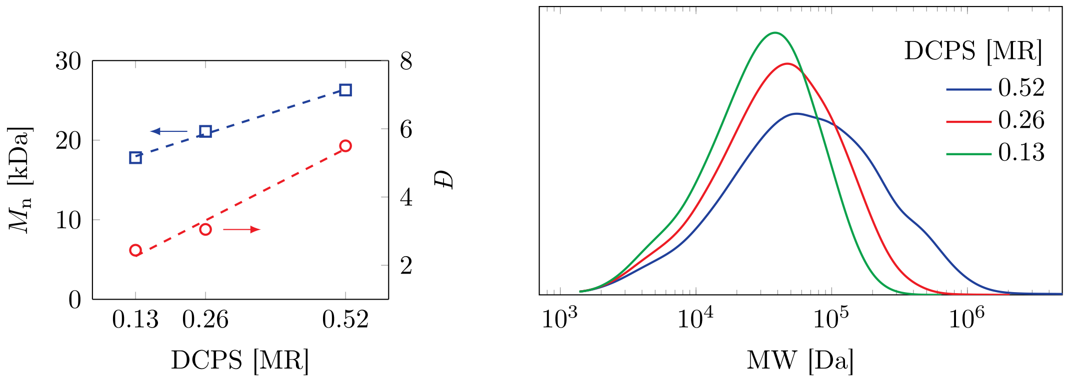

Figure 3.30: Effect of the DCPS concentration on the gelation of DCPS in the absence of St: M_n and $Đ$ versus DCPS MR (*left*), and GPC analysis (*right*) (entries P073–P075 of Table 3.15). The two straight lines on the left show the linear regression ($R^2_{M_n} = 0.996$, $R^2_{Đ} = 0.979$).

In conclusion, gelation was also observed for ARGET ATRP systems with DCPS as macroinitiator and without St monomer. Also dilution of the system or decreasing the concentration of DCPS yielded branched polymers. For the first time, branching was observed for a temperature greater than 90 °C. These results underline the importance of termination reactions in the branching phenomenon.

3.14 Catalytic radical termination

To have the formation of a macrocycle from a DCPS chain, both chain ends must be active (i.e. radicals, and not halogenated). However, in an ATRP system, the concentration of radicals is much lower than the concentration of halogenated chain ends. For that reason, the probability of having both radical chain ends on the same polymer is extremely low. The probability is calculated in the following subsection 3.14.1.

3.14.1 Probability of having two radicals on the same bifunctional polymer chain

With the following formulas, it can be estimated the probability of having three types of bifunctional polymer chains: *(i)* with two radical ends, *(ii)* with two halogenated ends, and *(iii)* with two different ends (i.e. one radical and one halogenated). Then, the population of the three polymer chain types is derived from the probability formulas. The formulas are then applied to the kinetic analysis (section 3.5) to convert the formulas into numbers.

Equations 3.1, 3.2, and 3.3 are used to calculate the probability of finding a bifunctional polymer with two radical ends, two halogenated ends, or two different ends, respectively. The number of radical chain ends is expressed by r, while x is the number of halogenated chain ends. The approximations are based on the fact that, in ATRP, the number of halogenated ends is much greater than the number of radical ends and that both of them are significantly greater than 1 ($x \gg r \gg 1$).

$$P_{rr} = \frac{r}{x+r} \cdot \frac{r-1}{x+r-1} \approx \left(\frac{r}{x}\right)^2 \tag{3.1}$$

$$P_{xx} = \frac{x}{x+r} \cdot \frac{x-1}{x+r-1} \approx 1 \tag{3.2}$$

$$P_{rx+xr} = \frac{r}{x+r} \cdot \frac{x}{x+r-1} + \frac{x}{x+r} \cdot \frac{r}{x+r-1} \approx \frac{2r}{x} \tag{3.3}$$

By multiplying the probabilities of Equations 3.1–3.3 with the number of the total polymer chains in the system, it is possible to calculate the number of chains with two radical ends, two halogenated ends, and two different ends (Equations 3.4, 3.5, and 3.6, respectively). The total number of bifunctional polymer chains is the half of the total number of chain ends ($\frac{x+r}{2}$), which is approximated to $\frac{x}{2}$.

$$N_{rr} \approx \left(\frac{r}{x}\right)^2 \cdot \frac{x}{2} = \frac{r^2}{2x} \tag{3.4}$$

$$N_{xx} \approx 1 \cdot \frac{x}{2} = \frac{x}{2} \tag{3.5}$$

$$N_{rx+xr} \approx \frac{2r}{x} \cdot \frac{x}{2} = r \tag{3.6}$$

As shown in Equation 3.7, the number of radical ends can be determined by multiplying together the concentration of radicals ($\mathrm{R}\cdot$), the volume of the reaction mixture (V), and the Avogadro constant (N_A). The number of halogenated ends is instead expressed in Equation 3.8 and can be approximated to the total number of chain ends, i.e. two times the number of polymer chains. The total number of chains depends only on the moles of initiator (n_{Ini}). The radical concentration of an ATRP system can be calculated with the Equation 1.3 of section 1.2. By plotting the values of $ln\frac{[\mathrm{M}]_0}{[\mathrm{M}]}$ against the time (t) (Figure 3.31), it is possible to calculate the radical concentration from the slope of the linear regression (m) (Equation 3.9). Since k_{p} of St is known and constant at constant temperature (Equation 3.10),[152] the radical concentration can be easily calculated. The linear regression of Figure 3.31 is based only on the first four points (including the origin) because after the 3.3 h the linearity is lost due to a decrease in the radical concentration.

$$r = [\mathrm{R}\cdot] \cdot V \cdot N_{\mathrm{A}} \tag{3.7}$$

$$x \approx 2 \cdot n_{\mathrm{Ini}} \cdot N_{\mathrm{A}} \tag{3.8}$$

$$m = k_{\mathrm{p}} \cdot [\mathrm{R}\cdot] \tag{3.9}$$

$$k_{\mathrm{p}} = 10^{7.630} \cdot e^{\frac{-32.51}{R \cdot T}} \tag{3.10}$$

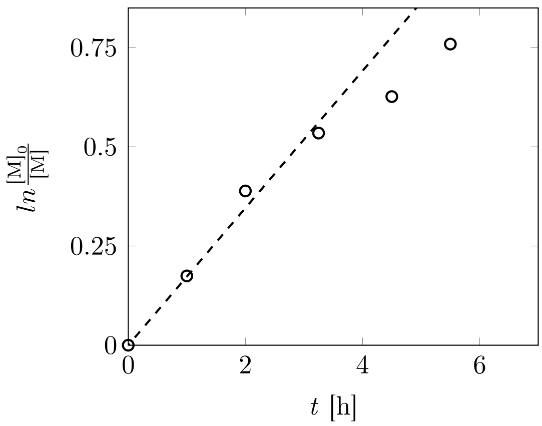

Figure 3.31: Semi-logarithmic plot of the kinetic analysis: monomer concentration versus time (entries of Table 3.5). The line shows the linear regression of the data in the interval 0–3.3 h, forcing the intercept at the origin ($R^2 = 0.994$).

Finally, all the experimental data and the values calculated with Equations 3.1–3.10 are shown hereafter. As a result, the probability of finding a chain with two radical chain ends is extremely small, near to 10^{-10}%. Instead, the probability of finding a chain with two different ends is close to 10^{-4}%. The remaining 99.9998% of the system is composed of chains completely inactive with two halogenated ends.

$V = 7.0 \cdot 10^{-3}\,\mathrm{L}$	$[\mathrm{R}\cdot] = 1.00 \cdot 10^{-7}\,\mathrm{mol\,L^{-1}}$	$N_{rx+xr} \approx 4.2 \cdot 10^{14}$ chains
$n_{\mathrm{Ini}} = 2.76 \cdot 10^{-4}\,\mathrm{mol}$	$r = 4.2 \cdot 10^{14}$ molecules	$P_{rr} \approx 1.6 \cdot 10^{-10}\,\%$
$T = 70\,°\mathrm{C}$	$x \approx 3.3 \cdot 10^{20}$ molecules	$P_{xx} \approx 100\,\%$
$m = 4.80 \cdot 10^{-5}\,\mathrm{s^{-1}}$	$N_{rr} \approx 2.7 \cdot 10^{8}$ chains	$P_{rx+xr} \approx 2.5 \cdot 10^{-4}\,\%$
$k_{\mathrm{p}} = 480\,\mathrm{L\,mol^{-1}\,s^{-1}}$	$N_{xx} \approx 1.7 \cdot 10^{20}$ chains	

3.14.2 Catalytic radical termination mechanism

The formation of macrocycles due to the presence of two radical chain ends appears to be discouraged from a statistical point of view. A catalytic radical termination (CRT) mechanism involving the catalyst was therefore formulated.[153] Even if in the literature are reported cases of CRT reactions only with acrylates,[154–156] the statistical analysis suggests that a more complex reaction mechanism underlies the branching phenomenon.

A CRT mechanism is highlighted in Scheme 3.4. The $\mathrm{Cu^{I}L}$ should be able to bond to the radical end of a polymer chain ($\mathrm{P_n}\cdot$), forming a stable organometallic compound ($\mathrm{P_n{-}Cu^{II}L}$). The stable organometal can then react with another radical chain end ($\cdot\mathrm{P_m}$) with two different paths. In the path above, a radical reaction expels the $\mathrm{Cu^{I}L}$ and a new covalent bond between two C atoms is formed. In the path below, a high-valent organometal is formed ($\mathrm{P_n{-}Cu^{III}L{-}P_m}$), which quickly follows a reductive elimination. In both pathways, the result is a dead polymer chain ($\mathrm{P_n{-}P_m}$). If $\mathrm{P_n}\cdot$ and $\cdot\mathrm{P_m}$ are part of the same bifunctional polymer chain, then the formed $\mathrm{P_n{-}P_m}$ species is a macrocycle.

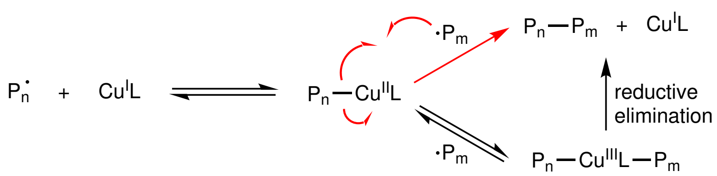

Scheme 3.4: Proposed CRT mechanisms.

It is however important to highlight that, using a bifunctional initiator, a termination reaction between two different polymer chains generates a still living bifunctional chain and not a dead polymer, as shown in the following reaction.

$$\mathrm{X{-}P_n{-}X} + \mathrm{X{-}P_m{-}X} \xrightarrow[\text{reaction}]{\text{termination}} \mathrm{X{-}P_n{-}P_m{-}X}$$

As a result, termination reactions decrease the number of chain ends, but do not generate dead polymer chains. The only exception is an intramolecular termination reaction, which yields a cyclic polymer without any reactive chain end.

3.14.3 Decreasing the load of catalyst

To understand if CRT reactions are occurring, a decrease in the load of Cu was studied in a system that gives gelation. As reported in Table 3.16, the MR of the Cu catalyst was progressively halved from 0.05 up to 0.00313 (entries P076–P080). Surprisingly, the gelation occurred with all the different amounts of catalyst. In the case of entry P080 with the lowest amount of catalyst, the reaction time was extended to 90 h because after 18 h the reaction mixture did not gel, but appeared very viscous. Therefore, the gel point (GP) is probably increasing by decreasing the amount of catalyst but, unfortunately, the GP was not recorded for this series of reactions. However, the conversions were estimated after treating the gels in Soxhlet with MeOH, as described in subsection 2.1.2. Even if the conversions are probably overestimated due to residues inside the gels, they are interestingly increasing as the amount of catalyst is decreased. In Figure 3.32, it is reported the conversion versus the logarithm of the catalyst MR. It seems that there is a linear dependence between the two. The increase in conversion after the decrease in the catalyst amount may seem strange, but it is expected behavior.[92] By decreasing the load of $CuCl_2$/TPMA and not the load of AsAc, it is increased the ratio between Cu^I and Cu^{II}. The overall amount of Cu is decreased, but the relative amount of Cu^I is increased if compared to Cu^{II}. This speeds up the ATRP process.

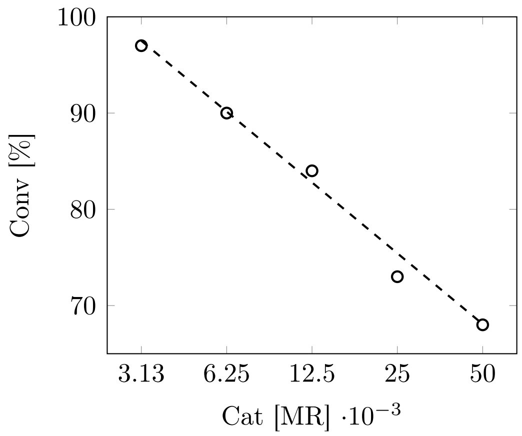

Figure 3.32: Conversion versus the logarithm of the catalyst amount (entries P076–P080 of Table 3.16). The line shows the linear regression with $R^2 = 0.986$.

Entry	**Cat**^{a} [MR]	t [h]	**Conv** [%]	M_n [kDa]	M_n^{th} [kDa]	ΔM_n%	$Đ$
P076	0.05	18	69 (gel)	—	—	—	—
P077	0.025	18	73 (gel)	—	—	—	—
P078	0.0125	18	84 (gel)	—	—	—	—
P079	0.00625	18	90 (gel)	—	—	—	—
P080	0.00313	90	97 (gel)	—	—	—	—
P081	—	90	13	107.8	1.5	99	2.76
P082^{b}	—	18	72	12.3	3.6	71	1.78
P083^{c}	0.05	18	32	4.4	3.4	24	1.53

Table 3.16: Effect of the catalyst load on gelation. Conditions: St:BC:AsAc:Na_2CO_3 = 100:1.04:0.5:1.5, $V_{St} = 3$ mL, $V_{EtOAc} = 3$ mL, $V_{EtOH} = 1$ mL, $T = 70$ °C. ^{a}$CuCl_2$/TPMA. ^{b}AIBN is used instead of BC, same MR. ^{c}"Normal" ATRP with transition metal in the lower oxidation state and without reducing agent: St:BC:CuCl/TPMA:AsAc:Na_2CO_3 = 100:1.04:0.05:0:1.5.

A reaction without any amount of catalyst was also performed (entry P081 of Table 3.16). In this case, no gelation was observed, but the conversion was particularly low, even if the reaction time was extended to 90 h. The low conversion and the large ΔM_n% suggest that the recovered PS is the product of self-initiation reactions.

An FRP experiment was also set up without catalyst (entry P082 of Table 3.16). The absence of any halogen in the system prevents the establishment of an ATRP-like mechanism.[154,157] This FRP system did not return any gelation of the system. Moreover, the branching phenomenon seems to be completely absent, due to the low value of $Đ$ and the monomodal GPC trace (Figure 3.33).

Lastly, a normal ATRP system was set up, with Cu^{I} and without any reducing agent (entry P083 of Table 3.16). Even if a reducing agent like AsAc was not added, Na_2CO_3 and TPMA can both act as reducing agents under specific conditions.[126] However, no gelation was observed. The relatively low values of ΔM_n% and $Đ$, and the monomodal GPC trace (Figure 3.33) suggest that the recovered PS is not branched.

Summarizing the results of Table 3.16, gelation was observed even with very low amounts of $CuCl_2$/TPMA. The gelation of the system seems to be unaffected by the amount of catalyst. However, decreasing the load of $CuCl_2$/TPMA should increase the relative amount of Cu^{I} compared to Cu^{II} and, consequently, it should increase the radical concentration and the termination reactions, which are fundamental for the gelation process. Therefore, it is not so unexpected that by decreasing the catalyst

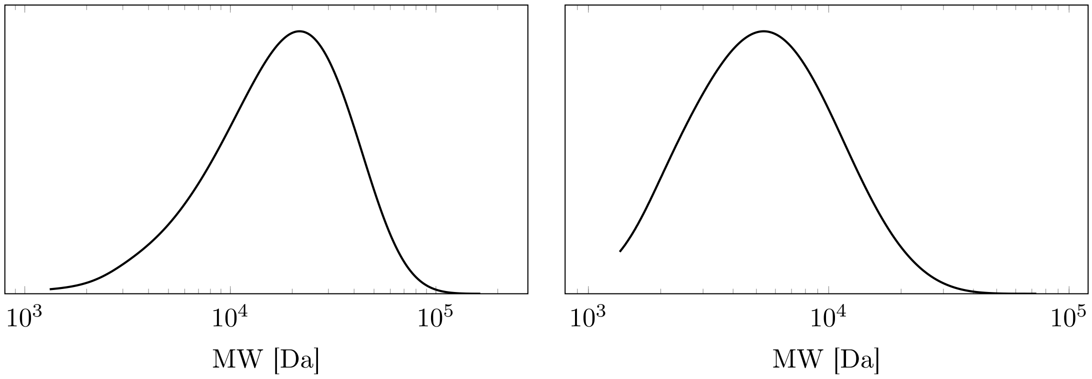

Figure 3.33: GPC analyses of an FRP (*left*) and a normal ATRP (*right*) (entries P082 and P083 of Table 3.16, respectively).

load there is still a gelation. Conversely, a more controlled ARGET ATRP process should be achieved by increasing the load of $CuCl_2$/TPMA. On the other hand, the $CuCl_2$/TPMA load had a more tangible effect on the conversion. Eventually, the gelation and the branching phenomenon were not observed without catalyst, or when the system was converted to an FRP, or with a normal ATRP.

Furthermore, the decrease in the quantity of catalyst makes the process more affordable and leaves less metallic impurities in the final gel. These two aspects are important for possible future applications and from an industrial point of view. For these reasons, several following experiments will use an MR of catalyst equal to 0.0125 (instead of 0.05).

3.14.4 Change of ligand

To better understand the role of the catalyst toward the gelation phenomenon and the CRT reactions, PMDETA and dNbpy were also tested as ligands. The ligands structures are reported in Figure 3.34 and the reactions are listed in Table 3.17. The reaction conditions are the ones that lead toward gelation but with an MR of the catalyst of 0.0125.

Differently from TPMA, no gelation was observed with PMDETA or dNbpy as ligands (entries P084 and P085 of Table 3.17, respectively). $\Delta M_n\%$ and $Đ$ values may be quite high (especially the $Đ$ of entry P085), but there does not seem to be any branching phenomenon. In fact, GPC analyses do not appear polymodal (Figure 3.35). The reason for the relatively high values of $\Delta M_n\%$ and $Đ$ is only due to the initial tail of both GPC traces. Probably, the tail is due to termination

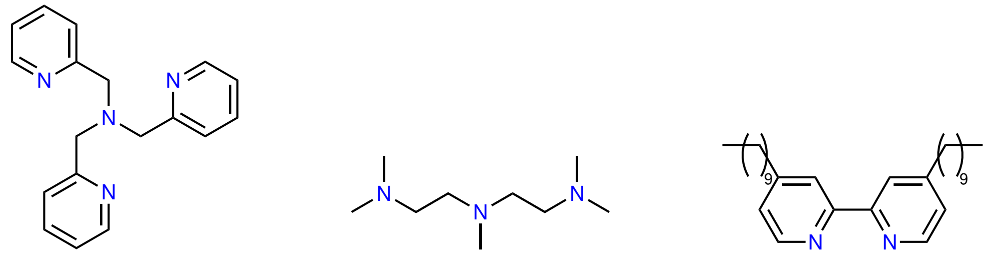

TPMA PMDETA dNbpy

Figure 3.34: Tested ligands.

Entry	**Ligand**	**Conv** [%]	$\boldsymbol{M_n}$ [kDa]	$\boldsymbol{M_n^{th}}$ [kDa]	$\boldsymbol{\Delta M_n}$**%**	$\boldsymbol{Đ}$
P078	TPMA	84 (gel)	—	—	—	—
P084	PMDETA	67	17.2	6.9	60	3.23
P085	dNbpy	75	15.4	7.7	50	1.89

Table 3.17: Effect of the ligand on gelation. Conditions: St:BC:$CuCl_2$/Ligand:AsAc:Na_2CO_3 = 100:1.04:0.0125[a]:0.5:1.5, $V_{St} = 3\,mL$, $V_{EtOAc} = 3\,mL$, $V_{EtOH} = 1\,mL$, $T = 70\,°C$. [a]The MR of dNbpy is doubled (MR = 0.025), in accordance with the stoichiometry of the complex.

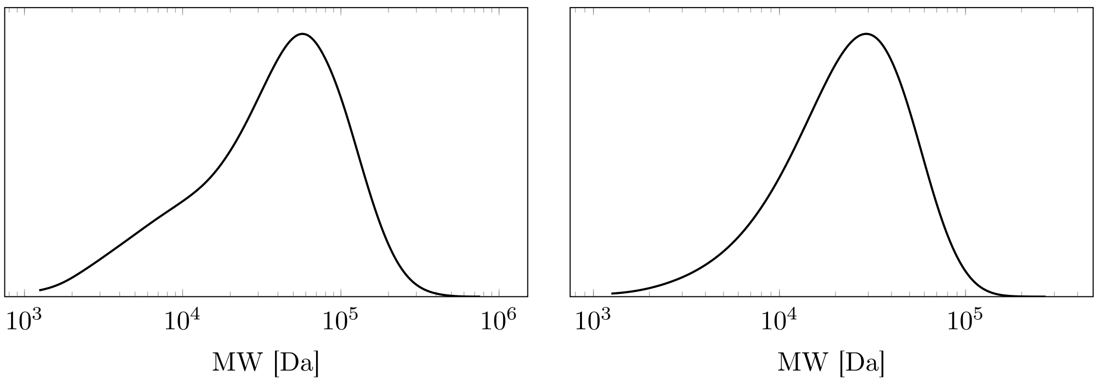

Figure 3.35: GPC analyses of ARGET ATRPs with PMDETA (*left*) and with dNbpy (*right*) (entries P084 and P085 of Table 3.17, respectively).

reactions that were consuming the halogenated chain end.

The ligand can regulate the activity of the Cu-catalyst by modulating its redox potential and by changing the coordination geometry. As a consequence, the overall ATRP process can be influenced. In this case, the anomalous gelation was not observed with PMDETA and dNbpy, but this does not mean that TPMA is necessarily involved in some way in the branching phenomenon. The conditions that lead toward gelation are so narrow that a change in the ligand (i.e. change in the catalytic activity) results in a missed gelation. Likely, reaction conditions can be tuned in order to reach gelation even with a ligand different from TPMA.

In conclusion, the results of this section cannot rule out the presence of CRT mechanisms. However, the gelation seems unaffected by the quantity of $CuCl_2$/TPMA and, in literature, CRT processes were never observed during the polymerization of St. Therefore, CRT reactions appear to be unlikely. A further investigation may be needed to definitely rule out the presence of CRT processes.

3.15 Effect of the solvent mixture on gelation

The effect of the solvent mixture on gelation was then investigated. First, it was increased the amount of St (subsection 3.15.1). St is the monomer, but it has also an important solvent effect. Then, it was investigated the effect of the ratio between EtOAc and EtOH on the gelation process (subsection 3.15.2).

3.15.1 Increasing the amount of styrene

Increasing the concentration of St should increase the rate of polymerization and decrease the rate of termination. At the same time, it should attenuate the catalyst regeneration and hence slow down the entire ATRP process. In fact, a less polar environment decreases the solubility of AsAc and Na_2CO_3, resulting in a smaller rate of catalyst regeneration.[92]

In the reactions of Table 3.18, the amount of St is simply progressively doubled for every reaction. The starting point is entry P086 with 3 mL of St, which is performed in the conditions that gave gelation. For reasons related to laboratory equipment, if the volume of St was not doubled, then all other reagents (including solvents) were halved (reactions conditions are listed in Table 3.19).

Doubling the amount of St (entry P087 of Table 3.18) returned a gel, like entry P086, but with higher conversion. The higher conversion is in agreement with the expected higher propagation over termination rate. The GP was also affected and was increased due to dilution with St. The fact that a gel was obtained was not particularly unexpected since doubling the volume of St did not significantly increase its $V/V\%$.

A four times higher volume of St (entry P088 of Table 3.18, compared with entry P086) returned a gel too. However, the gel was completely dissolved in Tol, meaning that a polymer network was not present. GPC or MALLS analyses were

Entry	**St**	**GP**	**Conv**	$M_\mathbf{n}$	$M_\mathbf{n}^\mathbf{th}$	$\Delta M_\mathbf{n}\%$	$Đ$
	[V/V%]	[h]	[%]	[kDa]	[kDa]		
P086	43	5.9	64 (gel)	—	—	—	—
P087	60	8.1	89 (gel)	—	—	—	—
P088	75	11.5	100 (gel)	—	—	—	—
P089	86	—	17	11.6	13.4	−16	1.38

Table 3.18: Increasing the amount of St. The conditions are reported in Table 3.19.

Entry	**St**	**BC**	**Cat**[a]	**AsAc**	$\mathbf{Na_2CO_3}$	**EtOAc**	**EtOH**	**St**
	[mL]	[MR]	[MR]	[MR]	[MR]	[mL]	[mL]	[V/V%]
P086	3	1.04	0.05	0.5	1.5	3	1	43
P087	6	0.52	0.025	0.25	0.75	3	1	60
P088	6	0.26	0.0125	0.125	0.375	1.5	0.5	75
P089	6	0.13	0.0063	0.063	0.019	0.75	0.25	86

Table 3.19: Conditions of the reactions of Table 3.18: $T = 70\,°\mathrm{C}$, $t = 18\,\mathrm{h}$. [a]$CuCl_2$/TPMA.

not performed on this PS sample. It is again important to stress that the gel does not come from the anomalous branching phenomenon.

In entry P089 (Table 3.18), the relative volume of St is increased by eight times and no gelation was observed. The conversion was quite small even after 18 h of reaction time, meaning that the concentration of reagents was too low at this point. The low $Đ$ and the monomodal GPC trace (Figure 3.36) demonstrate the non-branched nature of the recovered PS. As already observed,[92] a less polar reaction mixture (i.e. increasing the amount of St) attenuates the branching phenomenon.

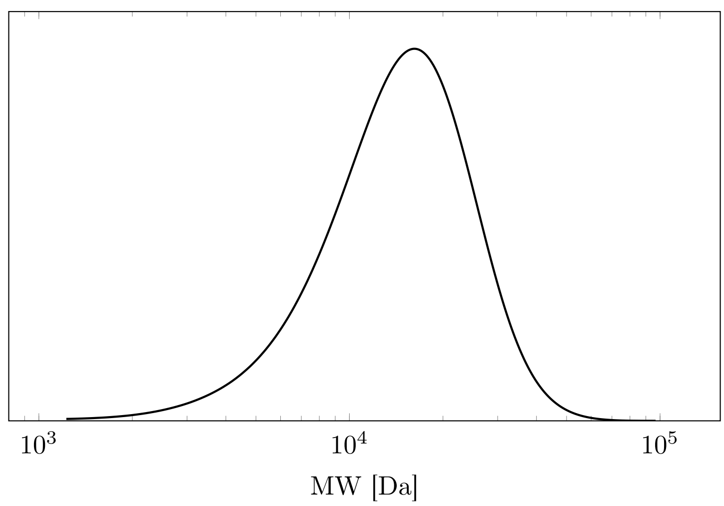

Figure 3.36: GPC analysis of ARGET ATRP with 86% (V/V) of St (entry P089 of Table 3.18).

3.15.2 Changing the ratio between EtOAc and EtOH

The polarity of the medium affects the reaction system and the gelation phenomenon. As already stated, a less polar environment decreases the solubility of AsAc and Na_2CO_3, decreasing the catalyst regeneration rate. This decreases the ratio between Cu^I and Cu^{II}, slowing down the process and preventing the branching phenomenon.[92]

In Table 3.20 are studied different reaction mixtures with different ratios between EtOAc and EtOH. Their total volume is always the same (4 mL). Different from the other reactions discussed in this section, EDCP is the initiator, not BC. However, it was previously discussed how EDCP and BC are equivalent in the ARGET ATRP system we developed (subsection 3.11.1). All the results are therefore comparable, regardless of the employed initiator. Even the hypotheses on the mechanism of the branching phenomenon are the same with any bifunctional initiator. Moreover, the reaction temperature is 60 °C and not 70 °C like the other reactions in this section. Again, this does not change the conclusions that are drawn for the series of reactions of Table 3.20. In addition, differently from the general procedure described in subsection 2.1.2, the obtained gels were dried in a vacuum oven skipping the Soxhlet extraction. Consequently, the conversions of gels are a bit overestimated (for entry P092 it even exceeds 100%). However, the conversions can still be compared within this series of reactions since all the gels were treated with the same procedure.

Entry	**EtOAc** [mL]	**EtOH** [mL]	**GP** [h]	**Conv** [%]	$\boldsymbol{M_n}$ [kDa]	$\boldsymbol{M_n^{th}}$ [kDa]	$\boldsymbol{\Delta M_n\%}$	**Đ**
P015	3.5	0.5	—	64	17.4	6.5	63	2.11
P090	3	1	13	72 (gel)	—	—	—	—
P091	2	2	8.2	94 (gel)	—	—	—	—
P092	1	3	4.8	104 (gel)	—	—	—	—
P093	0	4	0.8	5 (gel)	—	—	—	—

Table 3.20: Effect of the composition of the solvent mixture on gelation. Conditions: St:EDCP:$CuCl_2$/TPMA:AsAc:Na_2CO_3 = 100:1.06:0.05:0.5:1.5, V_{St} = 3 mL, T = 60 °C, t = 18 h.

The overall result of Table 3.20 is gelation for each volume of EtOH greater than 1 mL (i.e. 25% V/V with respect to the total volume of EtOAc and EtOH). For entries P090–P093, GP is also linearly decreasing by increasing the relative amount of EtOH, as depicted in Figure 3.37. This suggests that the branching phenomenon is accelerated by a higher quantity of EtOH. As expected, a greater amount of EtOH accelerates also the ARGET ATRP process and, as a consequence, the conversion is increased. The only exception is for entry P093 with only EtOH: in less than an hour, a small gel ball was separated from the reaction mixture and it did not grow further. Probably, termination reactions completely deteriorated the halogenated chain ends. When gelling occurs, the entire reaction mixture gels. In the case of entry P093 however, the event was more related to the precipitation of a gel with phase separation. Curiously, phase separation was also observed for entry P091 and two layers of very similar gels were formed (Figure 3.38).

EtOH is a poor solvent for PS and increasing its amount results in more contracted polymer chains in solution. The more the EtOH, the more affinity the PS chains

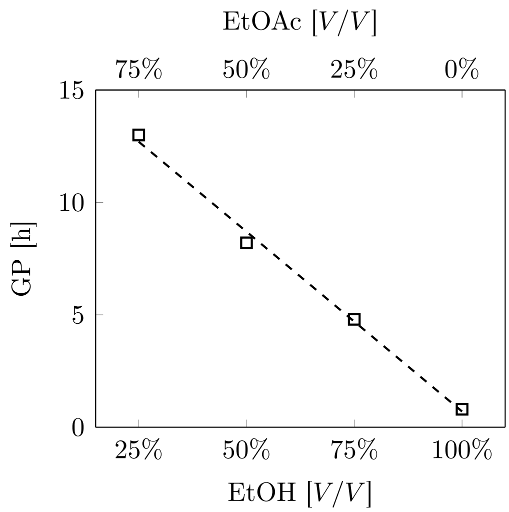

Figure 3.37: GP versus solvent mixture composition (entries P090–P093 of Table 3.20). The line shows the linear regression ($R^2 = 0.996$).

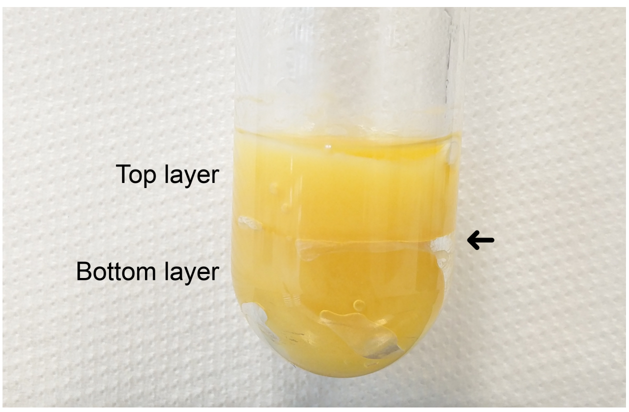

Figure 3.38: Phase separation and formation of two gel layers (entry P091 of Table 3.20). The arrow points out the interphase between the two gels.

have for themselves rather than for the solvent. Chemically speaking, the mixing ΔG between the PS and the solvent becomes greater than zero. In Figure 3.39 is represented the effect of the solvent on the polymer coil dimension. In θ conditions, the ΔG is equal to zero and the polymer coils behave like ideal chains. The outcome of a poor solvent is contracted coils, which can separate themselves from the solvent and can be bound together by termination reactions, even forming macrocycles in our case. In fact, in a relatively poor solvent, the polymer chains are led to a collapse, which increases the probability of ring closure.[158] However, the composition of the solvent mixture (i.e. the relative amounts of EtOAc and EtOH) is not the only parameter that is affecting the polymer coil dimension. Clearly, the chain length and the temperature are also influencing the solubility of the PS chains and the ΔG.[159]

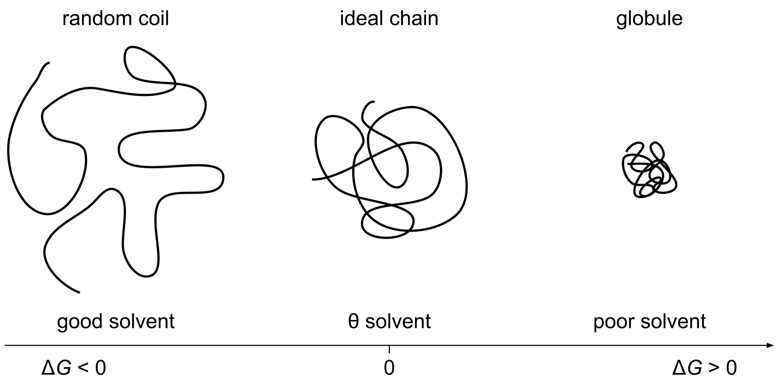

Figure 3.39: Schematic representation of polymer coils in solvents of different quality.

In conclusion, increasing the polarity of the reaction mixture has two effects. First, it increases the radical concentration by boosting the catalytic activity. Second, it pushes the PS chains toward a more globular conformation. These two effects enhance the gelation by formation of a polycatenane network. In fact, a decrease in GP was observed for an increased polarity of the reaction mixture.

3.16 Study of gel point

3.16.1 Effect of temperature and catalyst load

In section 3.1, it was discussed how the gelation phenomenon was only observed around 60 °C in specific reaction conditions. In this section, it is studied the temperature effect on gelation by measuring the GP. As reported in Table 3.21, the

Entry	**Cat**[a] [MR]	T [°C]	**GP** [h]	**Conv** [%]
P094	0.05	50	10.8	59
P095	0.05	60	7.2	64
P086	0.05	70	5.9	64
P096	0.0125	50	20.7	82
P097	0.0125	60	10.8	81
P078	0.0125	70	6.1	84

Table 3.21: Effect of temperature and catalyst concentration on GP. Conditions: St:BC:AsAc:Na_2CO_3 = 100:1.04:0.5:1.5, $V_{\mathrm{St}} = 3\,\mathrm{mL}$, $V_{\mathrm{EtOAc}} = 3\,\mathrm{mL}$, $V_{\mathrm{EtOH}} = 1\,\mathrm{mL}$, $t = 18\,\mathrm{h}$ (except for entry P096, where $t = 48\,\mathrm{h}$). [a]$CuCl_2$/TPMA.

temperature windows is 50–70 °C and two concentrations of $CuCl_2$/TPMA are chosen. In this way, the effect of the catalyst concentration on GP can also be evaluated.

The result is that GP is decreased by temperatures closer to 70 °C and by greater amounts of $CuCl_2$/TPMA (Figure 3.40). However, the difference in GP between the two series with different $CuCl_2$/TPMA concentrations becomes smaller as the temperature is increased. At 70 °C in fact, the GP is almost the same with the two different quantities of $CuCl_2$/TPMA.

Furthermore, as already observed in subsection 3.14.3, the conversions are higher when the load of $CuCl_2$/TPMA is lower. The temperature does not seem to have a particular effect on conversion.

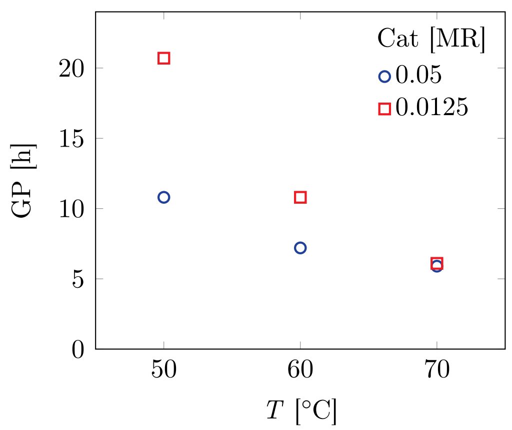

Figure 3.40: Effect of temperature and catalyst concentration on GP (entries of Table 3.21).

3.16.2 Effect of reagents quantities and their ratios

In entries P098–P101 of Table 3.22, it is studied the effect of the load of BC on the gelation phenomenon. The amount of BC is progressively doubled and the

Entry	**BC** [MR]	**AsAc** [MR]	**Na_2CO_3** [MR]	**GP** [h]	**Conv** [%]
P098	0.52	0.25	0.75	8.0	68
P099	1.04	0.5	1.5	6.3	83
P100	2.09	1	3	6.5	98
P101	4.18	2	6	10.6	103
P102[a]	1.04	1	1	—	77
P103	1.04	1	1.5	7.3	—

Table 3.22: Effect of BC amount and ratio between AsAc and Na_2CO_3 on gelation. Conditions: St:$CuCl_2$/TPMA = 100:0.0125, $V_{\mathrm{St}} = 3\,\mathrm{mL}$, $V_{\mathrm{EtOAc}} = 3\,\mathrm{mL}$, $V_{\mathrm{EtOH}} = 1\,\mathrm{mL}$, $T = 70\,°\mathrm{C}$, $t = 18\,\mathrm{h}$. [a] $M_{\mathrm{n}} = 16.0\,\mathrm{kDa}$, $M_{\mathrm{n}}^{\mathrm{th}} = 7.9\,\mathrm{kDa}$, $\Delta M_{\mathrm{n}}\% = 51$, $Đ = 1.77$.

ratios between BC, AsAc, and Na_2CO_3 are kept constant. These ratios are the ones that have always led to gelation (BC:AsAc:Na_2CO_3 = ~1:0.5:1.5). The MR of $CuCl_2$/TPMA is 0.0125.

The GP is the lowest when an MR of BC of ~1 or ~2 is used. For lower or higher amounts, the GP is increased. Apparently, the concentration of radical chain ends is influencing the termination reactions. As already stated, termination reactions are at the basis of the anomalous branching phenomenon (section 3.5).

Moreover, increasing the amount of BC increased conversion. This probably depends on the propagation rate due to the higher concentration of radicals. However, a higher amount of insoluble species (i.e. AsAc and Na_2CO_3) leads to a greater quantity of impurities in the final gel. In fact, the conversion of entry P101 exceeds 100%.

In entry P102 of Table 3.22, the stoichiometry between BC, AsAc, and Na_2CO_3 was re-established. As can be seen from the three reactions below, the stoichiometric ratio between BC, AsAc, and Na_2CO_3 is 1:1:1 ($1\,\mathrm{BC} = 2\,\mathrm{P_n{-}X}$). Termination reaction accumulate Cu^{II}, which is regenerated by AsAc. Na_2CO_3 quenches the acidity released by the regeneration. For a deeper insight into the reactions involving BC, AsAc, and Na_2CO_3, see Scheme 1.3.

$$
\begin{aligned}
2\,\mathrm{P_n{-}X} + 2\,\mathrm{Cu^{I}} &\longrightarrow \mathrm{P_n{-}P_n} + 2\,\mathrm{Cu^{II}} + 2\,\mathrm{X^{-}} \\
2\,\mathrm{Cu^{II}} + \mathrm{AsAc} &\longrightarrow 2\,\mathrm{Cu^{I}} + \mathrm{DHAs} + 2\,\mathrm{H^{+}} \\
2\,\mathrm{H^{+}} + \mathrm{Na_2CO_3} &\longrightarrow 2\,\mathrm{Na^{+}} + \mathrm{H_2O} + \mathrm{CO_2}
\end{aligned}
$$

The net result of these reactions which makes more explicit the stoichiometry between BC, AsAc, and Na_2CO_3 is reported in the reaction hereafter.

$$2\,P_n{-}X + AsAc + Na_2CO_3 \longrightarrow P_n{-}P_n + DHAs + 2\,Na^+X^- + H_2O + CO_2$$

The result of entry P102 with the re-established stoichiometry is a missed gelation. The only difference between the conditions of the re-established stoichiometry and the general conditions that lead to gelation is that the quantity of AsAc is doubled and the load of Na_2CO_3 is decreased by a third. Moreover, the recovered PS seems not to show the branching phenomenon due to the low $Đ$ and the bimodal GPC (Figure 3.41). The long reaction time and the quite high conversion are responsible for the onset of bimodality.

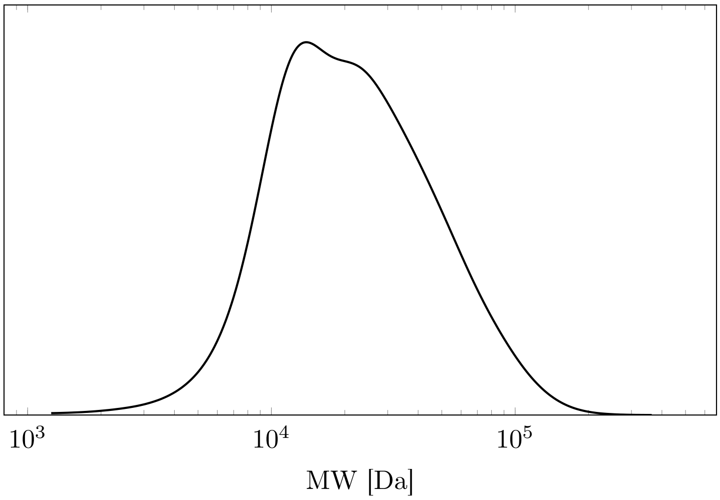

Figure 3.41: GPC analysis of ARGET ATRP with a re-established stoichiometry between BC, AsAc, and Na_2CO_3 (entry P102 of Table 3.22).

Since in entry P102 increasing the amount of AsAc and decreasing the load of Na_2CO_3 (compared to P099) led to a missed gelation, in entry P103 (Table 3.22), only AsAc is increased and Na_2CO_3 is kept constant. The result is gelation with a slightly higher GP (in comparison to P099). Apparently, the Na_2CO_3 needs to be in excess. However, it has to be taken into account the poor solubility of Na_2CO_3 in our reaction system. The Na_2CO_3 has three main roles in this reaction system. *(i)* It quenches the acidity released during the redox reaction between Cu^{II} and AsAc. *(ii)* Na_2CO_3 activates AsAc through deprotonation. *(iii)* Na_2CO_3 can also directly reduce Cu^{II} when combined with EtOH.[126] The importance of these three roles is underlined by the fact that polymerization was not observed without Na_2CO_3.[92] Thus, decreasing the load of Na_2CO_3 slows down these three effects and, consequently, the regeneration of Cu^{II} to Cu^{I}. This diminishes the concentration of radicals, the rate of propagation reaction, and termination by radical–radical coupling. As already stated, termination reactions seem to play a crucial role in the anomalous branching phenomenon.

It was then studied the effect that the amount of AsAc and Na_2CO_3 has on GP, but with a constant ratio between them (AsAc:Na_2CO_3 = 1:3). In Table 3.23, the usual loads of AsAc and Na_2CO_3 of entry P086 are slightly increased in entry P104, doubled in entry P105, and tripled in entry P106.

As expected, the overall result is a steep decrease in the GP by increasing the load of AsAc and Na_2CO_3. A higher amount of AsAc and Na_2CO_3 increases the catalyst regeneration rate and, consequently, the concentration of Cu^I and radical species. With more radicals, termination reactions are favored. The anomalous branching phenomenon was indeed associated with termination reactions. Furthermore, the small decrease in conversion after increasing the loads of AsAc and Na_2CO_3 could mean that the ratio between the rates of termination reactions and propagation reactions is increasing.

Entry	**AsAc** [MR]	**Na_2CO_3** [MR]	**GP** [h]	**Conv** [%]
P086	0.5	1.5	5.9	64
P104	0.55	1.65	4.3	66
P105	1	3	3.0	58
P106	1.5	4.5	2.8	54

Table 3.23: Effect of the AsAc and Na_2CO_3 amount on GP, with constant AsAc:Na_2CO_3 ratio of 1:3. Conditions: St:BC:$CuCl_2$/TPMA = 100:1.04:0.05, $V_{\mathrm{St}} = 3\,\mathrm{mL}$, $V_{\mathrm{EtOAc}} = 3\,\mathrm{mL}$, $V_{\mathrm{EtOH}} = 1\,\mathrm{mL}$, $T = 70\,°\mathrm{C}$, $t = 18\,\mathrm{h}$.

In conclusion, the temperature has a strong influence on the GP. A temperature closer to 70 °C is related to a lower GP. However, the investigated temperature window is narrow because gelation was not observed for temperatures greater than 90 °C (section 3.1). The catalyst concentration affects also the GP, but to a lesser extent. A higher concentration of catalyst corresponds to a lower GP. Furthermore, the AsAc/Na_2CO_3 ratio and the absolute amount of Na_2CO_3 seem to be fundamental for the gelation to occur. Increasing the load of AsAc and Na_2CO_3 and keeping constant the load of BC strongly decreases the GP.

3.17 Effect of the halogen on gelation

In this section, it is studied the effect that the halogen can have on the anomalous gelation. In addition to Cl, Br was the only other halogen tested, since these two are the most efficient halogens for ATRP. The nature of the halogen changes the reactivity of the halogenated chain end and the reactivity of the catalyst.[160] Clearly, the halogenated species in an ATRP system are two: the initiator and the catalyst. While BC and $CuCl_2$ were used in the Cl-ATRP, BB and $CuBr_2$ were used in the Br-ATRP.

In Table 3.24, three different gelation systems at 50, 60, and 70 °C are studied with both Cl and Br. All the reaction systems with Cl returned a gel. At 50 °C, the reactions times were extended from 18 h to 48 h, because for Cl it was observed a GP of 20.7 h (entry P096 of Table 3.24).

Entry	**X**	T [°C]	t [h]	**GP** [h]	**Conv** [%]	M_n [kDa]	M_n^{th} [kDa]	ΔM_n%	$Đ$
P078	Cl	70	18	6.1	84	—	—	—	—
P107	Br	70	18	9.7	87	—	—	—	—
P097	Cl	60	18	10.8	81	—	—	—	—
P108	Br	60	18	—	78	39.3	8.0	80	4.79
P096	Cl	50	48	20.7	82	—	—	—	—
P109	Br	50	48	—	84	38.7	8.6	78	4.18

Table 3.24: Effect of the halogen on the gelation. Conditions: St:BX[a]:CuX_2/TPMA:AsAc:Na_2CO_3 = 100:1.04:0.0125:0.5:1.5, V_{St} = 3 mL, V_{EtOAc} = 3 mL, V_{EtOH} = 1 mL. [a]BC when X = Cl, BB when X = Br.

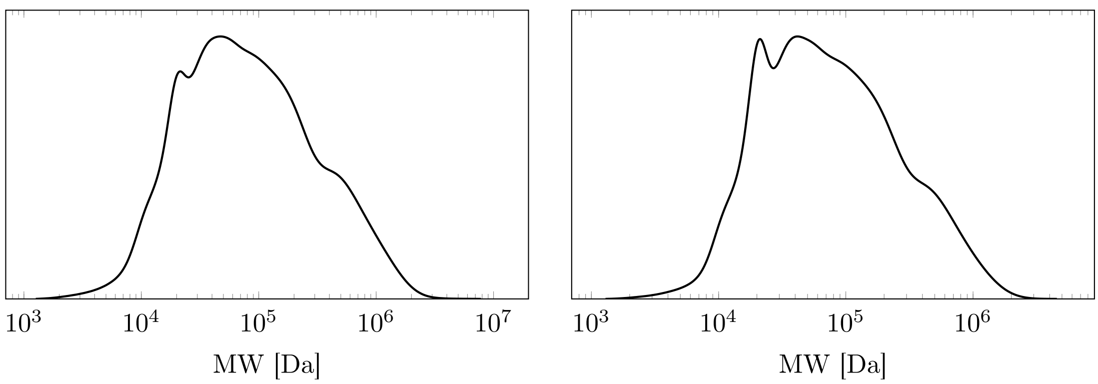

Figure 3.42: GPC analyses of ARGET Br-ATRP systems at 60 °C (*left*) and 50 °C (*right*) (entries P108 and P109 of Table 3.24, respectively).

Interestingly, Br was able to return a gel, but only at 70 °C (entry P107, Table 3.24). At 60 °C and 50 °C (entries P108 and P109 of Table 3.24, respectively), two branched PSs were recovered. The branched nature of these PSs is shown by the high values of $\Delta M_{\mathrm{n}}\%$ and $Đ$, by the polymodal GPC traces (Figure 3.42), and by the MALLS analysis (subsection 2.2.2). Furthermore, the traces of the two GPCs of Figure 3.42 are very similar.

The anomalous branching phenomenon is hence present even with a halogen different from Cl, like Br. However, the ATRP equilibrium is affected by the different reactivity of Br. For this reason, in some cases a gel was obtained from Cl, but not from Br. In any case, the PSs obtained from the Br-ATRP systems were branched.

Chapter 4

Conclusion

The anomalous gelation during the ARGET ATRP of St was studied. The ARGET ATRP is using a bifunctional initiator and is catalyzed by $CuCl_2$/TPMA, which is regenerated by a combination of AsAc and Na_2CO_3. The solvent is composed of a mixture of EtOAc and EtOH. This work investigated various critical variables that stimulate the branching phenomenon which leads to gelation.

Various aspects of the gelation were studied in order to understand the mechanism of the anomalous branching. The phenomenon was influenced by the following factors.

- **Temperature**. The increase in temperature caused the phenomenon to disappear (section 3.1 and subsection 3.16.1).
- **Relative quantities of initiator, AsAc, and $\mathbf{Na_2CO_3}$**. Their ratio should be close to Ini:AsAc:Na_2CO_3 = 2:1:3 (sections 3.2, 3.4, and subsection 3.16.2).
- **Polarity of the medium**. Decreasing the polarity (by increasing the content of EtOAc or St) decreases the solubility of AsAc and Na_2CO_3. In this way, the rate of reactivation of the catalyst is slowed down and the concentration of radicals is lower (sections 3.3 and 3.15).
- **Reducing agent**. Branching was observed only with AsAc, because of its activity as reducing agent (section 3.7).
- **Type of initiator**. The bifunctionality of the initiator is a fundamental requirement (section 3.11).

- **Termination reactions**. The kinetic analysis revealed that a decrease in radical concentration and a steep increase in the M_n is associated with the gelation phenomenon. Both these events indicate a high number of termination reactions (section 3.5). In fact, different monomers that have the tendency to terminate by disproportionation rather than coupling did not show the branching phenomenon (section 3.6). Furthermore, gelation was also achieved by forcing termination reactions in an ARGET ATRP system with DCPS and without St (section 3.13).

On the other hand, branching does not seem to be affected by the type of halogen. Gelation and branching were achieved both with Cl and Br (section 3.17). Even the load of $CuCl_2$/TPMA seems not to affect the gelation phenomenon. However, the branching phenomenon disappeared when the ligand was changed, but this is probably due to a change in the catalytic activity (section 3.14).

Various hypotheses have been formulated for the reasons behind the branching phenomenon: the inimer, the chain transfer, the unsaturation of PS chain ends, and the polycatenane (sections 3.8, 3.10, 3.9, and 3.12, respectively). However, the first three hypotheses were disproved by several experimental evidence and the polycatenane hypothesis seems to be the most plausible.

All the experimental data and the study of the polycatenane hypothesis allowed the formulation of the mechanistic framework about the reaction conditions that give the anomalous branching, depicted in Scheme 4.1.

The gelation depends on two things. First, the polymer chains are needed to collapse on themselves, with the two chain ends approaching each other. Then the two chain ends can react forming a bond following a termination reaction.

The collapse of the chains in solution mainly depends on the solubility of the chains. Therefore, it depends on the polarity of the medium. In fact, increasing the relative amount of EtOH (compared to EtOAc) makes the PS chains less soluble. Furthermore, the polarity of the medium is also influenced by the amount of St, which is present in not negligible volumes.

The collapse of the chains depends on the temperature as well, because the temperature affects the solubility. Lastly, it depends on the chain length: the longer the polymer, the less soluble it is.

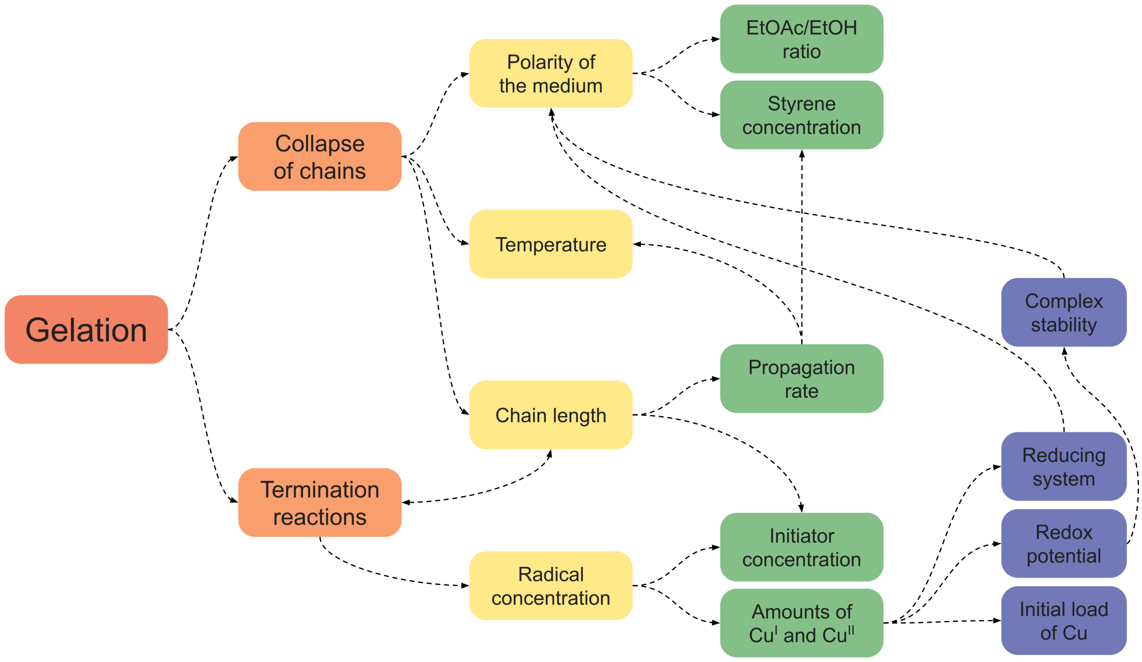

Scheme 4.1: Mechanistic framework of the branching phenomenon.

In its turn, the chain length depends on the quantity of initiator, because the amount of initiator determines the number of polymer chains that are growing together. The chain length depends also on the propagation rate, i.e. how quickly new St monomers are incorporated in the polymer backbone. The propagation rate is clearly influenced by the temperature,[152] but it is also increased by increasing the concentration of St (the more St in the system, the faster the radical addition).

On the other side, termination reactions depend on the chain length too. In fact, the probability of ring closure is related to the distance between two chain ends. However, the opposite is also true: the chain length depends on termination reactions. With a bifunctional initiator, a termination reaction between two different chains gives back a longer single chain with still two reactive chain ends, with the effect of increasing the chain length. Furthermore, termination reactions are related to the concentration of the radicals. In its turn, the radical concentration depends on the ATRP equilibrium and, therefore, it depends on the concentrations of the initiator and on the relative amounts of Cu^{I} and Cu^{II}.

The relative amounts of Cu^{I} and Cu^{II} depend on: the redox potential, the reducing system, and the initial load of Cu. The redox potential is influenced by the stability of the complex (or better, on its formation constant) and it depends therefore on the polarity of the medium for the same ligand. Next, the reducing system is composed of AsAc and Na_2CO_3, which are not completely soluble in our reaction mixture. Therefore, their activity depends on their solubility and therefore on the polarity of the medium too.

This scheme summarizes all the levers that can be pulled to drive the system toward a gelation or a controlled ATRP. By slightly changing one parameter, a gel or a perfectly controlled PS can be obtained. For example, a process that leads toward a controlled polymer can be pushed to gelation by simply increasing the amount of EtOH in the reaction mixture. More EtOH increases the polarity of the medium, which increases the collapse of the chains. It also increases the catalyst activity by better solubilizing the reducing system. Therefore, increasing the amount of EtOH increases the radical concentration and the termination reactions, which are the two key factors of the anomalous branching phenomenon.

4.1 Future perspectives

4.1.1 Labile initiator

To prove the polycatenane hypothesis, macrocycles with degradable bonds should be synthesized. If the macrocycles can be opened, then linear polymer chains are obtained (Scheme 4.2). In this way, the gel can be transformed into solubilizable linear PS chains, which are analyzable via GPC. Scheme 4.2 shows an example where the macrocycles are open by breaking a disulfide bond through a reduction. The disulfide bond could in fact be the most suitable bond for this purpose.

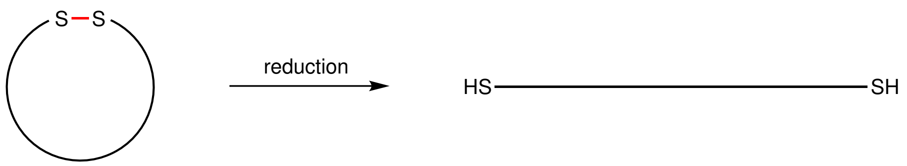

Scheme 4.2: Reduction of a disulfide bond to transform a macrocycle into a linear chain.

Nevertheless, other labile bonds may be considered to be inserted on the macrocycles. Esters, for example, can be easily broken by hydrolysis. Unfortunately, esters are probably too weak and they can give transesterification in our ARGET ATRP system, where an alcohol and a base are present (EtOH and Na_2CO_3). On the other hand, amide bonds are much stronger than ester bonds. However, hydrolysis of amides can require extreme conditions due to their high bond strength. Furthermore, hemiacetals can also be easily degraded. However, hemiacetals can form acetals in the presence of an alcohol like EtOH. Another possibility is to have an alkene as a degradable bond. The alkene needs to be substituted to prevent radical reactions, but it can be broken by ozonolysis. Nonetheless, the generation or the supply of ozone can be a problem from a laboratory procedure point of view. Moreover, ozone is a strong oxidant and it could also degrade the aromatic rings contained in the PS. Lastly, the retro-Diels–Alder can be exploited to open a ring by breaking two σ-bonds. However, very high temperatures may be required to make the retro-Diels–Alder process thermodynamically favorable. For all these reasons, the disulfide bond seems the most appropriate labile bond.

The disulfide bond can be reduced (and broken) after the gelation to disrupt the polymer network. Someone could argue that the ARGET ATRP process that gives gelation is a reducing environment and the disulfide bond could be broken during the polymerization. However, initiators and monomers with disulfide bonds were previously used in ATRP,[124,161] even in ARGET ATRP systems with AsAc.[162–164]

The easiest way to add a disulfide bond in the middle of the polymer chain is to incorporate it in the initiator. Since the anomalous branching occurs only with a generic bifunctional initiator, the disulfide bond should be placed between the two initiating sites. Therefore, the general structure of the required labile bifunctional non-geminal initiator is $Cl{-}R^1{-}S{-}S{-}R^2{-}Cl$. The chosen halogen is Cl, as in most of this study.

Among all possible R^1 and R^2 groups, one of the feasible initiator structures is highlighted in Scheme 4.3, together with its retrosynthetic pathway. This type of initiator is one of the best choices in terms of synthetic ease, availability of synthons, dangerousness of the reactants, and costs. In this initiator, the disulfide bond is found between two benzene rings and the initiating sites are secondary chlorides, which are sufficiently activated.

The retrosynthesis starts from 4′-iodoacetophenone. The first reaction (R1) should be the substitution of the aromatic iodide to obtain the thiophenol. Then, the ketone can be reduced to alcohol (R2) and substituted with a chloride (R3). The final step is the formation of the disulfide bond by oxidation (R4).

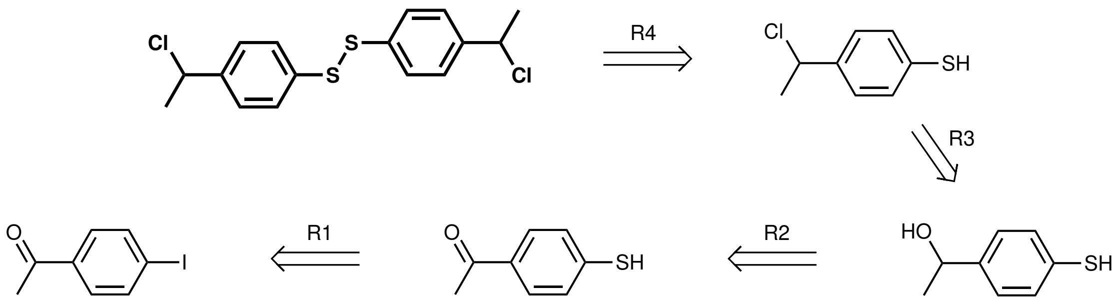

Scheme 4.3: Retrosynthesis of the target bifunctional initiator containing a disulfide bond.

The first aromatic substitution R1 can be easily performed with Na_2S[165] or S powder.[166] Alternatively, it can be performed with 1,2-ethanedithiol or 1,4-butanedithiol.[167] The mercapto group can be inserted on the benzene ring even using thiourea.[168] Generally, these reactions are Cu-catalyzed and performed in dimethyl sulfoxide (DMSO) or *N*,*N*-dimethylformamide (DMF), in the presence of a base.

The reaction R2 is a pretty straightforward reduction reaction. It can be performed with a simple reducing agent like $NaBH_4$.[169] Otherwise, the Meerwein–Ponndorf–Verley reduction could be a good alternative, which uses an alcohol as hydride donor as is catalyzed by an Al alkoxide (Scheme 4.4). If the sacrificial alcohol is isopropyl alcohol (IPA), the resulting acetone can be continuously removed from the reaction mixture by distillation, shifting the equilibrium toward the desired product. Interestingly, a reaction similar to the Meerwein–Ponndorf–Verley was performed even without any metal catalyst.[170]

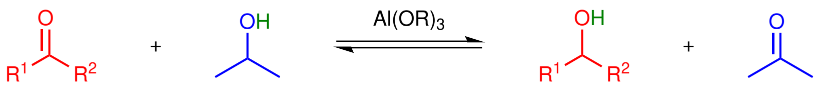

Scheme 4.4: Meerwein–Ponndorf–Verley reduction with IPA as hydride donor.

The nucleophilic substitution R3 can be performed with $SOCl_2$[171] or with $POCl_3$.[172] A more environmentally friendly process concerns the usage of HCl in H_2O.[173] An interesting alternative is the deoxygenative chlorination, which could execute R2 and R3 in a single reaction. The deoxygenative chlorination is a one-pot reaction and can be performed with $MeSiHCl_2$ and with $FeCl_3$ as catalyst[174] or with Me_2SiHCl and $In(OH)_3$.[175]

Finally, the formation of the dimer and the disulfide bond by oxidation (R4) can be accomplished with a simple oxidizing agent and the possibilities are many.[176]

There is a possibility that this reaction also occurs spontaneously when the reaction mixture is exposed to air. Furthermore, the disulfide bond could also be formed in all of the previous synthetic steps, which could make easier the purification of the product. In fact, the dimers should have higher melting temperatures and should be purified more easily by crystallization.

4.1.2 Analytical study of gels

In this work, if a system did not return a gel, the recovered PS was analyzed via GPC and MALLS. However, if a gel was obtained, no particular analyses were performed and limited amount of data about the PS gels have been collected. The only parameter to evaluate the quality of the gel was the GP. From a macroscopic point of view, the morphology was also roughly evaluated based on the consistency and the rubberiness of the gel, but this does not provide an objective parameter on which to make any inferences.

Therefore, a deeper study of the obtained PS gels should be done. In our research group, we have already started studying some aspects, such as the gel content and the swelling degree. Other analyses should be conducted on gels obtained in different reaction systems, such as thermogravimetric analysis (TGA), differential scanning calorimetry (DSC), and shear stress-strain tests. Besides, other SEM images of different gels (in different spots) could be collected.

Furthermore, particular attention should be directed to the physical properties of the gels. The polycatenane network could show interesting mechanical properties. In fact, a recently published article by Hu et al. investigates the elastomeric properties of cyclic polydimethylsiloxane.[146]

4.1.3 Gelation in dispersed media

Even though anomalous gelation is an interesting reaction, it has few applications, especially from an industrial point of view. The gelation of an entire reactor is not of particular interest. For this reason, it might be interesting to transfer the anomalous gelation into dispersed media.

With dispersion polymerization or oil-in-water emulsion polymerization, small droplets can be gelled, forming small spherical particles. These small spheres can be used as chromatographic packing materials, spacers in large liquid crystal displays, and colloid crystals. They can also be used as calibration standards in various instruments, like light scattering devices, electron microscopes, and particle size counters. They also find other applications such as controlled drug release vehicles, immunoassays, cell separation and cultivating, synthetic receptors, carriers for reagents, catalysts, and enzymes.[177]

Part II

Atom Transfer Radical Addition and Lactonization

Chapter 5

Introduction to atom transfer radical addition

ATRA is a powerful synthetic tool for the formation of C−C bonds.[178] It was first described in 1945 by Kharasch et al. as a free radical addition of CCl_4 and $CHCl_3$ to alkenes in an anti-Markovnikov way.[179] A modern ATRA process is usually catalyzed by a transition metal complex, generally formed by Cu and a N-based ligand. As shown in Scheme 5.1, in the activation step, the reduced form of the complex $[Cu^{I}L]^{+}$ can abstract a halogen atom from an alkyl halide ($R^1{-}X$). The result is the generation the corresponding oxidized $[X{-}Cu^{II}L]^{+}$ and the organic radical $\cdot R^1$. The radical can then react with the double bond of the alkene, generating the radical monoadduct. In the deactivation step, the $[X{-}Cu^{II}L]^{+}$ species quenches the radical, giving the desired halogenated monoadduct and completing the catalytic cycle.

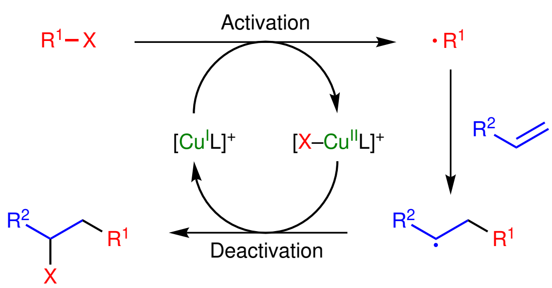

Scheme 5.1: Cu-catalyzed ATRA mechanism.

To achieve a high selectivity in an ATRA process, it is necessary to follow two rules. *(i)* It is important to avoid any further halogen abstraction from the product. Therefore, the substrates are usually chosen in a way that the radical monoadduct is much less stabilized than the initial radical. *(ii)* The avoidance of oligomerization/polymerization is also a significant concern. This can be achieved with a fast deactivation rate to give the halogenated monoadduct.[37]

These two rules, however, strongly limit the range of substrates that can undergo the ATRA. This study aims to break these rules by joining the ATRA with a subsequent lactonization reaction. A new type of reaction (called atom transfer radical addition and lactonization, ATRA-L) is then defined, which should drastically expand the use of ATRA.

5.1 The advantages of atom transfer radical addition and lactonization

ATRA-L is a new acronym that we are proposing to describe a class of reactions. The ATRA-L reaction (Scheme 5.2) generally occurs between an α-haloester and an alkene. After the addition takes place, the newly formed monoadduct undergoes a lactonization. Overall, two new bonds are formed: a C−C bond following the ATRA, and a C−O bond following the lactonization. ATRA-L can overcome the ATRA rules, which represent two significant limitations. If the lactonization is fast enough, the halogenated monoadduct cannot go through a further activation with halogen abstraction, breaking the *(i)* rule. Furthermore, if the lactonization occurs before the deactivation step, then there is no concern on any oligomerization/polymerization, breaking the *(ii)* rule. In this case, the lactonization occurs before the final deactivation step of ATRA and the halogenated monoadduct form is never reached. However, the cyclization mechanism is not fully understood yet and it is discussed in more detail in chapter 7.

Furthermore, ATRA-L can be applied for the preparation of inert or biologically relevant materials. As discussed in chapter 1, ATRP is a powerful technique

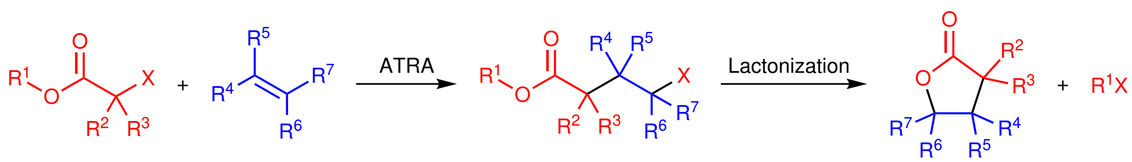

Scheme 5.2: ATRA-L reaction with the formation of γ-lactones.

used to create polymers with narrow molecular weight distributions and a post-functionalizable halogenated chain end. The halogen on the chain end is nevertheless unwanted for some biological applications and, with ATRA-L, it could be transformed into the relatively inert lactone.

Chapter 6

Literature review on atom transfer radical addition and lactonization

Various ATRA-L processes that are present in the scientific literature are investigated in this chapter. A meticulous investigation was done to gather all the information about this topic from the literature. However, the ATRA-L was never defined before as a topic for this type of chemical reaction. Consequently, the literature lacks a complete overview of this subject. This chapter aims to gather and link all the scientific information attributable to the ATRA-L reaction. Moreover, some of the examples described in this chapter cannot be considered ATRA-L reactions in the strictest sense, but they are still closely related to its definition. For that reason, these examples are important to be mentioned. Chapter 7 is also based only on the published scientific literature, but it was separated from this chapter because it is entirely focused on the mechanism. The topic of the mechanism is broad enough to deserve a whole chapter of its own.

6.1 First examples of ATRA-L

ATRA coupled with a lactonization was first described in 1948 by Kharash et al.[180] First, they performed an ATRA initiated by Ac_2O_2 (Scheme 6.1). Afterward, they observed the lactonization of the γ-brominated monoadduct during its distillation at high temperatures, with the loss of bromoethane. In esters and carboxylic acids, the carbonyl group can displace a γ- or δ-halogen to form γ- or δ-lactones, respectively.

However, this example can be considered a two-step process and it does not have the advantages of ATRA-L discussed in section 5.1. Other notable examples of two-step processes were achieved by other research groups, where the lactonization is only achieved in a second step after the ATRA reaction.[181–183]

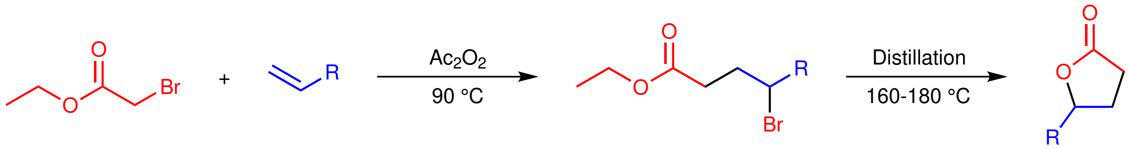

Scheme 6.1: Two-step ATRA-L from reference [180] (R = *n*-hexyl).

The very first single-step ATRA-L reaction was described by Freidlina et al. in 1967 during the telomerization of ethylene[184] and their work is described in subsection 6.9.1. The following year (1968), three research papers described proper ATRA-L reactions initiated by $Pb(OAc)_4$[185] or $Mn(OAc)_3$.[186,187] The usage of acetate salts in this reaction is discussed in section 6.3.

6.2 Catalysis

Various transition metal catalysts have been used in ATRA-L systems, like Fe,[184,188,189] Cr,[184] Mo,[188] V,[190] Ru,[191,192] Cu,[193,194] Ni,[195] Co,[196] and Mn.[197] Wei et al. were the first to employ a photocatalyst, based on Ir.[198] More recently, Triandafilli et al. not only used Ru and Ir as photocatalyst, but also thioxanthone, a metal-free one.[199] Acetate salts of Mn,[186,187,190,200,201] Pb,[185] and Ce[190] were also employed, but as initiators. Therefore, these acetate salts play the role of reagents and not catalysts, but the metal could have also been involved in some catalytic activities.

6.3 Acetate salts as initiators

Some of the first examples in the history of ATRA-L reported the use of $Mn(OAc)_3$ as reagent (Scheme 6.2).[186,187,190,200,201] Generally, these reactions are conducted in AcOH or Ac_2O or a mixture of the two. KOAc is used to increase the boiling point of the reaction mixture. High temperatures are required for the $Mn(OAc)_3$ to generate carboxymethyl radicals ($\cdot CH_2COOH$), which can give addition to an

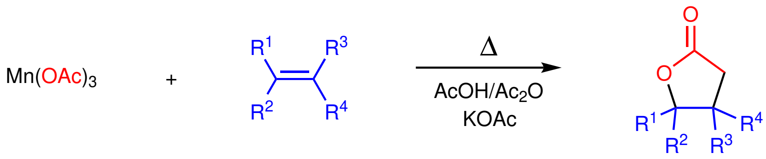

Scheme 6.2: ATRA-L initiated by $Mn(OAc)_3$.

alkene. The mechanism of lactonization of the radical monoadduct is discussed in subsection 7.3.1.

$Mn(OAc)_3$ is composed by trinuclear complexes with octahedral metal centers (Figure 6.1).[202] Three Mn^{III} ions are conjoined by oxo and acetate bridging ligands. An α-deprotonation of these acetates is facilitated by the electron deficiency of Mn^{III} and the outcome is a stable complex with a delocalized electron. As a result, this deprotonation can generate the equivalent of the reactive intermediate $\cdot CH_2COO^-$, starting the reaction.

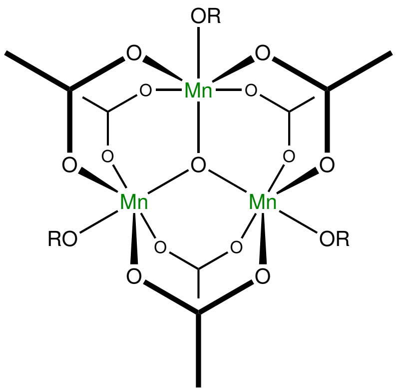

Figure 6.1: Structure of $Mn(OAc)_3$. OR groups are bridging AcO^- or AcOH.

A notable example of $Mn(OAc)_3$ usage is a double annulation able to generate polycyclic lactones.[200] In this system, $Mn(OAc)_3$ is only used to generate the radicals and the product originates from two intramolecular reactions of the substrate. An example of one of these reactions is depicted in Scheme 6.3.

In addition to $Mn(OAc)_3$, other metal acetates were used in an analogous way, like $Pb(OAc)_4$[185] and $Ce(OAc)_4$.[190] However, $Mn(OAc)_3$ is the most used due to its ready availability and high solubility. Moreover, $Pb(OAc)_4$ has a different structure compared to $Mn(OAc)_3$ and $Ce(OAc)_3$, and therefore a different mechanism of radical generation. $Pb(OAc)_4$ is believed to generate radicals through a decarboxylative pathway.

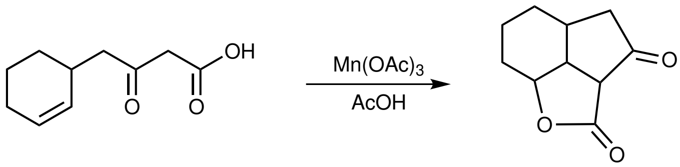

Scheme 6.3: Example of double annulation from reference [200].

6.4 Addition of Ac_2O to an alkene and lactonization

Huang et al. reported an interesting synthesis method for γ-lactones from alkenes involving O_2.[203] The reaction is highlighted in Scheme 6.4 and it is an oxidation catalyzed by $Cu(OTf)_2$ and LiBr. This type of oxidation is generally used for dihydroxylation reactions, where an alkene is converted to a vicinal diol.[204] Dihydroxylation reactions can usually go through acetylation of the double bond first, and then hydrolyzation. In this case however, the addition of Ac_2O to an alkene gave a γ-lactone. The authors proved that the mechanism is not radical by carrying out control experiments with radical quenching agents and observing no impact on the reaction. Therefore, the addition of Ac_2O on the alkene is not an ATRA process in this case. In fact, the authors proposed a non-radical addition mechanism, involving the nucleophilic attack by the enol of Ac_2O on the alkene.

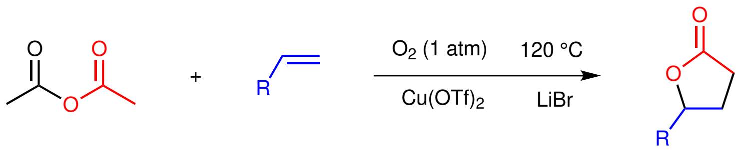

Scheme 6.4: Oxidation of an alkene to γ-lactone by Ac_2O from reference [203].

6.5 Sm-induced radical addition of ketones to alkenes and lactonization

γ-Lactones were also synthesized from a carbonyl and an alkene by Sm-induced radical addition.[205,206] Sm^{II} is a strong one-electron transfer reducing agent, able to generate a ketyl from a carbonyl and an allylic radical from an alkene (Scheme 6.5). Both these radical species can react with each other in a radical coupling, forming a monoadduct. Together with the radical coupling, a proton is incorporated on the α-C of the ester group. As a consequence, a protic species is needed to complete the reaction. The monoadduct can then cyclize into a γ-lactone. 2 equiv of Sm^{II}

are required for this reaction, one for the reduction of the carbonyl and one for the reduction of the alkene. Since Sm^{II} is consumed, it is not considered a catalyst, but a reagent.

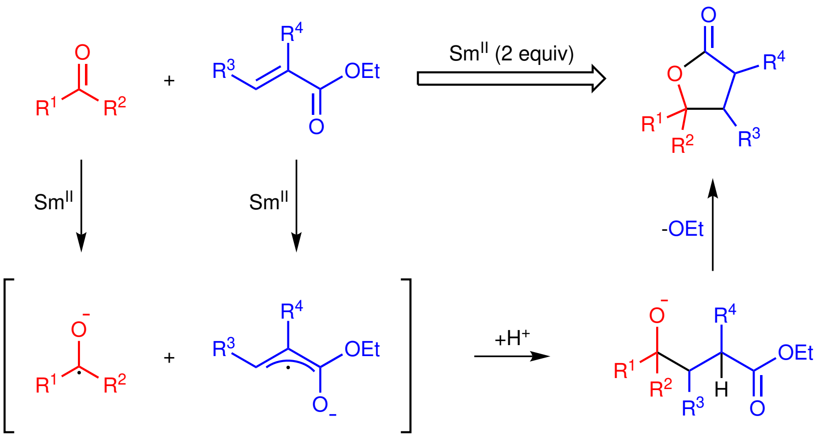

Scheme 6.5: Possible mechanism of formation of γ-lactones from a carbonyl and an alkene with Sm^{II}, from reference [205].

6.6 ATRA-L of stannyl and silyl esters

ATRA-L is generally initiated by an α-halo-alkyl ester or -carboxylic acid (Scheme 5.2). Differently, some examples in the literature report the usage of tributylstannyl esters[207–210] and one of trimethylsilyl ester.[192] The general reaction is depicted in Scheme 6.6 and tributyltin or trimethylsilyl halides (R^1X) are by-products of the lactonization reaction. The liability of O−Sn and O−Si bonds can promote the intramolecular lactonization of the monoadduct. For the reaction mechanism, see subsection 7.1.1.

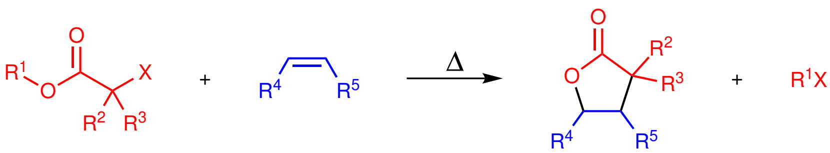

Scheme 6.6: ATRA-L between an alkene and a stannyl or silyl ester (R^1 = $-SnBu_3$ or $-SiMe_3$).

6.7 Electroreductive ATRA-L

Shono et al. proposed an ATRA-L initiated by electrochemical methods.[211] As shown in Scheme 6.7, they performed an electroreductive crossed hydrocoupling of α,β-

unsaturated esters with aldehydes or ketones in the presence of Me_3SiCl, obtaining γ-lactones. They proposed that the first radical is formed on the double bond of the α,β-unsaturated ester, following an electroreduction and leaving a radical anion. The radical can give addition to the aldehyde or the ketone because its carbonyl group is activated by coordination of the silicon from Me_3SiCl. After the addition, the $-SiMe_3$ remains attached to the O atom from the aldehyde or the ketone in the monoadduct, but it is rapidly expelled by the attack of the ester group, giving a γ-lactone. The mechanism, however, is not entirely clear and the addition may not be a radical one. Nevertheless, the peculiarities of this study are that the addition starts from the alkene and that the reaction is initiated by electrochemical methods.

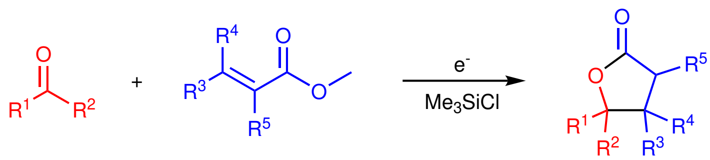

Scheme 6.7: Electroreductive crossed hydrocoupling of α,β-unsaturated esters with aldehydes or ketones from reference [211].

Another interesting study that is worth mentioning was proposed by Ihara et al.[195] They performed a Ni-catalyzed electroreductive cyclization of halogenated α,β-unsaturated esters, obtaining δ-lactones. Both the halogenated initiating site and the alkene reside on the same molecule, but an ester group is located between them on the backbone. This type of reactions is already discussed in section 6.13, but in this example, the reaction is performed with electrochemical procedures.

6.8 Addition of α-hydroxy radicals to an alkene and lactonization

Iwahama et al. reported an interesting ATRA-L example in the presence of O_2, highlighted in Scheme 6.8.[196] The initial radical is generated from a reaction between an alcohol and phthalimide *N*-oxyl (PINO), generating an α-hydroxy radical and *N*-hydroxyphthalimide (NHPI), respectively. NHPI is regenerated to PINO with the aid of a Co-based catalyst and O_2. The newly-formed α-hydroxy radical gives radical addition on an α,β-unsaturated ester to give the radical monoadduct. The radical of the monoadduct is then trapped by O_2 and converted into an alcohol, giving an α,γ-diol monoadduct. A lactonization with the elimination of MeOH yields the final lactone. The interesting aspects of this ATRA-L system are two. First, the carboxylate is located on the alkene, not on the initiator as usual. There is only one other example (discussed in subsection 6.9.2) where the carboxylate involved in the lactonization is located on the alkene monomer. Second, prior to lactonization, the γ-C is not halogenated, rather hydroxylated. Two other examples suggested a hydroxylation of the γ-C after addition and are discussed in section 7.2.

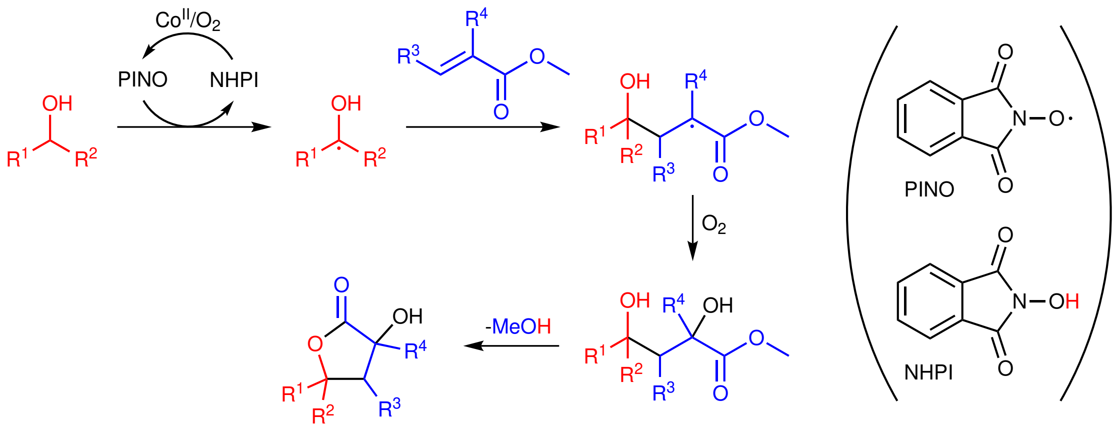

Scheme 6.8: Example of ATRA-L between an α-hydroxy radical and a (meth)acrylate ester from reference [196].

6.9 Lactonization during radical polymerization

In two examples, an ATRA-L reaction was reported during the radical polymerization of vinyl monomers. In the first case (subsection 6.9.1), the lactonization occurs as usual: after one addition, the ester group of the initiator can substitute the halogen in γ-position. In the second case instead (subsection 6.9.2), lactonization can happen at any time during the polymerization because every monomer possesses a carboxylic group and the chain end is always halogenated. In fact, the halogen is in the favorable γ-position compared to the carboxylic group of the penultimate monomer of the polymer chain.

6.9.1 Telomerization of ethylene

Freidlina et al.[184] reported an example of ATRA-L as a side reaction during the telomerization of ethylene with esters of trichloroacetic acid. The reaction is initiated by $Fe(CO)_5$ or $Cr(CO)_6$, and it is conducted at 140 °C and 100–150 atm. As shown in Scheme 6.9, they reported the formation of two different γ-lactones, depending on the number of reacted halogens of the initiator. Interestingly, no lactones were observed when using a peroxide initiator instead of a metal carbonyl.

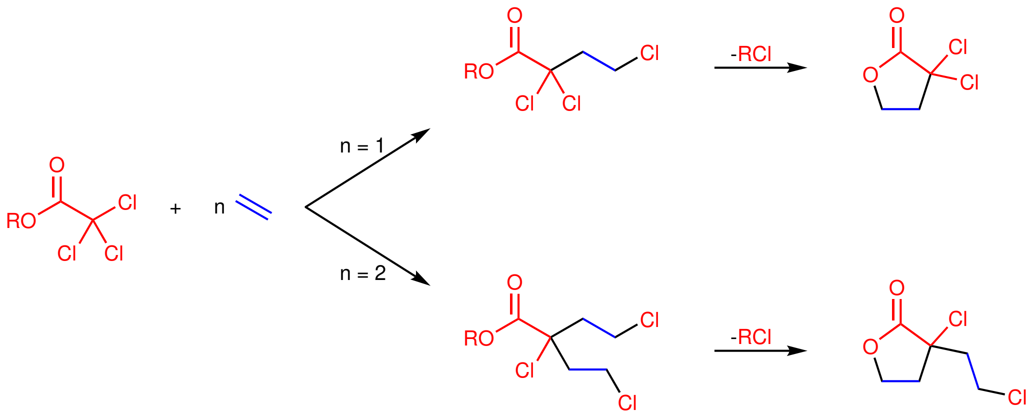

Scheme 6.9: Example of ATRA-L during the polymerization of ethylene from reference [184].

6.9.2 ATRP of methacrylic acid

Recently, Fantin et al.[212] observed a chain-end lactonization as a side reaction during the *e*ATRP and SARA ATRP of methacrylic acid (MAA) with α-bromoisobutyric acid (BiBA) as initiator (Scheme 6.10). The carboxylate of the penultimate MAA monomer unit can substitute the Br of the last monomer unit, giving a γ-lactone at the poly(methacrylic acid) (PMAA) chain end. Since the reaction is carried out in H_2O, the deprotonation of BiBA and the consequent rate of lactonization are directly dependent on the pH. This study is interesting because it shows that ATRA-L can be a new and interesting method for the defunctionalization of the halogenated polymer chain end obtained by ATRP. As discussed in section 5.1, the defunctionalization is a prerequisite for some biological applications.

6.10 ATRA-L during thermolysis

Maillard et al. studied the thermolysis of *tert*-butyl-4-peroxypentenoate (TBPP) at 120 °C in the presence of cyclohexane as solvent.[213] The thermal initiation step of TBPP and the propagation step are highlighted in Scheme 6.11. In the propagation step, t-BuO· can abstract a hydrogen from the cyclohexane, leaving a cyclohexyl

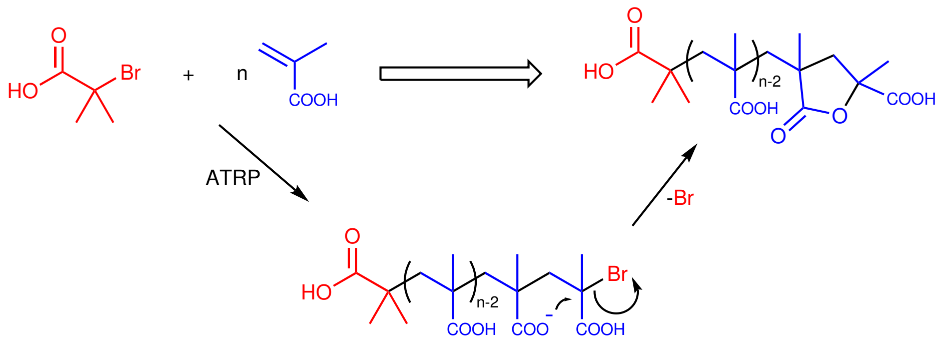

Scheme 6.10: PMAA chain-end lactonization during the ATRP of MAA from reference [212].

radical. The cyclohexyl radical can give radical addition to the TBPP double bond, which can lactonize, regenerating the t-BuO$\cdot$ and restarting the cycle. The authors reported several products generating from several radical reactions, but the final lactone of Scheme 6.11b was the major product obtained in 35% yield. Needless to say, t-BuOH was the other major product of the thermolysis with $\sim$100% yield. γ-Valerolactone was also obtained via radical cyclization of the pentenoate radical generated in Scheme 6.11a, but only in $\sim$1% yield. The reason why in Scheme 6.11b the t-BuO$\cdot$ seems to react preferentially with the cyclohexane and not other species is due to the high concentration of cyclohexane (TBPP:cyclohexane = 1:50).

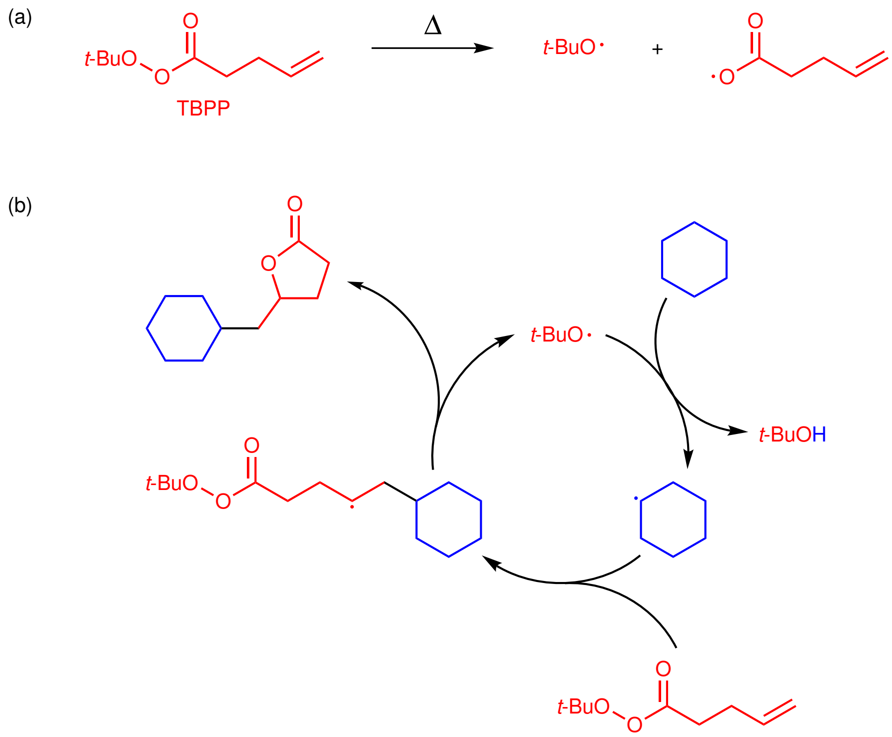

Scheme 6.11: Initiation (a) and propagation (b) steps of the thermolysis of TBPP from reference [213].

6.11 ATRA and iminolactonization or lactamization

If an amide replaces the ester in an ATRA-L with an alkene, the product is an iminolactone or a lactam, not a lactone. However, iminolactones can be easily hydrolyzed to lactones in mild acidic reaction conditions.[214] In the literature there are a few examples of iminolactones and lactams synthesis that exploit the ATRA-L protocol,[215–218] and one of them is highlighted in Scheme 6.12. The reaction is carried out between an α-bromoamide and an alkene bearing an electron withdrawing group (EWG) in the presence of a base and $BnBu_3NBr$, and it is catalyzed by $[Cu^{I}TPMA]^{+}$. Interestingly, the product was an iminolactone or a lactam depending on the employed reaction conditions. The polarity of the system influenced the mechanism of cyclization and consequently the product. Indeed, it was observed that stronger basic conditions and protic polar solvents preferably lead to lactams, whereas weak basic conditions and aprotic nonpolar solvents mainly yielded iminolactones.

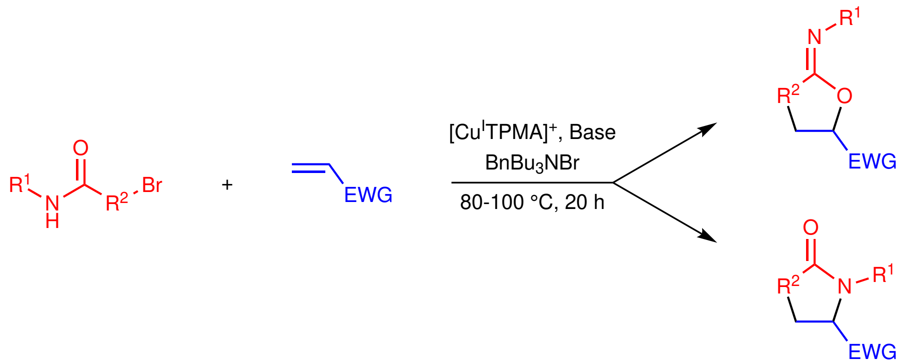

Scheme 6.12: ATRA and iminolactonization or lactamization from reference [216].

6.12 Atom transfer radical cyclization and lactonization

ATRC is an intramolecular ATRA and the product is a cyclic compound.[219] Both the generated radical and the alkene are on the same molecule and react with each other. Atom transfer radical cyclization and lactonization (ATRC-L) was developed by coupling ATRC with a subsequent lactonization.[210] ATRC-L can generate bicyclic structures, one from ATRC and the other from lactonization. In Scheme 6.13 is shown an example where ATRC is initiated by AIBN and the obtained

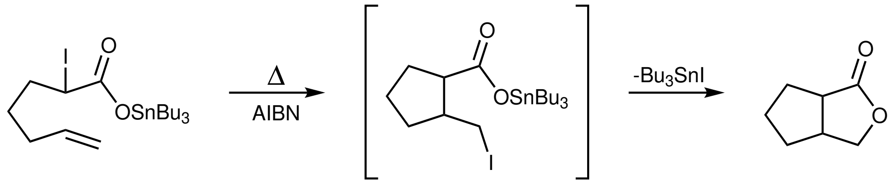

Scheme 6.13: Example of ATRC-L from reference [210].

5-*exo* product can lactonize. The mechanism of lactonization is probably the same as other tributylstannyl compounds, discussed in subsection 7.1.1.

A similar reaction was carried by Curran et al.[220] to obtain the same bicyclic lactone as the one of Scheme 6.13, but in a different way. The only difference is that the substrate was not a tributylstannyl ester, but a methyl ester. Anyhow, the reaction was initiated by organotin compounds, like $Bu_3SnSnBu_3$, and AIBN.

6.13 Radical cyclization of α-haloesters

ATRC or free-radical cyclization can also be used to generate lactones. However, the substrate molecule is required to have an ester group between the alkene moiety and the generated radical (Scheme 6.14a).[195,221–225] Coincidentally, esters groups are usually exploited because they can generate a radical from an α-halogen following an activation. Instead of esters, acetals can also be used to generate the radicals (Scheme 6.14b), but after the cyclization, they have to be oxidized to obtain a lactone.[195,226,227]

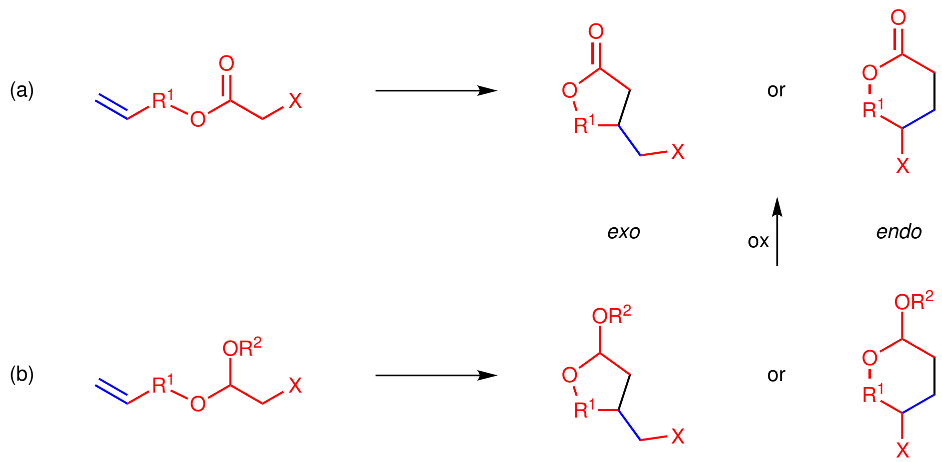

Scheme 6.14: *Exo* and *endo* ATRC or free-radical cyclization of ester (a) or acetal (b) substrates to give lactones.

6.14 Sequential atom transfer radical reactions

ATRA can be used in combination with ATRC to synthesize complex molecular structures. Like ATRA-L, this tandem ATRA-ATRC protocol exploits a cyclization reaction immediately after the ATRA. Some examples of ATRA-ATRC reactions are reported in literature[228–232] and one of them is highlighted in Scheme 6.15, where the ATRA and then the ATRC are able to generate interesting tricyclic structures.[233] Regarding the mechanism, the photo-generation of an alkyl radical occurs, which can give radical addition to the maleimide. The radical monoadduct is then able to give cyclization by attacking the benzene ring, resulting in a tricyclic structure. The aromaticity of the benzene ring is re-established by SET and loss of a proton.

Reversing the order, a tandem ATRC-ATRA was also developed taking advantage of a faster ATRC, which occurs before the ATRA.[234] Another type of tandem process is the succession of two cyclizations, namely ATRC-ATRC.[234–237]

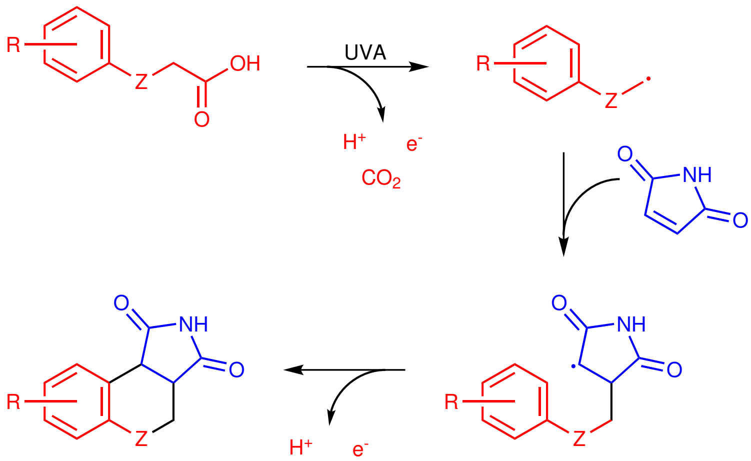

Scheme 6.15: Example of tandem ATRA-ATRC from reference [233] (Z = O, S).

6.15 Green ATRA-L

The development of green chemistry is fundamental to build more sustainable industrial processes in the future. For this reason, it is important to evaluate the ATRA-L research also from a green point of view.

Solvents are a major concern in green chemistry, due to their use in large quantities. As described in section 6.3, some of the first studies in the ATRA-L field employed acetate salts as initiators. Most of these reaction systems involved the usage of

AcOH as solvent,[185,187,190,200] which is generally considered a green choice. Other green solvents historically used are MeOH,[188,199,238,239] EtOH,[238,239] EtOAc,[218] and acetone alone[218] or acetone in combination with H_2O.[198] H_2O is undoubtedly the preferred solvent, but only a few studies performed the ATRA-L reaction in H_2O only.[212,238,239] However, the best solvent is no solvent at all. The possibility to operate a chemical reaction without solvents highly depends on the physical nature of the reagents, but some studies were able to develop solvent-free ATRA-L systems.[183,184,193] Lastly, Dupont et al.[181] described a system that does not belong to the categories just described regarding the solvent, but that is still interesting from a green point of view. They accomplished an ATRA without any solvent and a lactonization only in a second step, using just aqueous KOH.

ATRA-L systems, similar to ATRA, usually make use of transition metal catalysts. The efficient separation of reaction products from the catalyst and other substances present in the reaction mixture plays a major role in the green synthesis. It is thus important to keep the amount of catalyst and other additives as small as possible. Various pioneering studies on ATRA did not use any metal catalyst because they did not recognize how much transition metal complexes are efficient as halogen atom transfer agents. Similarly, some of the first ATRA-L processes did not use any metal catalyst, but only thermal radical initiators.[238–241] Interestingly, Triandafilli et al. recently developed a metal-free ATRA-L system, using thioxanthone as photocatalyst.[199] Noteworthy, some studies were able to reach less than 1% of catalyst load (compared to the alkene species).[188,191,192,196,198] Furthermore in ATRA and ATRP, different methods of catalyst regeneration allowed a strong decrease in the amount of required catalyst. These catalyst regeneration methods are nowadays very popular[37] and in a couple of examples, they were applied to ATRA-L systems.[199,212] For further information about these regeneration methods and how they work, see section 1.3. Finally, Iwasaki et al. recently described a simple ATRA-L process without ligands or other additives: just the two reagents, the solvent, and the catalyst.[189] Usually, simpler means also greener.

One of the principles of green chemistry concerns energy efficiency. Practically speaking, it means that temperatures and pressures of reactions should be as close as possible to the ambient ones. Various examples of ATRA-L at room temperature (and pressure) are present[200,212,217] and, as it usually is, some of them are electro-[195,211] or photo-catalyzed.[198,199]

Chapter 7

Lactonization mechanism

The mechanism of ATRA is well-established and discussed in chapter 5. The mechanism of the subsequent lactonization, on the other hand, is discussed in this chapter based on the published literature. As shown in Scheme 7.1, there are three possible mechanisms of lactonization:

- **Intramolecular nucleophilic substitution (S_Ni).** Lactonization occurs following an intramolecular nucleophilic attack on the halogen of the proper ATRA monoadduct.

- **Oxidative radical-polar crossover (ORPC).** A transition metal catalyst is generally required for this mechanism to occur. The radical C of the monoadduct is oxidized to a carbocation intermediate by the transition metal catalyst. Then, the carboxylate intramolecularly attacks the carbocation, giving the lactone.

- **Intramolecular homolytic substitution (S_Hi).** The radical monoadduct can directly undergo a cyclization without any other intermediate step.

The three mechanisms are all equally possible, but the prevalence of one over the others depends on the substrates used and the reaction conditions. However, Scheme 7.1 does not represent all the variants and the possibilities, but it only aims to summarize the main mechanisms. For the full discussion of S_Ni, ORPC, and S_Hi mechanisms, see sections 7.1, 7.2, and 7.3, respectively.

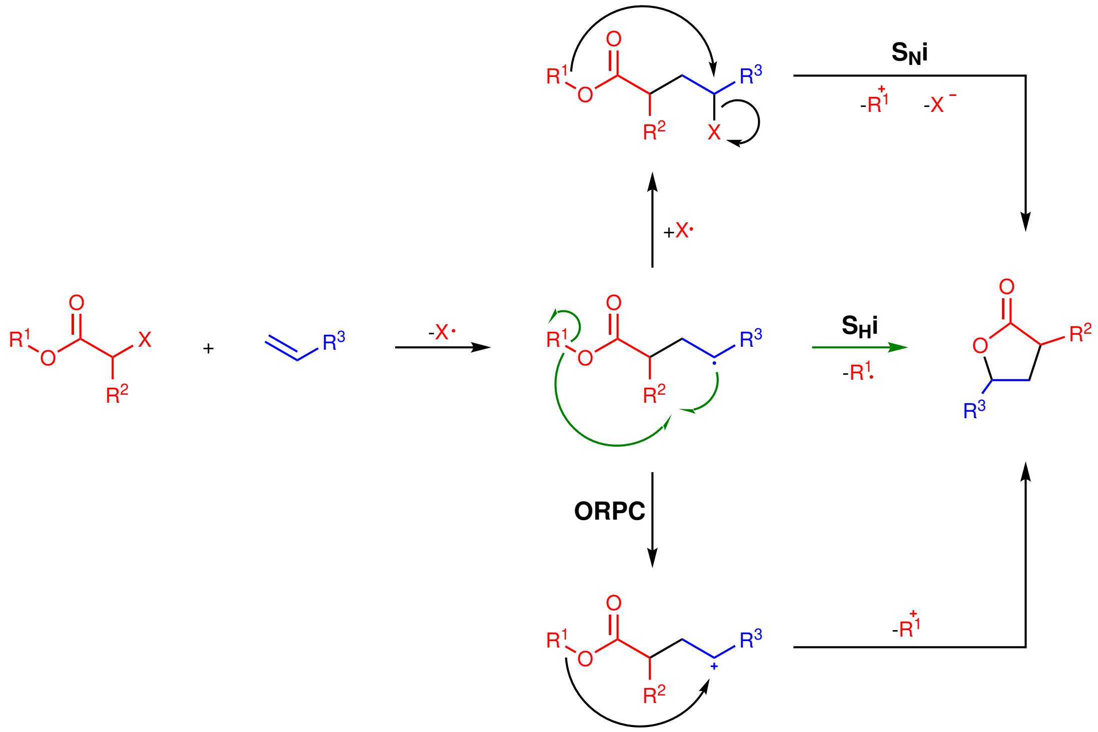

Scheme 7.1: Three main possible mechanisms for the lactonization after radical addition: S_Ni, ORPC, and S_Hi. For simplicity, only three substituents are shown (R^{1-3}), although the haloester could have one more and the alkene could have three more.

7.1 Intramolecular nucleophilic substitution

Some studies proposed the S_Ni to be the mechanism of lactonization, but without hard evidence.[212,241] On the other hand, Triandafillidi et al. recently brought solid evidence about the S_Ni mechanism taking place in their reaction system.[199] As shown in Scheme 7.2, the two reactants are an iodoacetic acid derivative and a 3,3-disubstituted propene. The reaction is performed in MeOH:MeCN (1:1) with a Ru photocatalyst regenerated by sodium ascorbate (NaAs). They collected evidence with high-resolution mass spectroscopy (HRMS) and NMR spectroscopy of the existence of the proper γ-iodinated ATRA product during the reaction. Therefore, they supposed that the ATRA product was converted to lactone via S_Ni by the attack of the carboxylic group to the γ-C bearing the iodine.

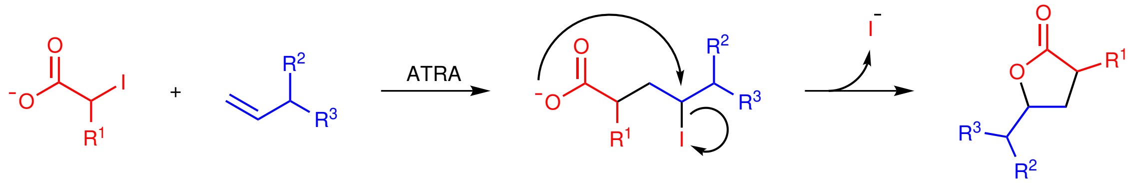

Scheme 7.2: Example of S_Ni mechanism from reference [199].

In their study, not only carboxylic acids but also esters gave lactonization, even if with slightly lower yields. If a carboxylate is required for the nucleophilic attack and the consequent lactonization, then a carboxylic acid just needs to be deprotonated, while an ester needs to be hydrolyzed. Therefore, the authors proposed that the basic conditions of their system could easily hydrolyze the ester. In fact, they used an equimolar amount of NaAs compared to the ester.

The fact that the hydrolysis can happen was proved by Iwasaki et al.[189] They performed an Fe-catalyzed ATRA-L in DMF, with 2 equiv of H_2O (compared to the alkene) and at 80 °C. As shown in Scheme 7.3, both the carboxylic acid (R = H) and the ester (R = Et) gave lactonization. However, ^{18}O from $H_2{}^{18}O$ was included in the lactone structure only when the ester was used (and not the carboxylic acid). Therefore, the ester requires hydrolysis in order to lactonize. They formulated an interesting mechanism, where the carbonyl O atom attacks the γ-C, forming a cyclic oxonium intermediate. Only at this point, the hydrolysis occurs and the ^{18}O consequently occupies the carbonyl position in the end. However, the authors were not sure about the nature of the γ-C of the addition monoadduct, if it was halogenated or if it was a carbocation intermediate. Consequently, in this study, it is undefined if the mechanism is a S_Ni or an ORPC. Anyhow, it is defined that the ester needs to be hydrolyzed to give lactonization.

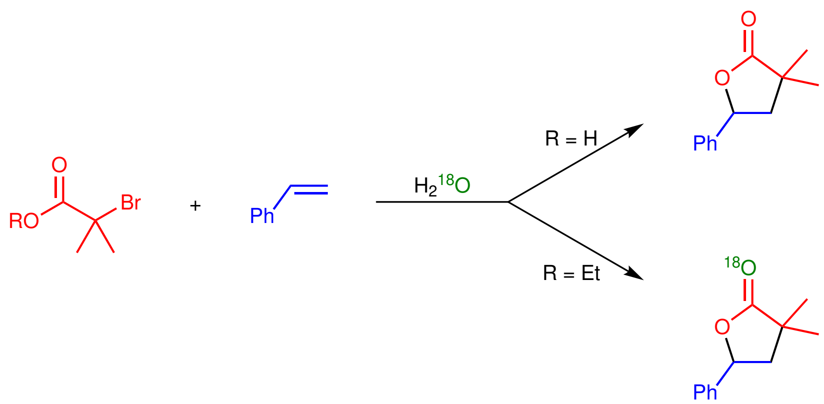

Scheme 7.3: Isotopic labeling experiment of ATRA-L from reference [189].

Furthermore, the experiment of Scheme 7.3 implicitly suggested that two S_Ni are mechanisms possible, depending on which O atom is attacking the γ-C (carbonyl or ethereal O). In the case of a deprotonated carboxylic acid however, the negative charge is delocalized between the two O atoms and they are equivalent towards the nucleophilic attack.

7.1.1 The case of tributylstannyl esters

The lactonization mechanism of tributylstannyl ester monoadducts was discussed by Kraus and Landgrebe whether it was S_Ni or S_Hi.[207,208] As depicted in Scheme 7.4, the S_Ni requires the deactivation step that brings the halogen back on the monoadduct, quenching the radical. Degueil-Castaing et al. showed in one experiment that the S_Hi is, in general, a slower process than the halogen abstraction by the radical monoadduct.[209] In other words, the radical monoadduct seems to preferably follow the halogen abstraction path of Scheme 7.4, not the S_Hi. Therefore, for the halogenated tributylstannyl ester monoadduct, the only possible mechanism of lactonization is the S_Ni.

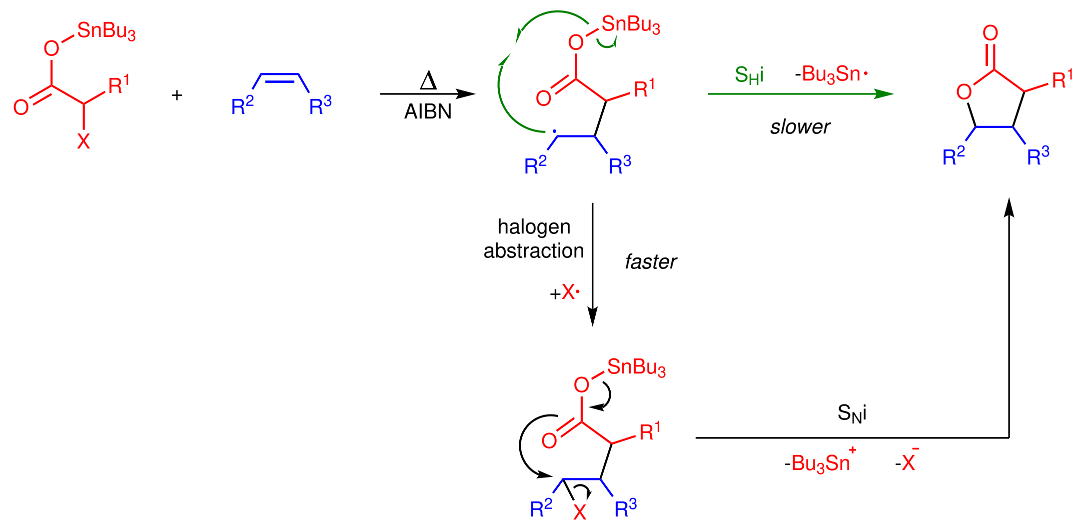

Scheme 7.4: Two possible ways of lactonization of tributylstannyl ester radical monoadducts from references [207–209].

7.2 Oxidative radical-polar crossover

Two different studies on ATRA-L reaction proposed the ORPC to be the mechanism of formation of a carbocation intermediate, which is then intramolecularly attacked by an O atom of the carboxylic group.[194,198] Both these studies perform a reaction in MeCN in the presence of H_2O, but one has an Ir photocatalyst,[198] while the other one has a Cu catalyst.[194] Besides this and other small differences, they propose two very similar mechanisms from isotopic labeling experiments, summarized in Scheme 7.5. The C−Br bond of the ester is homolytically broken by oxidation of the metal catalyst. Then, radical addition on the alkene double bond occurs. The newly generated radical monoadduct is oxidized by the metal catalyst, giving the carbocation. The nucleophilic attack on the carbocation by $H_2{}^{18}O$ results in the γ-hydroxybutyrate ester, able to lactonize. Overall, the metal catalyst is regenerated, because in one step is oxidized and in the other is reduced. The net result of this ATRA-L process is the elimination of HBr and R^1OH. Furthermore, a third study suggested the formation of a γ-hydroxy ester, but as a consequence of the oxidation of the radical γ-C by O_2, without involving carbocations and H_2O.[196] This third study is discussed in section 6.8.

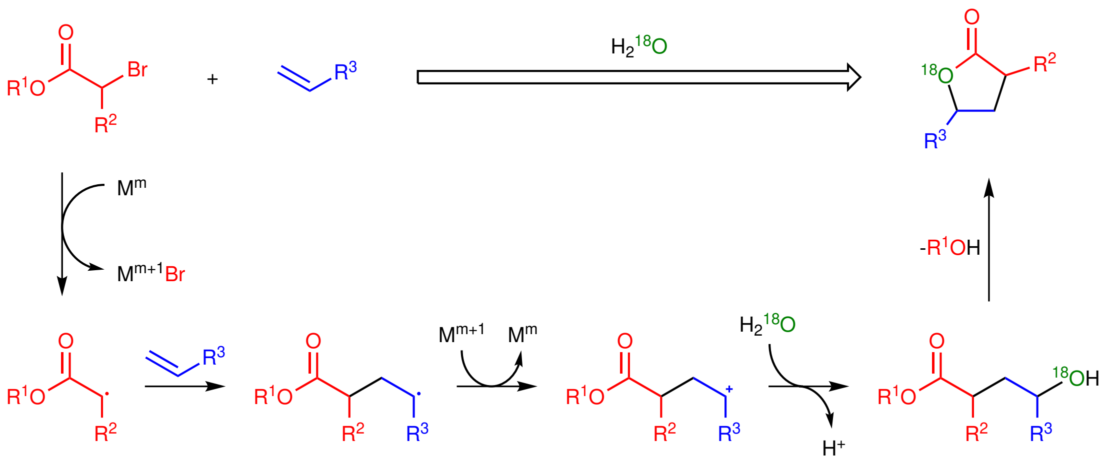

Scheme 7.5: Mechanism of isotopic labeling experiment of ATRA-L from references [194,198] (M = transition metal catalyst). For simplicity, only three substituents are shown (R^{1-3}), although the haloester could have one more and the alkene could have three more.

Someone could argue that a carbocation can also be formed as intermediate of a S_N1, as well as ORPC. Therefore, if the S_Ni mechanism described in section 7.1 reflects a S_N1 rather than a S_N2, then S_Ni and ORPC mechanisms are crossed. However, no published papers proposed that the carbocation is formed as S_N1 intermediate. It should only be kept in mind that the carbocation can be formed in both ways, but no evidence for S_N1 mechanisms was found in the literature.

7.3 Intramolecular homolytic substitution

The S_Hi can occur in two different ways, depending on the involved O atom, as shown in Scheme 7.6. The orange arrows describe the lactonization involving the ethereal O atom and the final product is obtained in a single step. The green arrows describe the attack of the radical to the carbonyl double bond, leading to a radical acetal which, in a second step, fragments into the final lactone. In the end, the two S_Hi mechanisms lead to the same product, but the positions of the two O atoms are inverted. To the best of my knowledge, no published papers proved the existence of one mechanism rather than the other in the field of ATRA-L reactions.

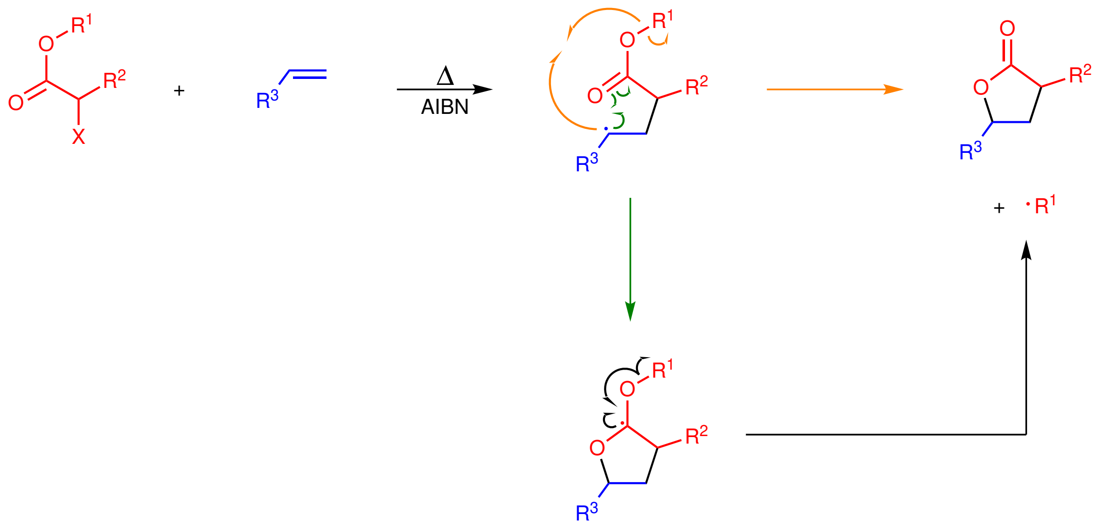

Scheme 7.6: Two possible mechanisms of S_Hi. For simplicity, only three substituents are shown (R^{1-3}), although the haloester could have one more and the alkene could have three more.

7.3.1 The case of $Mn(OAc)_3$

The ATRA-L with $Mn(OAc)_3$ discussed in section 6.3 can follow only the ORPC or the S_Hi mechanism, but not the S_Ni due to the absence of halogens. As shown in Scheme 7.7, $Mn(OAc)_3$ is able to generate carboxymethyl radicals when heated, which can give addition to an alkene, generating a radical monoadduct. Heiba et al. proposed the ORPC pathway, following electron transfer to Mn^{III}.[187,190] A carbocation is then obtained and it is intramolecularly attacked by the carboxylic O atom to give the γ-lactone. Nevertheless, the formation of the carbocation was disproved by Fristad and Peterson.[201] They used norbornene as alkene, obtaining the expected γ-lactone. However, 2-norbornyl cation is known to give rapid rearrangement,[242] while 2-norbornyl radical does not.[243] Therefore, the radical monoadduct can give lactonization without the intervention of carbocations, probably following a S_Hi mechanism.

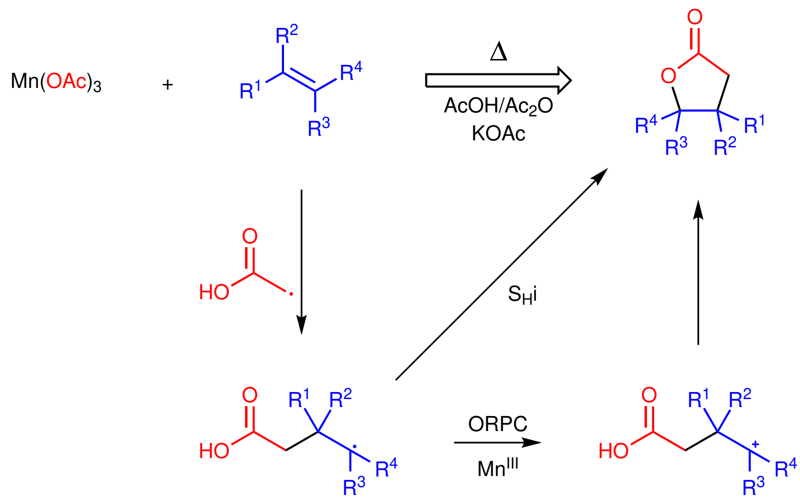

Scheme 7.7: Two possible mechanisms of ATRA-L with $Mn(OAc)_3$. The ORPC path was conceived in references [187,190], while the S_Hi one in reference [201].

7.4 Conclusion

Reagents and reaction conditions can play a crucial role in the selected reaction pathway, but the three main mechanisms (S_Ni, ORPC, and S_Hi) are all possible according to the published literature. Each one of these mechanisms is not rigid and can have some variations.

The S_Ni reaction pathway requires the completion of the ATRA reaction with the generation of the proper ATRA product. If the monoadduct is a carboxylic acid (or a carboxylate), the intramolecular nucleophilic attack is straightforward. If the monoadduct is an ester, the nucleophilic attack seems to be performed by the carbonyl O atom to form a cyclic oxonium intermediate, which is then hydrolyzed to a lactone. However, it is not possible to exclude other two S_Ni mechanisms of γ-haloester monoadducts. One is the hydrolysis to carboxylic acid before the nucleophilic attack. The other is the nucleophilic attack by the ethereal O atom.

Regarding the ORPC mechanism, two different pathways are possible. The first is the direct intramolecular nucleophilic attack of the carboxylic acid or the carbonyl group to the carbocation. The other one is the nucleophilic attack from an external H_2O molecule to the carbocation, giving a γ-hydroxybutyrate ester able to lactonize. Although there are only examples of the latter mechanism, the former also seems plausible.

The S_Hi mechanism can occur in two different ways, depending on the involved O atom. The result is the same lactone, but the O atoms are inverted. Nevertheless, the S_Hi seems to be a slower reaction than the S_Ni. Therefore, the only case where this mechanism should be considered is when no halogens are present in the reaction system.

Chapter 8

Materials and methods

Unless differently stated, the MR of a reactant is always referred to the absolute quantity of the alkene species.

8.1 Experimental section

8.1.1 Chemicals

BiBA (TCI, 98%), 2-hydroxyethyl 2-bromoisobutyrate (HEBiB) (Sigma-Aldrich, 95%), NaOH (Sigma-Aldrich, 97.0%), triethylamine (TEA) (Sigma-Aldrich, 99.5%), Na_2CO_3 (Sigma-Aldrich, 99%), Cs_2CO_3 (Sigma-Aldrich, 99%), $CuBr_2$ (Sigma-Aldrich, 99%), $Cu(MeCN)_4BF_4$ (TCI, 98%), TPMA (Ambeed, 97%), 2,2′-bipyridine (bpy) (Sigma-Aldrich, 99%), NaBr (Fisher Scientific, 99.0%), DMF (Sigma-Aldrich, 99.8%), DMSO (Sigma-Aldrich, 99.5%), phosphate-buffered saline (PBS) solution (Fisher Scientific), and 37% HCl aqueous solution (Fisher Scientific, ACS grade) are used without purification. The PBS solution (pH = 7.4) is an aqueous solution of KH_2PO_4 ($10.6\,\mathrm{mmol\,L^{-1}}$), $Na_2HPO_4 \cdot 7\,H_2O$ ($29.7\,\mathrm{mmol\,L^{-1}}$) and NaCl ($1.55\,\mathrm{mol\,L^{-1}}$). CuBr (Sigma-Aldrich, 98%) is purified under N_2 by washing three times with glacial AcOH, two times with EtOH, two times with Et_2O, and then dried overnight under N_2 flow. Acrylic acid (AA) (Sigma-Aldrich, 99%) and MAA (Sigma-Aldrich, 99%) are distilled under vacuum to remove polymerization inhibitors and are stored in a refrigerator under N_2 atmosphere. 2-(Dimethylamino)ethyl methacrylate (DMAEMA) (Sigma-Aldrich, 98%), 2-hydroxyethyl methacrylate (HEMA) (Sigma-Aldrich, 99%), and *N*-[3-(dimethylamino)propyl]methacrylamide (DMAPMAm) (Sigma-Aldrich, 99%)

are passed through basic alumina before use to remove inhibitors. Cu wire (Alfa Aesar, 99.9%) is washed for 30 min in MeOH/HCl (3:1, V/V) before use, then rinsed with MeOH and dried under N_2.

8.1.2 General procedures

Normal ATRA-L

Entry A01 of Table 8.2 is described as a typical experiment. 100 µL of MAA (101.5 g, 1.18 mmol), 1400 µL of H_2O, 500 µL of 1.18 mol L^{-1} NaBr stock solution (0.590 mmol), 62.1 µL of 19.0 mol L^{-1} NaOH stock solution (1.18 mmol), and DMF (9.13 µL) or DMSO (8.38 µL) as internal standard are added to a sealed vial for degassing (bubbling N_2 for 30 min). This solution is then transferred to the 4 mL reaction vial containing 197.0 mg of BiBA (1.18 mmol), 16.9 mg of CuBr (0.118 mmol), 68.5 mg of TPMA (0.236 mmol), a N_2 atmosphere, and a magnetic stirrer. The reaction vial is submerged in a water bath thermostated at 25 °C with a fast stirring. Small withdrawals from the reaction mixture are made to study the evolving of the reaction over time via ^{1}H NMR and to stop the reaction when the initiator or the alkene are completely consumed.

SARA ATRA-L

Entry A04 of Table 8.2 is described as a typical experiment. 100 µL of MAA (101.5 g, 1.18 mmol), 1300 µL of H_2O, 500 µL of 1.18 mol L^{-1} NaBr stock solution (0.590 mmol), 62.1 µL of 19.0 mol L^{-1} NaOH stock solution (1.18 mmol), 100 µL of 11.8 mmol L^{-1} $CuBr_2$ stock solution (1.18 mmol), and DMF (9.13 µL) or DMSO (8.38 µL) as internal standard are added to a sealed vial for degassing (bubbling N_2 for 30 min). This solution is then transferred to the 4 mL reaction vial containing 197.0 mg of BiBA (1.18 mmol), 6.8 mg of TPMA (24 mmol), a N_2 atmosphere, and Cu wire (d = 1 mm, l = 10 cm) wrapped around a magnetic stirrer. The reaction vial is submerged in a water bath thermostated at 25 °C with a fast stirring. Small withdrawals from the reaction mixture are made to study the evolving of the reaction over time via ^{1}H NMR and to stop the reaction when the initiator or the alkene are completely consumed.

Yield determination and kinetics

The yield is calculated based on ^{1}H NMR integrals and DMF or DMSO is used as internal standard. The mol % of DMF or DMSO is constant and it is defined at $t = 0$ compared to 100 mol % of the alkene monomer. If the reaction is so fast that at $t = 0$ a small amount of the lactone is already present, both the alkene monomer and the lactone contribute to the 100 mol %.

Various NMR spectra are collected during an experiment to perform a kinetic evaluation of the reaction. The values of NMR integrals are used to determine the relative amounts of all the species that are present at a certain time inside the reaction mixture. A reaction is stopped when one of the reagents is completely consumed or when no change is observed in the reaction mixture for a relatively long period. In this way, it is very difficult to know exactly when a reaction reached completion. This would require an unnecessary big number of withdrawal from the reaction mixture and NMR analyses. On the other hand, the kinetic evaluation can give a clear idea of how fast the reaction was.

pH measurement

The instrument is calibrated with a pH = 4 buffer solution before use. The temperature of the laboratory and the solution is (25 ± 2) °C for every measurement. The mixtures used to determine the pH are prepared as described in the general procedures (subsection 8.1.2), but scaled up three times. Regarding the normal procedure, CuBr is substituted with $CuBr_2$ and NaBr is decreased accordingly to the higher amount of Br^- coming from $CuBr_2$. Regarding the SARA procedure, Cu wire is the only reagent that is not added to the mixture. The pH is measured as soon as a base (NaOH or DMAEMA) is added, because over time the pH has the tendency to decrease due to initiator hydrolysis.

8.1.3 Instrumentation

^{1}H NMR spectra are obtained with an Avance III 500 MHz (Bruker) spectrometer. ^{13}C, HSQC, and HMBC NMR are obtained with an Avance Neo 500 MHz (Bruker) spectrometer. Deionized H_2O is further purified with the Barnstead Nanopure (Fisher

Scientific). pH is measured with an Orion Versa Star Pro (Fisher Scientific) and an Orion ROSS Ultra (8157BNUMD) (Fisher Scientific) electrode.

8.2 pH determination

The pH is a fundamental parameter for the reaction system of this study. Both the rate of activation of the ATRA and the rate of lactonization are pH-dependent, influencing the entire ATRA-L process. The hydrolysis side reaction is also highly influenced by the pH. Therefore, it is important to evaluate the pH for every reaction.

However, there are three different problems in experimentally measuring the pH of an ATRA-L reaction. *(i)* The hydrolysis of the initiator decreases the pH over time. As shown in the equilibrium below, the hydrolysis generates hydrogen halides, which are doubtless acidic. Hydrogen halides are formed in the time between mixing the reagents and receiving a response from the pH meter, resulting in an error in the measurement. The pH meter can take indeed a few minutes to perform a measurement, because the pH is not stable, but decreasing. In one experiment with a theoretical pH of 4.0, it was observed a pH decrease of 0.1 within the first three minutes and another 0.1 in the next seven minutes. It is difficult to avoid this systematic error.

$$\mathrm{R{-}X} + \mathrm{H_2O} \rightleftharpoons \mathrm{R{-}OH} + \mathrm{HX}$$

(ii) All the reactions of this study are performed in a non-oxidizing environment with an inert gas, where Cu^{I} is stable. Unfortunately, the measurement of the pH is open to the air and the O_2 can affect the reagents. This is not a problem since the only involved reaction should be the oxidation of Cu^{I} to Cu^{II}, which does not significantly interfere with the pH. However, this difference in the presence of O_2 could result in another systematic error.

(iii) A relatively large volume of the reaction mixture is required to measure the pH, resulting in a big waste. For instance, TPMA is one of the most expensive reagents used in this study, and one pH determination experiment could waste more than 200 mg of it. As a result, measuring the pH of every experiment can be a big waste of the research group resources.

For all these reasons, it was considered to determine the pH theoretically. However, the theoretical pH determination accepts some assumptions and approximations. The first one is that only the free ligand that is not bound to Cu is considered to influence the pH. When binding the Cu, the N atoms from the ligand do not have a free electron pair to accept any H^+. In other words, it is assumed that the ligand influences the pH, but its complex does not. For example, if in a system the ratio of Cu:TPMA is 1:2, then only half of the TPMA affects the pH because the other half is bound to Cu. Moreover, only one $\mathrm{p}K_\mathrm{a}$ is used for the ligands (TPMA and bpy) because no other data were found in the literature. Another assumption is about the use of theoretical $\mathrm{p}K_\mathrm{a}$ values. As reported in Table 8.1, half of the used $\mathrm{p}K_\mathrm{a}$ values are calculated. It is assumed that these values are correct or at least very close to the real ones. Finally, the second acidic dissociation of DMAPMAm is not considered because its $\mathrm{p}K_\mathrm{a2}$ value is relatively large (15.01 ± 0.46, theoretical and calculated like the other theoretical values of Table 8.1). The equilibrium is strongly shifted toward the undissociated form and this approximation is absolutely not significant.

Substance	**pK_a**	**Reference**
MAA	4.66	[244]
AA	4.25	[245]
DMAEMA	8.18 ± 0.28	calc[a]
DMAPMAm	9.39 ± 0.28	calc[a]
BiBA	2.91 ± 0.10	calc[a]
TPMA	4.96 ± 0.12	calc[a]
bpy	4.35	[246]
TEA	10.75	[245]

Table 8.1: $\mathrm{p}K_\mathrm{a}$ values for the used weak acids and bases. [a]Calculated using Advanced Chemistry Development (ACD/Labs) software v11.02 (© 1994–2021 ACD/Labs).

8.2.1 Example of pH calculation

Entry A01 of Table 8.2 is used as example of the method used for the theoretical determination of the pH. The conditions are MAA:BiBA:NaOH:NaBr:CuBr:TPMA = 1:1:1:0.5:0.1:0.2 with $C_\mathrm{MAA} = 0.590\,\mathrm{mol\,L^{-1}}$. Since NaBr and $\mathrm{Cu^I}$(TPMA)Br complex are not affecting the pH, the system can be simplified to MAA:BiBA:NaOH:TPMA = 1:1:1:0.1. Furthermore, it can be considered the quantitative reaction between

NaOH and one of the acids, like BiBA. Since BiBA and NaOH are present in equimolar amounts, all the BiBA is simply converted to α-bromoisobutyrate anion (BiB^-) and the system is further simplified to MAA:BiB^-:TPMA = 1:1:0.1. It is now possible to write the three equilibria below at $t = 0$ and at $t =$ equilibrium, where MAA is deprotonated to methacrylate anion (MA^-) and TPMA is protonated to tris(2-pyridylmethyl)ammonium cation ($TPMAH^+$).

t	**MAA**	$\rightleftharpoons$	$\mathbf{MA^-}$	+	$\mathbf{H^+}$
0	0.590		0		~ 0
eq	$0.590 - x$		x		x

	BiBA	$\rightleftharpoons$	$\mathbf{BiB^-}$	+	$\mathbf{H^+}$
0	0		0.590		~ 0
eq	y		$0.590 - y$		$-y$

	$\mathbf{TPMAH^+}$	$\rightleftharpoons$	**TPMA**	+	$\mathbf{H^+}$
0	0		0.059		~ 0
eq	z		$0.059 - z$		$-z$

From the definition of pK_a ($\frac{[A^-][H^+]}{[AH]} = 10^{-pK_a}$), it is possible to formulate the System of Equations 8.1. Being H^+ a common ion for the three equilibria, its concentration is equal to $x - y - z$. The system has a unique solution for positive x, y, and z. Sparing all the calculations, the pH is evaluated with Equation 8.2 and it is equal to approximately 4.0.

$$\begin{cases} \frac{x(x-y-z)}{0.590-x} & = & 10^{-4.66} \\ \frac{(0.590-y)(x-y-z)}{y} & = & 10^{-2.91} \\ \frac{(0.059-z)(x-y-z)}{z} & = & 10^{-4.96} \end{cases} \tag{8.1}$$

$$\text{pH} = -log_{10}[H^+] = -log_{10}(x - y - z) \approx 4.0 \tag{8.2}$$

8.2.2 Comparison between experimental and theoretical pH values

How accurate is the model for the determination of the theoretical pH? The answer to this question can be found in Table 8.2, where are reported both experimental and theoretical pH values from seven different reaction systems.

The difference between the two pH values (experimental and theoretical) is always smaller than 0.3. This is not true for entry A13 of Table 8.2, where the pH is so high and close to the neutrality that it is rapidly decreased by the fast BiBA hydrolysis. As a result, the experimental pH of entry A13 is highly underestimated.

Entry	**Monomer**	**Base** (MR)	$\mathbf{pH_{exp}}$	$\mathbf{pH_{th}}$
A01	MAA	NaOH (1)	3.8	4.0
A06	MAA	NaOH (0.5)	3.2	3.0
A07	MAA	—	1.9	2.0
A23	AA	NaOH (1)	3.7	3.7
A13	DMAEMA	—	5.0	6.1
A17[a]	MAA	NaOH (1)	3.8	4.1
A04[b]	MAA	NaOH (1)	3.7	3.8

Table 8.2: Experimental versus theoretical pH. Conditions: monomer:BiBA:CuBr:TPMA:NaBr = 1:1:0.1:0.2:0.5, $C_{\text{monomer}} = 0.590\,\text{mol}\,\text{L}^{-1}$. [a]bpy (with MR of 0.4) was used instead of TPMA. [b]Conditions (SARA): MAA:BiBA:$CuBr_2$:TPMA:NaBr = 1:1:0.001:0.02:0.5 and Cu wire 10 cm.

Since the hydrolysis of BiBA is decreasing the pH, the experimental values should be lower than the theoretical ones. Satisfyingly, this is true for all the entries of Table 8.2, except for entry A06, but there is a simple explanation for it. BiBA is not completely soluble in the reaction system of entry A06 because it is missing an equimolar amount of NaOH, which is generally required to completely solubilize BiBA in H_2O. As a result, the experimental pH of reaction A06 is higher because not all the BiBA can be solubilized.

From the satisfying results of Table 8.2, it is safe to assume that the model for the determination of the theoretical pH values is accurate and that it solves the problems encountered during the experimental determination of the pH values. The model is accurate enough to evaluate the difference in the pH between various reaction systems. Therefore, all the pH data reported in chapter 9 are theoretical and valid only at the beginning of the reaction. In fact, after the start of the reaction, the hydrolysis of the initiator can decrease the pH value.

8.3 Nuclear magnetic resonance characterization

In this section are shown the most significant examples of NMR spectra. The ^{1}H NMR spectra of the BiBA-initiated ATRA-L reactions with MAA, AA, HEMA, DMAEMA, and DMAPMAm are highlighted in Figures 8.1, 8.2, 8.3, 8.4, and 8.5, respectively. Figure 8.6 shows the NMR progression over time of a normal ATRA-L reaction between MAA and BiBA. ^{1}H, ^{13}C, HSQC, and HMBC NMR were collected of a SARA ATRA-L reaction in order to fully characterize the lactone (Figures 8.7 and 8.8).

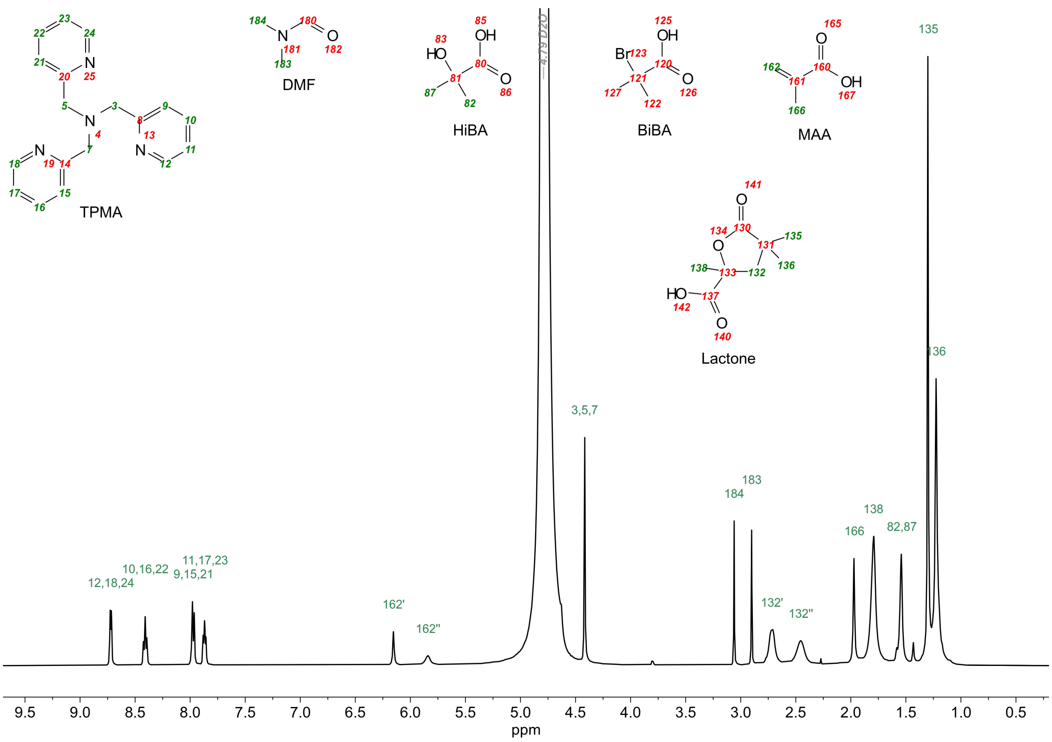

Figure 8.1: ^{1}H NMR spectrum of normal ATRA-L with MAA (entry A01 of Table 9.9 after 19 h).

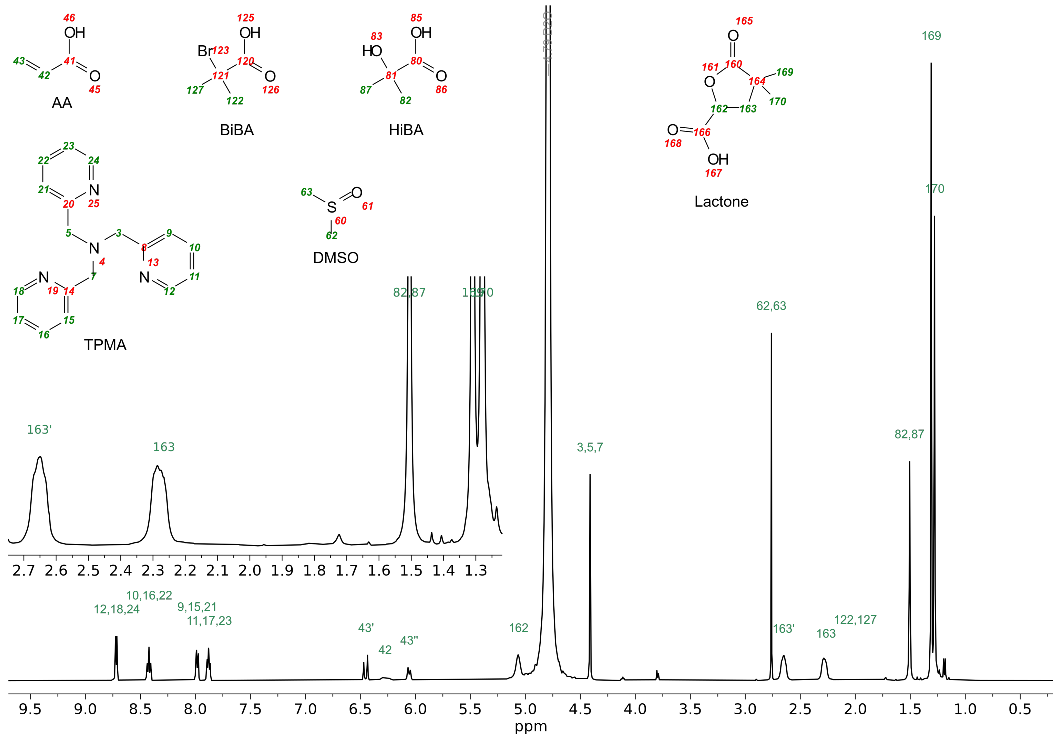

Figure 8.2: ^{1}H NMR spectrum of normal ATRA-L with AA (entry A23 of Table 9.9 after 22 h).

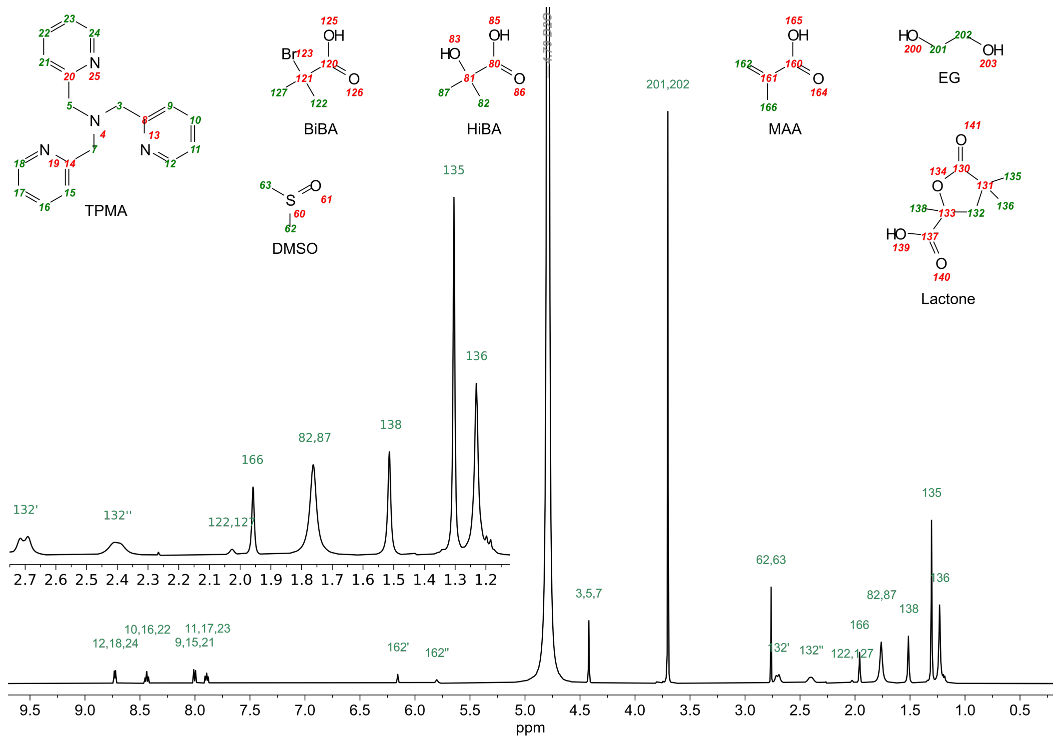

Figure 8.3: ^{1}H NMR spectrum of normal ATRA-L with HEMA (entry A08 of Table 9.9 after 3.5 h). HEMA was completely hydrolyzed into MAA and ethylene glycol (EG).

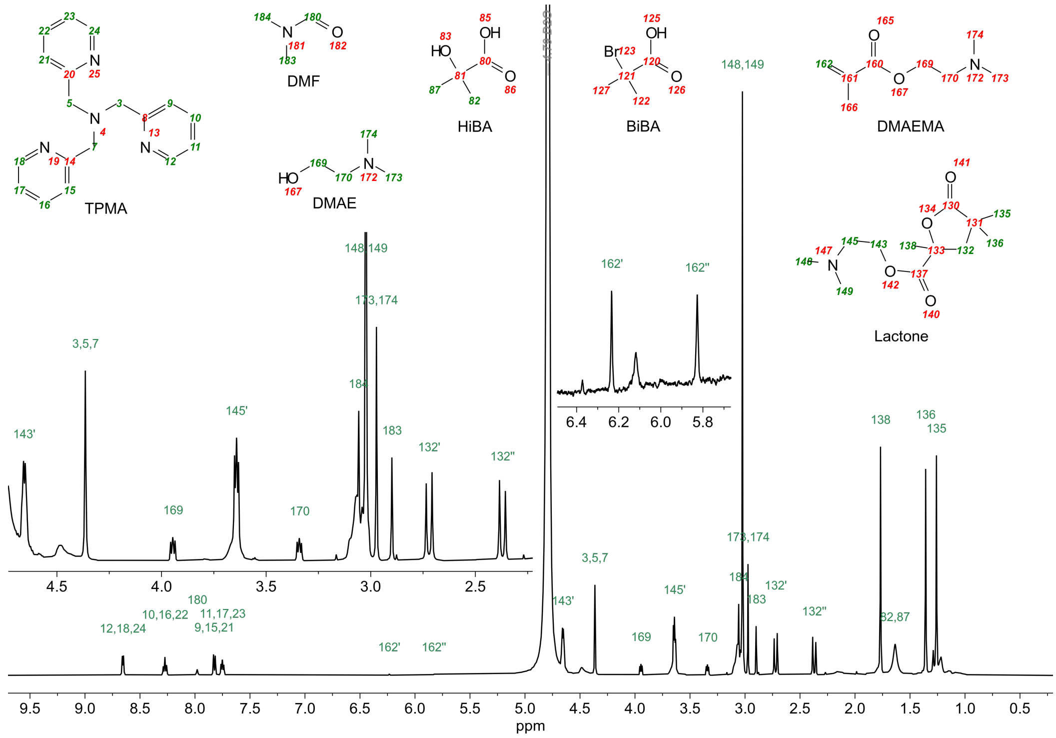

Figure 8.4: ^{1}H NMR spectrum of normal ATRA-L with DMAEMA (entry A13 of Table 9.9 after 5 h).

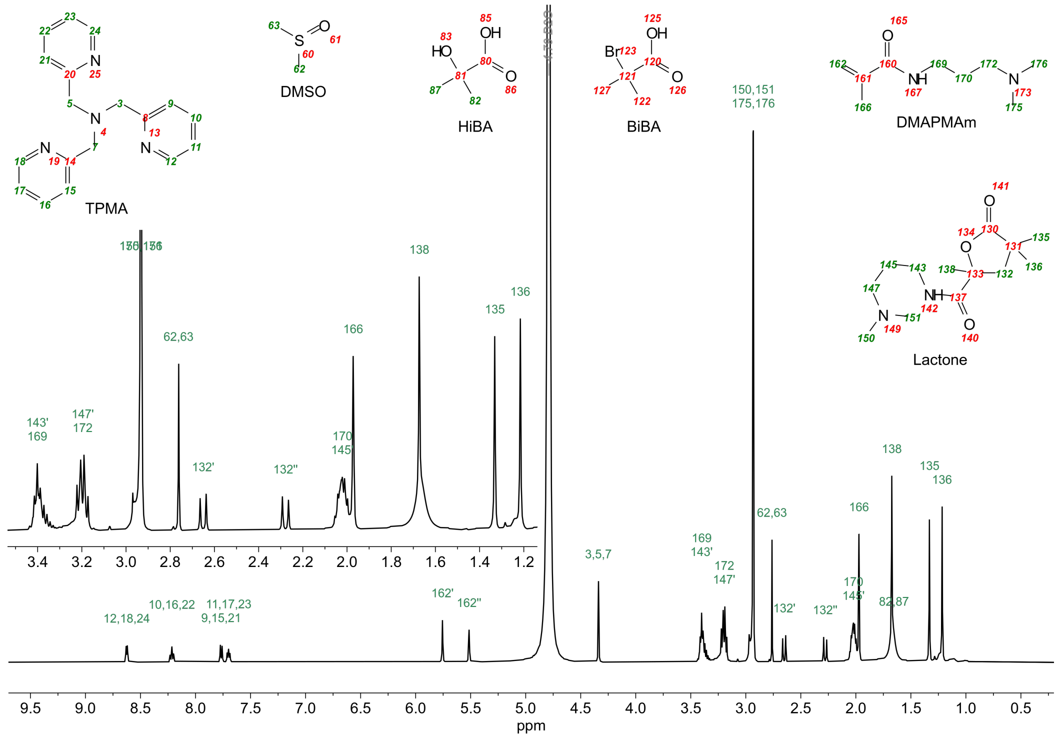

Figure 8.5: ^{1}H NMR spectrum of normal ATRA-L with DMAPMAm (entry A24 of Table 9.9 after 16 h).

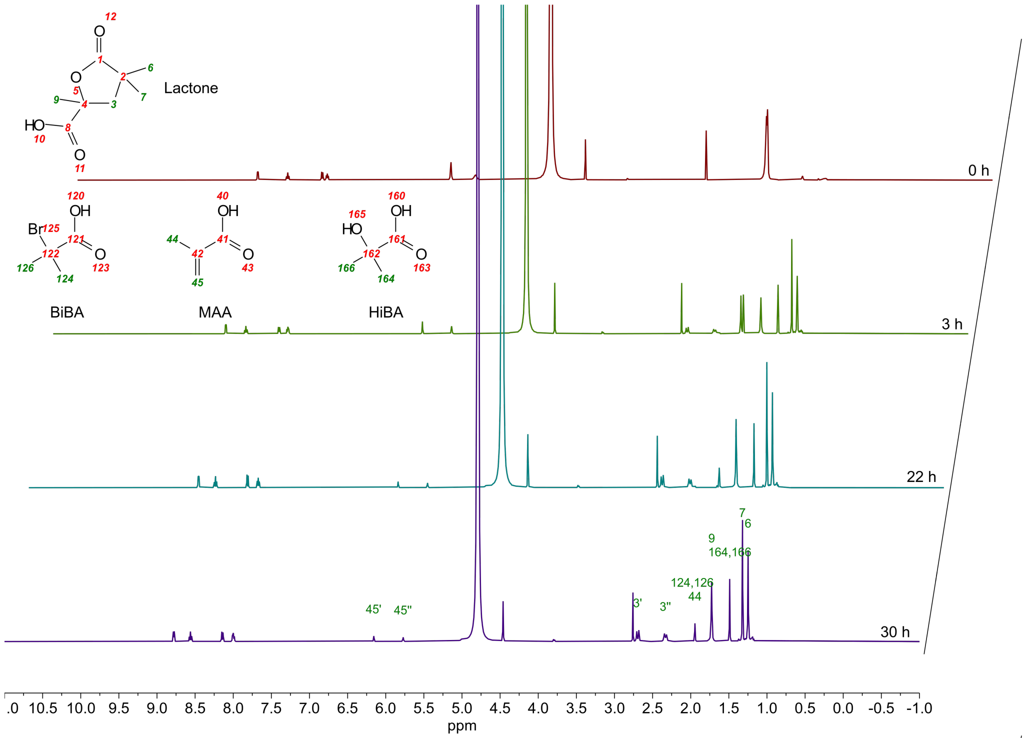

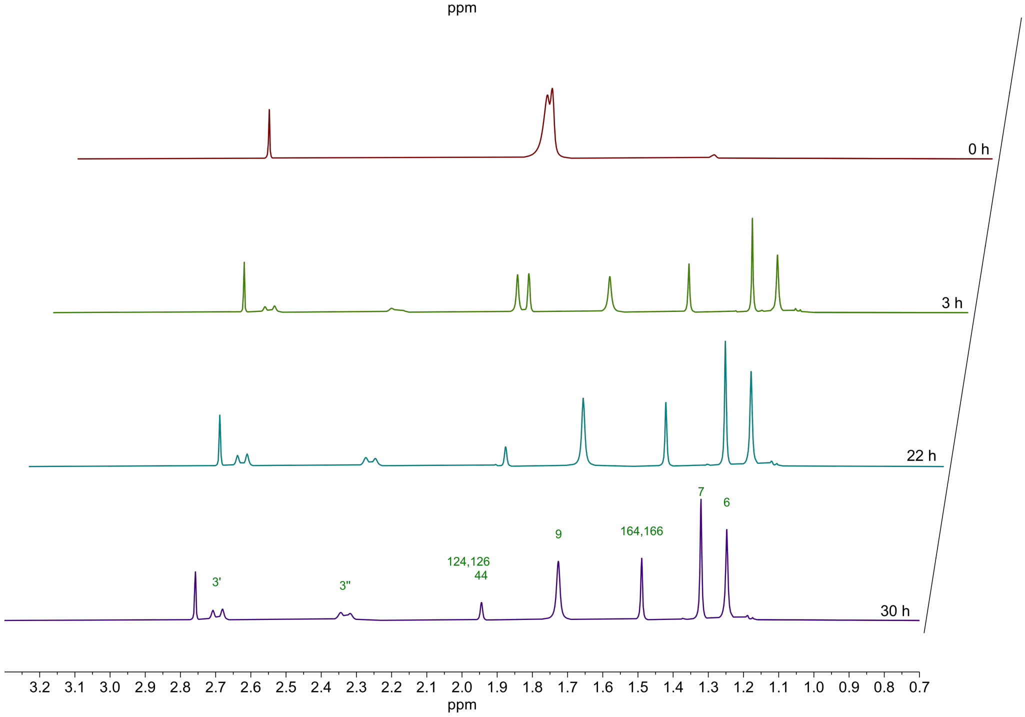

Figure 8.6: ^{1}H NMR spectra of normal ATRA-L with MAA versus time (entry A06 of Table 9.2) (*top*) and its expansion (*bottom*).

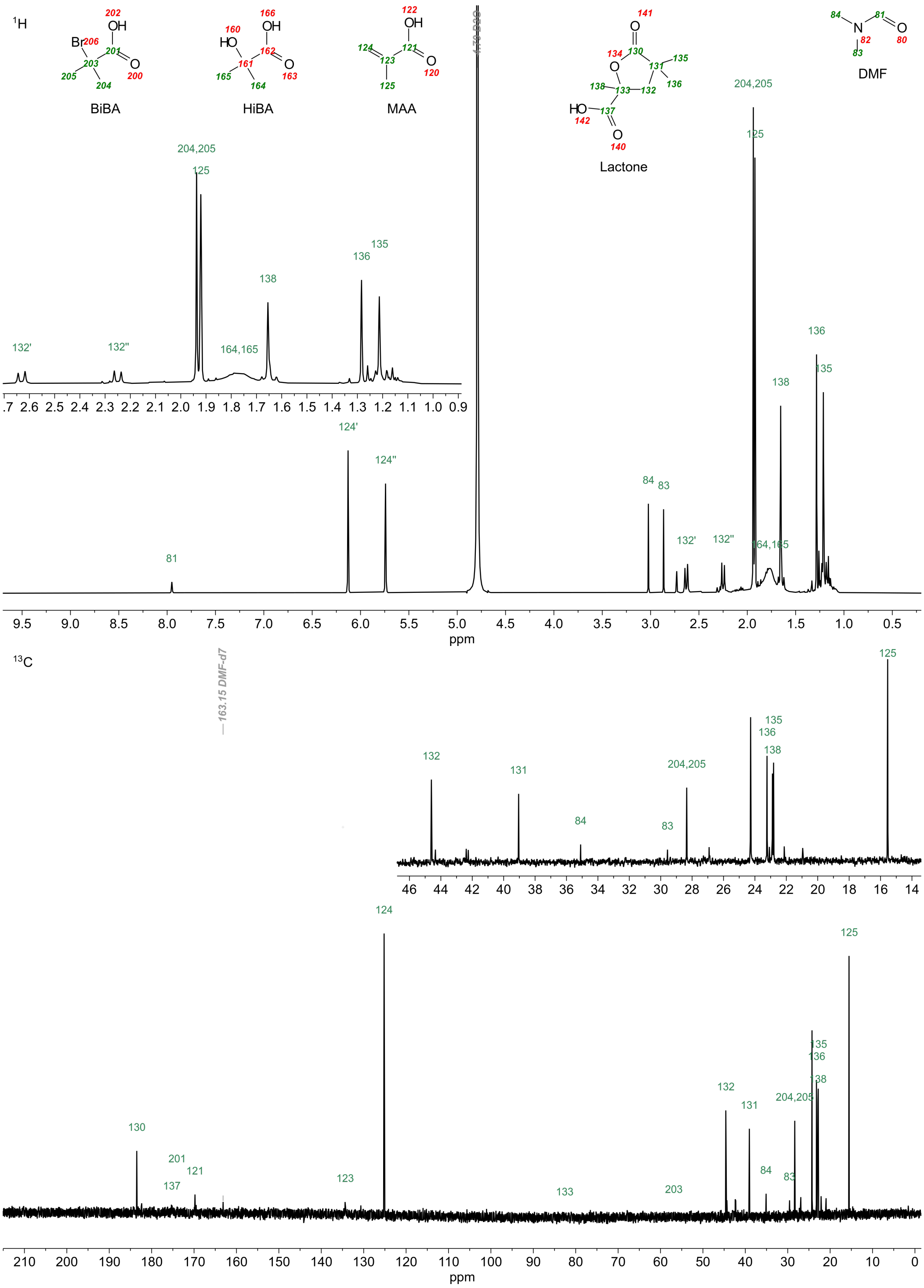

Figure 8.7: ^{1}H (*top*) and ^{13}C (*bottom*) NMR spectra of SARA ATRA-L with MAA (entry A05 of Table 9.1 after 6.3 h). HSQC and HMBC spectra are reported in Figure 8.8.

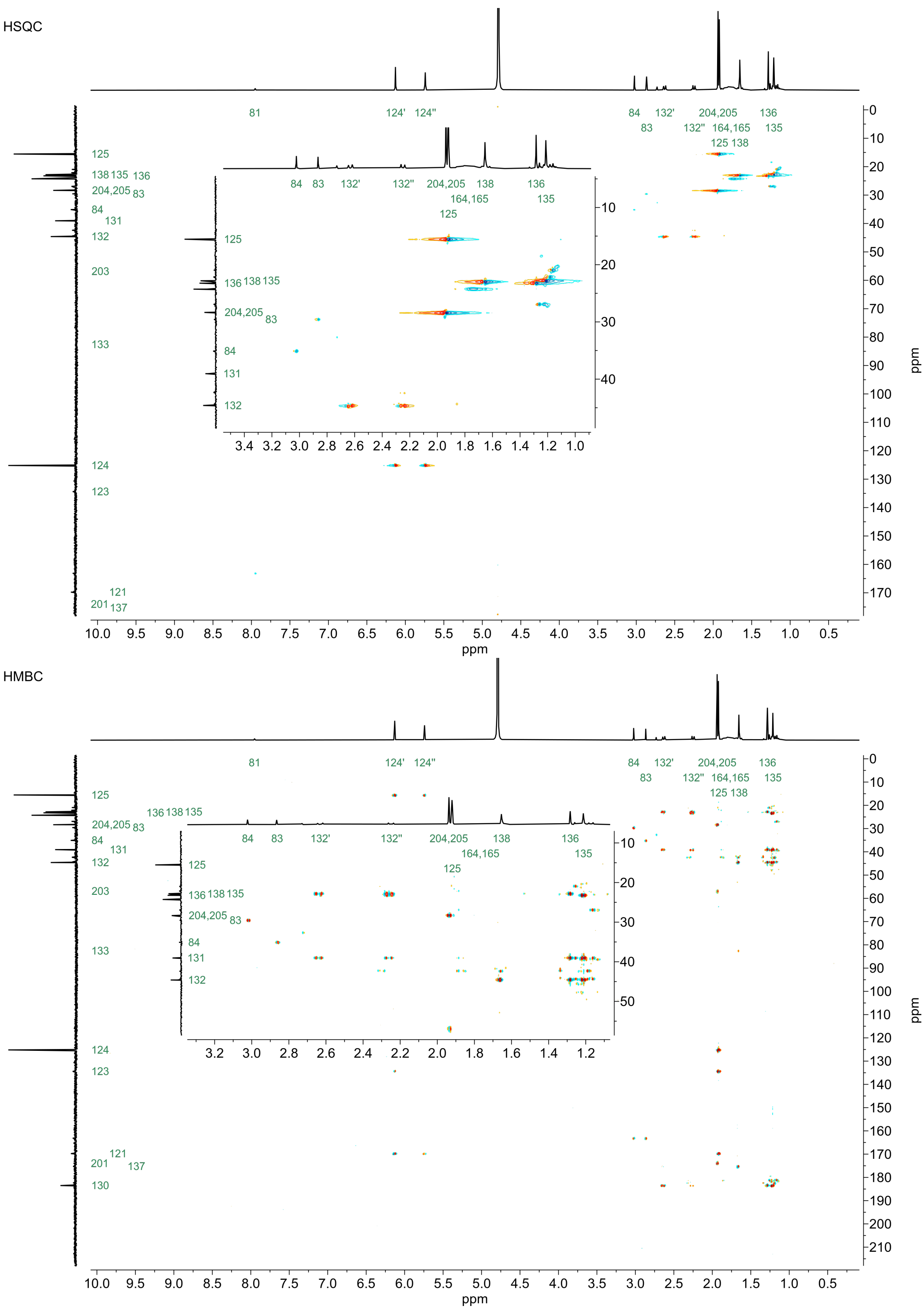

Figure 8.8: HSQC (*top*) and HMBC (*bottom*) NMR spectra of SARA ATRA-L with MAA (entry A05 of Table 9.1 after 6.3 h). ^{1}H and ^{13}C spectra are reported in Figure 8.7.

Chapter 9

Results and discussion

9.1 The aim of the study

As discussed in subsection 6.9.2, Fantin et al. observed a chain-end lactonization during the SARA ATRP of MAA in H_2O.[212] The lactonization occurs between the carboxylic acid of the penultimate monomer unit and the brominated C of the last monomer unit. The result is a PMAA ending with a γ-lactone. However, the chain-end lactonization was an unwanted side reaction for them. Contrarily, our study aims to exploit this lactonization to define a new type of organic reaction, the ATRA-L.

To better characterize the chain-end lactonization via NMR, Fantin et al. pushed the TDP as low as 10 in one experiment. The reaction conditions were the following: MAA:BiBA:$Cu(OTf)_2$:TPMA:NaBr = 10:1:0.001:0.03:5, Cu wire 10 cm, $C_{\mathrm{MAA}} = 0.590\,\mathrm{mol\,L^{-1}}$, 25 °C, and the resulting pH of 2.2. These conditions are used to define the starting point of our study, but with some differences. The most significant difference is the ratio between MAA and BiBA, which should be close to 1 in an ATRA reaction. The consequence is that the carboxyl group required for the lactonization comes from the initiator and not from the penultimate monomer unit. Moreover, it is important to avoid any polymerization by increasing the lactonization rate. This can be achieved by increasing the pH, and we decided to use a base in an equivalent amount to BiBA in order to deprotonate the carboxylic acid. MAA has a carboxylic acid too, but the pK_{a} of BiBA is lower (as reported in Table 8.1) and therefore BiBA should be the preferred species to be deprotonated. Finally, the

SARA regeneration method is removed and it is substituted by a normal ATRA. This implies the replacement of Cu^{II} with Cu^{I} and a strong increase in its amount.

Grouping all these considerations, the reaction conditions of entry A01 of Table 9.1 were defined. The reaction has an equimolar amount of MAA, BiBA, and NaOH with a resulting pH of 4.0. The catalyst is composed of a modest 10 mol % of CuBr and by a 20 mol % of TPMA. Lastly, the concentrations of NaBr and MAA were chosen to be very close to the ones used by Fantin et al. The reaction is highlighted in Scheme 9.1.

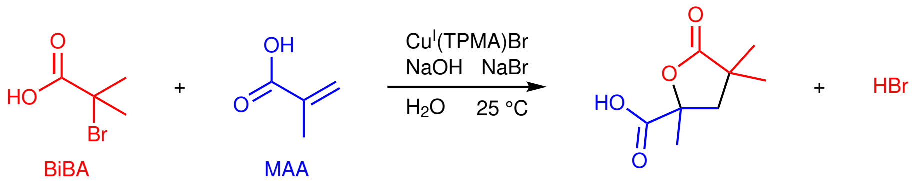

Scheme 9.1: Main ATRA-L reaction of this study.

In the following sections of this chapter, various reaction parameters are discussed: the amount of catalyst, the effect of the pH, the concentration of the reaction mixture, and the ratio between the alkene and BiBA. A SARA ATRA-L system similar to the one of Fantin et al. is also examined to have the regeneration of Cu^{II}. In a control experiment, it was also studied the BiBA side reactions, depending on the pH and on its addition method to the reaction mixture. A change of ligand, base, alkene, and solvent was also studied to expand the field of application of the ATRA-L process. Finally, a change of initiator proved the importance of a carboxylic acid on the initiator.

9.2 Effect of the catalyst amount

As discussed in section 9.1, reaction conditions of entry A01 of Table 9.1 were defined starting from the conditions of Fantin et al.[212] The result was a satisfying 75% lactone yield. From the NMR, multiple additions of MAA (telomerization) or unlactonized monoadduct were not observed. As a matter of fact, after the addition, one $-CH_2-$ is formed with two enantiotopic H atoms, which should give a singlet signal at the NMR. However, the $-CH_2-$ NMR signal is entirely split in two, meaning that it arises from two diastereotopic H atoms of a cycle. The only cycle that can be reasonably formed is a γ-lactone. Similarly, the same can be said for the two methyl groups from BiBA, which become diastereotopic after lactonization. In short, telomerization is not occurring and the monoadduct is quickly transformed into a lactone in this environment. Unless a few exceptions, telomerization was never observed in the ATRA-L study proposed here. Unlactonized monoadducts were also never observed, with the exception discussed in section 9.8, where HEBiB is used as the initiator. With HEBiB, the monoadduct cannot lactonize due to the absence of a carboxylic acid on the initiator.

Entry	**Type**	**Cu source (MR)**	**pH**	**Yield** [%]
A01	normal[a]	CuBr (0.1)	4.0	75
A02	normal[a]	CuBr (0.05)	3.9	49
A03	normal[a]	—	3.8	0
A04	SARA[b]	$CuBr_2$ (0.001)	3.8	47
A05	SARA[b]	$CuBr_2$ (0.0001)	3.8	32

Table 9.1: Effect of the catalyst load. Conditions: MAA:BiBA:NaOH:NaBr = 1:1:1:0.5, $C_{\mathrm{MAA}} = 0.590\,\mathrm{mol\,L^{-1}}$. [a]Cu:TPMA = 1:2. [b]Cu:TPMA = 1:20 and Cu wire 10 cm.

Unfortunately, at the end of reaction A01, a 21% of unreacted MAA was still present in the reaction mixture, while BiBA was completely consumed. A side reaction is clearly occurring and it is consuming BiBA before it can give radical addition, probably by removing its brominated function. From this observation and the NMR, the side reaction was identified to be the hydrolysis of BiBA into 2-hydroxyisobutyric acid (HiBA) (Scheme 9.2). The consumption of BiBA was what prevented the reaction to reach higher yields. For further information about BiBA hydrolysis, see section 9.3.

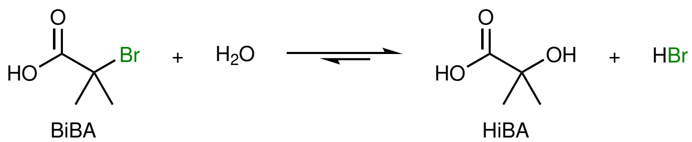

Scheme 9.2: Hydrolysis of BiBA into HiBA.

The first parameter we decided to evaluate is the load of the Cu^{I}. From a 10 mol % load of entry A01, we decreased it to 5 mol % and 0 mol %, entries A02 and A03 of Table 9.1 respectively. Entry A03 is clearly a control experiment without catalyst and, as expected, no lactonization was observed. Decreasing instead the Cu^{I} load from 10 mol % to 5 mol %, furnished a substantial decrease in the yield, from 75% to 49%. This is again due to the BiBA hydrolysis. While BiBA was completely consumed at the end of the reaction, 48% of unreacted MAA was still present. Nearly half of the BiBA was consumed by hydrolysis to HiBA.

The C−Br bond of BiBA is disputed between a homolytic cleavage (ATRA path) and a nucleophilic substitution (hydrolysis path). If the Cu^{I} load is decreased, then only the rate of the ATRA is slowed down and the hydrolysis can prevail. By decreasing the amount of Cu^{I} to 5% (entry A02), the two reaction pathways are almost perfectly balanced. In fact, half of the BiBA is giving the desired lactone (49% yield) and the other half is hydrolyzed to HiBA. Therefore, to counteract the hydrolysis, the load of Cu^{I} should be increased above 10%. However, even if metal-catalyzed ATRA can require a catalyst amount as high as 30 mol %,[37] we decided not to increase it further than 10 mol % for two reasons. First, we did not want to decrease the atom efficiency of the process. Second, we preferred to study other strategies to decrease the hydrolysis without increasing the load of the catalyst.

A good strategy to decrease the amount of the catalyst is to use a catalyst regeneration technique, like the ones discussed in section 1.3 for ATRP. In general, ATRA and ATRP share the same catalyst regeneration methods. Always following the experimental studies by Fantin et al. about the SARA ATRP,[212] we decided to test a SARA ATRA-L. In entries A04 and A05 (Table 9.1), only 0.1 mol % and 0.01 mol % of $CuBr_2$ were added respectively. However, the actual concentration of Cu ions in solution is higher due to the additional Cu wire, which provides a supplementary amount of catalyst. On the other hand, TPMA is as low as 2 mol % and 0.2 mol % (entries A04 and A05 respectively).

Satisfyingly, the SARA system worked. However, the yield was not as high as expected, but comparable to the normal reactions. The normal system of entry A02 with 5 mol % of Cu gave almost the same yield as entry A04, a SARA system with 0.1 mol % of Cu. As before, the main adverse effect that kept the yield from reaching a high value was the BiBA hydrolysis. BiBA hydrolysis had more time to take place in entry A05, because the reaction was slower than the one of entry A04, due to the lower amount of Cu. In fact, entry 5 took 21 hours to reach 94% BiBA conversion, while entry A04 took only 4 hours to reach 91% BiBA conversion.

In the SARA systems, after BiBA complete consumption, a good amount of unreacted MAA was still present in the reaction mixture, even if its amount was lower than expected. The expectation is based on the fact that the sum of the relative amounts of unreacted MAA and lactone should be close to the initial load of MAA, like it was observed for the normal conditions (entries A01 and A02). With the SARA system instead, the final unreacted MAA was only 18 mol % and 24 mol % for entries A04 and A05, respectively. The final lack of MAA could be explained by a telomerization, but multiple addition products were not observed via NMR.

Moreover, HiBA was observed from NMR in the SARA systems, but only at $t = 0$. After that, the HiBA signal disappeared from NMR and a broad signal appeared instead. In addition, the chemical shift of the broad signal was also not defined, it was easily shifting inside the alkyl region between NMR spectra of different reaction times. It was later discovered that the broad signal is probably generated by a complex between HiBA and Cu. In the SARA system, in fact, the concentration of Cu could be higher than the concentration of TPMA, forcing the Cu to form a complex with a new ligand. Since the broad signal was never observed in a normal ATRA-L, it is assumed that the stability constant of the Cu/TPMA complex is higher than the one of the Cu/HiBA complex, which is in accordance with the hard and soft acids and bases (HSAB) theory.[247–249] For further information on how the broad signal was assigned to the Cu/HiBA complex, see section 9.3.

Considering the problems that arose with the SARA system, we decided to focus on the simpler normal system to have a better understanding of the reaction mechanisms.

9.3 Hydrolysis of α-bromoisobutyric acid

The hydrolysis of BiBA (Scheme 9.2) turned out to be the weakness of the system of our studies from the beginning. We decided to deeply investigate the hydrolytic process in order to have an idea of how fast the hydrolysis can be.

We first studied the change of the relative amounts of BiBA and HiBA via NMR, by comparison of the CH_3 signals. The NMR tube was prepared with about 600 µL of 0.3 mol L^{-1} solution of BiBA in D_2O (pH = 1.7). The results are depicted in

Figure 9.1. In the charts, the mol % of BiBA and HiBA are relative to each other, meaning that their sum at a certain time is always 100 mol %. From the left chart, it is immediately clear that the equilibrium is shifted towards the hydrolyzed form (HiBA). However, the hydrolysis is particularly slow at a pH of 1.7, taking about 16 days to reach the same concentration of BiBA and HiBA. From a reaction point of view however, only the first hours of hydrolysis are important. For this reason, the right chart of Figure 9.1 shows only the first 50 hours of BiBA decrease. We theorized that, at this pH, the ATRA-L reaction could be much faster than the BiBA hydrolysis.

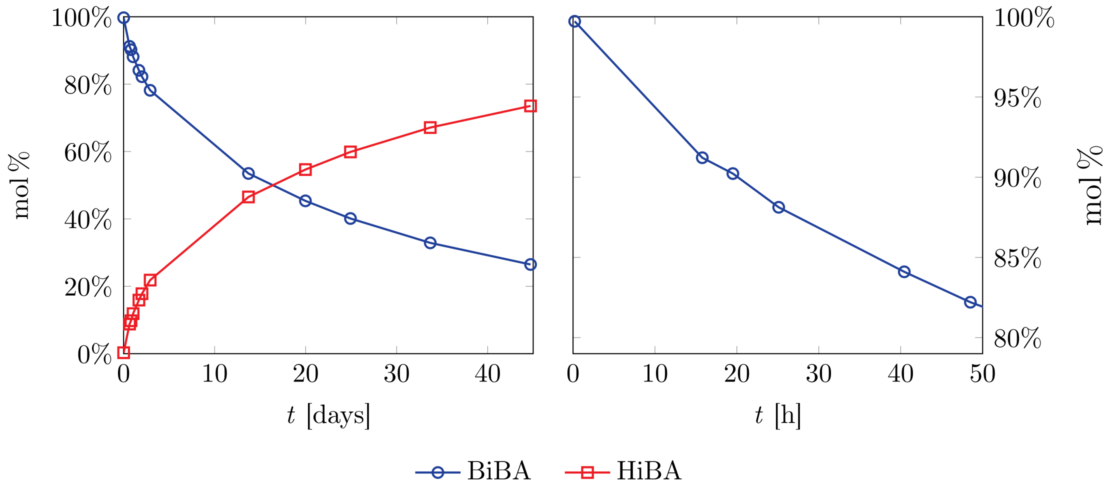

Figure 9.1: BiBA hydrolysis over time. *Left:* Relative amounts of BiBA and HiBA within 45 days. *Right:* Decrease of BiBA within 50 h (i.e. a magnification of the left top corner of the left chart).

The rate of BiBA hydrolysis is pH-dependent. The effect of the pH was then studied by preparing five BiBA solutions with five different amounts of TEA. The amounts of TEA were 0, 0.55, 0.92, 1.00, and 1.18 (as the ratios with respect to BiBA). The corresponding theoretical pH values were 1.6, 3.0, 4.0, 6.8, and 10.0. The results are shown in Figure 9.2 and, as expected, a lower pH corresponds to a greater hydrolysis rate. However, while the hydrolysis rate is highly increased by jumping from a pH of 1.6 to 4.0, the same cannot be said of the jump from 4.0 to 10.0. In any case, there is still room to achieve slower hydrolysis and faster ATRA reaction, aiming to increase the final lactone yield.

One of the products of the hydrolysis is HBr. This is true for BiBA, but also for any other brominated initiator. Since HBr is a strong acid, it is almost completely dissociated in solution and it can be found as H^+ and Br^-. If other species that

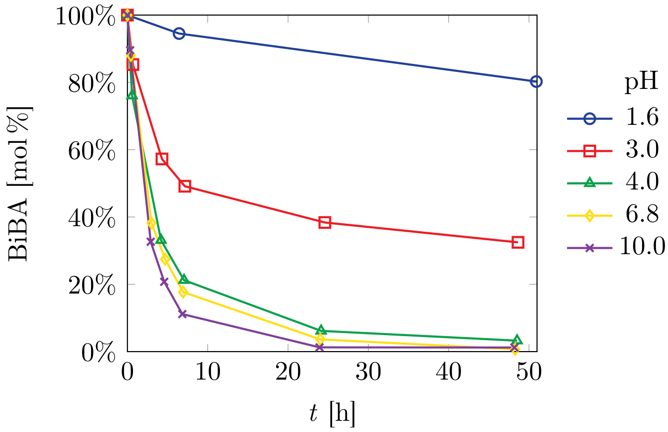

Figure 9.2: Effect of the pH on the decrease of concentration of BiBA in H_2O due to hydrolysis. Initial $C_{\mathrm{BiBA}} = 0.590\,\mathrm{mol\,L^{-1}}$.

release Br^- are added to the reaction mixture, then the hydrolysis should be slowed down. As a matter of fact, in the reaction system of our studies, Br^- is added to the reaction mixture as NaBr and CuBr or $CuBr_2$. Therefore, it became also important to study the effect of other reagents on the hydrolysis of BiBA. We then studied the hydrolysis in one of the more common reaction systems (similar to entry A01 of Table 9.1, but with $CuBr_2$ instead of CuBr and without TPMA). Five reaction mixtures were prepared by adding one of these reagents at a time, as shown in Figure 9.3. Again, most of the responsibility for the BiBA hydrolysis goes to the pH. The addition of MAA to BiBA slightly slowed down the hydrolysis because MAA marginally decreases the pH. The theoretical pH of both systems (BiBA alone and BiBA, MAA) is the same and it is equal to 1.6 because MAA is a weaker acid than BiBA. The addition of NaOH pushes the pH of the last three systems to 3.8 and the hydrolysis is therefore much faster. By adding NaBr in the penultimate system, no significant difference was observed in the hydrolysis rate. On the other hand, the addition of $CuBr_2$ in the latest system had the effect to decrease the hydrolysis, even if not significantly. This could be due to the increase of the concentration of Br^-, but only 0.2 equiv were added with $CuBr_2$, the other 0.5 equiv came from NaBr. The presence of Cu may have an unexpected effect on the hydrolysis.

Furthermore, the addition of $CuBr_2$ had a big impact on the NMR spectra. As shown in Figure 9.4, HiBA has a normal sharp signal as expected, unless $CuBr_2$ is present. With $CuBr_2$, the HiBA signal disappears and a broad signal arises. The only plausible hypothesis is that a Cu/HiBA complex is formed. HiBA should be

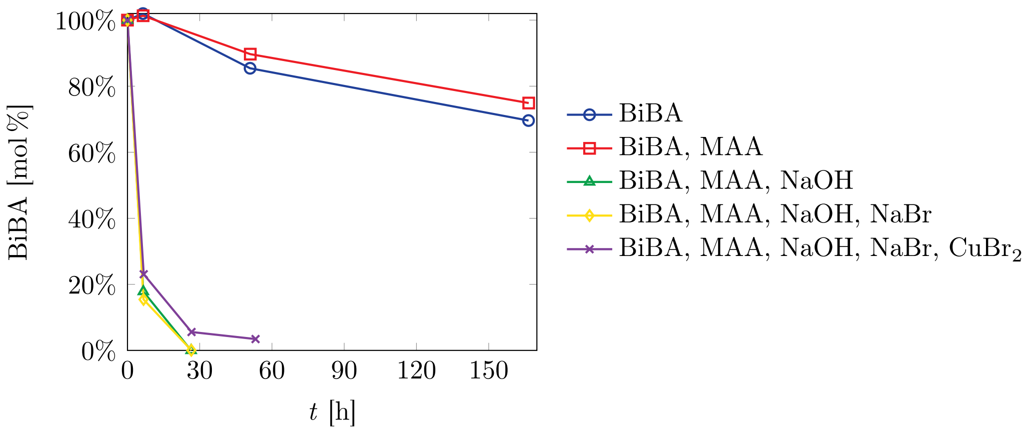

Figure 9.3: Effect of the reagents on the decrease of concentration of BiBA in H_2O due to hydrolysis. Initial $C_{\mathrm{BiBA}} = 0.590\,\mathrm{mol\,L^{-1}}$. The other reagents are added with the ratios BiBA:MAA:NaOH:NaBr:$CuBr_2$ = 1:1:1:0.5:0.1.

able to chelate Cu, forming a stable 5-membered ring. The broad signal was already observed in section 9.2 during SARA reactions, where the concentration of Cu could be higher than the concentration of TPMA, forcing the HiBA to bind to Cu. As already discussed, TPMA has a greater affinity for Cu than HiBA, therefore the Cu/HiBA complex is formed only when the concentration of TPMA is not as high as the concentration of Cu.

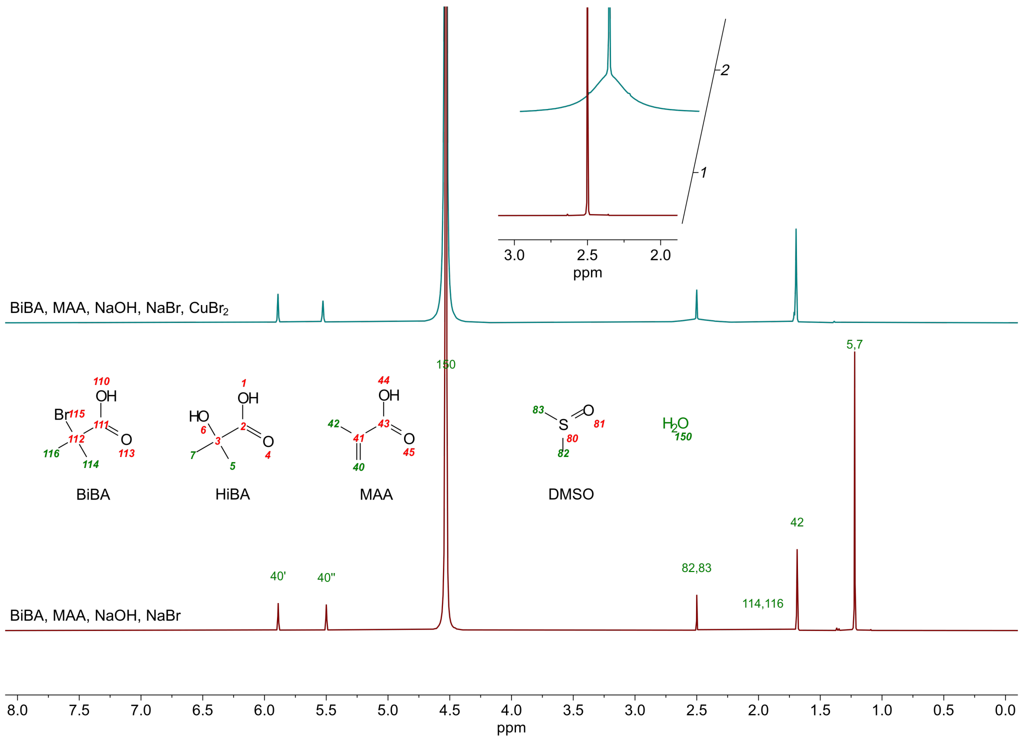

Figure 9.4: [1]H NMR spectra of HiBA generated by the complete hydrolyzation of BiBA, with (*top*) and without (*bottom*) $CuBr_2$. The expansion shows the broad signal which, unfortunately, has the same chemical shift as DMSO (the internal standard).

In conclusion, the hydrolysis of BiBA is mainly dependent on the pH. The hydrolysis is a very fast competitive reaction, but the ATRA-L can be very fast too. In fact, entry A01 of Table 9.1 furnished a relative high yield (75%). In order to achieve higher yields, some strategies about the reaction conditions can be adopted to boost the ATRA over the hydrolysis. To determine these strategies, it is important to know the effect of the reaction conditions on the reaction itself.

9.4 Side reactions of α-bromoisobutyric acid

As just discussed in section 9.3, BiBA is mainly hydrolyzed to HiBA. There are however other minor side reactions that are occurring. A control experiment with SARA conditions was set up with only BiBA and without any alkene. At first, this control experiment aimed to better characterize the broad signal. As already discussed, the broad signal appeared in the alkyl region of ^{1}H NMR only during SARA experiments and it was later assigned to the Cu/HiBA complex. In normal reaction conditions, the broad signal was not observed because Cu was complexed only by TPMA. The concentration of TPMA was in fact always higher than the concentration of Cu, and the Cu/TPMA complex has greater stability constant than the Cu/HiBA complex.

The reagents of the control experiment are BiBA:NaOH:NaBr:CuBr:TPMA = 1:0.725:0.5:0.001:0.002 with 10 cm of Cu wire. The reaction is carried out in H_2O and the resulting pH is 3.3. ^{1}H, $^{1}_{3}$C, HSQC, and HMBC NMR spectra were collected after 24 h and they are reported in Figures 9.5 and 9.6. From the NMR characterization, it was possible to identify several products from BiBA side reactions, as highlighted in Scheme 9.3. After 24 h, the relative amount of BiBA was found to be 38%, with 54% of HiBA, 3.3% of MAA, 1.7% of 2-methylpropanoic acid (MPA), and 0.6% of 2,2,3,3-tetramethylsuccinic acid (TMSA). Furthermore, a 3.0% of lactone was identified, formed by the ATRA-L reaction between BiBA and the generated MAA. Unfortunately, the percentage value of MAA may have been overestimated due to NMR signal overlapping. In short, HiBA is by far the main by-product, with only small amounts of other substances.

As previously discussed, HiBA is generated by BiBA hydrolysis (Scheme 9.2).

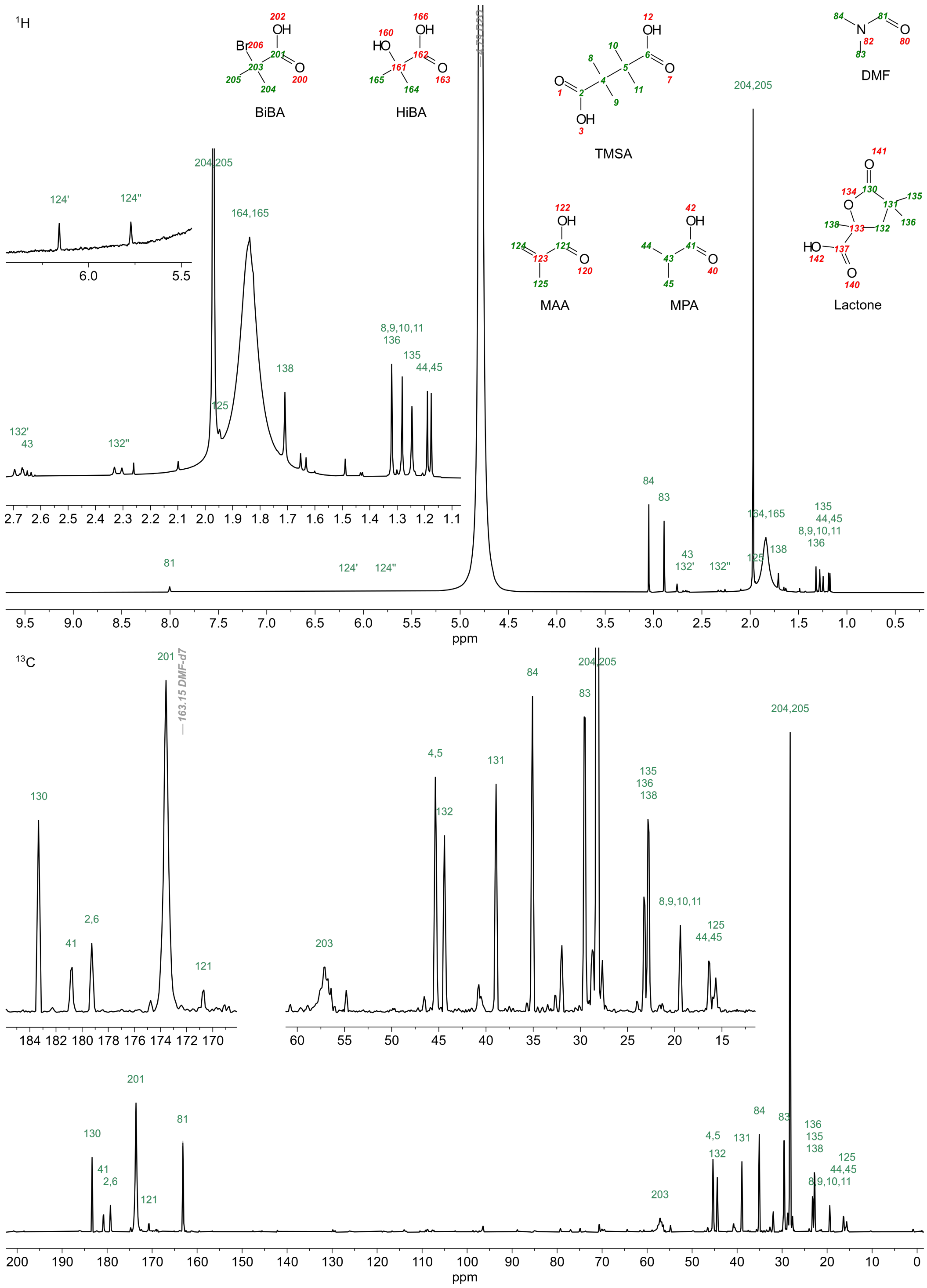

Figure 9.5: ^{1}H (*top*) and ^{13}C (*bottom*) NMR spectra of the control experiment without any alkene after 24 h. HSQC and HMBC spectra are reported in Figure 9.6.

MAA, on the other hand, is probably generated by a dehydrohalogenation reaction, releasing HBr. MPA may be formed by a termination reaction after activation of BiBA with the homolytic cleavage of the C−Br bond. TMSA is probably the product of a radical–radical termination after BiBA radical activation. However, the formation of MPA and TMSA may be suppressed in a regular ATRA-L with an

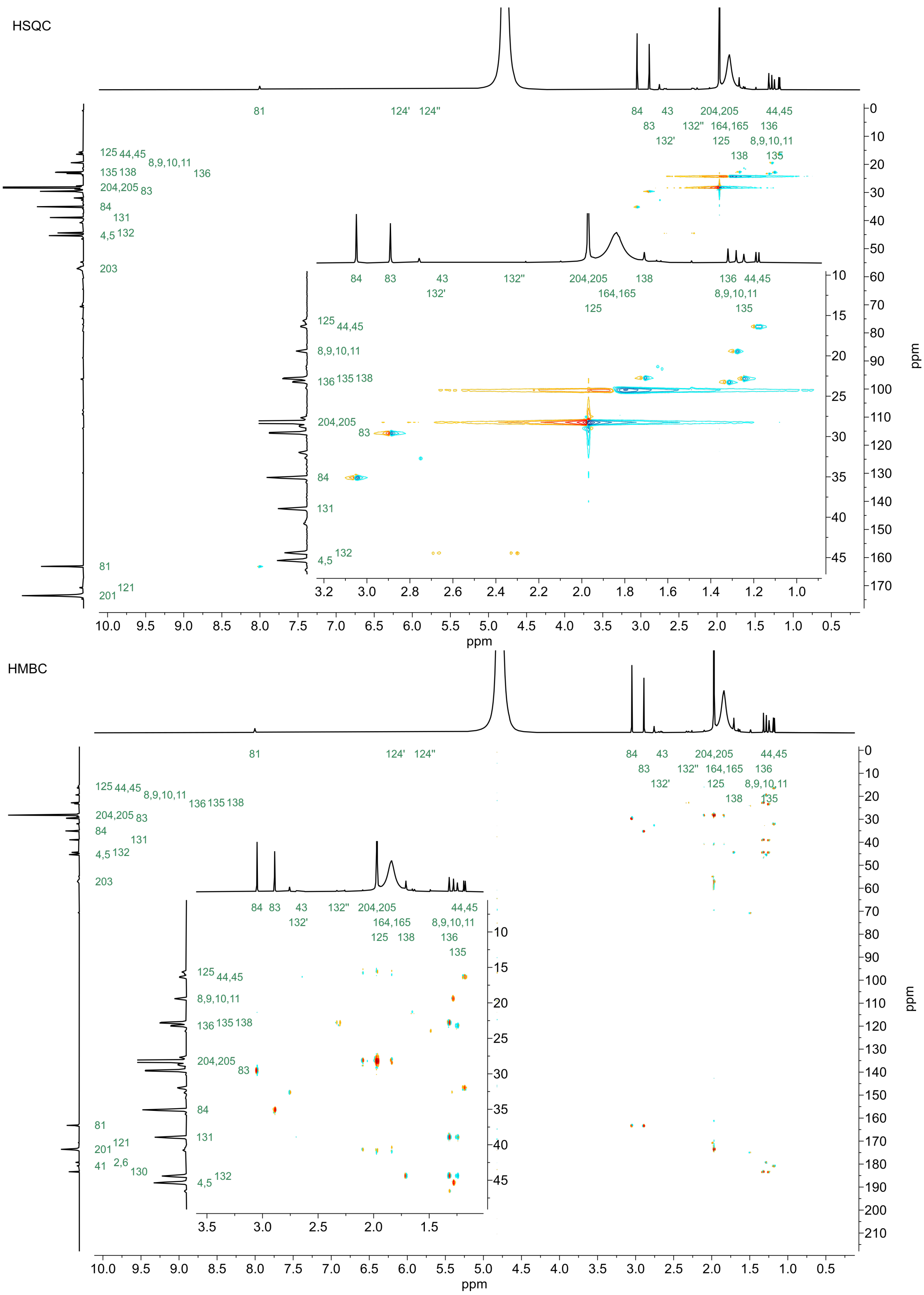

Figure 9.6: HSQC (*top*) and HMBC (*bottom*) NMR spectra of the control experiment without any alkene after 24 h. ^{1}H and ^{13}C spectra are reported in Figure 9.5.

alkene. In fact, the termination reactions (which are supposed to generate MPA and TMSA) have to compete with the ATRA reaction in the presence of an alkene.

In conclusion, no significant side reactions are consuming BiBA in our ATRA-L environment, with the only exception of hydrolysis. A small amount of MAA may also be generated from BiBA, but MAA or other (meth)acrylates are generally already present in the reaction mixture.

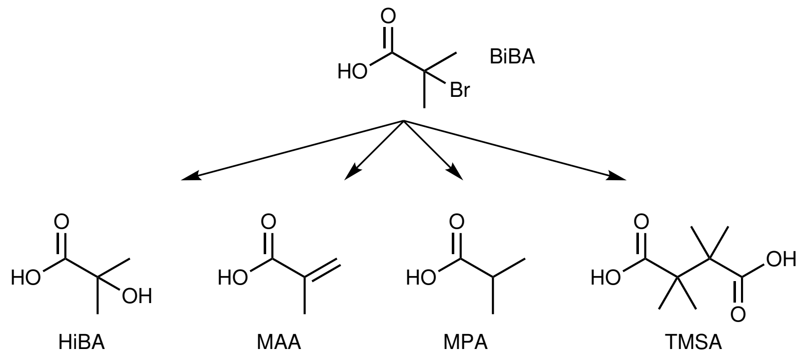

Scheme 9.3: Identified products from BiBA side reactions.

9.5 Effect of the pH

The pH was found to be the main responsible for the hydrolysis of BiBA, as analyzed in section 9.3. The aim of Table 9.2 is to study the effect of the pH on the final yield of our ATRA-L reaction system. The quantity of NaOH is changed to adjust the pH and two monomers are used: MAA (entries A01, A06, and A07) and HEMA (entries A08–A10). HEMA was studied as a monomer because, unlike MAA, it is not an acid and it should not interfere with the pH.

Entry	**Alkene**	**Base (MR)**	**pH**	**Yield** [%]
A01	MAA	NaOH (1)	4.0	75
A06	MAA	NaOH (0.5)	3.0	83
A07	MAA	—	2.0	63
A08	HEMA	NaOH (1)	8.9	82
A09	HEMA	NaOH (0.8)	3.8	82
A10	HEMA	—	2.0	55

Table 9.2: Effect of the pH of the reaction mixture. Conditions: alkene:BiBA:CuBr:TPMA:NaBr = 1:1:0.1:0.2:0.5, $C_{\mathrm{MAA}} = 0.590\,\mathrm{mol\,L^{-1}}$.

The decrease in the pH did not have the expected boost in the yield. For MAA, lowering the pH from 4.0 to 3.0 (entries A01 and A06, respectively) only slightly increased the yield. On the contrary, decreasing the pH further to 2.0 without adding any base (entry A07) registered the lowest yield. The same result was observed using HEMA as an alkene. While the two reactions with pH values of 8.9 and 3.9 (entries

A08 and A09, respectively) did not furnish different yields, entry A10 without any base saw a decrease in the yield from 82% to 55%. As discussed in section 9.3, the hydrolysis rates of BiBA at pH values of 8.9 and 3.9 (entries A08 and A09, respectively) should not be very different, but at 2.0 (entry A10) it should be highly discouraged. However and unexpectedly, the yield is decreasing when the BiBA hydrolysis should be slowed down.

The reason for this unexpected lower yield is because the pH has two effects on the reaction system. The first is the desired effect, or rather the decrease of BiBA hydrolysis. The second one is the unwanted decrease in the activation rate of the Cu^{I}(TPMA)Br catalyst. In other words, reducing the pH decreases the rates of both hydrolysis and ATRA. An effect of the pH on the activation rates of Cu/TPMA catalysts in H_2O was already observed.[250] Furthermore, if the concentration of H^+ or OH^- is too high, a generic Cu^{I}(TPMA)X catalyst can stop working, respectively for the protonation of the ligand or for the formation of the inactive Cu^{I}(TPMA)(OH) species. Moreover, the solubility rate of BiBA is pH-dependent too. If BiBA is not completely solubilized, then its lower concentration decreases the ATRA rate.

Figure 9.7 shows the lactone yield increasing over time for the three reactions with HEMA with different pH values. The rate of the ATRA-L reaction is clearly lower when the pH is 2.0, rather than 3.8 or 8.9. While reactions with pH values of 3.8 and 8.9 were complete in a few hours with total BiBA conversion, reaction with pH of 2.0 came to a stop after 5 days with 55% yield and only 85% BiBA conversion.

Moreover, it should not be forgotten that both the hydrolysis and the lactonization reactions release HBr, a strong acid. The acidity of the reaction is therefore increasing over time. The pH values of the various reaction systems are calculated before any hydrolysis or lactonization can take place. If BiBA is completely consumed and generates 1 equiv of HBr, then the pH of entries A07 and A10 can be as low as 0.3. As reported in the literature during an *e*ATRP,[250] the $[Cu(TPMA)]^{2+}$ catalyst was working at a pH of 1.5, but not at 0.5.

However, it is necessary to consider another reaction taking place. In these conditions, HEMA is easily hydrolyzed to MAA and EG, making little difference in the use of one alkene rather than the other. Two different lactones are therefore formed, as shown in Scheme 9.4. The hydrolysis of HEMA can occur before or

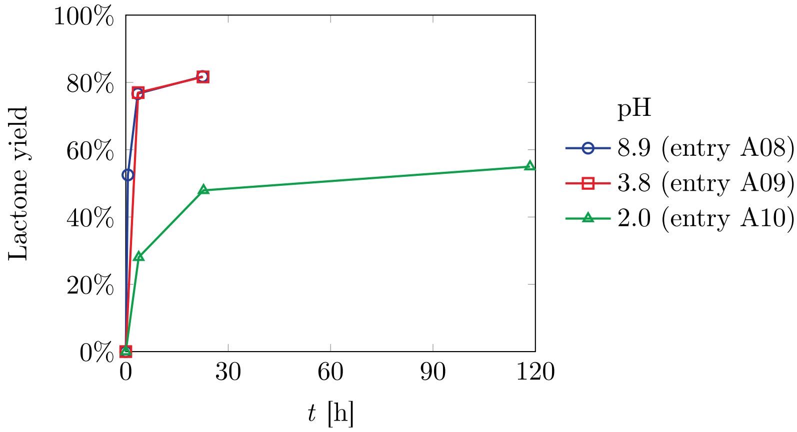

Figure 9.7: Increase in the lactone yield over time at different pH values (entries of Table 9.2).

after the formation of the lactone. Over time, the reaction system converges to the hydrolyzed lactone. After approximately one day of reaction, entry A09 (pH = 3.8) showed a ratio of about 4:1 between the two lactones, the hydrolyzed form being the majority. At the same time, entry A10 (pH = 2.0) showed a ratio of 1:9, with a minority of the hydrolyzed lactone instead. The ratio between the two lactones at the equilibrium was not evaluated, but probably it is highly shifted toward the hydrolyzed form. It is important to specify that all the lactone yields presented in this section are the sum of the two lactone products. No distinction was made between the two lactone forms for the calculation of the yield.

At the pH level of 2.0 (entries A07 and A10), telomerization may also be occurring.

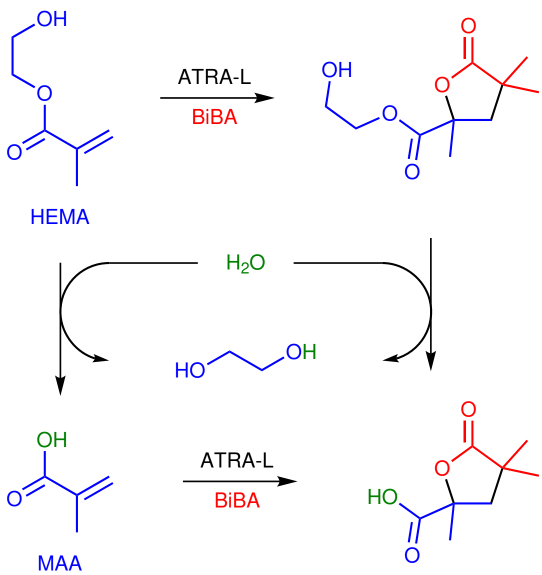

Scheme 9.4: Hydrolysis of HEMA and corresponding lactone. Hydrolysis reactions are generally equilibria, but highly shifted toward the hydrolyzed form in this case.

The lactonization of the monoadduct can be discouraged by the non-deprotonation of the carboxylic acid derived from BiBA, resulting in multiple additions. As a matter of fact, at the end of the reactions, the unreacted amount of BiBA was higher than the unreacted amount of the alkene (even if their starting ratio was 1:1). In entry A07, the amounts of unreacted MAA and BiBA were 10% and 11% respectively (both starting from 100%), with a 7% of HiBA generated by BiBA hydrolysis. The reaction of entry A10 stopped with 15% of unreacted BiBA and only 2% of unreacted HEMA, with 10% of HiBA. In both cases the alkene is consumed more than BiBA, especially taking into account the BiBA hydrolysis to HiBA. The excessive consumption of the alkene is probably due to multiple additions products. Multiple addition products of BiBA and MAA can still give lactones, as it was described in Scheme 6.10. On the other hand, multiple addition products of BiBA and HEMA can give γ-lactonization only when the ester group derived from HEMA is hydrolyzed to the carboxylic acid. For this reason, HEMA in entry A10 was consumed more than MAA in entry A07 (relative to BiBA), because the multiple addition product of HEMA needs to be hydrolyzed first in order to give lactonization. Once the lactonization occurs, no more additions can take place, because the Br atom is lost.

To summarize, changing the pH can decrease the hydrolysis of BiBA, but the rate of the ATRA reaction is also affected. The two effects are counterbalanced: reducing the pH decreases the yield, but also slows down the ATRA. The final result is that a small yield is observed. If the ATRA takes too long, then the hydrolysis has time to take place instead. It may be necessary to adopt another strategy to boost the yield by boosting the ATRA, but not the hydrolysis.

Importantly, the ATRA-L reaction was successfully performed with HEMA as an alkene, but the ester groups from HEMA and its generated lactone are easily hydrolyzed in the reaction conditions.

Moreover, if the pH is too low, multiple addition products can be formed. This may be due to the non-deprotonation of the carboxylic acid derived from BiBA, which is involved in the lactonization of the monoadduct. Multiple addition products of MAA or hydrolyzed HEMA can still give lactonization, but the final γ-lactones have clearly a different substituent from the one obtained by the monoadduct.

9.6 Addition method of α-bromoisobutyric acid to the reaction mixture

In sections 9.3 and 9.5, it was observed that a pH higher than 3.0 is required for the ATRA-L reaction to be fast, but these conditions greatly promote also the BiBA hydrolysis. All the BiBA is generally added to the reaction mixture at the beginning of the reaction (see subsection 8.1.2 for the general procedures), but a slow addition of it could stop its hydrolysis. If the concentration of BiBA in the reaction mixture is small compared to the Cu catalyst, BiBA may be rapidly intercepted and activated for the ATRA before the hydrolysis can occur.

In the experiment of entry A12 of Table 9.3, BiBA was slowly added within an hour to the reaction mixture. For the slow addition, BiBA was solubilized in H_2O and, as discussed in section 9.3, the BiBA hydrolysis is very little in a solution of BiBA alone with these concentrations. However, compared to the reaction model of entry A01 (Table 9.1), the concentration of reactions of section 9.3 is halved ($0.295\,\mathrm{mol\,L^{-1}}$). This is necessary to completely solubilize BiBA in H_2O without the addition of a base. The effect of the concentration of the reaction mixture is better discussed in section 9.7.

Entry	**BiBA addition method**	**Yield** [%]
A11	solid, at $t = 0$	71
A12	in solution, dropwise	69

Table 9.3: Effect of the BiBA addition method. Conditions: MAA:BiBA:NaOH:CuBr:TPMA:NaBr = 1:1:1:0.1:0.2:0.5, $C_{\mathrm{MAA}} = 0.295\,\mathrm{mol\,L^{-1}}$, pH = 4.0.

Unfortunately, there is a very small difference in the yield between the two reactions of Table 9.3. Apparently, the competition between ATRA-L and hydrolysis is independent of the concentration of BiBA in the reaction mixture.

There is however another extremely important fact about the experiment of entry A12. During the slow addition of BiBA, the concentration of MAA is always greater than the one of BiBA. In these conditions, polymerization can occur. However, from NMR, it was not observed the presence of any product coming from multiple additions. This is significant evidence that the lactonization reaction is faster than a second addition. The relevant consequence of this is that, in ATRA-L, it is possible to use alkenes that are generally forbidden in normal ATRA reactions. In ATRA in fact, to avoid polymerization, alkenes are chosen in a way that their monoadduct cannot be further activated. Therefore, ATRA is forced to exclude the use of (meth)acrylates and other alkenes that are typically used as monomers in ATRP. The goal of ATRP is indeed the opposite, or rather to obtain adducts that are still activated.

9.7 Concentration of the reaction mixture

The aim of Table 9.4 is to study the effect of the concentration of the reaction mixture on the yield and the BiBA hydrolysis. As expected, a more diluted system resulted in a lower yield and higher BiBA consumption by hydrolysis. Entry A01 with MAA furnished 75% yield, while halving the concentration yielded 69% (entry A11, Table 9.4).

Importantly, DMAEMA was also tested as alkene (entries A13 and A14 of Table 9.4). DMAEMA has a tertiary basic amine and fully satisfies the necessity of a base in the reaction mixture. With the double role of DMAEMA, it is possible to avoid the addition of NaOH to the system. Even with DMAEMA, a dilution of the system decreased the yield by increasing the BiBA hydrolysis. Compared to the reactions with MAA (entries A01 and A11) however, the yield difference with DMAEMA is higher by halving the concentration of the monomer. From entry A13 to A14, the concentration of DMAEMA was halved and the yield dropped from 74% to 60%. The higher decrease in the yield with DAMEMA may be due to the higher pH, making the reaction more sensitive to a change in reagents concentrations.

Entry	**Alkene**	$\boldsymbol{C}_{\mathbf{alkene}}$ [mol L^{-1}]	**NaOH** [MR]	**pH**	**Yield** [%]
A01	MAA	0.590	1	4.0	75
A11	MAA	0.295	1	4.0	69
A13	DMAEMA	0.590	—	6.1	74
A14	DMAEMA	0.295	—	6.1	60

Table 9.4: Effect of the concentration of the reaction mixture. Conditions: alkene:BiBA:CuBr:TPMA:NaBr = 1:1:0.1:0.2:0.5.

9.8 The importance of a carboxylic acid on the initiator

A carboxylic acid is thought to be required on the initiator to have lactonization after addition. To test this hypothesis and to have a better understanding of the reaction mechanism, an initiator without a carboxylic acid like HEBiB was tested. If the lactonization mechanism requires a carboxylic acid, then HEBiB should only give addition products.

BiBA and HEBiB (entries A01 and A15 of Table 9.5, respectively) share the same structure, with the exception that HEBiB is the ester of BiBA. Because of the loss of the carboxylic acid from BiBA to HEBiB, a base like NaOH was not added when HEBiB is used. Nevertheless, the two pH values are relatively close to each other (4.0 with BiBA and 3.7 with HEBiB).

Entry	**Initiator**	**NaOH** [MR]	**pH**	**Yield** [%]
A01	BiBA	1	4.0	75
A15	HEBiB	—	3.7	4

Table 9.5: Comparison between a carboxylic acid (BiBA) and an ester (HEBiB) as initiators. Conditions: MAA:initiator:CuBr:TPMA:NaBr = 1:1:0.1:0.2:0.5, $C_{\mathrm{MAA}} = 0.590\,\mathrm{mol\,L^{-1}}$.

BiBA and HEBiB furnished two very different lactone yields, 75% and 4% respectively. With HEBiB, the drastic drop in the yield is probably due to the absence of a carboxylic acid on the initiator. However, a small amount of lactone was present in the reaction mixture. There are three possible ways for the lactone to be formed from HEBiB and MAA (Scheme 9.5). One is the multiple additions with the formation of a telomer. If two or more MAA units are added, then there can be lactonization between the two last units of the chain. The same reaction was observed by Fantin et al. during the SARA ATRP in H_2O of MAA,[212] as discussed in subsection 6.9.2. A more plausible explanation for the formation of the lactone is the hydrolysis of HEBiB to BiBA, releasing EG. The hydrolysis can occur before or after the addition of MAA, splitting the hydrolysis hypothesis into two pathways. However, the resulting lactone is the same and it is identical to the one formed with BiBA.

From NMR, it was observed consumption of HEBiB and MAA close to 1:1,

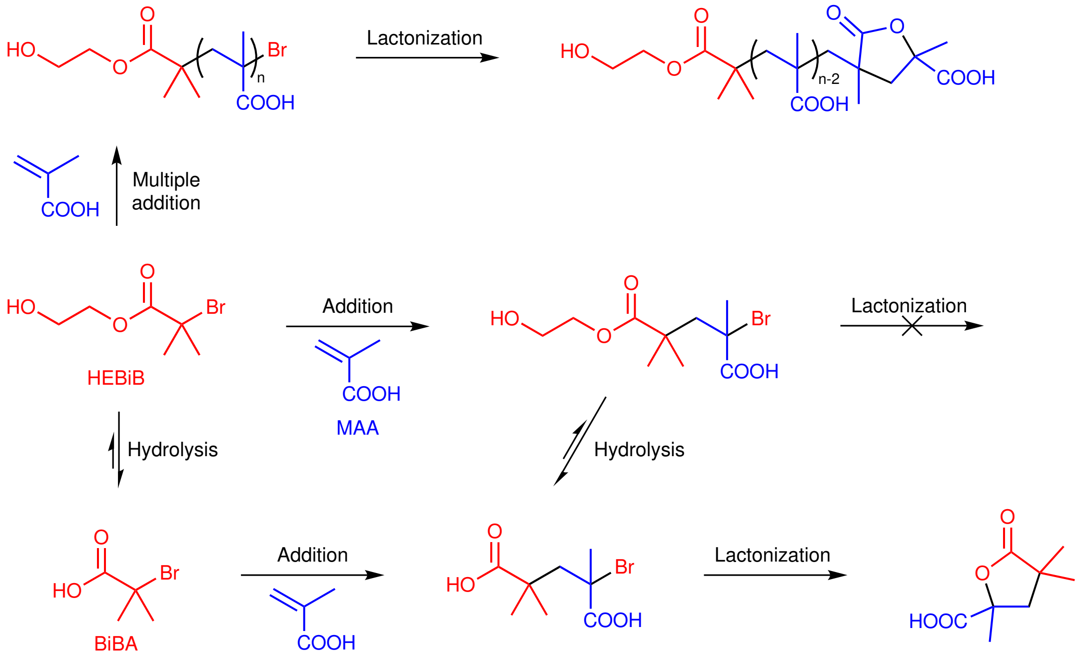

Scheme 9.5: Possible ways of lactone formation using HEBiB as initiator (n $\geq$ 2).

weakening the multiple addition hypothesis. However, there is the possibility that HEBiB was partially consumed by side reactions and that some telomers could be consequently formed. Generally in these reactions, the initiator is consumed by hydrolysis of the brominated function and, in the end, there is a good amount of residual alkene. For example, entry A01 reached complete BiBA consumption with only 79% of MAA conversion. The same did not happen for entry A15, where HEBiB and MAA reached 92% and 96% conversion, respectively. Reasonably, multiple additions occurred. Unfortunately, it was difficult to prove the hydrolysis of the C−Br bond of HEBiB from ^{1}H NMR due to peaks overlapping, but its hydrolysis is highly probable.

An increasing amount of EG was however present inside the reaction mixture. This is evidence of the hydrolysis of HEBiB into BiBA, before or after any addition reaction. The lactone yield was increasing over time, going from the tabulated 4% after 7 h to 14% after 23 h. However during this time, HEBiB and MAA have been consumed by only an additional 1 mol % and 3 mol %, respectively. EG was also increased during this time from 4 mol % to only 5 mol %. This means that hydrolysis of HEBiB was occurring, but it can explain only a 5% lactone yield, not 14%. The rest may be a lactonization of the last two monomer units of a multiple addition product.

In conclusion, a carboxylic acid on the initiator is required to give lactonization. When the carboxylic acid was made quiescent by esterification (turning BiBA to HEBiB), the lactonization was highly suppressed. However, a small amount of lactone was forming inside the reaction mixture, even when HEBiB and MAA were not reacting anymore. The lactone could have been formed by hydrolysis of the HEBiB ester to the corresponding carboxylic acid. Another hypothesis is the lactonization between the last MAA units of a multiple additions product. In both cases, a carboxylic acid is required for the lactonization.

9.9 Ratio between alkene and initiator

In general, the main problem of our ATRA-L system is the hydrolysis of the initiator. The hydrolysis keeps the yield from reaching values close to 100%. A good strategy is to increase the quantity of the initiator relative to the alkene in order to counterbalance side reactions involving the initiator. Furthermore, the initiator is generally in excess in ATRA systems to prevent telomerization.

During our ATRA-L studies, the ratio between alkene and initiator is always 1:1, like in entry A01 of Table 9.6, where MAA and BiBA are used. To increase the yield, we decided to increase the MR of BiBA from 1 to 1.3. Consequently, NaOH was increased accordingly for BiBA deprotonation and solubilization. In entry A01, 21 mol % of BiBA were consumed by hydrolysis, therefore it seemed reasonable to increase BiBA by 30 mol %. As a result, increasing the MR of BiBA from 1 to 1.3 increased the yield from 75% to 85%. However, the expectation was to reach a higher yield, but hydrolysis consumed a good part of BiBA. Indeed in entry A16 of Table 9.6, 36 mol % of BiBA (compared to MAA) were hydrolyzed, opposite to the 21 mol % of entry A01.

Faced with a yield increase of 10%, it is necessary to consider also the loss in

Entry	**BiBA** [MR]	**NaOH** [MR]	**Yield** [%]
A01	1	1	75
A16	1.3	1.3	85

Table 9.6: Effect of the ratio between alkene and initiator. Conditions: MAA:CuBr:TPMA:NaBr = 1:0.1:0.2:0.5, $C_{\mathrm{MAA}} = 0.590\,\mathrm{mol\,L^{-1}}$, pH = 4.0.

atom efficiency of the process. Both BiBA and NaOH were increased by 30 mol % for a not so significant increase in the yield. The result was a bit disappointing and it was decided to keep the 1:1 ratio between the alkene and the initiator.

9.10 Change of ligand

TPMA can build very active catalysts, suitable for a large number of atom transfer radical reactions. However, TPMA is expensive if compared to other ligands. Furthermore, an ATRA system like the one of our studies can require a quite good amount of catalyst. In order to develop a more affordable process for our ATRA-L system, we decided to test bpy as ligand instead of TPMA.

Usually, an excess of TPMA is used to bind all the Cu. In this study, a Cu:TPMA ratio of 1:2 is therefore used, even if only 1 mol of TPMA is necessary to bind to Cu. Differently, 2 mol of bpy should be required to form the complex with Cu.[251,252] Since TPMA is doubled to have an excess of it, we decided to double bpy too, reaching a Cu:bpy ratio of 1:4. In Table 9.7 are reported a reaction with TPMA, one with bpy and one without any ligand (entries A01, A17, and A18 respectively).

Entry	**Ligand** (MR)	**pH**	**Yield** [%]
A01	TPMA (0.2)	4.0	75
A17	bpy (0.4)	4.1	65
A18	—	3.8	0

Table 9.7: Change of ligand. Conditions: MAA:BiBA:NaOH:CuBr:NaBr = 1:1:1:0.1:0.5, $C_{\mathrm{MAA}} = 0.590\,\mathrm{mol\,L^{-1}}$.

Surprisingly, bpy yielded 65%, a value not too far from 75% with TPMA. TPMA is not only more expensive, but it is nearly one thousand times more active than bpy.[253] The reaction with bpy was however fast enough to generate the desired lactone before BiBA hydrolysis. As usual, a lower yield means a slower process and more time for the hydrolysis to occur.

Unfortunately, entry A17 with bpy showed overconsumption of MAA, which did not happen in entry A01 with TPMA. At the end of entry A17, BiBA reached full conversion, but it was partially (18%) hydrolyzed into HiBA. On the other side, MAA reached 99% conversion. Since the MAA:BiBA ratio is 1:1 and since BiBA did not fully react with MAA, probably some multiple additions occurred. On the contrary, with TPMA (entry A01), MAA reached only 79% when BiBA conversion was full. Even in this case, 15% of BiBA was hydrolyzed into HiBA. This suggests that the Cu complex may be involved in the lactonization mechanism. Unfortunately, no time was left to prove or disprove this idea.

The comparable results with both bpy and TPMA may indicate that the ligand is not that significant in the activation step of ATRA. However, entry A18 demonstrated that a proper ligand is required for Cu to activate the initiator. Indeed, no lactone formation was observed with CuBr alone, without any ligand.

9.11 Change of base

A base is generally required by the ATRA-L system of our research. The base has two main functions. First, it deprotonates and, consequently, it completely solubilizes BiBA. Second, the base keeps the environment from being too acidic, which would break the catalytic system by protonation of the ligand. So far, NaOH was mainly used as a base, but it can have some disadvantages. For instance, NaOH needs to be used in solution, but, even if stored in a closed vial, it is slowly neutralized by the CO_2 from the air. A saturated NaOH solution was therefore titrated and used, but, due to its high concentration, a small error in its withdrawal could result in a big change of pH in the reaction mixture. Fortunately, the reactions proved to be reproducible even if such a concentrated NaOH solution was used. However, it could be appropriate to study other bases, which can be weighted or withdrawn with bigger volumes. As reported in Table 9.8, TEA (entries A19 and A21), Na_2CO_3 (entry A20) and PBS (entry A22) were studied besides NaOH (entries A01 and A06). PBS is an aqueous buffer solution with a pH of 7.4 composed of KH_2PO_4, Na_2HPO_4 and NaCl (see subsection 8.1.1 for further information).

As a result, the change of the base does not make a big difference in the pH and thus in the lactone yield. Entries A01, A19, and A20 with 1 equiv of NaOH, TEA, and Na_2CO_3 respectively gave yields close to each other (75%, 82%, and 76% respectively). The pH of these three reactions was calculated to be 4.0 for all of them. The same can be said for entries A6 and A21 with half the amount of base from

Entry	**Base** (MR)	**pH**	**Yield** [%]
A01	NaOH (1)	4.0	75
A19	TEA (1)	4.0	82
A20	Na_2CO_3 (0.5)	4.0	76
A06	NaOH (0.5)	3.0	83
A21	TEA (0.5)	3.0	84
A22	PBS	2.3	83

Table 9.8: Change of base. Conditions: MAA:BiBA:CuBr:TPMA:NaBr = 1:1:0.1:0.2:0.5, $C_{\mathrm{MAA}} = 0.590\,\mathrm{mol\,L^{-1}}$.

previous entries and with a pH of 3.0. Respectively, the bases are NaOH and TEA and the yields are 83% and 84%. As already discussed in section 9.5, pH has both effects of slowing down the hydrolysis and also the ATRA reaction. For comparison, entry A19 with 1 equiv of TEA reached 83% BiBA conversion after 3 h, but it was probably complete in a few hours. Differently, entry A21 with 0.5 equiv of TEA took 23 h to reach 94% BiBA conversion and it was complete in less than 30 h.

Substituting NaOH with TEA is a good achievement for one reason in particular. It proves that tertiary amines can perfectly work as bases in our ATRA-L reaction system. As anticipated in section 9.7 and better discussed in section 9.12, alkenes containing a tertiary amine can be used to substitute NaOH. For instance, DMAEMA or DMAPMAm can act both as alkenes and as bases.

PBS (entry A22) was also tested as a solvent and no other base was added. The reaction yielded a good 83%, but its pH as low as 2.3 greatly slowed down the reaction. After 3 days, it reached 93% BiBA conversion and it was interrupted after 7 days with 95% BiBA conversion. The small concentration of phosphates inside PBS could not handle the high concentration of the weak acids like BiBA and MAA. Moreover, PBS contains NaCl, which can be dangerous for an atom transfer radical reaction based on another halogen like Br. The concentration of Cl^- in the PBS solution is more than four times higher than the concentration of Br^- in our system. Therefore, both chlorinated and brominated monoadducts could be formed. As previously observed, it should be more difficult for chlorinated monoadducts to lactonize if compared to brominated ones, in agreement with their BDEs.[212] Fortunately, no free monoadducts were observed from NMR and it was deduced that all the addition product were rapidly lactonized.

In short, the nature of the base is not important if the pH is maintained the same. This opens the door to a wide range of bases and in particular to alkenes with basic moieties.

9.12 Change of alkene

In order to have lactonization, the initiator is required to have a carboxylic acid. Furthermore, the active halogen of the initiator should be relatively close to the carboxyl group. In fact, the final lactone ring size depends on the distance between the active halogen and the carboxyl group (Scheme 9.6). For instance, an α-halogen and a β-halogen generate a γ-lactone and a δ-lactone, respectively. As known, γ- and δ-lactones are the most stable because of the number of members on the ring (5 and 6 respectively). However, the halogen needs to be in α position to be activated, limiting the obtainable lactones to only the γ-ones. For δ-lactone, a more complex structure of the initiator would be required to make the β-halogen active. Thus, there is not a wide range in the choice of the initiator and only two α-substituents can be changed. For this reason, different initiators from BiBA were not particularly studied.

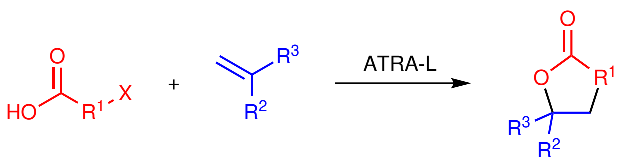

Scheme 9.6: ATRA-L generating different lactone ring sizes. The distance between the active halogen and the carboxylic acid (i.e. the length of R^1) determines the final size of the ring.

On the other hand, the choice of the alkene is less strict in our ATRA-L system. Anyway, vinyls were chosen for their fast addition. A fast addition can overcome the problem of the hydrolysis of the initiator. In addition, one of the main goals of this study is to use very active alkenes, which are usually forbidden in ATRA. As discussed in chapter 5, the fast lactonization of the monoadducts does not force the synthesis to only products with less active halogens. As displayed in Figure 9.8 and Table 9.9 in fact, (meth)acrylates and acrylamides were studied, which are so active that are generally used as monomers in radical polymerization processes, like ATRP.

Fantin et al. suggested that the mechanism of the lactonization could be a

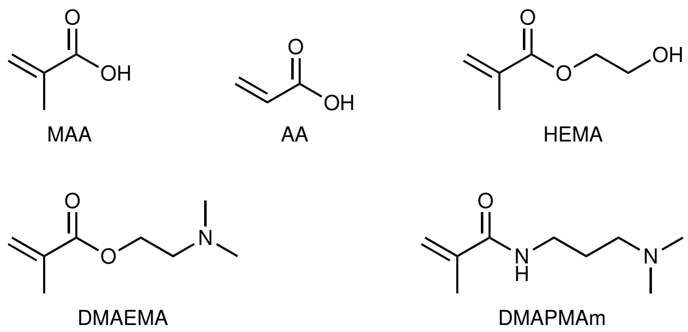

Figure 9.8: Studied alkenes.

Entry	**Alkene**	**NaOH** [MR]	**pH**	**Yield** [%]
A01	MAA	1	4.0	75
A23	AA	1	3.7	78
A08	HEMA	1	8.9	82
A13	DMAEMA	—	6.1	74
A24	DMAPMAm	—	6.7	49

Table 9.9: Testing different alkenes. Conditions: alkene:BiBA:CuBr:TPMA:NaBr = 1:1:0.1:0.2:0.5, $C_{\text{alkene}} = 0.590\,\text{mol}\,\text{L}^{-1}$.

nucleophilic substitution. They observed the lactonization between the last two monomer units of the polymer chain during the SARA ATRP of MAA in H_2O.[212] The lactonization mechanism of our system with BiBA and MAA could be the same and, in this case, it is a S_N1 or a S_N2 type? Four aspects should be considered about the halogenated C of the monoadduct (Scheme 9.7). *(i)* The S_N1 is very likely on a tertiary C due to steric hindrance. *(ii)* Furthermore, H_2O as solvent should stabilize the carbocation, promoting the S_N1 type. *(iii)* However, the carboxylate is a good nucleophile, leading to think that a S_N2 is more plausible. *(iv)* Lastly and most importantly, a S_N1 would take place via a carbenium ion intermediate, which would be extremely destabilized by the adjacent carboxyl group, a strong EWG. Therefore, the most plausible nucleophilic substitution mechanism is the S_N2.

If AA is used instead of MAA, the halogenated C involved in the lactonization changes from tertiary to secondary (Scheme 9.7). This difference can change the mechanism of the lactonization and the result of the reaction. A comparison between two reactions, one with MAA and one with AA (entries A01 and A23 of Table 9.9 respectively), can add a clue to understanding the mechanism. However, no big difference was found between the two reactions. In fact, the two final yields are very close to each other, 75% with MAA and 78% with AA. Unfortunately, this

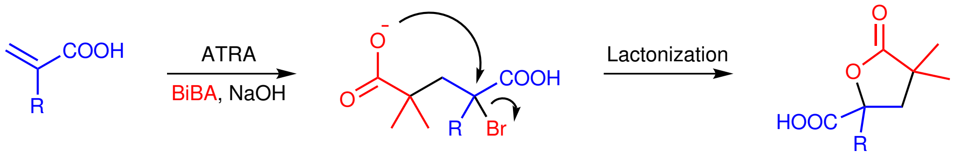

Scheme 9.7: ATRA-L via nucleophilic substitution of AA (R = H) or MAA (R = Me).

same result did not increase our understanding of the type of mechanism. On the other hand, our ATRA-L system is satisfyingly robust that can work both with methacrylates and acrylates.

Other methacrylates were also tested, like HEMA and DMAEMA (entries A08 and A13, respectively). The results with these two methacrylates are comparable with the ones with MAA and AA: HEMA and DMAEMA yielded 82% and 74% respectively. As discussed in section 9.5 however, HEMA and its generated lactone were hydrolyzed to MAA and its corresponding lactone. The same was observed for DMAEMA, which is hydrolyzed into MAA and 2-(dimethylamino)ethanol. A methacrylamide like DMAPMAm was therefore tested (entry A24, Table 9.9), which is highly less prone to hydrolysis. As expected, hydrolysis with DMAPMAm was not observed, but the yield dropped to 49%. Unfortunately, entry A24 was not repeated to confirm the result for a matter of time. As usual, a lower yield is symptomatic of a higher BiBA hydrolysis. However, the good result is that the ATRA-L system of our studies is working even with (meth)acrylamides, which are hardly hydrolyzable.

Importantly, DMAEMA and DMAPMAm (entries A13 and A24 respectively) can act both as alkenes and as bases, thanks to their amine groups. In fact, the addition of 1 equiv of NaOH is not necessary when this type of alkenes are used, simplifying the system.

In addition, DMAPMAm, DMAEMA, and HEMA do not have a carboxylic acid. This could be an advantage from a purification point of view of the final lactone. As a matter of fact, purification by chromatography can be quite inefficient when a carboxylic acid is present. However, DMAEMA and HEMA could be hydrolyzed to MAA, restoring the carboxylic acid. On the other hand, the amide of DMAPMAm hardly hydrolyzes.

In conclusion, various vinyls usually forbidden in ATRA were successfully tested in the ATRA-L system we developed. Methacrylates are easily hydrolyzed to MAA, therefore a methacrylamide was studied with encouraging results. A comparison between MAA and AA did not bring extraordinary new clues to the lactonization mechanism, which is thought to be a nucleophilic substitution. Lastly, alkenes with a tertiary amine group were proved to be an interesting replacement of NaOH, since 1 equiv of a base is required by the reaction system.

9.13 DMSO as solvent

One of the strengths of our ATRA-L system is the use of H_2O as a solvent. H_2O is inexpensive and the best solvent choice from a green point of view. However, other organic solvents are often a better choice for the synthesis of small organic molecules. Moreover, hydrolysis of the initiator is the main weakness of our reaction system and it is undoubtedly accelerated by the fact that H_2O is the solvent. Therefore, we decided to perform a few reactions with a polar aprotic solvent like DMSO. In the reactions of Table 9.10, DMSO-d_6 is used instead of normal DMSO for reasons related to the NMR analysis.

Entry	**Type**	**Initiator**	**Solvent**	**Yield** [%]
A14	normal[a]	BiBA	H_2O[b]	60
A25	normal[a]	BiBA	DMSO-d_6	40
A26	SARA[c]	BPAA	DMSO-d_6	0
A27	SARA[c]	BiBA	DMSO-d_6	0

Table 9.10: Testing DMSO as solvent. [a]Conditions: DMAEMA:BiBA:CuBr:TPMA = 1:1:0.1:0.2, $C_{\text{DMAEMA}} = 0.295\,\text{mol}\,\text{L}^{-1}$. [b]Added NaBr (MR = 0.5). [c]Conditions: St:initiator:Cs_2CO_3:$CuBr_2$:TPMA = 1:1:1:0.0002:0.002, Cu wire 6 cm, $C_{\text{St}} = 0.218\,\text{mol}\,\text{L}^{-1}$.

We decided to directly transfer the reaction system of entry A14 straight from H_2O to DMSO. Aside from the solvent, the only other difference is the usage of NaBr, which is not necessary in DMSO. In ATRP, the addition of halide salts in protic solvents is considered a good practice as it avoids the reversible dissociation of the halide from the Cu complex, sharpening the molecular weight distribution of the obtained polymer.[254,255] Entry A14 in H_2O with DMAEMA as alkene and base yielded 60%. Surprisingly, the same system transferred to DMSO (entry A25, Table 9.10) worked, but the yield was decreased to 40%. In both these reactions, BiBA was completely consumed in the end and the only side reaction observed from NMR was the hydrolysis of BiBA. Hydrolysis was possible also in DMSO due to the presence of H_2O as an impurity.

We hence designed a completely new reaction system in DMSO from scratch (entry A26, Table 9.10). St is the alkene, α-bromophenylacetic acid (BPAA) the initiator, and Cs_2CO_3 the base. $CuBr_2$/TPMA is the catalyst with a SARA regeneration method, letting the load of $CuBr_2$ to be as low as 200 ppm (plus 2000 ppm of TPMA and a Cu wire). Unfortunately, this SARA ATRA-L in DMSO never worked and the formation of any lactone was not observed. BPAA was rapidly consumed by other side reactions and the by-products were not thoroughly investigated. The reaction was repeated with BiBA as the initiator (entry A27, Table 9.10), but the same was observed. BiBA was only converted to a series of by-products and the alkene was nearly not consumed, as with BPAA. The BiBA side reaction products were probably HiBA, TMSA, and (α-bromopropionic acid) BPA, as discussed in section 9.4. If TMSA was formed, then the radical activation of BiBA was working even with the low load of the catalyst, but the generated radical did not react as expected. Moreover, H_2O was present in the reaction mixture due to impurities in the DMSO and to the acid–base reaction between BPAA/BiBA and Cs_2CO_3.

Given the poor results of the reaction systems in DMSO, we decided not to investigate this further. Apparently, the initiator is rapidly consumed into various side reactions into various by-products. In H_2O instead, hydrolysis of the initiator is by far the major side reaction. Moreover, DMSO is not as inexpensive and green as H_2O is. In literature, it was also pointed out that H_2O is required for some ATRA-L systems to work.[189,194,198,239]

9.14 Change of Cu^I source

When the reproducibility of the ATRA-L of this study was tested, no particular problems were found. Meticulous attention to detail let us develop an experimental procedure that minimizes experimental errors. Reproducibility has never been a problem. However, it was unfortunately discovered that the change of CuBr source could lead to very different results.

In Table 9.11 are reported six reactions with six different CuBr sources, including entry A01 which is generally taken as an example for comparisons in almost every section of this chapter. As can be seen from the Table 9.11, a wide range of lactone yields came out from the same reaction, ranging from 92% to 8%. However, the different sources of CuBr are not different vendors, but instead different chemists working in the same laboratory that used slightly different processes to purify the CuBr. Mipha, Daruk, Revali, and Urbosa are fantasy names for these chemists. The numbers following some of these names (1 and 2) indicate two different CuBr samples with two separate purification processes (but prepared with the same procedure by the same chemist).

Entry	**Cu^{I} source**	**Yield** [%]
A01	CuBr (Mipha-1)	75
A28	CuBr (Mipha-2)	92
A29	CuBr (Daruk)	27
A30	CuBr (Revali)	22
A31	CuBr (Urbosa-1)	10
A32	CuBr (Urbosa-2)	8
A33	$Cu(MeCN)_4BF_4$	0

Table 9.11: Effect of the Cu^{I} source. Conditions: MAA:BiBA:Cu^{I}:TPMA:NaBr = 1:1:0.1:0.2:0.5, $C_{\mathrm{MAA}} = 0.590\,\mathrm{mol\,L^{-1}}$, pH = 4.0.

The purification procedure of CuBr was the same for all the chemists, but with small differences. As reported in subsection 8.1.1, CuBr was washed several times with glacial AcOH, then with EtOH, and finally with Et_2O. Anyhow, some differences in the procedure are present: the number of times the CuBr was washed, the duration of the washings, the used solvent volumes, the drying method, and the chosen atmosphere during the washings (air or N_2). Independently on these small differences, however, all the CuBr prepared with this method were nearly pure with only small traces of Cu^{II}. CuBr from entry A32 (Table 9.11) furnished the lowest lactone yield and was therefore analyzed spectrophotometrically to determine the relative contents of Cu^{I} and Cu^{II}. Precisely, CuBr from Urbosa-2 was dissolved in DMF and a UV–Vis spectra was collected. From the absorbance and from the application of the Beer–Lambert law, the mole percent of Cu^{I} was found to be 95.8%, with only 4.2% of Cu^{II}. After this result, it would be logically incorrect to attribute the low 8% lactone yield of entry A32 to the Cu^{II} impurities inside the CuBr. In fact in section 9.2, a decrease in the quantity of the Cu/TPMA catalyst was studied, but the yield never dropped so significantly. There must be something else related to CuBr responsible for the poor efficiency of the system.

Another responsible for the poor efficiency of these reactions could be some residues of AcOH from the first washing of the CuBr. AcOH is undoubtedly acidic and the pH is one of the main concerns in our ATRA-L system. However, an NMR analysis of CuBr from Urbosa-2 revealed the absence of AcOH or any other organic impurity. The hypothesis of AcOH contamination was therefore discarded. So far, UV–Vis and NMR did not find anything wrong with the CuBr from Urbosa-2, nevertheless there is still a problem with it.

No problems were found with the CuBr sources and no hypothesis was confirmed about the strong impact of the CuBr sources on the yield. Actually, only one unverified hypothesis remained as a possible explanation. Small differences in the purification and drying process could have led to small differences in the morphology of the CuBr grains forming the powder. Any difference in the morphology of the CuBr powder could have consequences on the solubility of it and, as a result, on the rate of the ATRA process. As mentioned before, if the ATRA is not fast enough, the hydrolysis of the initiator compromises the reaction from reaching a satisfying yield. As a matter of fact, phase separation was observed at the beginning of the reactions that yielded the lowest values (entries A29, A30, A31, and A32 of Table 9.11). In these reactions, a small volume of a dark green liquid phase was initially formed. The dark green color may indicate that this phase was subtracting Cu catalyst from the other reaction mixture, slowing down the process.

In order to avoid the problems encountered with different CuBr sources, a reaction with $Cu(MeCN)_4BF_4$ was therefore studied (entry A33, Table 9.11). In addition, $Cu(MeCN)_4BF_4$ was added as a solution to have all the Cu^I ready at the beginning of the reaction. Unexpectedly, $Cu(MeCN)_4BF_4$ was completely unable to trigger the ATRA reaction. The reason is unknown and, unfortunately, no time was left to let me investigate why it did not work. The reaction was also repeated paying particular attention to the possible oxidation of Cu^I, but the same result was obtained and no lactone was observed from NMR. The reason for the non-functioning of the system with $Cu(MeCN)_4BF_4$ is unknown. Other studies successfully used $Cu(MeCN)_4BF_4$ as transition metal catalyst in atom transfer radical reactions.[250,256–260]

In conclusion, the morphology of the CuBr powder could alter its rate of solubilization in the first moments of the reaction. Subsequently, the rate of the ATRA is negatively affected and the hydrolysis can take over. However, this hypothesis is absolutely not confirmed. The explanation for the different yields from different CuBr sources could be another one. Interestingly, the Mipha-2 from entry A28 (Table 9.11) yielded 92%. This means that working on the CuBr source could boost the reaction system to relatively high yields.

Chapter 10

Conclusion

The SARA ATRP in H_2O of Fantin et al.[212] was successfully adapted to develop an efficient ATRA-L system (Scheme 10.1). Both a normal and a SARA ATRA-L were developed, depending on the catalytic system. A γ-lactone with two substituents is obtained from the process. Satisfyingly, it was possible to use alkenes that are generally forbidden in ATRA, like (meth)acrylates and methacrylamides. As a matter of fact, the fast lactonization prevents any reactivation of the obtained monoadduct. Furthermore, the ATRA-L reaction is carried out in H_2O and at 25 °C, making the process interesting from a green point of view.

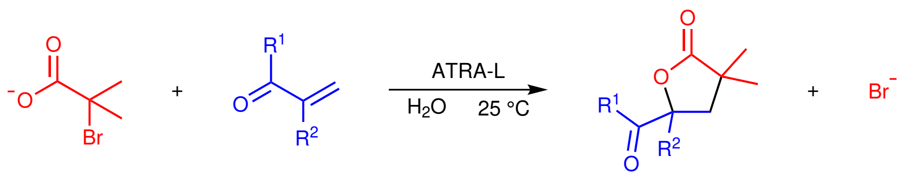

Scheme 10.1: Developed ATRA-L reaction. The catalytic system is Cu^{I}(TPMA)Br complex in normal conditions or [Cu^{II}(TPMA)Br][Br] coupled with Cu^0 in SARA conditions. NaBr is also added to increase the stability of the catalytic complex. R^1 and R^2 define the alkenes shown in Figure 9.8.

The biggest drawback of the studied ATRA-L process is the hydrolysis of the initiator. If the ATRA is not fast enough, the final lactone yield is compromised by the hydrolysis of the initiator. The pH resulted to be the main condition affecting the hydrolysis and lowering it decreases the hydrolysis rate. However, a lower pH decreases also the ATRA rate and these two effects almost cancel each other out. In order to reach higher yields, the concentration of Cu^{I}(TPMA)Br can be increased, accelerating the ATRA reaction. However, we wanted to avoid concentrations of Cu above 10 mol % for a principle of atom efficiency. In addition, the concentration of the solution can have a moderate effect in increasing the yield. A higher concentration of the reagents resulted in a decreased hydrolysis and therefore in higher yields. Lastly, increasing the amount of initiator relative to the alkene was proved to be a possible solution to the hydrolysis problem. In this way, the yield was increased, but it should be kept in mind that the atom efficiency of the process was actually decreased. Besides hydrolysis, other small side reactions are occurring. In the case of BiBA, HiBA from the hydrolysis is the major by-product, but also MPA, MAA, and TMSA were identified from NMR as minor by-products.

While pH is very important for the fate of the reaction, the type of base is not. Various organic and inorganic bases were tested, and they all returned similar results when the pH was the same. Interestingly, DMAEMA and DMAPMAm were used as both alkenes and bases. They are individually capable of both giving radical addition and quenching the acidity of an initiator like BiBA.

Apart from TPMA, bpy was found to be a good ligand for this ATRA-L system in H_2O. The yield with TPMA was higher than with bpy, but TPMA is a more expensive chemical substance. As a future development, other ligands can be tested and they can be chosen based on their activity and economical availability. Furthermore, a system without any ligand but with only Cu^I did not result in any radical addition reaction.

We successfully transferred the normal ATRA-L from H_2O to DMSO. However, the best results were obtained in H_2O. Probably, a deeper study of the ATRA-L in DMSO could return better results with higher yields, but H_2O should be preferred as solvent for its availability and greenness.

Some problems were encountered while changing the Cu^I source. Perhaps for solubility reasons, using slightly different purification methods of CuBr resulted in very different yields. This is clearly a disadvantage of the system, but developing a better understanding of the problem can be used to boost the ATRA and therefore to reach higher yields.

The more plausible mechanism of the lactonization is the S_Ni. In this case, it probably follows a S_N2 mechanism. Indeed, the S_N1 would require the highly unstable formation of a carbenium ion in α-position to a carboxylic group. However, other mechanisms found in literature like S_Hi and ORPC (Scheme 7.1) could not be totally excluded. Furthermore, the Cu catalyst may be involved in the lactonization mechanism. In fact, during the ATRP of MAA in H_2O, it was observed the lactonization of the last two monomer units with Cu/TPMA as catalyst,[212] but not with Fe/porphyrin.[261] This suggests that Cu/TPMA may have an active role on the lactonization mechanism. In addition, the usage of Cu/bpy instead of Cu/TPMA as catalyst (section 9.10) showed the formation of multiple addition products and therefore a slower lactonization rate.

10.1 Future perspectives

One of the most important aspects of this ATRA-L system that should be monitored is the hydrolysis of the initiator. However, only brominated initiators like BiBA were studied. Different halogens (Cl, Br, and I) can have important effects on ATRA, lactonization, and hydrolysis. Compared to Br, a chlorinated monoadduct should lactonize more slowly,[212] but the chlorinated initiator is less prone to hydrolysis. If the ATRA and the lactonization are fast even in a chlorinated system, then the hydrolysis could be highly suppressed. An iodinated system should also be studied in order to have a complete picture of the behaviors of the three halogens toward the three reactions (ATRA, lactonization, and hydrolysis). Obviously, changing the halogen on the initiator means changing the halogen of the entire system accordingly, taking into account all the other halogenated reagents. In the case of our ATRA-L system, BiBA was combined with CuBr and NaBr.

α-Haloamides can also be taken into consideration as initiators, instead of haloesters. The halogen from α-haloamides should be less prone to hydrolysis if compared to the one from α-haloesters. Therefore, the reactivity of haloamides toward hydrolysis and ATRA in our system should be studied. However, the formation of a lactone is only possible when a carboxyl group is present on the initiator. An amide could instead lead to the formation of a lactam or an iminolactone, as reported in the literature.[215–218] In any case, iminolactones are easily hydrolyzed to lactones in mild acidic conditions.[214]

The concentration of Br^- should also be investigated. The Br^- ions that are present in the reaction mixture come from four different sources: NaBr, CuBr, hydrolysis of the initiator, and lactonization of the monoadduct. Indeed, concentrations of Br^- affects the rate of hydrolysis and lactonization because these two reactions release Br^-. Furthermore, NaBr is generally added to increase the stability of the catalytic complex. A change in Br^- concentration could consequently alter the rate of the ATRA reaction. For these reasons, the effects of the Br^- concentration should be explored and also a control experiment without the addition of NaBr should be carried out.

In our ATRA-L study, BiBA was almost always used as the initiator. However, it would be interesting to study other initiators in order to have a comparison between the α-substituents. A simple example is shown in Scheme 10.2, where the α-substituents are methyl groups (two for BiBA, one for BPA, and no substituents for BAA). The ATRA activation rate constant should decrease as the number of methyl groups is decreasing. A less active initiator like BAA is generally forbidden in an ATRA with MAA, because the halogen of the generated monoadduct is more active than the initial BAA. In ATRA, the bad result of an initiator less active than the monoadduct is the telomerization. However, ATRA-L could possibly prevent this side effect typical of ATRA. If the lactonization is fast enough, then there is no concern on the relative activation rate constants of initiator and monoadduct. Lastly, it should be also taken into account the Thorpe–Ingold effect that the substituents have on the lactonization.[262]

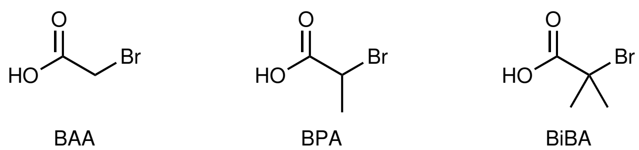

Scheme 10.2: Example of substituents change on the initiator.

By changing the two substituents on the initiator, it is possible to synthesize different lactones with a different couple of α-substituents. However, there are four more substituents than can be chosen that originate from the alkene, as shown in Scheme 5.2. A deeper study on substituents can open the doors to a wide range of γ-lactones. However, the rate of radical addition strongly depends on the alkene structure. Moreover, also the reactivity of the halogen of the monoadduct toward the lactonization depends on the structure of the alkene. So far, only (meth)acrylates and methacrylamides were tested, which are very reactive alkenes that lead to monoadducts with very reactive halogens. Therefore, the behavior of less reactive alkenes should be studied in our ATRA-L system.

The regeneration of the catalyst is a powerful method that allows the usage of small quantities of transition metal catalyst. Furthermore, the metal can be added to the reaction mixture in its higher oxidation state, which is more stable in air and less expensive. Alongside a normal ATRA-L in fact, also a SARA ATRA-L with catalyst regeneration was set up. As a future development, the SARA system should be studied more thoroughly in order to let it reach the same results as the normal system. Furthermore, other catalyst regeneration techniques should be tested for the same advantages described above. For example, since the reaction is carried out in H_2O, AsAc can be used in an ARGET system. Additionally, another strategy can be adopted to decrease one of the two components of the catalyst. The catalyst is a complex formed by a transition metal and a proper ligand. Throughout the entire ATRA-L study of normal conditions, the ligand was always present in a double amount compared to the stoichiometry of the complex. As a future perspective, the ratio between the ligand and the transition metal could be driven to a value closer to the stoichiometric one. The goal is to increase the atom efficiency of the process.

The solvent of the reaction is another point that can be expanded in the future. So far, all the reactions were carried out in H_2O, except only one good result in DMSO. H_2O is a great solvent since it is cheap and the best choice from a green point of view. However, using different solvents from H_2O could suppress the problem of hydrolysis of the initiator. Other possible organic polar solvents are for example DMF, THF, acetone, MeCN, and EtOAc. Alcohols as solvents may give esterification of the carboxylic acid of the initiator, compromising the lactonization. Lastly, a complete apolar system could be also tested, with apolar solvent and reagents.

The temperature is another aspect that was not explored. All the proposed reactions of this study were performed at 25 °C. Therefore, the effect of the temperature could be studied in the future.

In the ATRA-L study here presented, the lactonization is performed by the carboxyl group of the initiator. However, the lactone ring closure could be performed by any carboxyl group present on the monoadduct. The only requirement is the distance between the halogenated C and the carboxyl group, on which the final size of the lactone ring depends. Therefore, the carboxyl group could be found on the alkene instead of on the initiator. As shown in Scheme 10.3a, the monoadduct is always a γ-halocarboxylic acid, but the carboxylic group comes from the alkene. The distance between the halogenated C and the carboxyl group allows the formation of the stable γ-lactone. Ideally, the 4-pentenoic acid could be replaced by a 5-hexenoic acid and a δ-lactone should be obtained instead. The same principle is applied in Scheme 10.3b for the synthesis of phthalides.

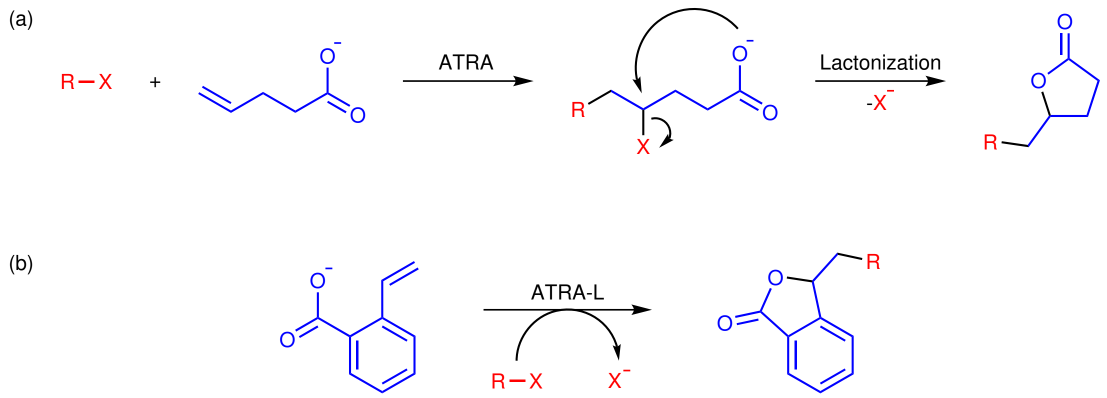

Scheme 10.3: Examples of ATRA-L with the lactonization performed by a carboxyl group from alkene.

Acknowledgments

First of all, this work would not have been possible without the valuable support of my supervisors, Prof. Franco Ghelfi and Francesca Parenti. Their motivation, their scientific observations, and their teachings guided me through this entire project. A special thank goes also to all the present and past members of our research group: PhD student Niccolò Braidi, and graduating students Alberto Menabue, Valentina Buzzoni, and Maria Federica Marchesi for their significant contribution regarding the anomalous gelation of polystyrene; Prof. Marco Borsari for the electrochemical analyses; and graduating students Maria Serena Schenetti, Eleonora Adonella Salati, Manuel Imperato, Andrea Bignardi, Gaia Serafini, and Nicola Porcelli for their important work in the ARGET ATRP of styrene.

My deep gratitude goes to Versalis (Eni) S.p.A. for financial support and to all the brilliant people who work at the "Claudio Buonerba" Research Center of Mantua, especially to Aldo Longo, Angelo Ferrando, and Elena Bedogni.

My great appreciation goes also to the Electrocatalysis and Applied Electrochemistry Group of the University of Padua. A special thank to Prof. Armando Gennaro and Prof. Abdirisak Ahmed Isse.

Many thanks to Prof. Maria Letizia Focarete and Chiara Gualandi from the University of Bologna for their support in understanding the physical nature of the polymer gel materials.

I am particularly grateful to all the amazing people that form the Matyjaszewski Polymer Group. My grateful thanks to Prof. Krzysztof Matyjaszewski, Francesca Lorandi, Marco Fantin, Grzegorz Szczepaniak, Sajjad Dadashi Silab, and Adam Gorczynski for working with me on the ATRA-L project.

Thanks also to all the friends and co-workers from the Department of Chemical and Geological Sciences of the University of Modena and Reggio Emilia, especially to Prof. Andrea Cornia and Alessio Nicolini for sharing with me their laboratory equipment.

My gratitude goes also to Alice Ballerini for helping me with the graphical representation of all the "worms" (i.e. polymer chains).

Bibliography

[1] D. A. Shipp, Reversible-deactivation radical polymerizations, *Polymer Reviews* **51**(2), 99–103 (2011), DOI: 10.1080/15583724.2011.566406.

[2] K. Matyjaszewski, Atom transfer radical polymerization (ATRP): Current status and future perspectives, *Macromolecules* **45**(10), 4015–4039 (2012), DOI: 10.1021/ma3001719.

[3] S. Perrier, 50th anniversary perspective: RAFT polymerization—A user guide, *Macromolecules* **50**(19), 7433–7447 (2017), DOI: 10.1021/acs.macromol.7b00767.

[4] T. Junkers, C. Barner-Kowollik, and J. Lalevée, Recent developments in nitroxide mediated polymerization, in *Nitroxide mediated polymerization: From fundamentals to applications in materials science*, edited by D. Gigmes, chapter 6, pages 264–304, Royal Society of Chemistry, 2016, DOI: 10.1039/9781782622635-00264.

[5] L. E. Allan, M. R. Perry, and M. P. Shaver, Organometallic mediated radical polymerization, *Progress in Polymer Science* **37**(1), 127–156 (2012), DOI: 10.1016/j.progpolymsci.2011.07.004.

[6] N. V. Tsarevsky and K. Matyjaszewski, Atom transfer radical polymerization (ATRP), in *Fundamentals of controlled/living radical polymerization*, edited by N. V. Tsarevsky and B. S. Sumerlin, chapter 8, pages 287–357, Royal Society of Chemistry, 2013, DOI: 10.1039/9781849737425-00287.

[7] T. G. Ribelli, F. Lorandi, M. Fantin, and K. Matyjaszewski, Atom transfer radical polymerization: Billion times more active catalysts and new initiation

systems, *Macromolecular Rapid Communications* **40**(1), 1800616 (2019), DOI: 10.1002/marc.201800616.

[8] M. Kato, M. Kamigaito, M. Sawamoto, and T. Higashimura, Polymerization of methyl methacrylate with the carbon tetrachloride/dichlorotris-(triphenylphosphine)ruthenium(II)/methylaluminum bis(2,6-di-*tert*-butylphenoxide) initiating system: Possibility of living radical polymerization, *Macromolecules* **28**(5), 1721–1723 (1995), DOI: 10.1021/ma00109a056.

[9] J.-S. Wang and K. Matyjaszewski, Controlled/"living" radical polymerization. Atom transfer radical polymerization in the presence of transition-metal complexes, *Journal of the American Chemical Society* **117**(20), 5614–5615 (1995), DOI: 10.1021/ja00125a035.

[10] F. Lorandi and K. Matyjaszewski, Why do we need more active ATRP catalysts?, *Israel Journal of Chemistry* **60**(1–2), 108–123 (2020), DOI: 10.1002/ijch.201900079.

[11] P. L. Golas and K. Matyjaszewski, Marrying click chemistry with polymerization: Expanding the scope of polymeric materials, *Chemical Society Reviews* **39**(4), 1338–1354 (2010), DOI: 10.1039/B901978M.

[12] D. F. Grishin and I. D. Grishin, Controlled radical polymerization: Prospects for application for industrial synthesis of polymers (review), *Russian Journal of Applied Chemistry* **84**(12), 2021–2028 (2011), DOI: 10.1134/s1070427211120019.

[13] K. Matyjaszewski and N. V. Tsarevsky, Macromolecular engineering by atom transfer radical polymerization, *Journal of the American Chemical Society* **136**(18), 6513–6533 (2014), DOI: 10.1021/ja408069v.

[14] P. Krys and K. Matyjaszewski, Kinetics of atom transfer radical polymerization, *European Polymer Journal* **89**, 482–523 (2017), DOI: 10.1016/j.eurpolymj.2017.02.034.

[15] T. Ando, M. Kamigaito, and M. Sawamoto, Iron(II) chloride complex for living radical polymerization of methyl methacrylate, *Macromolecules* **30**(16), 4507–4510 (1997), DOI: 10.1021/ma961478j.

[16] K. Matyjaszewski, M. Wei, J. Xia, and N. E. McDermott, Controlled/"living" radical polymerization of styrene and methyl methacrylate catalyzed by iron complexes, *Macromolecules* **30**(26), 8161–8164 (1997), DOI: 10.1021/ma971010w.

[17] Y. Wang and K. Matyjaszewski, ATRP of MMA in polar solvents catalyzed by $FeBr_2$ without additional ligand, *Macromolecules* **43**(9), 4003–4005 (2010), DOI: 10.1021/ma1002276.

[18] Y. A. Kabachii, S. Y. Kochev, L. M. Bronstein, I. B. Blagodatskikh, and P. M. Valetsky, Atom transfer radical polymerization with Ti(III) halides and alkoxides, *Polymer Bulletin* **50**(4), 271–278 (2003), DOI: 10.1007/s00289-003-0157-9.

[19] C. Granel, P. Dubois, R. Jérôme, and P. Teyssié, Controlled radical polymerization of methacrylic monomers in the presence of a bis(ortho-chelated) arylnickel(II) complex and different activated alkyl halides, *Macromolecules* **29**(27), 8576–8582 (1996), DOI: 10.1021/ma9608380.

[20] H. Uegaki, Y. Kotani, M. Kamigaito, and M. Sawamoto, Nickel-mediated living radical polymerization of methyl methacrylate, *Macromolecules* **30**(8), 2249–2253 (1997), DOI: 10.1021/ma961367k.

[21] G. Moineau, M. Minet, P. Dubois, P. Teyssié, T. Senninger, and R. Jérôme, Controlled radical polymerization of (meth)acrylates by ATRP with $NiBr_2(PPh_3)_2$ as catalyst, *Macromolecules* **32**(1), 27–35 (1999), DOI: 10.1021/ma980995u.

[22] B. Wang, Y. Zhuang, X. Luo, S. Xu, and X. Zhou, Controlled/"living" radical polymerization of MMA catalyzed by cobaltocene, *Macromolecules* **36**(26), 9684–9686 (2003), DOI: 10.1021/ma035334y.

[23] P. Lecomte, I. Drapier, P. Dubois, P. Teyssié, and R. Jérôme, Controlled radical polymerization of methyl methacrylate in the presence of palladium acetate, triphenylphosphine, and carbon tetrachloride, *Macromolecules* **30**(24), 7631–7633 (1997), DOI: 10.1021/ma970890b.

[24] F. Simal, A. Demonceau, and A. F. Noels, Highly efficient ruthenium-based catalytic systems for the controlled free-radical polymerization of vinyl monomers, *Angewandte Chemie International Edition* **38**(4), 538–540 (1999), DOI: 10.1002/(SICI)1521-3773(19990215)38:4<538::AID-ANIE538>3.0.CO;2-W.

[25] M. Haas, E. Solari, Q. T. Nguyen, S. Gautier, R. Scopelliti, and K. Severin, A bimetallic ruthenium complex as a catalyst precursor for the atom transfer radical polymerization of methacrylates at ambient temperature, *Advanced Synthesis & Catalysis* **348**(4–5), 439–442 (2006), DOI: 10.1002/adsc.200505318.

[26] J. A. M. Brandts, P. van de Geijn, E. E. van Faassen, J. Boersma, and G. van Koten, Controlled radical polymerization of styrene in the presence of lithium molybdate(V) complexes and benzylic halides, *Journal of Organometallic Chemistry* **584**(2), 246–253 (1999), DOI: 10.1016/S0022-328X(99)00149-7.

[27] E. Le Grognec, J. Claverie, and R. Poli, Radical polymerization of styrene controlled by half-sandwich Mo(III)/Mo(IV) couples: All basic mechanisms are possible, *Journal of the American Chemical Society* **123**(39), 9513–9524 (2001), DOI: 10.1021/ja010998d.

[28] S. Maria, F. Stoffelbach, J. Mata, J.-C. Daran, P. Richard, and R. Poli, The radical trap in atom transfer radical polymerization need not be thermodynamically stable. A study of the $MoX_3(PMe_3)_3$ catalysts, *Journal of the American Chemical Society* **127**(16), 5946–5956 (2005), DOI: 10.1021/ja043078e.

[29] G. Moineau, C. Granel, P. Dubois, R. Jérôme, and P. Teyssié, Controlled radical polymerization of methyl methacrylate initiated by an alkyl halide in the presence of the Wilkinson catalyst, *Macromolecules* **31**(2), 542–544 (1998), DOI: 10.1021/ma971123f.

[30] J. Sedláček and J. Vohlídal, Controlled and living polymerizations induced with rhodium catalysts. A review, *Collection of Czechoslovak Chemical Communications* **68**(10), 1745–1790 (2003), DOI: 10.1135/cccc20031745.

[31] W. A. Braunecker, Y. Itami, and K. Matyjaszewski, Osmium-mediated

radical polymerization, *Macromolecules* **38**(23), 9402–9404 (2005), DOI: 10.1021/ma051877r.

[32] H. Uegaki, Y. Kotani, M. Kamigaito, and M. Sawamoto, Living radical polymerization of acrylates with rhenium(V)-based initiating systems: $ReO_2I(PPh_3)_2$/alkyl iodide, in *Transition metal catalysis in macromolecular design*, pages 196–206, American Chemical Society, 2000, DOI: 10.1021/bk-2000-0760.ch012.

[33] Y. Kotani, M. Kamigaito, and M. Sawamoto, Living radical polymerization of para-substituted styrenes and synthesis of styrene-based copolymers with rhenium and iron complex catalysts, *Macromolecules* **33**(18), 6746–6751 (2000), DOI: 10.1021/ma000624p.

[34] Y. Shen, H. Tang, and S. Ding, Catalyst separation in atom transfer radical polymerization, *Progress in Polymer Science* **29**(10), 1053–1078 (2004), DOI: 10.1016/j.progpolymsci.2004.08.002.

[35] M. Ding, X. Jiang, L. Zhang, Z. Cheng, and X. Zhu, Recent progress on transition metal catalyst separation and recycling in ATRP, *Macromolecular Rapid Communications* **36**(19), 1702–1721 (2015), DOI: 10.1002/marc.201500085.

[36] X. Su, P. G. Jessop, and M. F. Cunningham, ATRP catalyst removal and ligand recycling using CO_2-switchable materials, *Macromolecules* **51**(20), 8156–8164 (2018), DOI: 10.1021/acs.macromol.8b01432.

[37] T. Pintauer and K. Matyjaszewski, Atom transfer radical addition and polymerization reactions catalyzed by ppm amounts of copper complexes, *Chemical Society Reviews* **37**(6), 1087–1097 (2008), DOI: 10.1039/b714578k.

[38] N. V. Tsarevsky and K. Matyjaszewski, "Green" atom transfer radical polymerization: From process design to preparation of well-defined environmentally friendly polymeric materials, *Chemical Reviews* **107**(6), 2270–2299 (2007), DOI: 10.1021/cr050947p.

[39] K. Matyjaszewski, W. Jakubowski, K. Min, W. Tang, J. Huang, W. A. Braunecker, and N. V. Tsarevsky, Diminishing catalyst concentration in atom trans-

fer radical polymerization with reducing agents, *Proceedings of the National Academy of Sciences of the United States of America* **103**(42), 15309–15314 (2006), DOI: 10.1073/pnas.0602675103.

[40] M. Lamson, M. Kopeć, H. Ding, M. Zhong, and K. Matyjaszewski, Synthesis of well-defined polyacrylonitrile by ICAR ATRP with low concentrations of catalyst, *Journal of Polymer Science Part A: Polymer Chemistry* **54**(13), 1961–1968 (2016), DOI: 10.1002/pola.28055.

[41] J. Sun, Y. Zhang, J. Li, Q. Ren, C. Wang, and Z. Xu, Low concentration limitations of catalyst and conventional free radical polymerization in ICAR ATRP of butyl methacrylate with PMDETA as the ligand, *Journal of Macromolecular Science, Part A* **52**(8), 609–616 (2015), DOI: 10.1080/10601325.2015.1050632.

[42] P. Krys, H. Schroeder, J. Buback, M. Buback, and K. Matyjaszewski, The borderline between simultaneous reverse and normal initiation and initiators for continuous activator regeneration ATRP, *Macromolecules* **49**(20), 7793–7803 (2016), DOI: 10.1021/acs.macromol.6b01765.

[43] K. A. Payne, D. R. D'hooge, P. H. Van Steenberge, M.-F. Reyniers, M. F. Cunningham, R. A. Hutchinson, and G. B. Marin, ARGET ATRP of butyl methacrylate: Utilizing kinetic modeling to understand experimental trends, *Macromolecules* **46**(10), 3828–3840 (2013), DOI: 10.1021/ma400388t.

[44] N. Chan, S. Boutti, M. F. Cunningham, and R. A. Hutchinson, Continuous atom transfer radical polymerization with low catalyst concentration in a tubular reactor, *Macromolecular Reaction Engineering* **3**(5–6), 222–231 (2009), DOI: 10.1002/mren.200900012.

[45] L. Bai, L. Zhang, Z. Cheng, and X. Zhu, Activators generated by electron transfer for atom transfer radical polymerization: Recent advances in catalyst and polymer chemistry, *Polymer Chemistry* **3**(10), 2685–2697 (2012), DOI: 10.1039/c2py20286g.

[46] W. Jakubowski and K. Matyjaszewski, Activators regenerated by electron transfer for atom-transfer radical polymerization of (meth)acrylates and related

block copolymers, *Angewandte Chemie International Edition* **45**(27), 4482–4486 (2006), DOI: 10.1002/anie.200600272.

[47] M. Chen, D. Fan, S. Liu, Z. Rao, Y. Dong, W. Wang, H. Chen, L. Bai, and Z. Cheng, Fabrication of self-healing hydrogels with surface functionalized microcapsules from stellate mesoporous silica, *Polymer Chemistry* **10**(4), 503–511 (2019), DOI: 10.1039/c8py01402g.

[48] A. Simakova, S. E. Averick, D. Konkolewicz, and K. Matyjaszewski, Aqueous ARGET ATRP, *Macromolecules* **45**(16), 6371–6379 (2012), DOI: 10.1021/ma301303b.

[49] S. Hansson, E. Östmark, A. Carlmark, and E. Malmström, ARGET ATRP for versatile grafting of cellulose using various monomers, *ACS Applied Materials and Interfaces* **1**(11), 2651–2659 (2009), DOI: 10.1021/am900547g.

[50] K. Min, H. Gao, and K. Matyjaszewski, Use of ascorbic acid as reducing agent for synthesis of well-defined polymers by ARGET ATRP, *Macromolecules* **40**(6), 1789–1791 (2007), DOI: 10.1021/ma0702041.

[51] K. Y. Simanskaya, I. D. Grishin, M. V. Pavlovskaya, and D. F. Grishin, Controlled synthesis of polymers on the basis of stearyl methacrylate and their use as depressor additives, *Polymer Science, Series B* **61**(2), 155–162 (2019), DOI: 10.1134/S1560090419020118.

[52] Y. Kwak and K. Matyjaszewski, ARGET ATRP of methyl methacrylate in the presence of nitrogen-based ligands as reducing agents, *Polymer International* **58**(3), 242–247 (2009), DOI: 10.1002/pi.2530.

[53] H. Tang, Y. Shen, B.-G. Li, and M. Radosz, Tertiary amine — Enhanced activity of ATRP catalysts CuBr/TPMA and CuBr/Me_6TREN, *Macromolecular Rapid Communications* **29**(22), 1834–1838 (2008), DOI: 10.1002/marc.200800378.

[54] J. Queffelec, S. G. Gaynor, and K. Matyjaszewski, Optimization of atom transfer radical polymerization using Cu(I)/tris(2-(dimethylamino)ethyl)amine as a catalyst, *Macromolecules* **33**(23), 8629–8639 (2000), DOI: 10.1021/ma000871t.

[55] T. Guliashvili, P. V. Mendonça, A. C. Serra, A. V. Popov, and J. F. J. Coelho, Copper-mediated controlled/“living” radical polymerization in polar solvents: Insights into some relevant mechanistic aspects, *Chemistry—A European Journal* **18**(15), 4607–4612 (2012), DOI: 10.1002/chem.201102183.

[56] Y. Kwak, A. J. D. Magenau, and K. Matyjaszewski, ARGET ATRP of methyl acrylate with inexpensive ligands and ppm concentrations of catalyst, *Macromolecules* **44**(4), 811–819 (2011), DOI: 10.1021/ma102665c.

[57] K. Matyjaszewski, S. Coca, S. G. Gaynor, M. Wei, and B. E. Woodworth, Zerovalent metals in controlled/“living” radical polymerization, *Macromolecules* **30**(23), 7348–7350 (1997), DOI: 10.1021/ma971258l.

[58] B. M. Rosen and V. Percec, Single-electron transfer and single-electron transfer degenerative chain transfer living radical polymerization, *Chemical Reviews* **109**(11), 5069–5119 (2009), DOI: 10.1021/cr900024j.

[59] A. Anastasaki, V. Nikolaou, G. Nurumbetov, P. Wilson, K. Kempe, J. F. Quinn, T. P. Davis, M. R. Whittaker, and D. M. Haddleton, Cu(0)-mediated living radical polymerization: A versatile tool for materials synthesis, *Chemical Reviews* **116**(3), 835–877 (2016), DOI: 10.1021/acs.chemrev.5b00191.

[60] P. Chmielarz, M. Fantin, S. Park, A. A. Isse, A. Gennaro, A. J. D. Magenau, A. Sobkowiak, and K. Matyjaszewski, Electrochemically mediated atom transfer radical polymerization (*e*ATRP), *Progress in Polymer Science* **69**, 47–78 (2017), DOI: 10.1016/j.progpolymsci.2017.02.005.

[61] S. Park, P. Chmielarz, A. Gennaro, and K. Matyjaszewski, Simplified electrochemically mediated atom transfer radical polymerization using a sacrificial anode, *Angewandte Chemie International Edition* **54**(8), 2388–2392 (2015), DOI: 10.1002/anie.201410598.

[62] N. Bortolamei, A. A. Isse, A. J. D. Magenau, A. Gennaro, and K. Matyjaszewski, Controlled aqueous atom transfer radical polymerization with electrochemical generation of the active catalyst, *Angewandte Chemie International Edition* **50**(48), 11391–11394 (2011), DOI: 10.1002/anie.201105317.

[63] A. J. D. Magenau, N. C. Strandwitz, A. Gennaro, and K. Matyjaszewski, Electrochemically mediated atom transfer radical polymerization, *Science* **332**(6025), 81–84 (2011), DOI: 10.1126/science.1202357.

[64] S. Dadashi-Silab, S. Doran, and Y. Yagci, Photoinduced electron transfer reactions for macromolecular syntheses, *Chemical Reviews* **116**(17), 10212–10275 (2016), DOI: 10.1021/acs.chemrev.5b00586.

[65] S. Shanmugam, J. Xu, and C. Boyer, Photocontrolled living polymerization systems with reversible deactivations through electron and energy transfer, *Macromolecular Rapid Communications* **38**(13), 1700143 (2017), DOI: 10.1002/marc.201700143.

[66] X. Pan, M. A. Tasdelen, J. Laun, T. Junkers, Y. Yagci, and K. Matyjaszewski, Photomediated controlled radical polymerization, *Progress in Polymer Science* **62**, 73–125 (2016), DOI: 10.1016/j.progpolymsci.2016.06.005.

[67] Z. Wang, X. Pan, L. Li, M. Fantin, J. Yan, Z. Wang, Z. Wang, H. Xia, and K. Matyjaszewski, Enhancing mechanically induced ATRP by promoting interfacial electron transfer from piezoelectric nanoparticles to Cu catalysts, *Macromolecules* **50**(20), 7940–7948 (2017), DOI: 10.1021/acs.macromol.7b01597.

[68] H. Mohapatra, M. Kleiman, and A. P. Esser-Kahn, Mechanically controlled radical polymerization initiated by ultrasound, *Nature Chemistry* **9**(2), 135–139 (2017), DOI: 10.1038/nchem.2633.

[69] Y. Ni, L. Zhang, Z. Cheng, and X. Zhu, Iodine-mediated reversible-deactivation radical polymerization: A powerful strategy for polymer synthesis, *Polymer Chemistry* **10**(20), 2504–2515 (2019), DOI: 10.1039/C9PY00091G.

[70] X. Pan, C. Fang, M. Fantin, N. Malhotra, W. Y. So, L. A. Peteanu, A. A. Isse, A. Gennaro, P. Liu, and K. Matyjaszewski, Mechanism of photoinduced metal-free atom transfer radical polymerization: Experimental and computational studies, *Journal of the American Chemical Society* **138**(7), 2411–2425 (2016), DOI: 10.1021/jacs.5b13455.

[71] G. M. Miyake and J. C. Theriot, Perylene as an organic photocatalyst for the radical polymerization of functionalized vinyl monomers through oxidative quenching with alkyl bromides and visible light, *Macromolecules* **47**(23), 8255–8261 (2014), DOI: 10.1021/ma502044f.

[72] G. Wang, M. Xi, L. Bai, Y. Liang, L. Yang, W. Wang, H. Chen, and H. Yang, Pickering emulsion of metal-free photoinduced electron transfer-ATRP stabilized by cellulose nanocrystals, *Cellulose* **26**(10), 5947–5957 (2019), DOI: 10.1007/s10570-019-02528-4.

[73] D. Wei, Y. Xu, C. Liu, Y. Zhai, H. Chen, L. Bai, H. Yang, L. Yang, W. Wang, and Y. Niu, Visible light-induced metal-free atom transfer radical polymerization: An efficient approach to polyacrylonitrile, *Journal of Polymer Science Part A: Polymer Chemistry* **57**(12), 1265–1269 (2019), DOI: 10.1002/pola.29386.

[74] L. Bai, X. Jiang, Z. Sun, Z. Pei, A. Ma, W. Wang, H. Chen, H. Yang, L. Yang, and D. Wei, Self-healing nanocomposite hydrogels based on modified cellulose nanocrystals by surface-initiated photoinduced electron transfer ATRP, *Cellulose* **26**(9), 5305–5319 (2019), DOI: 10.1007/s10570-019-02449-2.

[75] K. Matyjaszewski, Advanced materials by atom transfer radical polymerization, *Advanced Materials* **30**(23), 1706441 (2018), DOI: 10.1002/adma.201706441.

[76] J. J. Griebel, R. S. Glass, K. Char, and J. Pyun, Polymerizations with elemental sulfur: A novel route to high sulfur content polymers for sustainability, energy and defense, *Progress in Polymer Science* **58**, 90–125 (2016), DOI: 10.1016/j.progpolymsci.2016.04.003.

[77] H. Gao and K. Matyjaszewski, Synthesis of functional polymers with controlled architecture by CRP of monomers in the presence of cross-linkers: From stars to gels, *Progress in Polymer Science* **34**(4), 317–350 (2009), DOI: 10.1016/j.progpolymsci.2009.01.001.

[78] H. Gao and K. Matyjaszewski, Modular approaches to star and miktoarm star polymers by ATRP of cross-linkers, *Macromolecular Symposia* **291–292**(1), 12–16 (2010), DOI: 10.1002/masy.201050502.

[79] K. Matyjaszewski, S. G. Gaynor, A. Kulfan, and M. Podwika, Preparation of hyperbranched polyacrylates by atom transfer radical polymerization. 1. Acrylic AB* monomers in "living" radical polymerizations, *Macromolecules* **30**(17), 5192–5194 (1997), DOI: 10.1021/ma970359g.

[80] N. Ide and T. Fukuda, Nitroxide-controlled free-radical copolymerization of vinyl and divinyl monomers. 2. Gelation, *Macromolecules* **32**(1), 95–99 (1999), DOI: 10.1021/ma9805349.

[81] R. Casolari, F. Felluga, V. Frenna, F. Ghelfi, U. M. Pagnoni, A. F. Parsons, and D. Spinelli, A green way to γ-lactams through a copper catalyzed ARGET-ATRC in ethanol and in the presence of ascorbic acid, *Tetrahedron* **67**(2), 408–416 (2011), DOI: 10.1016/j.tet.2010.11.025.

[82] F. Bellesia, A. J. Clark, F. Felluga, A. Gennaro, A. A. Isse, F. Roncaglia, and F. Ghelfi, Efficient and green route to γ-lactams by copper-catalysed reversed atom transfer radical cyclisation of α-polychloro-N-allylamides, using a low load of metal (0.5 mol %), *Advanced Synthesis & Catalysis* **355**(8), 1649–1660 (2013), DOI: 10.1002/adsc.201300132.

[83] A. J. Clark, A. Cornia, F. Felluga, A. Gennaro, F. Ghelfi, A. A. Isse, M. C. Menziani, F. Muniz-Miranda, F. Roncaglia, and D. Spinelli, Arylsulfonyl groups: The best cyclization auxiliaries for the preparation of ATRC γ-lactams can be acidolytically removed, *European Journal of Organic Chemistry* **2014**(30), 6734–6745 (2014), DOI: 10.1002/ejoc.201402769.

[84] H. Li, D. Yang, Y. Gao, H. Li, and J. Xu, Dual responsive macroemulsion stabilized by Y-shaped amphiphilic AB_2 miktoarm star copolymers, *RSC Advances* **5**(117), 96377–96386 (2015), DOI: 10.1039/C5RA16399D.

[85] X. Guan, F. Chen, Z. Li, H. Zhou, and X. Ma, Influence of a rigid polystyrene block on the free volume and ionic conductivity of a gel polymer electrolyte based on poly(methyl methacrylate)-*block*-polystyrene, *Journal of Applied Polymer Science* **133**(38), 43901 (2016), DOI: 10.1002/app.43901.

[86] F. Fu, H. Xu, Y. Dong, M. He, Z. Zhang, T. Luo, Y. Zhang, X. Hao, and C. Zhu, Design of polyphosphazene-based graft copolystyrenes with alkylsulfonate

branch chains for proton exchange membranes, *Journal of Membrane Science* **489**, 119–128 (2015), DOI: 10.1016/j.memsci.2015.04.016.

[87] L. Yang, E. Allahyarov, F. Guan, and L. Zhu, Crystal orientation and temperature effects on double hysteresis loop behavior in a poly(vinylidene fluoride-*co*-trifluoroethylene-*co*-chlorotrifluoroethylene)-*graft*-polystyrene graft copolymer, *Macromolecules* **46**(24), 9698–9711 (2013), DOI: 10.1021/ma401660k.

[88] S. L. Hilburg, A. N. Elder, H. Chung, R. L. Ferebee, M. R. Bockstaller, and N. R. Washburn, A universal route towards thermoplastic lignin composites with improved mechanical properties, *Polymer* **55**(4), 995–1003 (2014), DOI: 10.1016/j.polymer.2013.12.070.

[89] F. Bellesia, F. D'Anna, F. Felluga, V. Frenna, F. Ghelfi, A. F. Parsons, F. Reverberi, and D. Spinelli, Breakthrough in the α-perchlorination of acyl chlorides, *Synthesis* **44**(4), 605–609 (2012), DOI: 10.1055/s-0031-1289678.

[90] F. Bellesia, M. Boni, F. Ghelfi, and U. M. Pagnoni, Methyl α,α-dichloroesters by oxidation-chlorination of cyclic acetals with trichloroisocyanuric acid, *Tetrahedron Letters* **35**(18), 2961–2964 (1994), DOI: 10.1016/S0040-4039(00)76672-X.

[91] L. De Buyck, F. Casaert, C. De Lepeleire, and N. Schamp, α,α-Dichloroaldehydes and α,α-dichlorocarboxylic acids from long chain 1-alkanols. Improved chlorination in the system DMF-$CHCl_3$-$MgCl_2$, *Bulletin des Sociétés Chimiques Belges* **97**(7), 525–533 (1988), DOI: 10.1002/bscb.19880970708.

[92] N. Braidi, M. Buffagni, F. Ghelfi, M. Imperato, A. Menabue, F. Parenti, A. Gennaro, A. A. Isse, E. Bedogni, L. Bonifaci, G. Cavalca, A. Ferrando, A. Longo, and I. Morandini, Copper-catalysed "activators regenerated by electron transfer" "atom transfer radical polymerisation" of styrene from a bifunctional initiator in ethyl acetate/ethanol, using ascorbic acid/sodium carbonate as reducing system, *Macromolecular Research* **28**(8), 751–761 (2020), DOI: 10.1007/s13233-020-8091-3.

[93] L. S. Connell, J. R. Jones, and J. V. M. Weaver, Transesterification of functional methacrylate monomers during alcoholic copper-catalyzed atom transfer radical

polymerization: Formation of compositional and architectural side products, *Polymer Chemistry* **3**(10), 2735–2738 (2012), DOI: 10.1039/c2py20280h.

[94] Y. Kagawa, P. B. Zetterlund, H. Minami, and M. Okubo, Atom transfer radical polymerization in miniemulsion: Partitioning effects of copper(I) and copper(II) on polymerization rate, livingness, and molecular weight distribution, *Macromolecules* **40**(9), 3062–3069 (2007), DOI: 10.1021/ma062786c.

[95] Y. Yang, F. Chen, Q. Chen, J. He, T. Bu, and X. He, Synthesis and characterization of grafting polystyrene from guar gum using atom transfer radical addition, *Carbohydrate Polymers* **176**, 266–272 (2017), DOI: 10.1016/j.carbpol.2017.08.081.

[96] Y. Kitayama, Y. Kagawa, H. Minami, and M. Okubo, Preparation of micrometer-sized, onionlike multilayered block copolymer particles by two-step AGET ATRP in aqueous dispersed systems: Effect of the second-step polymerization temperature, *Langmuir* **26**(10), 7029–7034 (2010), DOI: 10.1021/la904296h.

[97] Y. Wang, S. Zhang, L. Wang, W. Zhang, N. Zhou, Z. Zhang, and X. Zhu, The Suzuki coupling reaction as a post-polymerization modification: A promising protocol for construction of cyclic-brush and more complex polymers, *Polymer Chemistry* **6**(25), 4669–4677 (2015), DOI: 10.1039/C5PY00551E.

[98] L. Bai, L. Zhang, Z. Zhang, Y. Tu, N. Zhou, Z. Cheng, and X. Zhu, Iron-mediated AGET ATRP of styrene in the presence of catalytic amounts of base, *Macromolecules* **43**(22), 9283–9290 (2010), DOI: 10.1021/ma1013594.

[99] G.-X. Wang, M. Lu, Z.-H. Hou, and H. Wu, Homogeneous Fe-mediated AGET ATRP of methyl methacrylate in PEG-400 in the presence of Na_2CO_3, *Journal of Macromolecular Science, Part A* **52**(3), 186–192 (2015), DOI: 10.1080/10601325.2015.996939.

[100] L. Bai, L. Zhang, Z. Zhang, J. Zhu, N. Zhou, Z. Cheng, and X. Zhu, Rate-enhanced ATRP in the presence of catalytic amounts of base: An example of iron-mediated AGET ATRP of MMA, *Journal of Polymer Science Part A: Polymer Chemistry* **49**(18), 3980–3987 (2011), DOI: 10.1002/pola.24838.

[101] W. He, L. Zhang, L. Bai, Z. Zhang, J. Zhu, Z. Cheng, and X. Zhu, Iron-mediated AGET ATRP of methyl methacrylate in the presence of catalytic amounts of base, *Macromolecular Chemistry and Physics* **212**(14), 1474–1480 (2011), DOI: 10.1002/macp.201100073.

[102] T. Guo, L. Zhang, H. Jiang, Z. Zhang, J. Zhu, Z. Cheng, and X. Zhu, Catalytic amounts of sodium hydroxide as additives for iron-mediated AGET ATRP of MMA, *Polymer Chemistry* **2**(10), 2385–2390 (2011), DOI: 10.1039/c1py00184a.

[103] X.-R. Shen, Y.-J. Ding, and J.-G. Gao, Ethyl lactate, a new green solvent for ARGET ATRP of methyl acrylate, *Chemistry Letters* **46**(5), 690–692 (2017), DOI: 10.1246/cl.170107.

[104] A. Moreno, D. Garcia, M. Galià, J. C. Ronda, V. Cádiz, G. Lligadas, and V. Percec, SET-LRP in the neoteric ethyl lactate alcohol, *Biomacromolecules* **18**(10), 3447–3456 (2017), DOI: 10.1021/acs.biomac.7b01130.

[105] W. T. Eckenhoff, A. B. Biernesser, and T. Pintauer, Kinetic and mechanistic aspects of atom transfer radical addition (ATRA) catalyzed by copper complexes with tris(2-pyridylmethyl)amine, *Inorganic Chemistry* **51**(21), 11917–11929 (2012), DOI: 10.1021/ic3018198.

[106] W. T. Eckenhoff and T. Pintauer, Structural comparison of copper(I) and copper(II) complexes with tris(2-pyridylmethyl)amine ligand, *Inorganic Chemistry* **49**(22), 10617–10626 (2010), DOI: 10.1021/ic1016142.

[107] N. Chan, M. F. Cunningham, and R. A. Hutchinson, ARGET ATRP of methacrylates and acrylates with stoichiometric ratios of ligand to copper, *Macromolecular Chemistry and Physics* **209**(17), 1797–1805 (2008), DOI: 10.1002/macp.200800328.

[108] Y. Zhang, Y. Wang, C.-h. Peng, M. Zhong, W. Zhu, D. Konkolewicz, and K. Matyjaszewski, Copper-mediated CRP of methyl acrylate in the presence of metallic copper: Effect of ligand structure on reaction kinetics, *Macromolecules* **45**(1), 78–86 (2012), DOI: 10.1021/ma201963c.

[109] O. Repič, *Principles of process research and chemical development in the pharmaceutical industry*, Wiley, 1st edition, 1998.

[110] N. Kanbayashi, K. Takenaka, T.-a. Okamura, and K. Onitsuka, Asymmetric auto-tandem catalysis with a planar-chiral ruthenium complex: Sequential allylic amidation and atom-transfer radical cyclization, *Angewandte Chemie International Edition* **52**(18), 4897–4901 (2013), DOI: 10.1002/anie.201300485.

[111] H. R. Hudson and G. R. de Spinoza, Factors in the formation of isomerically and optically pure alkyl halides. Part X. Reactions of saturated aliphatic alcohols with thionyl chloride, *Journal of the Chemical Society, Perkin Transactions 1* (1), 104–108 (1976), DOI: 10.1039/p19760000104.

[112] M. Al-Harthi, L. S. Cheng, J. B. P. Soares, and L. C. Simon, Atom-transfer radical polymerization of styrene with bifunctional and monofunctional initiators: Experimental and mathematical modeling results, *Journal of Polymer Science Part A: Polymer Chemistry* **45**(11), 2212–2224 (2007), DOI: 10.1002/pola.21988.

[113] D. Braun, H. Cherdron, M. Rehahn, H. Ritter, and B. Voit, *Polymer synthesis: Theory and practice*, Springer, 5th edition, 2013, DOI: 10.1007/978-3-642-28980-4.

[114] F. Ghelfi, A. Ferrando, A. Longo, and M. Buffagni, Polymerization process for the synthesis of vinyl aromatic polymers with a controlled structure, 2019, Patent number WO2019215626.

[115] X. Wang and H. Gao, Recent progress on hyperbranched polymers synthesized via radical-based self-condensing vinyl polymerization, *Polymers* **9**(6), 188 (2017), DOI: 10.3390/polym9060188.

[116] W. Huang, Y. Zheng, B. Jiang, D. Zhang, J. Chen, Y. Yang, C. Liu, G. Zhai, L. Kong, and F. Gong, Studies on the atom transfer radical branching copolymerization of styrene and acrylonitrile with divinyl benzene as the branching agent, *Macromolecular Chemistry and Physics* **211**(20), 2211–2217 (2010), DOI: 10.1002/macp.201000224.

[117] W. Huang, H. Yang, X. Xue, B. Jiang, J. Chen, Y. Yang, H. Pu, Y. Liu, D. Zhang, L. Kong, and G. Zhai, Polymerization behaviors and polymer branching structures in ATRP of monovinyl and divinyl monomers, *Polymer Chemistry* **4**(11), 3204–3211 (2013), DOI: 10.1039/c3py00338h.

[118] W. Wang, Y. Zheng, E. Roberts, C. J. Duxbury, L. Ding, D. J. Irvine, and S. M. Howdle, Controlling chain growth: A new strategy to hyperbranched materials, *Macromolecules* **40**(20), 7184–7194 (2007), DOI: 10.1021/ma0707133.

[119] T. Zhao, Y. Zheng, J. Poly, and W. Wang, Controlled multi-vinyl monomer homopolymerization through vinyl oligomer combination as a universal approach to hyperbranched architectures, *Nature Communications* **4**(1), 1873 (2013), DOI: 10.1038/ncomms2887.

[120] Q. Xu, S. A, P. McMichael, J. Creagh-Flynn, D. Zhou, Y. Gao, X. Li, X. Wang, and W. Wang, Double-cross-linked hydrogel strengthened by UV irradiation from a hyperbranched PEG-based trifunctional polymer, *ACS Macro Letters* **7**(5), 509–513 (2018), DOI: 10.1021/acsmacrolett.8b00138.

[121] K. Kanamori, J. Hasegawa, K. Nakanishi, and T. Hanada, Facile synthesis of macroporous cross-linked methacrylate gels by atom transfer radical polymerization, *Macromolecules* **41**(19), 7186–7193 (2008), DOI: 10.1021/ma800563p.

[122] P. Polanowski, J. K. Jeszka, K. Krysiak, and K. Matyjaszewski, Influence of intramolecular crosslinking on gelation in living copolymerization of monomer and divinyl cross-linker. Monte Carlo simulation studies, *Polymer* **79**, 171–178 (2015), DOI: 10.1016/j.polymer.2015.10.018.

[123] A. Debuigne, M. Hurtgen, C. Detrembleur, C. Jérôme, C. Barner-Kowollik, and T. Junkers, Interpolymer radical coupling: A toolbox complementary to controlled radical polymerization, *Progress in Polymer Science* **37**(7), 1004–1030 (2012), DOI: 10.1016/j.progpolymsci.2012.01.003.

[124] X. Jiang, Y. Chen, and F. Xi, Stepwise cleavable star polymers and polymeric gels thereof, *Macromolecules* **43**(17), 7056–7061 (2010), DOI: 10.1021/ma101460n.

[125] C. Li and Q. Wang, Characterization of polymer network by combination of tailored synthesis and direct analysis of its decrosslinked components, *Polymer* **99**, 594–597 (2016), DOI: 10.1016/j.polymer.2016.07.064.

[126] N. Braidi, M. Buffagni, F. Ghelfi, F. Parenti, A. Gennaro, A. A. Isse, E. Bedogni, L. Bonifaci, G. Cavalca, A. Ferrando, A. Longo, and I. Morandini, ARGET ATRP of styrene in EtOAc/EtOH using only Na_2CO_3 to promote the copper catalyst regeneration, *Journal of Macromolecular Science, Part A* (2021), DOI: 10.1080/10601325.2020.1866434.

[127] Y. Nakamura, T. Ogihara, and S. Yamago, Mechanism of Cu(I)/Cu(0)-mediated reductive coupling reactions of bromine-terminated polyacrylates, polymethacrylates, and polystyrene, *ACS Macro Letters* **5**(2), 248–252 (2016), DOI: 10.1021/acsmacrolett.5b00947.

[128] C. Ünaleroğlu, B. Zümreoğlu-Karan, Y. Zencir, and T. Hökelek, pH-independent decomposition reactions of L-ascorbic acid in aqueous metal solutions—I. Formation and structures of Co^{II} and Gd^{III} oxalates, *Polyhedron* **16**(13), 2155–2161 (1997), DOI: 10.1016/S0277-5387(96)00563-3.

[129] G. M. Tsivgoulis, P. A. Afroudakis, and P. V. Ioannou, Preparation of dehydro-L-(+)-ascorbic acid dimer by oxidation of ascorbic acid with arsenic acid/iodine and formation of complexes between arsenious acid and ascorbic acid, *Journal of Inorganic Biochemistry* **98**(4), 649–656 (2004), DOI: 10.1016/j.jinorgbio.2004.01.016.

[130] M. Nath, R. Jairath, G. Eng, X. Song, and A. Kumar, New organotin(IV) ascorbates: Synthesis, spectral characterization, biological and potentiometric studies, *Spectrochimica Acta Part A: Molecular and Biomolecular Spectroscopy* **61**(1–2), 77–86 (2005), DOI: 10.1016/j.saa.2004.03.018.

[131] T. Xiaolin, T. Dafeng, W. Zhongyan, and M. Fengkui, Synthesis and evaluation of chitosan-vitamin C complexes, *Journal of Applied Polymer Science* **114**(5), 2986–2991 (2009), DOI: 10.1002/app.30918.

[132] T. Sarbu, K.-Y. Lin, J. Ell, D. J. Siegwart, J. Spanswick, and K. Matyjaszewski, Polystyrene with designed molecular weight distribution by atom

transfer radical coupling, *Macromolecules* **37**(9), 3120–3127 (2004), DOI: 10.1021/ma035901h.

[133] K. Matyjaszewski, K. Davis, T. E. Patten, and M. Wei, Observation and analysis of a slow termination process in the atom transfer radical polymerization of styrene, *Tetrahedron* **53**(45), 15321–15329 (1997), DOI: 10.1016/S0040-4020(97)00965-4.

[134] W. Jakubowski, B. Kirci-Denizli, R. R. Gil, and K. Matyjaszewski, Polystyrene with improved chain-end functionality and higher molecular weight by ARGET ATRP, *Macromolecular Chemistry and Physics* **209**(1), 32–39 (2008), DOI: 10.1002/macp.200700425.

[135] M. B. Smith, *March's advanced organic chemistry: Reactions, mechanisms, and structure*, Wiley, 7th edition, 2013.

[136] K. J. Laidler, *Chemical kinetics*, Harper & Row, 3rd edition, 1987.

[137] H. Fischer and L. Radom, Factors controlling the addition of carbon-centered radicals to alkenes—An experimental and theoretical perspective, *Angewandte Chemie International Edition* **40**(8), 1340–1371 (2001), DOI: 10.1002/1521-3773(20010417)40:8%3C1340::AID-ANIE1340%3E3.0.CO;2-%23.

[138] C. Yoshikawa, A. Goto, and T. Fukuda, Reactions of polystyrene radicals in a monomer-free atom transfer radical polymerization system, *e-Polymers* **2**(1), 013 (2002), DOI: 10.1515/epoly.2002.2.1.172.

[139] T. M. Kruse, O. S. Woo, H.-W. Wong, S. S. Khan, and L. J. Broadbelt, Mechanistic modeling of polymer degradation: A comprehensive study of polystyrene, *Macromolecules* **35**(20), 7830–7844 (2002), DOI: 10.1021/ma020490a.

[140] P. H. M. Van Steenberge, J. Vandenbergh, M.-F. Reyniers, T. Junkers, D. R. D'hooge, and G. B. Marin, Kinetic Monte Carlo generation of complete electron spray ionization mass spectra for acrylate macromonomer synthesis, *Macromolecules* **50**(7), 2625–2636 (2017), DOI: 10.1021/acs.macromol.7b00333.

[141] S. C. Thickett and R. G. Gilbert, Midchain transfer to polymer in styrene–poly(butyl acrylate) systems: Direct evidence of retardative effects, *Macromolecules* **38**(23), 9894–9896 (2005), DOI: 10.1021/ma051666m.

[142] A. F. Voter and E. S. Tillman, An easy and efficient route to macrocyclic polymers via intramolecular radical–radical coupling of chain ends, *Macromolecules* **43**(24), 10304–10310 (2010), DOI: 10.1021/ma102319r.

[143] Z. Niu and H. W. Gibson, Polycatenanes, *Chemical Reviews* **109**(11), 6024–6046 (2009), DOI: 10.1021/cr900002h.

[144] Z. Rigbi and J. E. Mark, Concurrent chain extension and crosslinking of hydroxyl-terminated poly(dimethyl siloxane): Possible formation of catenate structures, *Journal of Polymer Science Part B: Polymer Physics* **24**(2), 443–449 (1986), DOI: 10.1002/polb.1986.090240217.

[145] J. Goff, S. Sulaiman, B. Arkles, and J. P. Lewicki, Soft materials with recoverable shape factors from extreme distortion states, *Advanced Materials* **28**(12), 2393–2398 (2016), DOI: 10.1002/adma.201503320.

[146] P. Hu, J. Madsen, Q. Huang, and A. L. Skov, Elastomers without covalent cross-linking: Concatenated rings giving rise to elasticity, *ACS Macro Letters* **9**(10), 1458–1463 (2020), DOI: 10.1021/acsmacrolett.0c00635.

[147] K. Endo, T. Shiroi, and N. Murata, Thermal polymerization of 1,2-dithiane, *Polymer Journal* **37**(7), 512–516 (2005), DOI: 10.1295/polymj.37.512.

[148] B. Vollmert and J. X. Huang, Synthesis and characterization of ring- and catena-polystyrene with high molecular weight by reaction of polystyrene dianions with *p*-dibromoxylene, *Die Makromolekulare Chemie, Rapid Communications* **2**(6–7), 467–472 (1981), DOI: 10.1002/marc.1981.030020621.

[149] H. R. Kricheldorf, S. M. Weidner, and F. Scheliga, Synthesis of cyclic polymers and flaws of the Jacobson–Stockmayer theory, *Polymer Chemistry* **11**(14), 2595–2604 (2020), DOI: 10.1039/D0PY00226G.

[150] H. R. Kricheldorf, Cyclic polymers: Synthetic strategies and physical properties, *Journal of Polymer Science Part A: Polymer Chemistry* **48**(2), 251–284 (2010), DOI: 10.1002/pola.23755.

[151] E. M. Carnicom and E. S. Tillman, Polymerization of styrene and cyclization to macrocyclic polystyrene in a one-pot, two-step sequence, *Reactive & Functional Polymers* **80**, 9–14 (2014), DOI: 10.1016/j.reactfunctpolym.2013.10.009.

[152] M. Buback, R. G. Gilbert, R. A. Hutchinson, B. Klumperman, F.-D. Kuchta, B. G. Manders, K. F. O'Driscoll, G. T. Russell, and J. Schweer, Critically evaluated rate coefficients for free-radical polymerization, 1. Propagation rate coefficient for styrene, *Macromolecular Chemistry and Physics* **196**(10), 3267–3280 (1995), DOI: 10.1002/macp.1995.021961016.

[153] T. G. Ribelli, S. M. Wahidur Rahaman, J.-C. Daran, P. Krys, K. Matyjaszewski, and R. Poli, Effect of ligand structure on the $Cu^{II}-R$ OMRP dormant species and its consequences for catalytic radical termination in ATRP, *Macromolecules* **49**(20), 7749–7757 (2016), DOI: 10.1021/acs.macromol.6b01334.

[154] K. Matyjaszewski and B. E. Woodworth, Interaction of propagating radicals with copper(I) and copper(II) species, *Macromolecules* **31**(15), 4718–4723 (1998), DOI: 10.1021/ma980473e.

[155] K. Schröder, D. Konkolewicz, R. Poli, and K. Matyjaszewski, Formation and possible reactions of organometallic intermediates with active copper(I) catalysts in ATRP, *Organometallics* **31**(22), 7994–7999 (2012), DOI: 10.1021/om3006883.

[156] Y. Wang, N. Soerensen, M. Zhong, H. Schroeder, M. Buback, and K. Matyjaszewski, Improving the "livingness" of ATRP by reducing Cu catalyst concentration, *Macromolecules* **46**(3), 683–691 (2013), DOI: 10.1021/ma3024393.

[157] J. Xia and K. Matyjaszewski, Controlled/"living" radical polymerization. Homogeneous reverse atom transfer radical polymerization using AIBN as the initiator, *Macromolecules* **30**(25), 7692–7696 (1997), DOI: 10.1021/ma9710085.

[158] Z. Jia and M. J. Monteiro, Cyclic polymers: Methods and strategies, *Journal of Polymer Science Part A: Polymer Chemistry* **50**(11), 2085–2097 (2012), DOI: 10.1002/pola.25999.

[159] T. Kawakatsu, *Statistical physics of polymers*, Springer, 2004, DOI: 10.1007/978-3-662-10024-0.

[160] S. Lanzalaco, M. Fantin, O. Scialdone, A. Galia, A. A. Isse, A. Gennaro, and K. Matyjaszewski, Atom transfer radical polymerization with different halides (F, Cl, Br, and I): Is the process "living" in the presence of fluorinated initiators?, *Macromolecules* **50**(1), 192–202 (2017), DOI: 10.1021/acs.macromol.6b02286.

[161] N. V. Tsarevsky and K. Matyjaszewski, Reversible redox cleavage/coupling of polystyrene with disulfide or thiol groups prepared by atom transfer radical polymerization, *Macromolecules* **35**(24), 9009–9014 (2002), DOI: 10.1021/ma021061f.

[162] T. Zhao, H. Zhang, B. Newland, A. Aied, D. Zhou, and W. Wang, Significance of branching for transfection: Synthesis of highly branched degradable functional poly(dimethylaminoethyl methacrylate) by vinyl oligomer combination, *Angewandte Chemie* **126**(24), 6209–6214 (2014), DOI: 10.1002/ange.201402341.

[163] H. Kim, B. Kim, C. Lee, J. L. Ryu, S.-J. Hong, J. Kim, E.-J. Ha, and H.-j. Paik, Redox-responsive biodegradable nanogels for photodynamic therapy using chlorin e6, *Journal of Materials Science* **51**(18), 8442–8451 (2016), DOI: 10.1007/s10853-016-0104-4.

[164] J. Gu, J. R. Clegg, L. A. Heersema, N. A. Peppas, and H. D. C. Smyth, Optimization of cationic nanogel PEGylation to achieve mammalian cytocompatibility with limited loss of gram-negative bactericidal activity, *Biomacromolecules* **21**(4), 1528–1538 (2020), DOI: 10.1021/acs.biomac.0c00081.

[165] H. Xue, B. Jing, S. Liu, J. Chae, and Y. Liu, Copper-catalyzed direct synthesis of aryl thiols from aryl iodides using sodium sulfide aided by catalytic 1,2-ethanedithiol, *Synlett* **28**(17), 2272–2276 (2017), DOI: 10.1055/s-0036-1588482.

[166] Y. Jiang, Y. Qin, S. Xie, X. Zhang, J. Dong, and D. Ma, A general and efficient approach to aryl thiols: CuI-catalyzed coupling of aryl iodides with sulfur and subsequent reduction, *Organic Letters* **11**(22), 5250–5253 (2009), DOI: 10.1021/ol902186d.

[167] Y. Liu, J. Kim, H. Seo, S. Park, and J. Chae, Copper(II)-catalyzed single-step synthesis of aryl thiols from aryl halides and 1,2-ethanedithiol, *Advanced Synthesis & Catalysis* **357**(10), 2205–2212 (2015), DOI: 10.1002/adsc.201400941.

[168] S. Qiao, K. Xie, and J. Qi, Copper-catalyzed coupling of thiourea with aryl iodides: The direct synthesis of aryl thiols, *Chinese Journal of Chemistry* **28**(8), 1441–1443 (2010), DOI: 10.1002/cjoc.201090246.

[169] K. Jeyakumar, R. D. Chakravarthy, and D. K. Chand, Simple and efficient method for the oxidation of sulfides to sulfones using hydrogen peroxide and a Mo(VI) based catalyst, *Catalysis Communications* **10**(14), 1948–1951 (2009), DOI: 10.1016/j.catcom.2009.07.009.

[170] A. Ouali, J.-P. Majoral, A.-M. Caminade, and M. Taillefer, NaOH-promoted hydrogen transfer: Does NaOH or traces of transition metals catalyze the reaction?, *ChemCatChem* **1**(4), 504–509 (2009), DOI: 10.1002/cctc.200900237.

[171] T. Delgado-Abad, J. Martínez-Ferrer, A. Caballero, A. Olmos, R. Mello, M. E. González-Núñez, P. J. Pérez, and G. Asensio, Supercritical carbon dioxide: A promoter of carbon–halogen bond heterolysis, *Angewandte Chemie International Edition* **52**(50), 13298–13301 (2013), DOI: 10.1002/anie.201303819.

[172] R. Scholz, G. Hellmann, S. Rohs, D. Özdemir, G. Raabe, C. Vermeeren, and H.-J. Gais, Enantioselective synthesis, configurational stability, and reactivity of lithium α-*tert*-butylsulfonyl carbanion salts, *European Journal of Organic Chemistry* **2010**(24), 4588–4616 (2010), DOI: 10.1002/ejoc.201000410.

[173] G. Wang, K. Ding, L. Xu, C. Wang, G. Wang, H. Yin, M. Qi, and Y. Xu, Method for synthesizing pesticide intermediate 2,4-dichloroacetophenone by recycling epoxypropane coproduct, 2019, Patent number CN109180418.

[174] Z. Li, C. Sheng, H. Qiu, and Y. Zhang, Ferric chloride-catalyzed deoxygenative chlorination of carbonyl compounds to halides, *Organic Preparations and Procedures International* **39**(4), 412–415 (2007), DOI: 10.1080/00304940709458597.

[175] Y. Onishi, D. Ogawa, M. Yasuda, and A. Baba, Direct conversion of carbonyl compounds into organic halides: Indium(III) hydroxide-catalyzed deoxygenative halogenation using chlorodimethylsilane, *Journal of the American Chemical Society* **124**(46), 13690–13691 (2002), DOI: 10.1021/ja0283246.

[176] B. Mandal and B. Basu, Recent advances in S−S bond formation, *RSC Advances* **4**(27), 13854–13881 (2014), DOI: 10.1039/c3ra45997g.

[177] H. Zhang, Controlled/"living" radical precipitation polymerization: A versatile polymerization technique for advanced functional polymers, *European Polymer Journal* **49**(3), 579–600 (2013), DOI: 10.1016/j.eurpolymj.2012.12.016.

[178] T. Pintauer, Towards the development of highly active copper catalysts for atom transfer radical addition (ATRA) and polymerization (ATRP), *Chemical Papers* **70**(1), 22–42 (2016), DOI: 10.1515/chempap-2015-0183.

[179] M. S. Kharasch, E. V. Jensen, and W. H. Urry, Addition of carbon tetrachloride and chloroform to olefins, *Science* **102**(2640), 128 (1945), DOI: 10.1126/science.102.2640.128.

[180] M. S. Kharasch, P. S. Skell, and P. Fisher, Reactions of atoms and free radicals in solution. XII. The addition of bromo esters to olefins, *Journal of the American Chemical Society* **70**(3), 1055–1059 (1948), DOI: 10.1021/ja01183a053.

[181] G. Dupont, R. Dulou, and C. Pigerol, Sur la fixation radicalaire du trichloroacétate d'éthyle sur l'heptène-I et l'étude de la déchlorhydratation, par les alcalis, du trichloro-2,2,4 nonanoate d'éthyle, *Bulletin de la Société Chimique de France* **22**, 1011–1106 (1955).

[182] I. Somech and Y. Shvo, Synthesis of γ-lactones and unsaturated bis γ-lactones via Cu−Fe-mediated reductive cyclization of di- and tri-α-halogenated carboxylic esters, *Journal of Organometallic Chemistry* **601**(1), 153–159 (2000), DOI: 10.1016/S0022-328X(00)00056-5.

[183] B. T. Lee, T. O. Schrader, B. Martín-Matute, C. R. Kauffman, P. Zhang, and M. L. Snapper, $(PCy_3)_2Cl_2Ru{=}CHPh$ Catalyzed Kharasch additions. Application in a formal olefin carbonylation, *Tetrahedron* **60**(34), 7391–7396 (2004), DOI: 10.1016/j.tet.2004.06.066.

[184] R. K. Freidlina, E. T. Chukovskaya, and A. B. Terent'ev, Telomerization of ethylene with esters of dichloroacetic and trichloroacetic acids, *Bulletin of the Academy of Sciences of the USSR, Division of chemical science* **16**(11), 2355–2359 (1967), DOI: 10.1007/BF00911844.

[185] E. I. Heiba, R. M. Dessau, and W. J. Koehl, Oxidation by metal salts. II. The formation of γ-lactones by the reaction of lead tetraacetate with olefins in acetic acid, *Journal of the American Chemical Society* **90**(10), 2706–2707 (1968), DOI: 10.1021/ja01012a051.

[186] J. B. Bush and H. Finkbeiner, Oxidation reactions of manganese(III) acetate. II. Formation of γ-lactones from olefins and acetic acid, *Journal of the American Chemical Society* **90**(21), 5903–5905 (1968), DOI: 10.1021/ja01023a048.

[187] E. I. Heiba, R. M. Dessau, and W. J. Koehl, Oxidation by metal salts. IV. A new method for the preparation of γ-lactones by the reaction of manganic acetate with olefins, *Journal of the American Chemical Society* **90**(21), 5905–5906 (1968), DOI: 10.1021/ja01023a049.

[188] Y. Mori and J. Tsuji, Organic syntheses by means of metal complexes —VIII: Reactions of methyl trichloroacetate with olefins catalyzed by metal carbonyls, *Tetrahedron* **28**(1), 29–35 (1972), DOI: 10.1016/0040-4020(72)80051-6.

[189] M. Iwasaki, N. Miki, Y. Ikemoto, Y. Ura, and Y. Nishihara, Regioselective synthesis of γ-lactones by iron-catalyzed radical annulation of alkenes with α-halocarboxylic acids and their derivatives, *Organic Letters* **20**(13), 3848–3852 (2018), DOI: 10.1021/acs.orglett.8b01436.

[190] E. I. Heiba, R. M. Dessau, and P. G. Rodewald, Oxidation by metal salts. X. One-step synthesis of γ-lactones from olefins, *Journal of the American Chemical Society* **96**(26), 7977–7981 (1974), DOI: 10.1021/ja00833a024.

[191] H. Matsumoto, T. Nakano, K. Ohkawa, and Y. Nagai, Reaction of trichloro- and dichloro-acetic acid with 1-alkenes catalyzed by dichlorotris-(triphenylphosphine)ruthenium(II). A convenient route to 2-chlorinated 4-alkyl-γ-butyrolactones, *Chemistry Letters* **7**(4), 363–366 (1978), DOI: 10.1246/cl.1978.363.

[192] H. Matsumoto, K. Ohkawa, S. Ikemori, T. Nakano, and Y. Nagai, A one-step and convenient synthesis of α-chloro-γ-butyrolactones, precursors of $\Delta^{\alpha,\beta}$-butenolides and α-methylene γ-butyrolactones, *Chemistry Letters* **8**(8), 1011–1014 (1979), DOI: 10.1246/cl.1979.1011.

[193] J. O. Metzger and R. Mahler, Radical additions of activated haloalkanes to alkenes initiated by electron transfer from copper in solvent-free systems, *Angewandte Chemie International Edition* **34**(8), 902–904 (1995), DOI: 10.1002/anie.199509021.

[194] G.-H. Pan, R.-J. Song, and J.-H. Li, Radical-mediated synthesis of γ-lactones by copper-catalyzed intermolecular carboesterification of alkenes with α-carbonyl alkyl bromides and H_2O, *Organic Chemistry Frontiers* **5**(2), 179–183 (2018), DOI: 10.1039/c7qo00579b.

[195] M. Ihara, A. Katsumata, F. Setsu, Y. Tokunaga, and K. Fukumoto, Synthesis of six-membered compounds by environmentally friendly cyclization using indirect electrolysis, *Journal of Organic Chemistry* **61**(2), 677–684 (1996), DOI: 10.1021/jo951653e.

[196] T. Iwahama, S. Sakaguchi, and Y. Ishii, Catalytic α-hydroxy carbon radical generation and addition. Synthesis of α-hydroxy-γ-lactones from alcohols, α,β-unsaturated esters and dioxygen, *Chemical Communications* (7), 613–614 (2000), DOI: 10.1039/b000707m.

[197] L. Wu, Z. Zhang, J. Liao, J. Li, W. Wu, and H. Jiang, MnO_2-promoted carboesterification of alkenes with anhydrides: A facile approach to γ-lactones, *Chemical Communications* **52**(12), 2628–2631 (2016), DOI: 10.1039/c5cc08867d.

[198] X. J. Wei, D.-T. Yang, L. Wang, T. Song, L.-Z. Wu, and Q. Liu, A novel

intermolecular synthesis of γ-lactones via visible-light photoredox catalysis, *Organic Letters* **15**(23), 6054–6057 (2013), DOI: 10.1021/ol402954t.

[199] I. Triandafillidi, M. G. Kokotou, and C. G. Kokotos, Photocatalytic synthesis of γ-lactones from alkenes: High-resolution mass spectrometry as a tool to study photoredox reactions, *Organic Letters* **20**(1), 36–39 (2018), DOI: 10.1021/acs.orglett.7b03256.

[200] E. J. Corey and M. C. Kang, New and general synthesis of polycyclic γ-lactones by double annulation, *Journal of the American Chemical Society* **106**(18), 5384–5385 (1984), DOI: 10.1021/ja00330a076.

[201] W. E. Fristad and J. R. Peterson, Manganese(III)-mediated γ-lactone annulation, *Journal of Organic Chemistry* **50**(1), 10–18 (1985), DOI: 10.1021/jo00201a003.

[202] L. W. Hessel and C. Romers, The crystal structure of "anhydrous manganic acetate", *Recueil des Travaux Chimiques des Pays-Bas* **88**(5), 545–552 (1969), DOI: 10.1002/recl.19690880505.

[203] L. Huang, H. Jiang, C. Qi, and X. Liu, Copper-catalyzed intermolecular oxidative [3 + 2] cycloaddition between alkenes and anhydrides: A new synthetic approach to γ-lactones, *Journal of the American Chemical Society* **132**(50), 17652–17654 (2010), DOI: 10.1021/ja108073k.

[204] L. Emmanuvel, T. M. A. Shaikh, and A. Sudalai, $NaIO_4$/LiBr-mediated diastereoselective dihydroxylation of olefins: A catalytic approach to the Prevost–Woodward reaction, *Organic Letters* **7**(22), 5071–5074 (2005), DOI: 10.1021/ol052080n.

[205] S. I. Fukuzawa, A. Nakanishi, T. Fujinami, and S. Sakai, Samarium(II) di-iodide induced reductive coupling of α,β-unsaturated esters with carbonyl compounds leading to a facile synthesis of γ-lactone, *Journal of the Chemical Society, Perkin Transactions 1* (7), 1669–1675 (1988), DOI: 10.1039/P19880001669.

[206] W. Wang, M.-H. Xu, X. S. Lei, and G.-Q. Lin, Chiral sulfonamide induced enantioselective protonation of samarium enolate in the reaction of

α,β-unsaturated ester with ketone, *Organic Letters* **2**(24), 3773–3776 (2000), DOI: 10.1021/ol006429c.

[207] G. A. Kraus and K. Landgrebe, The transformation of alkenes into γ-lactones using α-iodoesters, *Tetrahedron Letters* **25**(36), 3939–3942 (1984), DOI: 10.1016/0040-4039(84)80035-0.

[208] G. A. Kraus and K. Landgrebe, Stannyl ester cyclizations, *Tetrahedron* **41**(19), 4039–4046 (1985), DOI: 10.1016/S0040-4020(01)97182-0.

[209] M. Degueil-Castaing, B. Oe Jeso, G. A. Kraus, K. Landgrebe, and B. Maillard, Mechanism of the addition of tributyltin iodoacetate to alkenes, *Tetrahedron Letters* **27**(49), 5927–5930 (1986), DOI: 10.1016/S0040-4039(00)85364-2.

[210] D. P. Curran and C.-T. Chang, Atom transfer cyclization reactions of α-iodo esters, ketones, and malonates: Examples of selective 5-exo, 6-endo, 6-exo, and 7-endo ring closures, *Journal of Organic Chemistry* **54**(13), 3140–3157 (1989), DOI: 10.1021/jo00274a034.

[211] T. Shono, H. Ohmizu, S. Kawakami, and H. Sugiyama, Electroreductive hydrocoupling of activated olefins with ketones or aldehydes in the presence of trimethylchlorosilane, *Tetrahedron Letters* **21**(52), 5029–5032 (1980), DOI: 10.1016/S0040-4039(00)71124-5.

[212] M. Fantin, A. A. Isse, A. Venzo, A. Gennaro, and K. Matyjaszewski, Atom transfer radical polymerization of methacrylic acid: A won challenge, *Journal of the American Chemical Society* **138**(23), 7216–7219 (2016), DOI: 10.1021/jacs.6b01935.

[213] B. Maillard, A. Kharrat, and C. Gardrat, Deplacements homolytiques intramoleculaires—I: Etude de la decomposition du perpentene-4 oate de *t*-butyle dans les cyclanes. Synthese de cycloalkyl-5 pentanolides-4, *Tetrahedron* **40**(18), 3531–3537 (1984), DOI: 10.1016/S0040-4020(01)91505-4.

[214] G. L. Schmir and B. A. Cunningham, Iminolactones. I. The mechanism of hydrolysis, *Journal of the American Chemical Society* **87**(24), 5692–5701 (1965), DOI: 10.1021/ja00952a030.

[215] D. Liu, S. Tang, H. Yi, C. Liu, X. Qi, Y. Lan, and A. Lei, Carbon-centered radical addition to O=C of amides or esters as a route to C−O bond formations, *Chemistry—A European Journal* **20**(47), 15605–15610 (2014), DOI: 10.1002/chem.201404607.

[216] Y. Yamane, K. Miyazaki, and T. Nishikata, Different behaviors of a Cu catalyst in amine solvents: Controlling N and O reactivities of amide, *ACS Catalysis* **6**(11), 7418–7425 (2016), DOI: 10.1021/acscatal.6b02309.

[217] T. Nishikata, K. Itonaga, N. Yamaguchi, and M. Sumimoto, Amine-controlled divergent reaction: Iminolactonization and olefination in the presence of a Cu(I) catalyst, *Organic Letters* **19**(10), 2686–2689 (2017), DOI: 10.1021/acs.orglett.7b01020.

[218] Y. Lv, W. Pu, S. Mao, X. Ren, Y. Wu, and H. Cui, Cu-catalyzed intermolecular oxyalkylation of styrenes under air: Access to diverse iminolactones, *RSC Advances* **7**(66), 41723–41726 (2017), DOI: 10.1039/c7ra07306b.

[219] A. J. Clark, Copper catalyzed atom transfer radical cyclization reactions, *European Journal of Organic Chemistry* **2016**(13), 2231–2243 (2016), DOI: 10.1002/ejoc.201501571.

[220] D. P. Curran and C.-T. Chang, Atom transfer cyclization reactions of α-iodo carbonyls, *Tetrahedron Letters* **28**(22), 2477–2480 (1987), DOI: 10.1016/S0040-4039(00)95445-5.

[221] D. P. Curran and J. Tamine, Effects of temperature on atom transfer cyclization reactions of allylic α-iodo esters and amides, *Journal of Organic Chemistry* **56**(8), 2746–2750 (1991), DOI: 10.1021/jo00008a032.

[222] E. Lee, C. H. Yoon, and T. H. Lee, 8-Endo cyclization of (alkoxycarbonyl)methyl radicals generated from bromoacetates, *Journal of the American Chemical Society* **114**(27), 10981–10983 (1992), DOI: 10.1021/ja00053a056.

[223] E. Lee, C. H. Yoon, T. H. Lee, S. Y. Kim, T. J. Ha, Y.-s. Sung, S.-H. Park, and S. Lee, 8-Endo cyclization of (alkoxycarbonyl)methyl radicals: Radical

ways for preparation of eight-membered-ring lactones, *Journal of the American Chemical Society* **120**(30), 7469–7478 (1998), DOI: 10.1021/ja980908d.

[224] J. Wang and C. Li, Investigation of bis(tributyltin)-initiated free radical cyclization reactions of 4-pentenyl iodoacetates, *Journal of Organic Chemistry* **67**(4), 1271–1276 (2002), DOI: 10.1021/jo0109568.

[225] S. Hanessian, R. Di Fabio, J. F. Marcoux, and M. Prud'homme, The synthesis of substituted lactones by intramolecular chirality transfer with stereodifferentiating chiral α-ester radical intermediates, *Journal of Organic Chemistry* **55**(11), 3436–3438 (1990), DOI: 10.1021/jo00298a005.

[226] D. L. J. Clive and P. L. Beaulieu, Formation of carbon–carbon bonds by ring closure of β-phenylselenocrotonates, *Journal of the Chemical Society, Chemical Communications* (6), 307–309 (1983), DOI: 10.1039/C39830000307.

[227] J. L. Belletire and N. O. Mahmoodi, Direct butyrolactone production using tin hydride, *Tetrahedron Letters* **30**(33), 4363–4366 (1989), DOI: 10.1016/S0040-4039(00)99361-4.

[228] J. M. Muñoz-Molina, T. R. Belderraín, and P. J. Pérez, Copper-catalyzed synthesis of 1,2-disubstituted cyclopentanes from 1,6-dienes by ring-closing Kharasch addition of carbon tetrachloride, *Advanced Synthesis & Catalysis* **350**(14-15), 2365–2372 (2008), DOI: 10.1002/adsc.200800364.

[229] C. Ricardo and T. Pintauer, Copper catalyzed atom transfer radical cascade reactions in the presence of free-radical diazo initiators as reducing agents, *Chemical Communications* (21), 3029–3031 (2009), DOI: 10.1039/b905839g.

[230] M. N. C. Balili and T. Pintauer, Photoinitiated ambient temperature copper-catalyzed atom transfer radical addition (ATRA) and cyclization (ATRC) reactions in the presence of free-radical diazo initiator (AIBN), *Dalton Transactions* **40**(12), 3060–3066 (2011), DOI: 10.1039/c0dt01764g.

[231] S. Kamijo, S. Matsumura, and M. Inoue, Microwave-assisted atom transfer radical addition of polychlorinated compounds to olefins without addition

of metal catalysts, *Tetrahedron Letters* **53**(33), 4368–4371 (2012), DOI: 10.1016/j.tetlet.2012.06.027.

[232] Y. Gao, P. Zhang, Z. Ji, G. Tang, and Y. Zhao, Copper-catalyzed cascade radical addition–cyclization halogen atom transfer between alkynes and unsaturated α-halogenocarbonyls, *ACS Catalysis* **7**(1), 186–190 (2017), DOI: 10.1021/acscatal.6b03033.

[233] D. W. Manley, A. Mills, C. O'Rourke, A. M. Z. Slawin, and J. C. Walton, Catalyst-free photoredox addition–cyclisations: Exploitation of natural synergy between aryl acetic acids and maleimide, *Chemistry—A European Journal* **20**(18), 5492–5500 (2014), DOI: 10.1002/chem.201304929.

[234] S.-i. Iwamatsu, H. Kondo, K. Matsubara, and H. Nagashima, Copper-catalyzed facile carbon-carbon bond forming reactions at the α-position of α,α,γ-trichlorinated γ-lactams, *Tetrahedron* **55**(6), 1687–1706 (1999), DOI: 10.1016/S0040-4020(98)01198-3.

[235] M. Helliwell, D. Fengas, C. K. Knight, J. Parker, P. Quayle, J. Raftery, and S. N. Richards, Bifurcate, tandem ATRC reactions: Towards 2-oxabicyclo[4.3.0]nonane core of eunicellins, *Tetrahedron Letters* **46**(42), 7129–7134 (2005), DOI: 10.1016/j.tetlet.2005.08.104.

[236] D. Yang, Y.-L. Yan, B.-F. Zheng, Q. Gao, and N.-Y. Zhu, Copper(I)-catalyzed chlorine atom transfer radical cyclization reactions of unsaturated α-chloro β-keto esters, *Organic Letters* **8**(25), 5757–5760 (2006), DOI: 10.1021/ol0623264.

[237] C. V. Stevens, E. Van Meenen, K. G. Masschelein, Y. Eeckhout, W. Hooghe, B. D'hondt, V. N. Nemykin, and V. V. Zhdankin, A copper-catalyzed domino radical cyclization route to benzospiro-indolizidinepyrrolidinones, *Tetrahedron Letters* **48**(40), 7108–7111 (2007), DOI: 10.1016/j.tetlet.2007.07.211.

[238] H. Yorimitsu, K. Wakabayashi, H. Shinokubo, and K. Oshima, Radical addition of 2-iodoalkanamide or 2-iodoalkanoic acid to alkenols using a water-soluble radical initiator in water. A facile synthesis of γ-lactones, *Tetrahedron Letters* **40**(3), 519–522 (1999), DOI: 10.1016/S0040-4039(98)02391-0.

[239] H. Yorimitsu, K. Wakabayashi, H. Shinokubo, and K. Oshima, Radical addition of 2-iodoalkanamide or 2-iodoalkanoic acid to alkenes with a water-soluble radical initiator in aqueous media: Facile synthesis of γ-lactones, *Bulletin of the Chemical Society of Japan* **74**(10), 1963–1970 (2001), DOI: 10.1246/bcsj.74.1963.

[240] T. Nakano, M. Kayama, H. Matsumoto, and Y. Nagai, Free radical addition of α-bromocarboxylic acids to olefins leading to γ-butyrolactones, *Chemistry Letters* **10**(3), 415–418 (1981), DOI: 10.1246/cl.1981.415.

[241] T. Nakano, M. Kayama, and Y. Nagai, Free radical addition of 2-bromoalkanoic acids to alkenes, *Bulletin of the Chemical Society of Japan* **60**(3), 1049–1052 (1987), DOI: 10.1246/bcsj.60.1049.

[242] D. I. Davies and M. D. Dowle, The acid-catalysed lactonisation of the norborn-5-en-2-ylacetic acids, *Journal of the Chemical Society, Perkin Transactions 1* (3), 227–231 (1978), DOI: 10.1039/p19780000227.

[243] G. M. Whitesides and J. San Filippo, The mechanism of reduction of alkylmercuric halides by metal hydrides, *Journal of the American Chemical Society* **92**(22), 6611–6624 (1970), DOI: 10.1021/ja00725a039.

[244] E. V. Piletska, A. R. Guerreiro, M. Romero-Guerra, I. Chianella, A. P. Turner, and S. A. Piletsky, Design of molecular imprinted polymers compatible with aqueous environment, *Analytica Chimica Acta* **607**(1), 54–60 (2008), DOI: 10.1016/j.aca.2007.11.019.

[245] D. R. Lide, *Handbook of chemistry and physics*, CRC Press, 84th edition, 2003.

[246] H. Xiong, W. Mo, J. Hu, R. Bai, and G. Li, CuCl/phen/NMI in homogeneous carbonylation for synthesis of diethyl carbonate: Highly active catalyst and corrosion inhibitor, *Industrial and Engineering Chemistry Research* **48**(24), 10845–10849 (2009), DOI: 10.1021/ie901139e.

[247] R. G. Pearson, Hard and soft acids and bases, *Journal of the American Chemical Society* **85**(22), 3533–3539 (1963), DOI: 10.1021/ja00905a001.

[248] R. G. Pearson, Hard and soft acids and bases, HSAB, part I: Fundamental principles, *Journal of Chemical Education* **45**(9), 581–587 (1968), DOI: 10.1021/ed045p581.

[249] R. G. Pearson, Hard and soft acids and bases, HSAB, part II: Underlying theories, *Journal of Chemical Education* **45**(10), 643–648 (1968), DOI: 10.1021/ed045p643.

[250] M. Fantin, A. A. Isse, A. Gennaro, and K. Matyjaszewski, Understanding the fundamentals of aqueous ATRP and defining conditions for better control, *Macromolecules* **48**(19), 6862–6875 (2015), DOI: 10.1021/acs.macromol.5b01454.

[251] S. Tyagi, B. Hathaway, S. Kremer, H. Stratemeier, and D. Reinen, Crystal structure of bis(2,2′-bipyridyl)monochlorocopper(II) hexafluorophosphate monohydrate at 298 K and the electron spin resonance spectra of some bis(2,2′-bipyridyl)copper(II) complexes to 4.2 K, *Dalton Transactions* (10), 2087–2091 (1984), DOI: 10.1039/DT9840002087.

[252] M. Munakata, S. Kitagawa, A. Asahara, and H. Masuda, Crystal structure of bis(2,2′-bipyridine)copper(I) perchlorate, *Bulletin of the Chemical Society of Japan* **60**(5), 1927–1929 (1987), DOI: 10.1246/bcsj.60.1927.

[253] W. Tang and K. Matyjaszewski, Effect of ligand structure on activation rate constants in ATRP, *Macromolecules* **39**(15), 4953–4959 (2006), DOI: 10.1021/ma0609634.

[254] N. V. Tsarevsky, T. Pintauer, and K. Matyjaszewski, Deactivation efficiency and degree of control over polymerization in ATRP in protic solvents, *Macromolecules* **37**(26), 9768–9778 (2004), DOI: 10.1021/ma048438x.

[255] N. V. Tsarevsky, W. A. Braunecker, A. Vacca, P. Gans, and K. Matyjaszewski, Competitive equilibria in atom transfer radical polymerization, *Macromolecular Symposia* **248**, 60–70 (2007), DOI: 10.1002/masy.200750207.

[256] N. Bortolamei, A. A. Isse, V. B. Di Marco, A. Gennaro, and K. Matyjaszewski, Thermodynamic properties of copper complexes used as catalysts in atom

transfer radical polymerization, *Macromolecules* **43**(22), 9257–9267 (2010), DOI: 10.1021/ma101979p.

[257] A. Bunha, M. C. Tria, and R. Advincula, Polymer catenanes via a supramolecularly templated ATRP initiator, *Chemical Communications* **47**(32), 9173–9175 (2011), DOI: 10.1039/c1cc13162a.

[258] A. A. Isse, N. Bortolamei, P. De Paoli, and A. Gennaro, On the mechanism of activation of copper-catalyzed atom transfer radical polymerization, *Electrochimica Acta* **110**, 655–662 (2013), DOI: 10.1016/j.electacta.2013.04.132.

[259] M. Knorn, T. Rawner, R. Czerwieniec, and O. Reiser, [Copper(phenanthroline)-(bisisonitrile)]$^{+}$-complexes for the visible-light-mediated atom transfer radical addition and allylation reactions, *ACS Catalysis* **5**(9), 5186–5193 (2015), DOI: 10.1021/acscatal.5b01071.

[260] S. Tan, Y. Zhang, Z. Niu, and Z. Zhang, Copper(0) mediated single electron transfer controlled radical polymerization toward C−F bonds on poly(vinylidene fluoride), *Macromolecular Rapid Communications* **39**(4), 1700561 (2018), DOI: 10.1002/marc.201700561.

[261] L. Fu, A. Simakova, M. Fantin, Y. Wang, and K. Matyjaszewski, Direct ATRP of methacrylic acid with iron-porphyrin based catalysts, *ACS Macro Letters* **7**(1), 26–30 (2018), DOI: 10.1021/acsmacrolett.7b00909.

[262] R. M. Beesley, C. K. Ingold, and J. F. Thorpe, CXIX.—The formation and stability of spiro-compounds. Part I. spiro-Compounds from cyclohexane, *Journal of the Chemical Society, Transactions* **107**, 1080–1106 (1915), DOI: 10.1039/CT9150701080.

Acronyms and abbreviations

In square brackets are reported the CAS registry numbers of chemical substances.

AA	Acrylic acid [79-10-7]
Ac	Acetyl group $-C(=O)CH_3$
AIBN	Azobisisobutyronitrile [78-67-1]
ARGET	Activator regenerated by electron transfer
AsAc	Ascorbic acid [50-81-7]
ATRA	Atom transfer radical addition
ATRA-L	Atom transfer radical addition and lactonization
ATRC	Atom transfer radical cyclization
ATRC-L	Atom transfer radical cyclization and lactonization
ATRP	Atom transfer radical polymerization
BB	Benzal bromide [618-31-5]
BC	Benzal chloride [98-87-3]
BDE	Bond-dissociation energy
BiBA	α-Bromoisobutyric acid [2052-01-9]
BiB$^-$	α-Bromoisobutyrate anion [18526-77-7]
Bn	Benzyl group $-CH_2C_6H_5$
BPA	α-Bromopropionic acid [598-72-1]
BPAA	α-Bromophenylacetic acid [4870-65-9]

bpy	2,2′-Bipyridine [366-18-7]
Bu	Butyl group $-C_4H_9$
Cat	Catalyst
Conv	Conversion
CRT	Catalytic radical termination
Đ	Dispersity
DBPS	α,ω-Dibromopolystyrene [9003-53-6]
DCPS	α,ω-Dichloropolystyrene [9003-53-6]
DF	Dilution factor
DHAs	Dehydroascorbic acid [490-83-5]
DMAEMA	2-(Dimethylamino)ethyl methacrylate [2867-47-2]
DMAPMAm	*N*-[3-(Dimethylamino)propyl]methacrylamide [5205-93-6]
DMF	*N*,*N*-Dimethylformamide [68-12-2]
DMSO	Dimethyl sulfoxide [67-68-5]
dNbpy	4,4′-Dinonyl-2,2′-bipyridine [142646-58-0]
DSC	Differential scanning calorimetry
EA	Ethyl acrylate [140-88-5]
***e*ATRP**	Electrochemically mediated ATRP
ECA	Ethyl 2-chloroactylate [687-46-7]
ECiB	Ethyl 2-chloroisobutyrate [62554-44-3]
EDCP	Ethyl 2,2-dichloropropionate [17640-03-8]
EG	Ethylene glycol [107-21-1]
EMA	Ethyl methacrylate [97-63-2]
Et	Ethyl group $-CH_2CH_3$
EWG	Electron withdrawing group
FEG	Field emission gun

FRP	Free-radical polymerization
GC	Gas chromatography
GP	Gel point
GPC	Gel permeation chromatography
HEBiB	2-Hydroxyethyl 2-bromoisobutyrate [189324-13-8]
HEMA	2-Hydroxyethyl methacrylate [868-77-9]
HiBA	2-Hydroxyisobutyric acid [594-61-6]
HPLC	High-performance liquid chromatography
HRMS	High-resolution mass spectroscopy
HSAB	Hard and soft acids and bases
ICAR	Initiators for continuous activator regeneration
Ini	Initiator
IPA	Isopropyl alcohol [67-63-0]
IPIAA	5,6-O,O-Isopropylidene-ascorbic acid [15042-01-0]
LRP	Living radical polymerization
M	Monomer
MAA	Methacrylic acid [79-41-4]
MA^-	Methacrylate anion [18358-13-9]
MALLS	Multiangle laser light scattering
MCA	Methyl 2-chloroactylate [80-63-7]
MDCB	Methyl 2,2-dichlorobutanoate [18545-44-3]
Me	Methyl group $-CH_3$
Mechano-ATRP	Mechanically induced ATRP
$\boldsymbol{M}_n$	Number average molar mass
$\boldsymbol{M}_n^{th}$	Theoretical number average molar mass
MPA	2-Methylpropanoic acid [79-31-2]

MR	Molar ratio
Mt	Transition metal
MW	Molecular weight
$\boldsymbol{M}_{\mathrm{w}}$	Mass average molar mass
$\boldsymbol{M}_{\mathrm{w}}^{\mathrm{GPC}}$	Mass average molar mass (determined by GPC)
$\boldsymbol{M}_{\mathrm{w}}^{\mathrm{MALLS}}$	Mass average molar mass (determined by MALLS)
NaAs	Sodium ascorbate [134-03-2]
NHPI	*N*-Hydroxyphthalimide [524-38-9]
NMP	Nitroxide-mediated radical polymerization
NMR	Nuclear magnetic resonance
OMRP	Organometallic-mediated radical polymerization
ORPC	Oxidative radical-polar crossover
OTf	Triflate group $-OSO_2CF_3$
PBS	Phosphate-buffered saline
PEMA	Poly(ethyl methacrylate) [9003-42-3]
Ph	Phenyl group $-C_6H_5$
Photo-ATRP	Photoinduced ATRP
PINO	Phthalimide *N*-oxyl [3229-40-1]
PMAA	Poly(methacrylic acid) [25087-26-7]
PMDETA	N,N,N',N'',N''-Pentamethyldiethylenetriamine [3030-47-5]
PS	Polystyrene [9003-53-6]
RA	Reducing agent
RAFT	Reversible addition-fragmentation chain transfer
RDRP	Reversible-deactivation radical polymerization
RP	Radical polymerization
SARA	Supplemental activator and reducing agent

SEM	Scanning electron microscope
SET	Single-electron transfer
$\mathbf{S_Hi}$	Intramolecular homolytic substitution
$\mathbf{S_N1}$	Unimolecular nucleophilic substitution
$\mathbf{S_N2}$	Bimolecular nucleophilic substitution
$\mathbf{Sn(EH)_2}$	Tin(II) 2-ethylhexanoate [301-10-0]
$\mathbf{S_Ni}$	Intramolecular nucleophilic substitution
St	Styrene [100-42-5]
TBC	4-*tert*-Butylcatechol [98-29-3]
TBPP	*tert*-Butyl-4-peroxypentenoate [84210-61-7]
TDP	Targeted degree of polymerization
TEA	Triethylamine [121-44-8]
TGA	Thermogravimetric analysis
THF	Tetrahydrofuran [109-99-9]
TMSA	2,2,3,3-Tetramethylsuccinic acid [630-51-3]
Tol	Toluene [108-88-3]
TPMA	Tris(2-pyridylmethyl)amine [16858-01-8]
$\mathbf{TPMAH^+}$	Tris(2-pyridylmethyl)ammonium cation
VISCO	Viscometer
X	Halogen

List of schemes

List of figures

List of tables